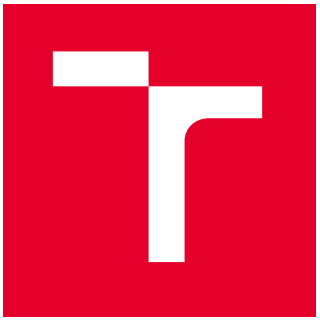

BRNO UNIVERSITY OF TECHNOLOGY

VYSOKÉ UČENÍ TECHNICKÉ V BRNĚ

FACULTY OF MECHANICAL ENGINEERING

FAKULTA STROJNÍHO INŽENÝRSTVÍ

INSTITUTE OF MACHINE AND INDUSTRIAL DESIGN

ÚSTAV KONSTRUOVÁNÍ

THE INFLUENCE OF HYALURONIC ACID ON FRICTION AND LUBRICATION OF FASCIA

VLIV KYSELINY HYALURONOVÉ NA TŘENÍ A MAZÁNÍ FASCIÍ

DOCTORAL THESIS

DIZERTAČNÍ PRÁCE

AUTHOR — **Ing. Alexandra Streďanská**

AUTOR PRÁCE

SUPERVISOR — **prof. Ing. Martin Vrbka, Ph.D.**

ŠKOLITEL

BRNO 2025

STATEMENT

I hereby declare that I have written the PhD thesis *The influence of hyaluronic acid on friction and lubrication of fascia* on my own according to the advice of my supervisor Professor Martin Vrbka, PhD, co-supervisor Assoc. Professor David Nečas, PhD, and using the sources listed in the references.

…….
Alexandra Streďanská

BIBLIOGRAPHICAL REFERENCE

STREĎANSKÁ, Alexandra. *The influence of hyaluronic acid on friction and lubrication of fascia*. Doctoral Thesis. Martin VRBKA (supervisor). Brno: Brno University of Technology, Faculty of Mechanical Engineering, 2025.

ACKNOWLEDGEMENT

I would like to express my sincere thanks to all those who helped and supported me during the work on this dissertation. I would like to thank my thesis supervisor, Professor Martin Vrbka, PhD and co-supervisor Assoc. Professor David Nečas, PhD for their professional guidance, valuable advice and constant support throughout the whole period of my dissertation. Their guidance was invaluable in shaping my ideas and conducting my research.

I would also like to thank my colleagues, with special thanks to those in the office who have been supportive during the day-to-day research activities and discussions. Their support has contributed to the improvement of this thesis.

Many thanks also go to my family and special ones for their support, patience and understanding throughout my educational journey. Finally, a million thanks to my sister K., my greatest fellow in arms.

"You must go on a long journey before you can really find out how wonderful home is." Comet in Moominland

ABSTRACT

The growing prevalence of non-specific lower back pain (NSLBP) represents significant socioeconomic challenges, necessitating the development of effective treatment strategies. This study, conducted in collaboration with Contipro, a.s., aims to address this need by developing a hyaluronic acid (HA)-based viscosupplement intended for injection into the thoracolumbar fascia to mitigate the adhesion of pathological fascial tissues, a condition often associated with NSLBP. The research was divided into fundamental and applied objectives. The fundamental objective focused on developing six unique tribological models of the thoracolumbar fascia to accurately simulate the frictional behavior of fascial tissues under *in vivo*-like conditions. These models were crucial for investigating the mechanisms through which HA-based solutions influence frictional properties and for identifying the material parameters essential for accurately replicating the behavior of fascial tissue. In addition to extensive tribological measurements, pharmacokinetic study was conducted to further verify the results. The applied objective aimed to consider the impact of various HA-based solution compositions on reducing friction in fascial tissues, ultimately leading to the development of an optimized viscosupplement for treating NSLBP. Key findings demonstrated that sliding velocity, material stiffness, pin radius, preload, and HA molecular weight and concentration are critical factors influencing the frictional behavior of the thoracolumbar fascia. Lower molecular weight HA solutions, particularly those with reduced viscosity, were found to significantly reduce friction by facilitating smoother movement between tissue surfaces. The study also identified the mechanisms of friction reduction in HA-lubricated adhesive fascial tissues, providing a scientific basis for the development of a novel viscosupplement.

KEYWORDS

hyaluronic acid, tribological model, friction, fascia, lower back pain, compliant contact

ABSTRAKT

Rastúci počet pacientov trpiacich nešpecifických bolestí chrbta predstavuje významné sociálno-ekonomické výzvy, ktoré si vyžadujú hľadanie účinných liečebných stratégií. Cieľom tejto štúdie, ktorá sa uskutočnila v spolupráci so spoločnosťou Contipro, a.s., je riešiť túto potrebu vývojom viskosuplementu na báze kyseliny hyalurónovej určeného na injekčné podanie do torakolumbálnej fascie na zmiernenie adhézie patologických fasciálnych tkanív, čo je stav často spojený s nešpecifickou bolesťou dolnej časti chrbta. Výskum bol rozdelený na základné a aplikované ciele. Základný cieľ bol zameraný na vývoj šiestich jedinečných tribologických modelov torakolumbálnej fascie na presnú simuláciu trecieho správania fasciálnych tkanív v podmienkach podobných podmienkam *in vivo*. Tieto modely boli nevyhnutné na skúmanie mechanizmov, ktorými roztoky na báze kyseliny hyalurónovej ovplyvňujú trecie vlastnosti, a na identifikáciu materiálových parametrov rozhodujúcich pre replikáciu správania fasciálneho tkaniva. Aplikovaný cieľ bol zameraný na posúdenie vplyvu rôznych zložení roztokov na báze kyseliny hyalurónovej na zníženie trenia vo fasciálnych tkanivách, čo v konečnom dôsledku viedlo k vývoju optimalizovaného viskózneho doplnku na liečbu nešpecifickej bolesti dolnej časti chrbta. Kľúčové zistenia ukázali, že rýchlosť pohybu, tuhosť materiálu, polomer pinu, predopnutie fascie a molekulová hmotnosť a koncentrácia kyseliny hyalurónovej sú rozhodujúcimi faktormi ovplyvňujúcimi trenie v torakolumbálnej fascii. Zistilo sa, že roztoky kyseliny hyalurónovej s nižšou molekulovou hmotnosťou, najmä tie so zníženou viskozitou, výrazne znižujú trenie tým, že uľahčujú hladší pohyb medzi povrchmi tkaniva. Štúdia tiež identifikovala mechanizmy zníženia trenia v adhezívnych fasciálnych tkanivách mazaných kyselinou hyalurónovou, čím poskytla vedecký základ pre vývoj nového viskosuplementu. Okrem rozsiahlych tribologických meraní sa na ďalšie overenie výsledkov uskutočnila farmakokinetická štúdia.

KĽÚČOVÉ SLOVÁ

kyselina hyalúronová, tribologický model, trenie, bolesť krížov, poddajný kontakt

CONTENT

1	**INTRODUCTION**	**8**
2	**STATE OF THE ART**	**10**
2.1	Thoracolumbar fascia	10
2.1.1	The fascia specification and causality of non-specific lower back pain	10
2.1.2	Possibilities and effectiveness of a fascial therapy	11
2.2	Hyaluronic acid and its role within the fascia friction	13
2.2.1	Treatment of selected medical diagnoses focused on hyaluronic acid	17
2.3	Friction of compliant contacts	19
2.3.1	Biotribological models of human body parts today	19
2.3.2	The compliant contact tribology	21
3	**ANALYSIS AND CONCLUSION OF LITERATURE REVIEW**	**28**
3.1	Non-specific lower back pain	28
3.2	Hyaluronic acid-based treatment	28
3.3	Thoracolumbal fascia tribological model	29
4	**AIMS OF THE THESIS**	**30**
4.1	Scientific questions & Hypotheses	30
5	**MATERIALS AND METHODS**	**33**
5.1	Experimental equipment	33
5.1.1	Bruker UMT TriboLab	33
5.1.2	Rheological Testing Equipment	34
5.1.3	Scanning electron microscope	34
5.2	Experimental specimens	35
5.2.1	Model development	35
5.2.2	Lubricants	38
5.3	Experimental design	39
5.3.1	The influence of material hardness and motion speed on fascia model friction (Study I)	39
5.3.2	Hyaluronic acid properties scale estimation (Study II)	40
5.3.3	Tribological model development (Study III)	40
5.3.4	Hyaluronic acid frictional properties (Study III and Study IV)	41
5.3.5	Statistical methods	41
5.4	Thesis layout	44
6	**RESULTS AND DISCUSSION**	**46**
6.1	First publication [I.]	46
6.2	Second publication [II.]	46
6.3	Third publication [III.]	47
6.4	Fourth publication [IV.]	49
7	**LIMITATIONS**	**100**
8	**CONCLUSIONS**	**101**
9	**LIST OF PUBLICATIONS**	**104**
10	**LITERATURE**	**105**
LIST OF FIGURES		**116**
LIST OF TABLES		**117**
LIST OF ABBREVIATIONS AND SYMBOLS		**118**

1 INTRODUCTION

Lower back pain (LBP) is a prevalent issue that can affect people of all ages, with working-age individuals being the most affected. Surveys suggest that nearly all adults have experienced this problem at least once in their lives, and a concerning 23% suffer from chronic back pain, lasting for more than 6-12 weeks. This chronic condition disables around 11-12% of the population [1]. Consequently, LBP ranks among the leading causes of disability globally, impacting not only the individual's well-being (Fig. 1) but also carrying socioeconomic implications for their communities and society at large.

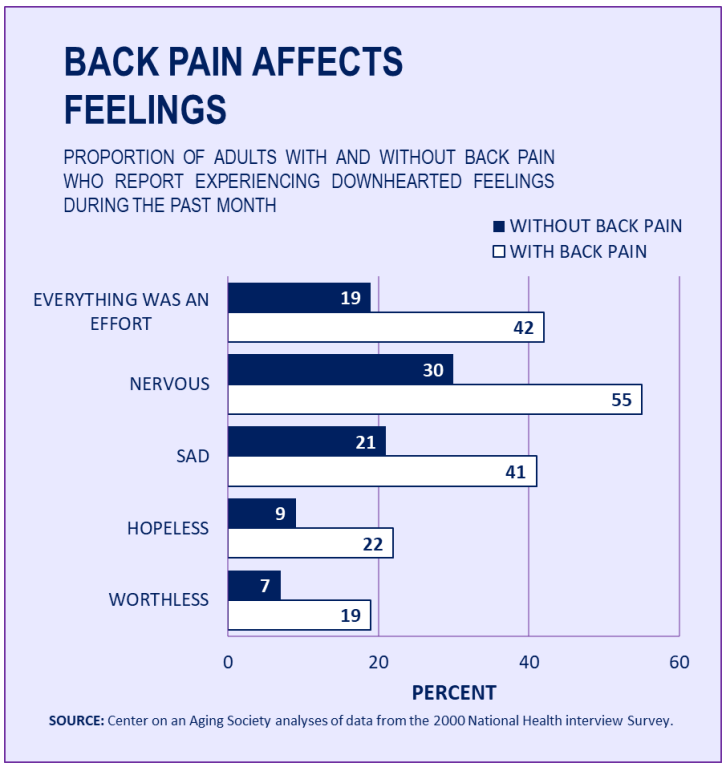

Fig. 1 How back pain affects feelings. Graphs are taken and adapted from [2]

Although age-standardized rates have experienced a modest decline over the last three decades, projections indicate that by 2050, over 800 million individuals worldwide will suffer from low back pain [3]. Treatment, particularly in developed countries, incurs high costs, both directly and indirectly, deteriorated by the inability to work due to the condition [4], see Fig. 2. Unfortunately, in 85-90% of cases [5], doctors struggle to identify the exact cause of a patient's pain, like degenerative spinal changes or bulging intervertebral discs, which are typically visible on scans. And are called non-specific LBP (NSLBP). It remains a leading cause for visiting general practitioners or physicians globally, with an average care-seeking prevalence of 58% [6-8]. Recent research points to the thoracolumbar fascia (TLF) as a potential source of this pain [9]. The TLF, with its layers lubricated by hyaluronic acid

(HA), normally facilitates smooth movement and force transfer between muscles [10]. However, lifestyle and health factors can alter the fascia, leading to pain [11; 12]. Although NSLBP is very common worldwide, however, the treatments that are recommended tend to have only moderate effectiveness [8; 9]. Considering these factors, discussed later in this thesis, there is a belief that an injectable viscosupplement could relief pain and restore proper fascial function.

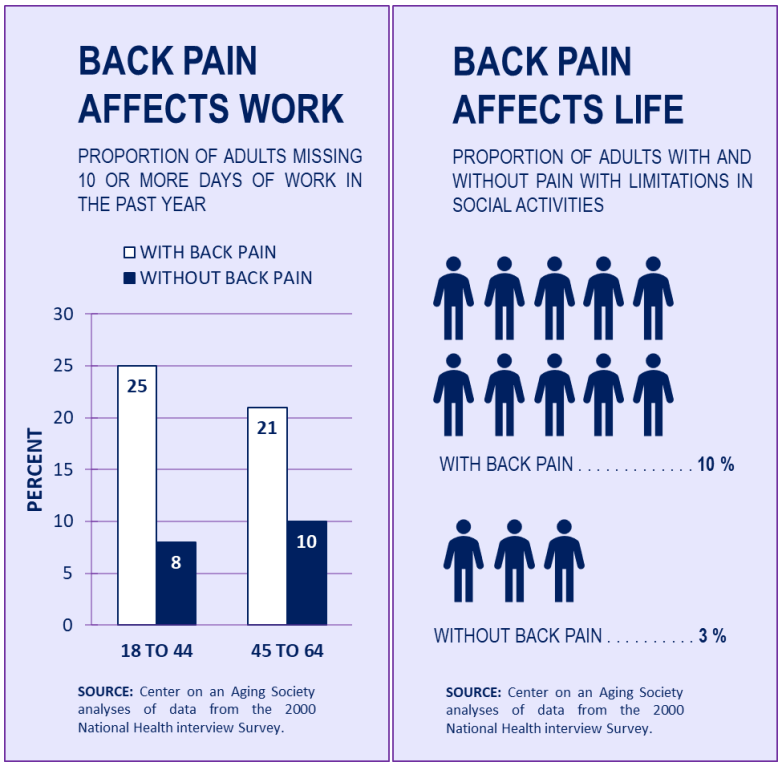

Fig. 2 How back pain affects work and social life. Graphs are taken and adapted from [2]

Motivation

The biotechnology company Contipro, a.s. proposed a HA-based treatment idea and approached The Biotribology Research Group at FME BUT for a joint project. However, to move beyond mere ideas, the first goal of the project is to develop an accurate tribological model of fascia. Consequently, it aims to identify the ideal chemical properties of HA that minimize friction between fascia layers. This information will be shared with Contipro, a.s., where scientists will manufacture the specified agent for inclusion in clinical trials. The ultimate objective is to introduce a remedy to the market within five years, offering relief to numerous patients and restoring them to normal life.

2 STATE OF THE ART

Biotribology is the science that studies friction, lubrication, and wear in biological systems. From joint replacements and food processing to the application of cosmetics, tooth brushing, contact lens friction, and even the mutual friction of internal organs, biotribology helps improve our quality of life and safety. Like other research fields, whether in healthcare or engineering, biotribology seeks ways to investigate its problems under laboratory conditions. This is because testing the systems under study in real environments is often expensive, sometimes impossible, and subject to medical ethics. Therefore, tribological models exist that aim to closely replicate reality, allowing us to study tribological processes in joints, eyes, skin, and the tongue, for example. However, it must be noted that despite the extensive number of existing models, as shown later, none simulate and study human fascia. What exactly is fascia? Perhaps the most well-known fascia is the epimysium surrounding muscles. However, the fascial system covers the entire human body, holding our organs, muscles, bones, joints, blood vessels, and nerves together [13].

2.1 Thoracolumbar fascia

2.1.1 The fascia specification and causality of non-specific lower back pain

Fascia (Fig. 3) is a tissue multilayered structure of 2-3 layers of densely packed collagen fibers. These layers are separated by loose connective tissue containing adipose cells, sulphated glycosaminoglycans and cells called fasciacytes [14]. These cells, similar to fibroblasts, produce HA, allowing the layers of fascia to glide over each other without causing pain. However, as mentioned, recent research suggests a connection between the TLF and NSLBP [11; 15; 16]. The TLF is the fascia located in the lower back, shaped like a diamond. The TLF is a key connective tissue that links the trunk, upper limbs, and lower limbs. It helps transfer forces between the lower and upper parts of the body [17]. The TLF has three layers: posterior, middle, and anterior. The posterior layer attaches to the lumbar and sacral spine, the supraspinous ligaments, the iliac crest, the lower edge of the 12th rib, and the lumbocostal ligament [18]. The posterior layer is the focus of this study and will henceforth be referred to only as TLF later. It works with muscles like the gluteus maximus, latissimus dorsi, and lower fibers of the trapezius to form a structure that supports movement and load transfer in the body [19]. The posterior layer has two layers an outer layer made of parallel collagen fibers, mainly from the latissimus dorsi and serratus posterior inferior muscles, and a deep layer with a sheath that surrounds the paraspinal muscles [18].

The individual layers of TLF often suffer due to the lifestyle of the person, where prolonged sitting, improper posture, age, overusing syndromes etc. [20-25] lead to pathological changes called fibrosis and densification [9; 12]. While fibrosis alters the fibrous tissue and the entire structure of the fascia, densification results in the thickening of the tissue and changes its mechanical sliding properties. The TLF shear stress decreases in patients with chronic NSLBP up to ~20% lower [11; 26]. And there is no exception that fibrosis and densification coexist. The body responds to these changes by increasing the production of high viscosity HA [27], which overwhelms the system and causes the fascia layers to stick together. This may be perceived by patients as an increase of fascial stiffness. Because the fascia is full of nerve endings [28; 29], stiffness is not the only sensation in fascial changes, but results in pain.

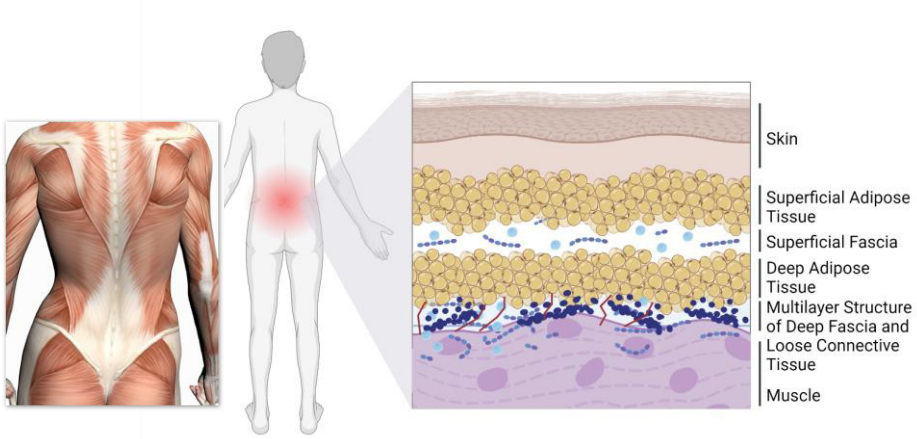

Fig. 3 NSLBP caused by TLF and placement of TLF under the skin. Created by Biorender.com

2.1.2 Possibilities and effectiveness of a fascial therapy

The WHO has issued recommendations on its website [30] regarding the treatment of LBP. It urges that painkillers should never be the first treatment option. And if the patient is already taking them, they should be combined with primary non-pharmacological treatment. Pharmacological treatment should always be combined with non-pharmacological treatment. It can be deduced that painkillers only address the symptoms of NSLBP, not the causes, as with many other conditions. Most treatment strategies recommended by primary care health professionals are not consistent with guidelines for the treatment of LBP and most patients reported that these treatments were ineffective, leading to their dissatisfaction [31]. Often offering generic advice, such as suggesting group exercise [32; 33]. They place little focus on personalized treatment plans or on how to effectively combine physical activity with other factors affecting the LBP experience. As the review study [34] about 2,674 participants showed - exercise therapy might not significantly impact pain or functional status in the short term for individuals with acute NSLBP when compared to sham/placebo treatments or no treatment at all, but the evidence

is highly uncertain. This highlights the gap between what patients feel they need and the current recommendations for LBP management.

The several techniques aimed directly at the fascia. One of them is Fascial Manipulation (FM), which involves pinpointing the exact site of pain and applying a lot of pressure by the therapist on that site. It is described by the coauthors [35] of FM as time-consuming, painful but effective. However, according to a review [36] on the FM which examined 13 studies using this technique for pain relief, this is more likely to be low- to moderate-quality evidence of the effect of FM on pain improvement. This technique was also partially addressed in the review study [37], which also found no evidence for the effectiveness of this method. Moreover, the technique was found to be widespread only in Italy and India, which is considered a major limitation. Alternative methods include exercises aimed at relaxing muscle fascia not specifically associated with pain. These include soft tissue mobilization using tools, self-myofascial release using a foam roller, and various massage tools such as rods and sticks [38]. However, despite their widespread use, scientific understanding of their physiological impact remains unclear and there is no agreed optimal programme to enhance athletic flexibility, recovery, and performance [39].

After going through the basic recommendations of a specialist, a desperate patient may look around for less traditional modalities such as laser acupuncture. Even here, however, the efficacy is somewhat questionable. Based on review of 20 studies [40], the pain scores reported by patients who received local laser acupuncture were statistically comparable to those of the control group at both short-term (4-8 weeks post-treatment) and long-term (12 months) follow-ups. For patients with chronic NSLBP, this may offer immediate pain relief.

From the preceding subsection, it may appear that the treatment of NSLBP is challenging. This underscores the need for innovative approaches to address this issue. Painkillers merely alleviate symptoms without targeting the underlying cause, and rehabilitation, while effective, is often short-effective, demanding rigorous adherence and incurring significant costs. In the description of fascia, it was noted that this tissue contains fasciacytes, which are cells responsible for producing HA. The proposed function of HA is to facilitate smooth gliding between structures during movement and to aid in the transmission of force generated by muscle contraction. If the properties of HA in loose connective tissue is reduced due to injury or other pathological conditions, the behavior of the entire deep fascia and the underlying perimysium could be compromised. Treatments that address the role of HA may therefore hold promise.

2.2 Hyaluronic acid and its role within the fascia friction

HA is a non-sulfated glycosaminoglycan consisting of repeating polymeric disaccharides made up of D-glucuronic acid and N-acetyl-D-glucosamine, connected by a glucuronidic β (1→3) bond. It was named HA after its biological origin - hyaloid, and its major component, uronic acid. HA is present extracellularly in most human tissues, with over 50% found in the skin, lungs, and intestines [41]. Under physiological conditions, nearly all HA molecules exist as their salts, known as hyaluronate. The term 'hyaluronan' was introduced to include both the free acid and its salts, regardless of the degree of dissociation or the type of counterion. In the literature, the acronym HA can refer to hyaluronic acid, hyaluronate, or hyaluronan, depending on the context [42; 43].

The biological functions of HA include a wide range of critical roles. These include maintaining the viscoelasticity of liquid connective tissues, such as joint synovial fluid and the vitreous humor of the eye. HA also plays a key role in regulating tissue hydration and facilitating water transport. Additionally, it is involved in the supramolecular assembly of proteoglycans within the extracellular matrix. Beyond these structural and regulatory functions, HA participates in numerous receptor-mediated processes that influence cell detachment, mitosis, migration, tumor development and metastasis, as well as inflammation [44; 45]. Numerous studies have shown that HA can prevent tissue adhesion formation in various locations, such as subcutaneous tissue, arthritic joints, tendons, and peritoneal tissues [46-50]. Also, in preventing peritoneal tissue adhesion HA proved highly effective and did not cause any abnormal tissue responses during wound healing. Based on these findings, it was concluded that HA shows promise as a clinical injectable tissue adhesion barrier [51]. Additionally, HA induced abnormal inflammatory reactions during wound healing [51-53]. Both the *in vitro* and *in vivo* degradation experiments showed that HA was biodegradable [53]. HA has varied effects on fibroblast proliferation and migration, influenced by its molecular weight and the origin of the fibroblasts. HA promotes fibroblast proliferation [54-56] and migration [57; 58], while inhibiting the expression of α-smooth muscle actin [59]. However, some studies have found that HA can inhibit proliferation [60] or have no effect at all [59]. HA enhances wound healing by upregulating genes associated with scarless healing, such as type III collagen and TGF-β3 [55; 58]. It also modulates inflammatory responses by inhibiting the production of pro-inflammatory cytokines [61].

HA is removed from the body through a combination of local cleavage reactions and systemic elimination mechanisms involving the liver, lymphatic system, and kidneys. At the cellular level, HA is subject to non-specific degradation by free radicals as well as specific depolymerization catalysed by various enzymes [62]. The turnover rate of endogenous HA in the human body is relatively rapid, exhibiting a half-life of approximately 2 to 5 minutes in the bloodstream [63], while its half-life in tissues extends

to a few days [64]. When exogenous HA is administered at low doses, around μg/kg, its elimination mirrors that of endogenous HA, occurring swiftly. Conversely, when HA is administered at higher doses, typically in the range of mg/kg, the elimination process shifts to saturable kinetics, leading to a significantly prolonged half-life that can extend to several hours, see Tab 1.

Tab 1 Concentration and turnover of HA in different tissues. Adapted and modified from [65]

Tissue and species	Concentration of HA in		$t_{1/2}$ (days)
	tissue (μg/ml)	injectate (mg/ml)	
Vitreous body			
Rhesus monkey	100-180	10	10-20
Owl monkey	300-900	10	20-30
Rabbit	14-52	0.02	70
Joints			
Horse	300-500	10	1
Rabbit	(134)	0.3	0.5
Rabbit	3800	20	0.5
Skeletal muscle			
Rabbit	26-28*	10	1.25
Skin			
Rabbit	840*		1.9-.7
Rabbit		0.07	0.5
Rabbit		10	2

* μg/g

Because of relatively rapid degradation, the creation of biocompatible and more stable alternatives to HA holds great potential for various biomedical applications. To improve the residence stability of HA, various studies have investigated the use of crosslinkable HA systems. These include chemically modified HA combined with polyethylene glycol [66], crosslinkable HA derivatives [67; 68], and the application of stabilizers like carboxymethylcellulose [69; 70]. For instance, the study [71] describes a derivative of HA

where some carboxyl groups are converted to primary alcohols. These modified HAs, characterized by a MW greater than 400 kDa and a substitution degree exceeding 75%, as well as other forms with a MW over 1,000 kDa and about 30% substitution, has been evaluated *in vitro* on mouse fibrotic cells. The results indicated that these derivatives exhibit enhanced enzymatic stability compared to the native HA, suggesting it may degrade more slowly *in vivo*. While various derivatization methods exist, not all result in improved durability.

One of the most notable characteristics of HA solutions is high viscosity. Specific viscosity η_{sp} is the term used to describe the change in viscosity of a solution when a polymer is added to it, compared to a pure solvent. Viscosity η is a measure of a fluid's resistance to flow, and specific viscosity shows us how the presence of a polymer affects the viscosity of a solution. The intrinsic viscosity $[\eta]$ is a measure of the ability of a polymer to increase the viscosity of the solvent in which it is dissolved. This parameter is key in characterizing the properties of polymers, particularly their MW (molecular weight) and interaction with the solvent. The intrinsic viscosity is important because it is independent of concentration and provides information on the MW and structure of the polymer. The specific viscosity η_{sp} in homogenous solution at zero shear rate is a function of the concentration c and the intrinsic viscosity $[\eta]$:

$$\eta_{sp} = c[\eta] + k'(c[\eta])^2 + \frac{(k')^2}{2!}(c[\eta])^3 + \frac{(k')^3}{3!}(c[\eta])^4 \qquad (1)$$

where k' is Huggins constant. Its value is 0.4, derivated from Stokes-Einstein equation for the viscosity of a suspension of spheres. Experimental data [72] for HA in physiological saline demonstrates a significant rise in viscosity as both concentration and intrinsic viscosity increase. These findings are based on experiments conducted under low shear conditions. The study [73] showed zero-shear viscosity as a function of solution concentration for HA at three different MWs, see Fig. 4. For any given MW of HA, viscosity increases by a factor of 10 with a tenfold increase in concentration. Additionally, at a concentration of 10 mg/ml, viscosity increases by a factor of 1,000 when the MW rises from 0.35×10^6 to 1.8×10^6 Da.

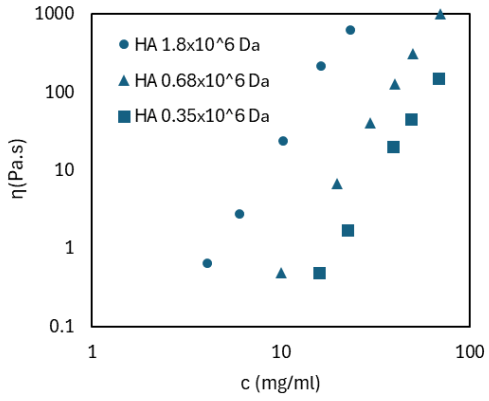

Fig. 4 Zero-rate viscosity of HA as the function of concentration. Adapted from [73]

The phenomenon described by [73] can be explained as follows. For a semi-flexible polymer like HA, each chain occupies a large volume. Most of this volume consists of water that is not bound to the polymer. While the polymer shape constantly changes, the water still contributes to the effective size of each molecule due to frictional interactions with closely spaced polymer segments. This means that the larger the polymer, the lower the average density, as the volume grows faster than the mass [74]. As the total concentration increases, the reduced probability of finding space for movement makes the effective concentration of HA greater and solutions is far from ideal. Due to its unique molecular structure and interaction with water HA exhibits viscoelastic properties and shear-thinning behavior in time.

Viscoelastic and shear-thinning behavior was widely researched. Fig. 5 from [44] illustrates an example of the curves obtained from the viscoelastic measurements. The region before the intersection (crossover point) of the two curves representing the dynamic elastic modulus G' and the dynamic viscous modulus G" of hylan (HA-based gel) is referred to as the viscous region. In this region, the input of mechanical energy deforms the dense hyaluronan molecular network at a slow rate, allowing the molecular chains to return to their original equilibrium configuration due to Brownian motion. Under these conditions, complete stress relaxation occurs, and the sample behaves as a viscous solution. Beyond the intersection, or the crossover point of the dynamic moduli curves, the rate of input of mechanical energy is too rapid for the network to relax. Consequently, the network absorbs the energy elastically, preventing stress relaxation and causing the sample to behave as an elastic solid. Due to the different mechanisms of energy dissipation in viscous flow versus temporary storage (which is eventually dissipated as heat), the elastic dynamic modulus G' is also known as the storage modulus, while the viscous modulus G" is referred to as the loss modulus. As can be seen from the Fig. 5, at a frequency of 0.01 Hz, hylan exhibits elastic behavior, while the hyaluronan solution does not exhibit elastic properties even at the highest frequencies.

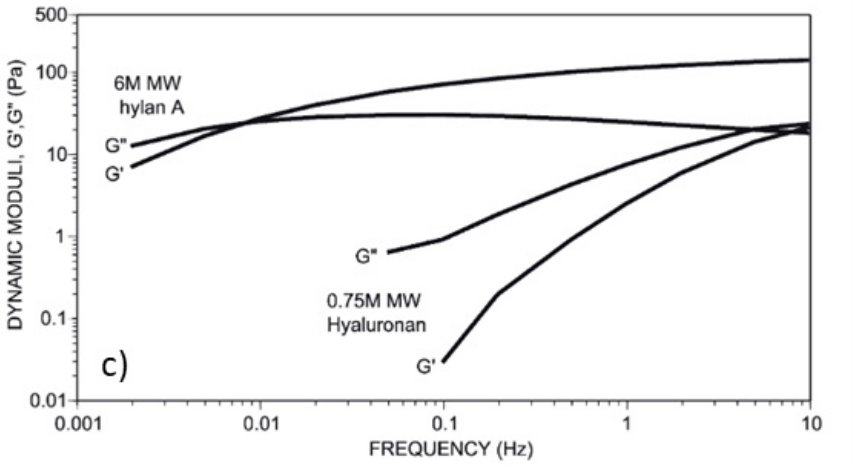

Fig. 5 The dependence of dynamic moduli (G' and G" in Pa) of HA and hylan (HA-based gel) preparation on frequency. The concentration is 10 mg/ml. MW is MW [44]

Viscoelastic properties have also been investigated in the study [75]. In steady shear tests with ranging from 0.01 to 5,000 s^{-1} and small-amplitude oscillatory shear tests, it was showed that higher MWs correspond to stronger viscoelastic properties. At a concentration of 20 mg/ml, four HAs with MWs of 77 kDa, 640 kDa, 1,060 kDa, and 2,010 kDa were measured. Only HA with a MW of 2,010 kDa, see Fig. 6, exhibited elastic behavior even at low frequencies. (Note: This means the crucial role of HA in synovial fluid for cartilage protection.) Additionally, no shear-thinning behavior was observed for the low MW HA of 77 kDa. For the remaining solutions, the viscosity decreased with increasing shear rate.

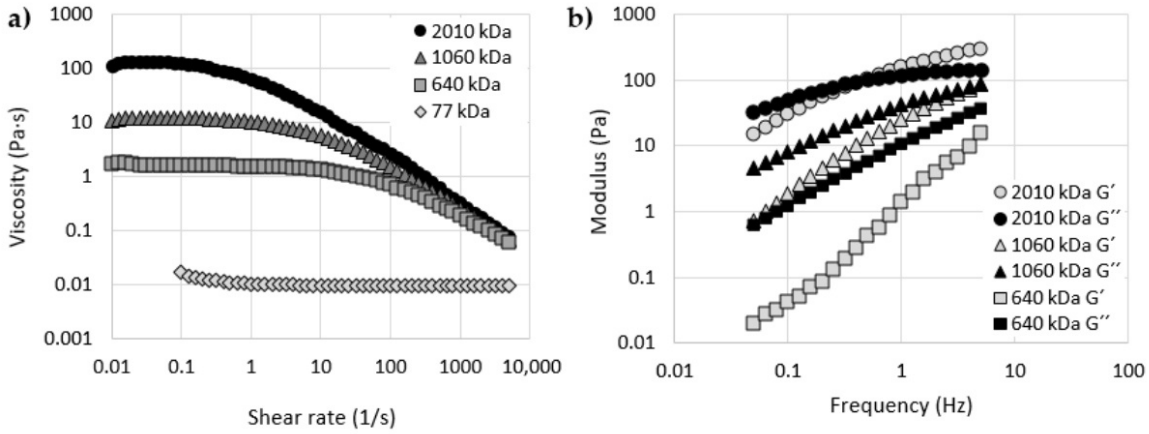

Fig. 6 Viscosity as a function of shear rate for HA solutions with different MWs; (b) Elastic (G′) and viscous (G″) moduli as a function of frequency for HA solutions with different MW [75]

2.2.1 Treatment of selected medical diagnoses focused on hyaluronic acid

HA is not yet widely used directly for the treatment of various diagnoses. It is rather widespread in the field of aesthetic medicine and cosmetics. However, a few applications exist. HA is often described as keeping our body functioning smoothly, like a well-oiled machine, provided all systems are operating correctly. In our world of rapid progress and advanced medicine, we have the means to support our bodies through both existing and potential treatments involving injected HA.

Tissue adhesion

The tendon is the closest fascia-like organ, often transitioning directly into the fascia. Tendons are implicated in “trigger finger”, where they may require transplantation. Due to increased friction, excessive wear, recurrent damage occurs. HA injections have emerged as a potential treatment for these issues. In study [76], 48 turkey feet were dissected and divided into four groups for friction testing: one control group and three groups treated with carbodiimide-derivatized HA and gelatin (cd-HA-gelatin) solutions of varying MWs. The results suggested that using lower MW gelatin in the cd-HA-gelatin formulation may

reduce tendon gliding friction, potentially minimizing adhesion formation post-surgery. In related research [77], 36 tendons from the flexor digitorum profundus in canine hind paws were studied. They were divided randomly into three groups to investigate the frictional force over 1,000 motion cycles. The researchers also examined the tendons' surfaces for remaining hyaluronic acid levels and smoothness. The study found that treating the lyophilized tendons with a mixture of cd-HA-gelatin restored the frictional force to normal levels. Moreover, modifying the tendon surfaces with cd-HA-gelatin helped counteract the negative effects of lyophilization on tendon frictional force.

Limb stiffness

Patients suffering from NSLBP often report a sensation of stiffness in their back. Study [78] focused on individuals experiencing stiffness in their upper limbs following cerebral injury. Instead of using HA, the researchers employed hyaluronidase, an enzyme that breaks down HA and disperses it within the muscle tissue. Twenty patients with stiffness in their upper limb muscles received intramuscular injections of recombinant hyaluronidase mixed with saline. Evaluations were conducted before the injections, and subsequently at 2 weeks, 4-6 weeks, and 3-5 months after treatment. The findings indicated that this treatment led to increased passive and active joint movements in patients with cerebral-origin spasticity, lasting for at least 3 months post-application.

Viscosupplementation of knee with osteoarthritis

Viscosupplementation is a medical treatment primarily used to relieve pain and improve joint function in individuals with osteoarthritis (OA), especially of the knee. This procedure involves injecting HA or its derivatives directly into the affected joint. The injected HA helps to restore the viscoelastic properties of the synovial fluid, which may be degraded due to osteoarthritis. The added HA can provide cushioning and lubrication, thereby reducing pain and discomfort during joint movement. The concept of joint viscosupplementation has been utilized for over 50 years. Despite its long history, opinions on its efficacy remain divided. A recent comprehensive review [79] summarizes the side that suggests only moderate effectiveness in reducing pain for patients with OA. This review examines results from 24 large-scale clinical studies. According to the review, viscosupplementation shows only modest results compared to a placebo, but it has a significantly higher risk of adverse effects. The review has been widely cited and adopted by many healthcare professionals, particularly general practitioners, rather than specialists such as orthopaedists. However, it is important not to take this review as definitive. A closer examination of the included studies reveals that no significant attention was given to the properties, structure, or form of the HA used in viscosupplements. As highlighted earlier in this chapter and further discussed later, these factors are crucial when considering

the use of HA. Additionally, the review does not account for the varying stages of OA progression. In contrast, another recent review [80] discusses the effectiveness of specific preparations. This review analyses systematic reviews, meta-analyses, and randomized controlled trials published in the last five years concerning substances used in viscosupplementation. It categorizes viscosupplements into native vs. crosslinked and low MW vs. high MW HA. Current treatment options include Hylan G-F 20, sodium hyaluronate (Supartz Fx, Euflexxa, Gelsyn-3, Durolane, Hyalgan), single-injection products (Gel-One, Synvisc-One, Monovisc), and hyaluronate (Orthovisc, Monovisc, Hymovis). Evidence of their effectiveness is provided for each of these products.

The mechanism why viscosupplementation has the possibility to work is hidden in the interaction of HA with collagen fibers, as described in the study [81]. The collagen fibril network in cartilage plays a crucial role in managing the distribution and movement of HA molecules. The complex, anisotropic pore matrix formed by the collagen network acts as a structural barrier, effectively trapping HA molecules within its pores. During compression, the network deforms, consolidating the pores and tightly entrapping HA, which in turn stores elastic energy. This stored energy is released during the recovery phase, facilitating the rapid reuptake of fluid and maintaining cartilage integrity.

2.3 Friction of compliant contacts

2.3.1 Biotribological models of human body parts today

The complexity of the human body is also shown in the issue of biotribology. This field of science can be categorized based on the primary focus of investigation into several groups: joint tribology, skin tribology, oral tribology, tribology of other human tissues, medical devices, animal tribology, and plant tribology. Recently, these groups have been divided so that joint tribology constitutes approximately 40%, skin tribology 20%, and oral tribology 10% of the total research [82]. The remaining portion is distributed among the other groups. To investigate how HA influences friction and lubrication, it is necessary to use the most faithful conditions and tribological model of the fascia interface.

Tab 2 Body parts models in the biotribological studies. Poly(dimethylsiloxane) mentioned as PDMS

Contact pair - origin	Model contact pair	Lubricant	Friction coefficient (-)
Tendon			
Tendon-sheat	Chicken tendon-sheat	Tendon sheat fluid	0.07~ 0.08 [83]

Tendon-sheat	Human tendon-sheat		~0.045 [84]
Tendon-sheat	Canine tendon-sheat	HA-gelatin	[77]
Tendon-sheat	Turkey tendon-sheat	HA-gelatin	[76]
Oral tissue			
Tongue-mouth	Pig tongue-pig oesophagus	Saliva	0.1~0.3 [85]
Tongue-mouth	Steel-silicone elastomer	Guar and xanthan gum, corn syrup	0.1~0.5 [86]
Tongue-mouth	Steel-PDMS	Red wine, saliva	0.2~0.6 [87]
Tongue-mouth	Pig tongue/PDMS-glass	Food emulsion	[88]
Tongue-mouth	PDMS Glass	Gelatin, agar, xanthan	[89]
Tongue-mouth	Steel- styrene rubber	Yoghurt	0.05~0.8 [90; 91]
Eye			
Eye-eyelid	Human eye-silicone rubber	Tear-like fluid	0.006~0.015 [92]
Eye-eyelid	Silicon wafer-PDMS	HA, poly(vinylpyrrolidone)	0.002~1 [93]
Eye-eyelid-lens	PDMS-PDMS	HA, eye drops	0.046~0.1 [94]
Eye-eyelid-lens	PDMS-glass	HA	0.1~0.25 [95]

Since articular cartilage is a relatively stiffer tissue compared to the fascia studied in this research, Tab 2 includes modeling methods for macular tissues such as tendon, tongue, and eye. As shown in Tab 2, both biological and engineering materials have been used to model selected contact pairs from the human body, but none reflects the fascia. While biological materials are generally considered more faithful models, they have several drawbacks, including poor repeatability, high cost, limited availability, perishability, degradation etc. Therefore, many studies prefer using engineering materials, often with one or both samples of the contact pair being compliant. Research indicates that Poly(dimethylsiloxane) (PDMS) is the most preferred elastomer for tissue modeling.

2.3.2 The compliant contact tribology

In general, friction in a lubricated contact is primarily the result of hydrodynamic and surface forces. In the hydrodynamic regime of lubrication, where the pressure from the fluid and the generated lift force are large enough to separate the lubricated surfaces, the viscous drag of the fluid is considered to be the main reason for the frictional force [96]. However, in compliant contacts, pressure from the fluid can generate viscoelastic hysteresis losses, which also contribute significantly to friction. Similarly, but even more significantly, lubricant viscosity plays a role in boundary and mixed-mode lubrication [97; 98]. In dry contact, frictional forces are due to the interference of adhesive bonds that form on contact and subsurface deformations that arise from motion and normal force. In the case of viscoelastic lubricants, both plastic deformations (fluid-viscous losses) and hysteresis losses within the compliant material are accounted for [99]. An experimental investigation [100] found the configuration of the compliant contact (soft-on-hard, hard-on-soft, soft-on-soft) affected the friction coefficient, with configurations using a soft disc resulting in higher hysteresis. However, the same configurations do not affect the friction coefficient in the full-film lubrication regime after accounting for hysteretic losses [101].

The study [102] investigated friction in a rolling-sliding, lubricated, steel ball on elastomer flat contact, and uses a novel experimental technique to measure and separate the rolling friction and sliding friction components, generating separate Stribeck curves for each, in order to identify the various mechanisms that contribute to friction in compliant contacts. It was shown that sliding friction arises primarily from two sources: asperity adhesion at low entrainment speeds and Couette flow of the lubricant film at high entrainment speeds. Rolling friction consists mainly of elastic hysteresis and Poiseuille flow of the lubricant, with an additional unexplained component emerging at high entrainment speeds. While friction due to surface adhesion, elastic hysteresis, and Poiseuille flow remains largely independent of sliding speed, friction resulting from Couette flow is directly proportional to the slide-roll ratio. Also, in the lubricated state, increased normal loads and speeds result in adhesion and deformation friction contributing equally, with each accounting for 50% of the total friction [103].

The conceptual model on Fig. 7 addressing processes in compliant contact is offered by Selway [104], building on the work of [105]. It was claimed that four viscoelastic lubrication mechanisms coexist in compliant contact. From a macroscopic perspective (I), hysteresis losses arise from bulk deformations of the elastomer initiated by normal and shear forces acting on the material surface. The properties of the lubricant do not contribute to friction directly, as it originates within the material; however, the degree of deformation is influenced by mechanisms such as adhesion, which indirectly depend on lubricant properties. From the perspective of surface asperities (II), the asymmetry of lubricant pressure between asperities generates additional hysteresis losses in the elastomer. Depending on the surface roughness peaks (III), local dewetting and film extrusion occur

from the nominal contact area. The degree of dewetting and extrusion depends on the viscosity and wettability, subsequently influencing whether the friction component associated with the material, or the lubricant will dominate. At the molecular level (IV), interfacial friction is determined by adhesive bonds between two bodies, which stretch during sliding until they break, relax, and reattach. If a lubricating film is present between the contact bodies, the viscosity of the lubricant governs this molecular movement, bringing us back to point (I).

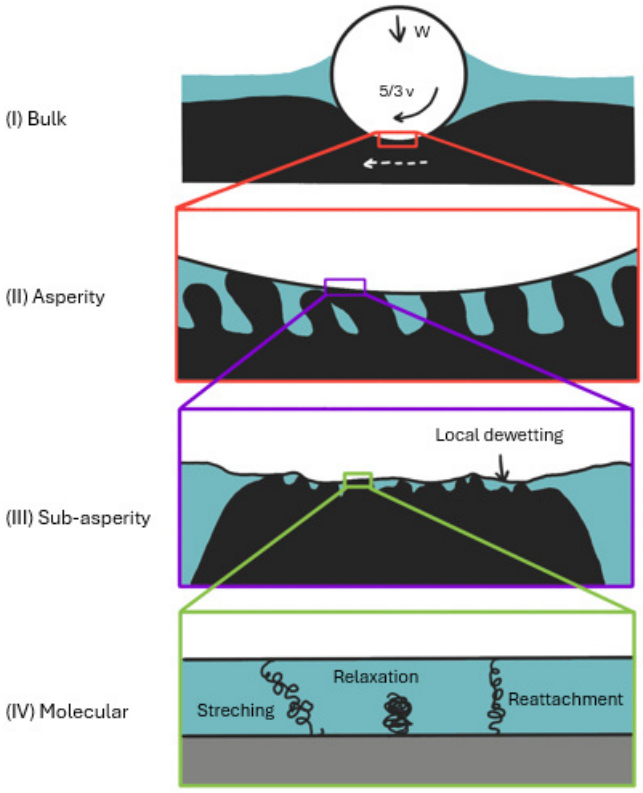

Fig. 7 A multi-scale viscoelastic conceptual model has been proposed to elucidate the effects of lubricant viscosity and static wetting on the tribological characteristics of both smooth and rough contacts. Adapted from [104].

It is also possible to look at the issue of friction of compliant contacts in a less general way, the final value of friction is dependent on several factors. The first that can be mentioned is the contact area and the hardness or stiffness of the materials under investigation. In the study [106] Ethylene-Propylene-Diene-Rubber plates with varying ShA hardness values of 40, 50, 60, and 70 were used. The plates were 2 mm thick, and the surface pressure was varied from 0 to 0.51 MPa based on cut geometry. To determine the friction and adhesion of the substrates on a macroscopic level, a "Universal Material Tester (UMT3)" system from CETR in a pin-on-disc configuration was utilized. Additionally, a tensile setup was applied to measure the friction force during linear motion, using a "Z020" tensile testing machine from Zwick/Roell. All tests were performed without lubrication. As was shown, the friction of elastomers is primarily influenced by the real contact area, especially in low-

velocity friction tests. This contact area depends on the hardness and other bulk properties of the materials, see Fig. 8. If tribological tests were conducted with equal contact areas, the friction force would likely increase with increasing hardness.

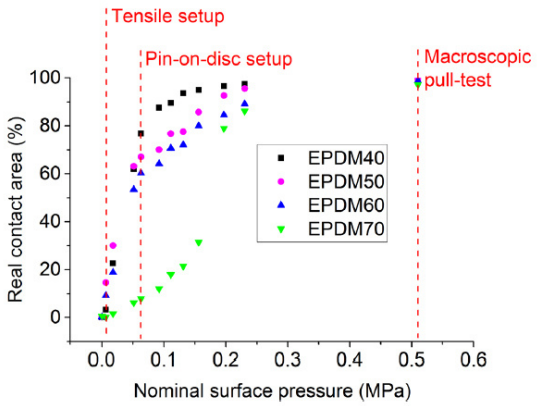

Fig. 8 Real contact area (%) dependence of growing nominal surface pressure of elastomers [106]

In study [103], three pin materials (Noryl, PTFE, and aluminum) were tested in both rolling and sliding modes under dry and lubricated conditions. The dynamic friction was analyzed by taking a subset of the stroke where the friction was relatively stable. The probe geometry has a negligible effect on the relative contributions of adhesion and deformation friction in both dry and lubricated conditions. However, the probe material impacts these contributions in the dry state. PTFE exhibits a higher proportion of deformation friction (30%) compared to aluminum and Noryl (20%). In contrast, the material does not significantly affect the relative contributions in the lubricated state. This study also found that deformation friction contributes a relatively significant proportion to total friction, especially in conditions with high normal loads and speeds, and should not be ignored.

The effect of elastomer stiffness on friction is also addressed in studies [107] and [108]. The study [107] employed a Mini Traction Machine (MTM) to measure friction in a lubricated contact between a steel ball and a polymer disc. Tests were conducted at four different applied loads (0.5, 1, 3, and 5 N), a fixed temperature of 35°C, and a constant slide-roll ratio of 50%. Friction measurements were taken over an entrainment speed range of 5-1,200 mm/s. Additionally, the viscoelastic properties of the polymer discs were assessed using dynamic mechanical analysis (DMA). The conclusion of the study showed that the elasticity of the substrates had contrasting effects on sliding and rolling friction in the isoviscous-elastic regime, with sliding friction increasing and rolling friction converging to a constant value as elastic modulus decreased.

The study [108] investigated the influence of viscoelasticity on dry and lubricated sliding friction in tribopairs, revealing that the loss modulus is a critical factor in determining

the friction coefficient. It also highlighted that the conventional Stribeck curve model fails to adequately describe the behavior of highly compliant tribopairs. To explore this, PDMS tribopairs with varying viscoelastic properties were fabricated by adjusting the weight ratios of the base to curing agent (10:1, 20:1, 30:1, 40:1). The tribopairs consisted of a PDMS hemispherical probe and flat PDMS substrates. Deionized water and glycerol, with different viscosities, were used as lubricants. Sliding friction experiments were conducted using a universal macro-tribometer, with the flat PDMS substrate moving laterally against the stationary PDMS pin under constant preloads and sliding velocities.

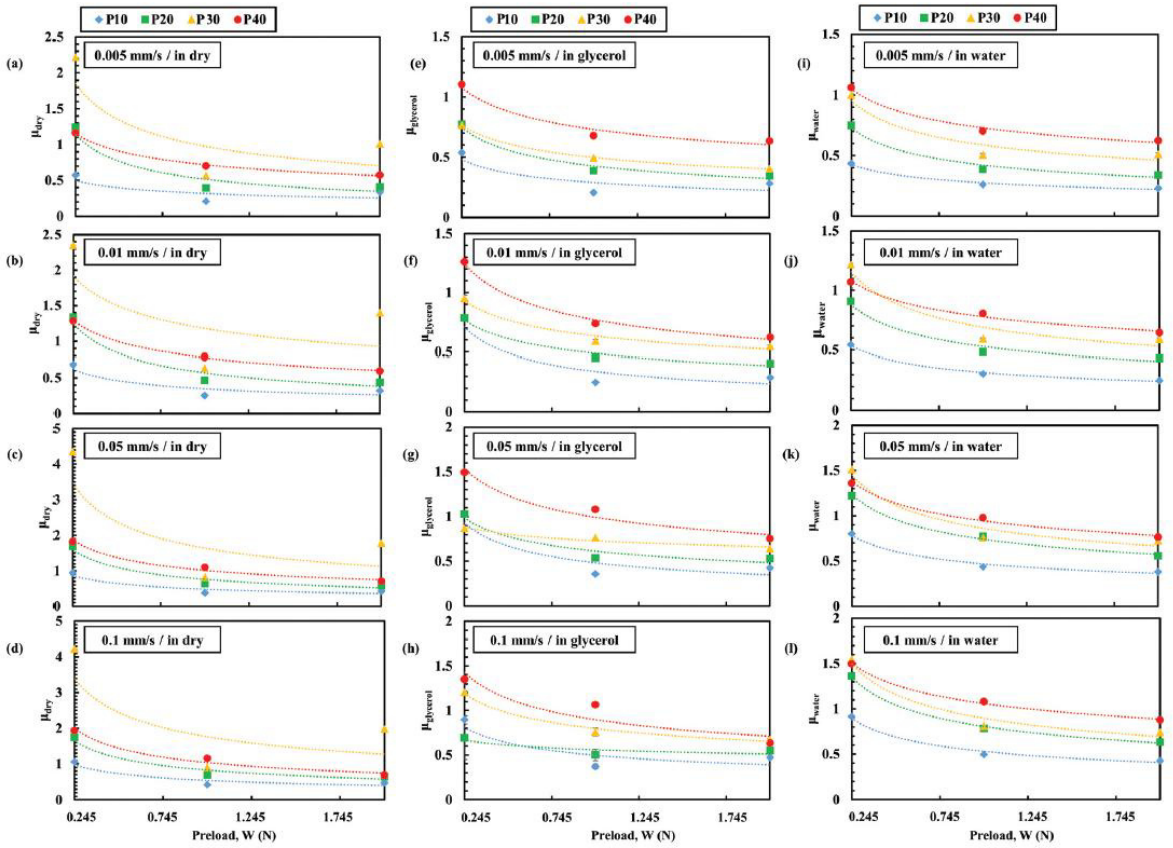

Fig. 9 Plot of the friction coefficient against the preload at each sliding velocity of dry, glycerol and water friction [108]

The viscoelastic behavior of the tribopairs, indicated by the loss modulus and loss tangent, is crucial in determining the friction coefficient in both dry and lubricated sliding contacts. In dry conditions, the influence of viscoelasticity on the friction coefficient is approximately six times greater than in lubricated conditions. For lubricated systems, the friction coefficient scales with preload similarly to the friction in the lubricant film within the Hertzian contact region, suggesting reduced interfacial adhesion between the PDMS tribopairs due to the presence of the thin lubricant film.

Another property that influences the friction of compliant contacts is material roughness and surface wettability. According to [109], rubber adhesion is influenced by three primary factors: bulk viscoelasticity, surface roughness, and the molecular mobility of uncrosslinked chains. The impact of surface roughness on adhesion varies with the rubber's stiffness. For stiffer compounds, surface roughness reduces adhesion, whereas for softer compounds, it increases adhesion. Two experimental setups were employed in the study. The first, the UF setup, utilized an acrylic ball, with the contact region observed optically to measure the contact radius over time. An optical microtribometer performed load-unload experiments between the acrylic ball and PDMS, recording force, penetration, and contact radius over time. The second, the Jülich setup, used a glass ball, measuring force and displacement without observing the contact region. The paper highlights key findings on how surface roughness, crack tip velocity, cleaning method, surface contaminants, and strain softening at the crack tip affect the work of adhesion for various elastomers, including PDMS, NBR, EPDM, GECO, and HNBR. In the study [110], PDMS elastomer surfaces were fabricated by casting between glass plates, with some surfaces roughened by sandblasting. PDMS spheres and disks were used as the tribological contact. Friction measurements were conducted using a MTM at 35°C. A normal load was applied, and the ball and disk were rotated at different speeds to create a slide-to-roll ratio. The paper concludes that surface roughness and lubricant-substrate contact angle have a large influence on the tribological properties of soft contacts, and that modeling biolubrication requires using surfaces that imitate the topography and chemistry of biological surfaces. As can be seen on Fig. 10, the friction coefficient in the boundary regime decreases with a lower contact angle of the lubricant on the PDMS substrate. For rough surfaces, the friction coefficient in the boundary regime is influenced by the entrainment speed U rather than the product of speed and viscosity U_η. Additionally, the transition from full-film to mixed lubrication regimes is primarily influenced by surface roughness [101]. Greater surface roughness shifts this transition to higher U_η values, but it does not affect the friction coefficient in the elastohydrodynamic lubrication (EHL) regime.

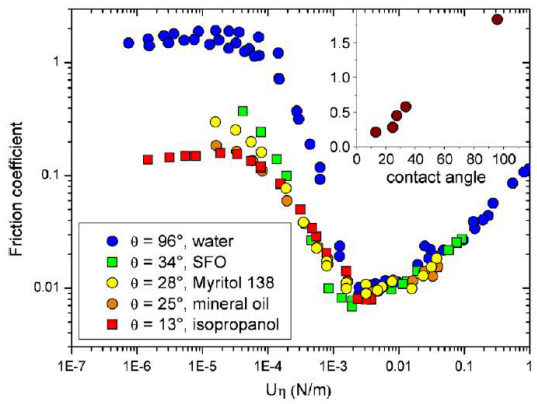

Fig. 10 Stribeck curves for a hydrophobic–hydrophobic tribopair (disk roughness = 382 nm) [110]

That viscosity and lubricant wettability have a significant effect on lubrication in viscoelastic contacts, not only on the direct contribution of viscous losses showed [104]. Four different tribo-pairs were tested: smooth PTFE ball with smooth PDMS disc, smooth PTFE ball with rough PDMS disc, smooth PDMS ball with smooth PDMS disc, and smooth PDMS ball with rough PDMS disc. The PDMS discs were fabricated by casting a two-component silicone elastomer kit, with smooth discs cast against a glass plate and rough discs cast against a sandblasted aluminium plate. Three lubricant series were evaluated: glycerol-water mixtures, glycerol-ethanol-water mixtures with 10% glycerol, and glycerol-ethanol-water mixtures with 40% glycerol. The tribological properties were characterized using a ball-on-disc tribometer, measuring friction force as a function of entrainment speed ranging from 1 to 3000 mm/s. In conclusion, in smooth contacts, lubrication is primarily influenced by fluid entrapment and molecular-scale viscoelastic effects. In contrast, in rough contacts, fluid-asperity interactions and rapid fluid drainage modify the shape of the Stribeck curve. Additionally, from [110], glycerol-water mixtures exhibit reduced friction compared to water on medium-rough hydrophilic PDMS, likely due to glycerol's preferential wetting on the hydrophilic surface.

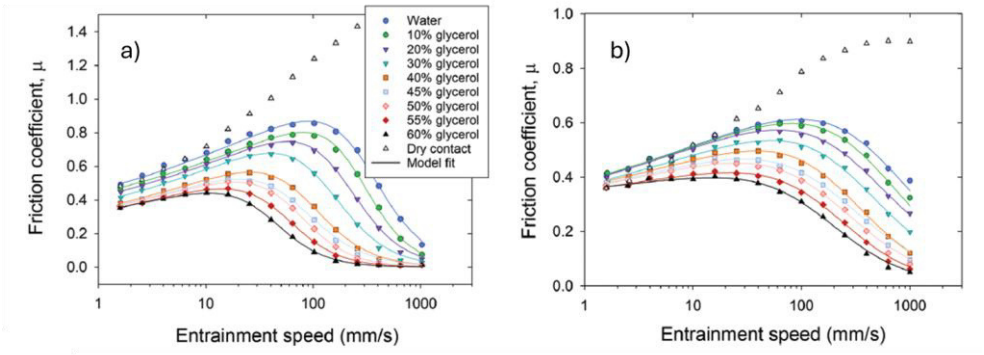

Fig. 11 The friction coefficient of PTFE ball tribological contact with (A) a smooth and (B) a rough PDMS disc [104]

Another group of what influences the friction of compliant contacts are the experimental conditions. In the study [111], a custom-built high-speed pin-on-disk microtribometer was employed to measure friction. Hydrogel samples were prepared with 7.5% NIPAM and 0.3% bisacrylamide crosslinker. One sample was a 4.5 mm thick disk, while the other was a hemispherical probe with a 2 mm radius. The probe was lowered onto the disk with a normal force of 2 mN, and the disk was rotated to induce sliding. Both normal and tangential friction forces were measured, with the sliding speed varied during the experiments. In the study [111], hydrogel-hydrogel interfaces display exceptionally low friction coefficients, approximately 0.01, at slow sliding speeds, with minimal variation up to 5 mm/s. Beyond this speed, the friction coefficient increases slightly, scaling with the square root of the sliding speed. When the hydrogels are destabilized above

the lower critical solution temperature of the polymer, the friction coefficient becomes very high and irregular, approaching levels similar to dry friction.

This state-of-the-art review is part of a study that is purely experimental in nature and does not incorporate numerical analyses. However, it is important to acknowledge that numerical studies play a crucial role in scientific research and bring insight into the theory of lubrication of compliant contacts. The study [112] proposed a numerical solution for viscoelastic half-space line contact lubrication, revealing asymmetric pressure profiles and reduced film thickness at the flow outlet, as also observed by [105], [113], and [114]. The study [105] found that in viscoelastic systems, the minimum film separation does not monotonically increase with sliding velocity across lubrication regimes, challenging the traditional Stribeck curve approach used for elastic solids. The viscoelasto-hydrodynamic lubrication regime, characterized by the coupling of fluid flow and solid hysteresis, is now recognized as distinct. The study [115] developed a point contact lubrication model, later extended by [116] and [117], showing that the compliant contacts friction is influenced by both viscous losses and viscoelastic hysteresis. Recent studies [118] and [119] further explored the compliant contact friction, including non-steady-state conditions and layered materials with imperfect bonding.

The lubrication regime between fascia involves the flow of HA as a non-Newtonian fluid, which can be modeled using Squeeze Film Lubrication theory. This theory describes the behavior of lubrication films between two surfaces, where one surface experiences pressure and tangential velocity. During manual therapies, such as sliding, vertical vibrations, and oscillations, the deformation of fascia causes a significant increase in HA fluid pressure. This pressure variation drives HA toward the edges of the manipulated fascial area, enhancing lubrication [120; 121].

3 ANALYSIS AND CONCLUSION OF LITERATURE REVIEW

3.1 Non-specific lower back pain

NSLBP is a significant and growing health issue that affects individuals and society. Identifying its exact cause is challenging. However, in some cases, NSLBP is associated with the TLF in the sacral region [11; 15; 16]. The TLF consists of three layers separated by loose connective tissue containing fascial cells that produce HA [14]. Healthy fascia glides smoothly and painlessly, aided by HA as a lubricant. An unhealthy lifestyle [20-25], often due to sedentary jobs and other factors, can lead to changes in fascia tissue, including adhesion and fibrosis [9; 12]. The body responds to these changes by producing high viscosity HA [27], which patients experience as back stiffness [28; 29]. It suggests that when HA accumulates in high concentrations within the fascia, as a result of injury or other pathological conditions, it could impair the functionality of the fascia and the tissues beneath it. Current treatments for NSLBP are often expensive, time-consuming, and frequently ineffective or provide only short-term relief [31]. Therapy [32-40] typically focuses on massages, rehabilitation, laser acupuncture, or pain relief medications that suppress symptoms rather than addressing the underlying problem.

Knowledge gap: The thickening of HA due to TLF and its pathological changes have been implicated in the onset and progression of NSLBP. Treating this pain can be challenging, often requiring time-consuming and costly interventions with uncertain outcomes. Given the increasing prevalence of NSLBP across generations and globally, there is an urgent need to address its diagnosis and seek effective therapeutic solutions.

3.2 Hyaluronic acid-based treatment

HA is a naturally occurring polysaccharide that is widely distributed in body tissues and intracellular fluids [41; 65]. Due to its biocompatibility, HA plays several crucial roles [44-61], including serving as a lubricant in the fascia. One of HA's defining features is its high viscosity, which increases with both its concentration and MW in solution [72-74]. Additionally, HA exhibits notable viscoelastic properties [44; 75], particularly at higher viscosities. HA's natural compatibility with the body, among other advantages listed in Tab 3, makes it an ideal candidate for viscosupplementation. It is also being explored for potential applications in preventing tissue adhesion following toe tendon transplantation and in treating upper extremity stiffness [76-80]. Upon injection, HA has a relatively rapid half-life [62-64], which varies depending on the dosage and application

site [65]. However, its therapeutic potential to alleviate pain has been demonstrated in knee viscosupplementation and limb stiffness treatments. Furthermore, the half-life of HA can be extended through chemical modification, enhancing its clinical efficacy [71].

Tab 3 HA advantages in medical usage [44-61]

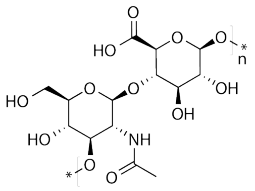

- Lubricant
- Wound healing, pro-inflammatory effect
- Easily covering of injured tissue
- Optional crosslinking, injectable ability
- Effects on proliferation and migration of fibroblast

Knowledge gap: HA serves as a lubricant within the fascia, facilitating smooth gliding and reducing pain. However, pathological changes lead to HA thickening and increased fascial adhesion. One potential treatment approach involves the application of exogenous HA via intrafascial injections directly into the fascial layers. This addition of HA with suitable properties could potentially decrease friction and alleviate tissue adhesion. Despite HA's established uses in medicine, such as viscosupplementation for joints, there are currently no products on the market specifically targeting fascial applications. Consequently, the optimal properties of HA for reducing fascial friction and adhesion remain unknown.

3.3 Thoracolumbal fascia tribological model

Biotribology addresses and simulates many situations in the human body, literally from hair to toe [82]. For its research, it mainly uses models in laboratory conditions. The models use biological samples or engineering materials. The work deals with the problem of soft tissue contacts. Commonly used models in the practice of compliant contacts are the eyelid [92-95], tendon and tendon sheath [76; 77; 83; 84] or tongue internal tissues of the oral cavity [85-91]. As mentioned, there is an attempt to use true tissues from the human body (e.g., eye from deceased) or animal models (e.g., canine tendon). However, much more use is made of technical materials, various rubbers, silicones, etc. PDMS is used in the greatest quantity.

Knowledge gap: Despite the extensive range of topics explored in biotribology and the various models employed for the studies, no research to date has specifically addressed TLF or utilized a tribological model for fascial tissues.

4 AIMS OF THE THESIS

The thesis focuses on two main objectives, which can be categorized into fundamental and applied research. The primary goal of the basic research is to develop a tribological model of the TLF, specifically targeting the experimental analysis of the friction coefficient. The applied research aims to evaluate the impact of HA-based solutions on the friction of the tribological model of the fascia.

To accomplish these main objectives, several sub-objectives need to be addressed:

- selection of technical materials to represent both muscle and fascial tissue, followed by tribological validation of their combinations, with a focus on material properties,
- assessment of the influence of geometry, loading, and kinematics on the friction of compliant contacts,
- experimental verification of friction of technical materials, compared with biological fascia,
- definition of a tribological model of the TLF,
- assessment of the influence of HA-based solutions using the developed model,
- evaluation of results, drawing conclusions, and engaging in critical discussion based on the research findings.

4.1 Scientific questions & Hypotheses

Q1: What material parameters are crucial in developing a tribological model to accurately simulate fascial tissues and reliably identify the adhesive mechanisms in pathological conditions?

H1: When developing a tribological model to accurately simulate fascial tissues and reliably identify adhesion mechanisms under pathological conditions, it is essential to incorporate specific material parameters. Mechanical properties such as elastic modulus, tensile strength, and viscoelasticity are crucial for replicating the stiffness, elasticity, and time-dependent behavior of fascial tissues. Additionally, surface properties like surface roughness and surface energy significantly influence adhesion and wetting characteristics, ensuring realistic interaction between fascial layers. An accurate representation of frictional properties, including the coefficient of friction (COF) and the behavior of HA-based lubricants, will ensure a realistic simulation of lubrication conditions. By integrating these material parameters, the model will more effectively simulate fascial tissue behavior and identify adhesion mechanisms involved in pathological conditions.

Fundamental explanations: To simulate the tribological behavior of fascial tissues and study adhesive mechanisms in pathological conditions, it is crucial to look at key material parameters into the model. These parameters are essential for understanding and predicting how these tissues interact with surfaces and lubricants under various conditions. Viscoelastic properties [97-100; 105; 106; 108] are central to this simulation, as fascial tissues exhibit both elastic and viscous responses to deformation. This dual nature affects how tissues deform and recover under load, which influences friction and adhesion. Properly modeling these viscoelastic properties ensures that the model reflects the real-time-dependent behavior of the tissues. Material stiffness and hardness [103; 107; 108] play a significant role in how fascial tissues interact with contacting surfaces. Stiffness, or the modulus of elasticity, determines the extent of deformation under applied forces. Hardness affects how much a material deforms and can impact the real contact area, thereby influencing frictional resistance. Harder materials typically deform less but might increase friction, while softer materials show different frictional characteristics. Surface roughness and wettability [101; 104; 109] are critical factors in determining the nature of friction and adhesion. Surface roughness affects the real area of contact between materials, altering frictional interactions. Wettability, or how well a lubricant spread on a surface, influences the lubricant's effectiveness in reducing friction. Smooth surfaces generally exhibit different frictional behavior compared to rough surfaces, and the interaction between the lubricant and the surface is crucial for accurate friction predictions. Lubricant properties [104] also significantly impact the tribological behavior. Key properties include viscosity, MW, and chemical composition. These properties determine how well a lubricant can separate surfaces and reduce friction. While high viscosity lubricants might reduce friction effectively in some scenarios, they could also increase resistance if not matched well with surface conditions. Adhesive bonding [103] characteristics between contacting surfaces influence both friction and wear. Strong adhesive bonds can increase friction, while weaker bonds might lead to higher wear rates. Understanding how these bonds behave under various conditions helps in predicting potential frictional behavior and failure modes. Deformation characteristics of the materials [102], whether elastic, plastic, or viscoelastic, affect how surfaces interact during sliding. Elastic deformation recovers after load removal, while plastic deformation results in permanent changes. Viscoelastic materials show time-dependent deformation, impacting friction development over time. Normal load and sliding speed [107] are additional parameters that influence friction and wear. The magnitude of the applied normal load and the sliding speed affect how materials interact and how lubricants perform. Higher loads typically increase friction and wear rates, while varying sliding speeds can alter the efficiency of lubrication and the nature of material interactions.

Incorporating these material parameters into a tribological model allows for a more accurate simulation of fascial tissues' behavior under various conditions, including pathological

states. This comprehensive approach enables better predictions of how these tissues will perform, facilitating improved design and treatment strategies in biomedical applications.

Q2: What is the mechanism of friction reduction of HA lubricated adhesive fascial tissue induced by various solution compositions?

H2: The reduction in friction in HA-lubricated fascial tissue is due to the balance between the molecular weight and concentration of the HA solution and its interaction with the collagen fibers. Lower molecular weight solutions generally offer better lubrication by reducing resistance, while the structural integration with collagen enhances the overall effectiveness in minimizing friction.

Fundamental explanations: The mechanism of friction reduction in HA-lubricated adhesive fascial tissue due to varying solution compositions involves several interrelated factors. The mechanism of friction reduction in HA-lubricated adhesive fascial tissue is primarily influenced by the interaction between the HA solution and the tissue structure, particularly the MW and concentration of the HA [72-74]. HA exhibits viscoelastic properties [44; 75] that significantly contribute to its lubricating effects. HA solutions with different MWs and concentrations impact friction differently. Higher MW HA typically results in a more viscous solution [73]. This viscosity can reduce friction by increasing the distance between the contacting surfaces, thus minimizing direct surface contact and resistance [104]. However, excessively high viscosity might lead to higher friction under certain conditions due to the dense polymer chains creating resistance [74]. Lower MW HA solutions are less viscous, which can be advantageous for lubrication [76]. The reduced viscosity allows for smoother movement by decreasing resistance. Another critical factor is the interaction between HA and the collagen fibers within fascial tissue. HA molecules can integrate with the collagen matrix [81], aiding in friction reduction. This interaction helps to minimize direct contact between surfaces and reduces frictional forces. Collagen fibers in the tissue can trap HA molecules, enhancing lubrication by providing structural support and reducing wear.

5 MATERIALS AND METHODS

5.1 Experimental equipment

5.1.1 Bruker UMT TriboLab

To conduct the tribological tests, we utilized the UMT TriboLab (Bruker, Massachusetts, USA), a versatile and advanced tribometer designed for a wide range of tribological applications. This instrument is well-suited for precisely measuring friction, wear, and lubrication properties under various conditions. The modular platform allows for easy configuration and customization of the test setup to meet specific experimental requirements. Equipped with high sensitivity sensors, the UMT TriboLab accurately measures frictional forces and wear rates. The data acquisition system captures these measurements in real-time, allowing for detailed analysis of the tribological behavior of the materials. The UMT TriboLab supports multiple testing modes, including reciprocating, rotational, block-on-ring, and ball-on-disk, among others. For this study, the reciprocating mode by lower probe, in pin-on-plate configuration, was primarily used to simulate the sliding motion typical of fascia interactions. The normal force is applied using a loading mechanism in upper probe that ensures accurate and consistent application of force during tribological testing. A highly sensitive load cell is integrated into the system to measure the applied normal force in real-time. The load cell provides feedback to the control system, ensuring that the desired normal force is accurately maintained throughout the test.

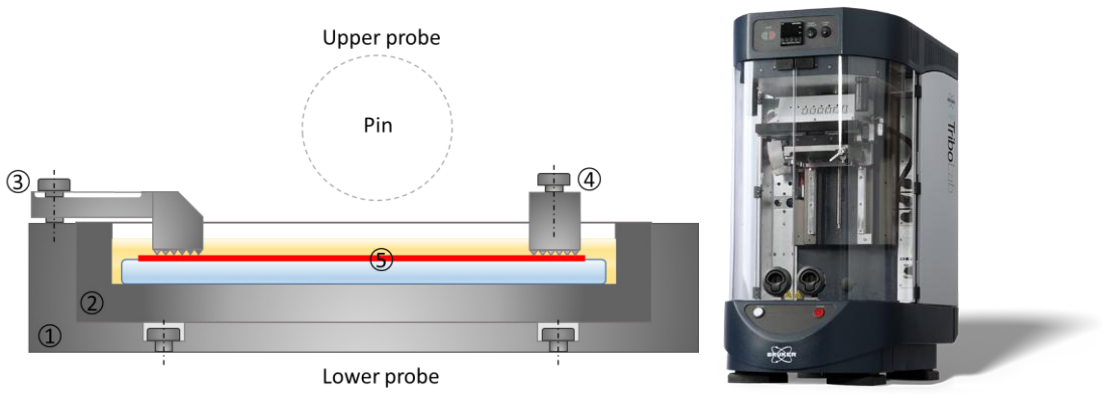

Fig. 12 Developed fascia holder for tribological testing and promo picture of UMT Tribolab from Bruker.com

For the purpose of this work, a sample adapter was constructed to attach to the lower probe used further throughout the study. As can be seen in Fig. 12, it consists of four main parts.

The outer tub (1), which is used to clamp directly to the tribometer. The inner pot (2) serves as the sample and lubricant storage (5). The samples are then firmly clamped, pre-stressed and pushed against the inner pot by means of two holders. The holder (4) is static, and the fascia is tensioned by the holder (3) by means of axial displacement after pushing. Both are fixed to the outer tub (1) by means of screws. All experimental conditions related to the UMT TriboLab device are listed in 5.3 Experimental design, according to how they were used in the different parts of the study.

5.1.2 Rheological Testing Equipment

The viscosity of the samples was measured using the Discovery HR-30 rheometer (TA Instruments, New Castle, DE, USA). This advanced rheometer is designed for precise measurement of the flow properties of materials. The experiments were conducted in cone-plate configuration at 37 °C for viscosity measurements. The experiments were carried out using a stainless-steel cone and plate geometry (40 mm diameter with a 1° cone angle). The experiments were conducted under constant shear conditions, where the viscosity of the samples was assessed across a range of shear rates from 0.01 to 3,000 s^{-1}. Prior to each measurement, all HA solution samples were allowed to stabilize for 2 minutes. The relationship between viscosity and shear rate was then analyzed, and viscosity flow curves were generated using a logarithmic scale. Each measurement was performed in triplicate using fresh samples. The zero-shear viscosity of the HA solutions was determined using the Carreau-Yasuda model through TRIOS software. Results are reported as average values, see Tab 4.

5.1.3 Scanning electron microscope

A scanning electron microscope (SEM), MIRA3 (TESCAN, Czech Republic), was employed to study the morphology of the dried material sample. The MIRA3 SEM provides high-resolution imaging, which is essential for detailed morphological studies. It offers a magnification range from 20x to 1,000,000x, enabling comprehensive analysis of microstructural features. Images were captured in secondary electron emission mode, using the DEPTH scan mode. The beam density was set to 10, and the high voltage was 10 kV. The working distance was maintained at 15 mm. Prior to imaging, the surface of the sample was coated with a 15 nm thin layer of gold using an EM ACE 600 (Leica Microsystems, Wetzlar, Germany) to enhance conductivity and image quality.

For SEM, the material sample underwent washing with ultrapure water (Type II as per ISO 3696, produced using an Elix 5 UV Water Purification System, Merck, Germany).

The specimen was then freeze-dried using an Epsilon 2-10D machine (Martin Christ, Osterode am Harz, Germany) to prepare it for electron microscopy analysis.

5.2 Experimental specimens

5.2.1 Model development

The models representing muscles and fascia were constructed using various materials, including PDMS, polyurethan (PU) gels, polyvinyl alcohol (PVA) hydrogel, and rabbit fascia. Fig. 13 lists the individual material pairs used for each model. Technical materials were carefully chosen to mimic the essential mechanical properties of fascial tissue, although the inherent complexity of biological fascia could not be fully captured. The PDMS plates used for both the pin and the base were 3.5 mm thick, while the PU gel Phantom was 8 mm thick. The interlayer materials had a thickness ranging from 0.75 to 1 mm.

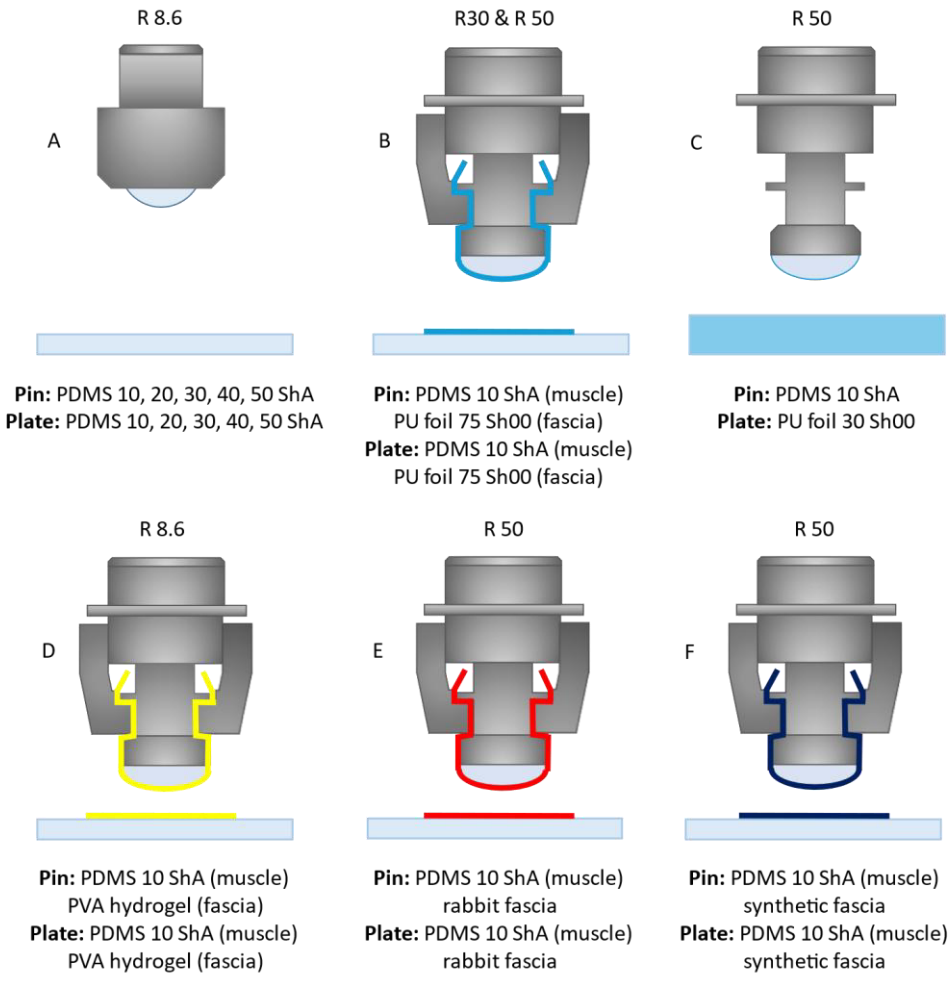

Fig. 13 Models configuration presentation

Model A: The initial model was based on a basic PDMS-PDMS with (acetoxy-PDMS, Elastosil® E43 Transparent, Wacker Chemie AG, Germany) used in many biotribology studies to simulate compliant contact. Stiffness of model varied by 10 from 10 to 50 ShA. Pin was made of PDMS sphere with radius of 8.6 mm. Plate made of the same material and stiffness was 70 mm length, 35 mm wide and 3.5 mm thick.

Model B: This model consisted of PDMS-PDMS 10 ShA (acetoxy-PDMS, Elastosil® E43 Transparent, Wacker Chemie AG, Germany), with a surface roughness (Ra) of 1.08 µm and a tensile strength of 3000 kPa. Interlayers of PU gel 75 Sh00 Phantom (BTG Standard 75, Technogel®, Germany) with Ra = 211.2 nm and tensile strength greater than 800 kPa were included to mimic the fascia layers on muscle tissue. This model aimed to replicate the actual state of the human body, where fascia acts as a membrane over muscles or adipose tissue. Redesigned pin with a linear contact and a radius of 30 and 50 mm was used.

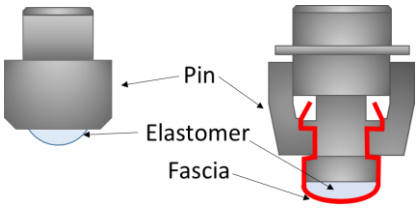

Fig. 14 Redesigned pin from point contact to linear contact with R30 and R50. Fascia is prestressed over the glued PDMS and hold with two rough holders avoiding slipping on the sides

Model C: This model featured a PDMS 10 ShA pin and a PU gel plate labelled Phantom (BTG S 130 AX, Technogel®, Germany) with 30 Sh00 stiffness, Ra = 1.1 µm, and a tensile strength of 60-70 kPa. This setup was designed to more accurately mimic muscle tissue due to the higher compliance of the PU gel compared to PDMS. The pin was radius of 50 mm to maintain linear contact.

Model D: Returning to a PDMS-PDMS configuration, this model incorporated interlayers of PVA hydrogel with Ra = 793.42 nm, chosen for its hydrophilic surface properties.

PVA hydrogel preparation: To prepare the 15 wt% PVA solution, a systematic approach was followed to secure uniform mixing and proper handling of the hydrogel material. Pure water (127.5 g) was measured and added to a glass jar equipped with a stir disc. Using a magnetic stirrer set to 500 rpm, the water was stirred continuously while gradually adding PVA powder (22.5 g) over a period of approximately two minutes. This initial mixing phase lasted for 10 minutes to achieve complete dissolution of the PVA powder. Subsequently,

the glass jar containing the PVA solution was placed in a large glass beaker filled with approximately 300 ml of water. The water bath was heated using a magnetic stirrer with controlled heating, maintaining a temperature range of 150°C to 160°C. Throughout this heating process, a plastic lid was loosely placed on the jar to prevent excessive evaporation and maintain the integrity of the solution. As the solution heated, the stirring speed was gradually reduced from 500 rpm to 80–100 rpm over a period of 10 minutes. This gradual reduction in stirring speed ensured that the PVA solution was heated uniformly without causing rapid evaporation or overheating. Once the heating phase was completed, the glass jar was carefully removed from the hot water bath and placed on a normal stirrer set at 250 rpm. Over the next 10 minutes, the stirring speed was gradually decreased from 250 rpm to 80–100 rpm as the solution cooled down. The final mixing continued until all bubbles disappeared and the PVA solution appeared clear, indicating thorough homogenization.

Following this, the plastic lid was removed, and any surface crust that had formed on the solution was gently removed. Using a syringe or pipette, the clear PVA solution was transferred into molds prepared for casting the hydrogel. Special care was taken to remove any residual bubbles from the solution using the pipette, ensuring the final hydrogel would be clear and bubble-free. After filling the molds, excess hydrogel was pressed out by firmly placing the top part of the mold. The molds were then tightly wrapped first with stretch foil and then with newspapers to protect them during the setting process. Finally, the wrapped molds containing the PVA hydrogel were placed in a temperature chamber set to cycle between -20°C (for 8 hours) and 4°C (for 16 hours) over a period of four days. This controlled temperature cycling helped to secure proper curing and solidification of the PVA hydrogel. This methodical approach secured the preparation of white, homogeneous PVA hydrogel suitable for subsequent experimental use.

Model E: The reference model and the most realistic one, consisted of PDMS-PDMS with interlayers of rabbit fascia, which has a tensile strength of 21±4 MPa. Mechanical properties of the fascia were measured in by Contipro, a.s. in [122]. The surface roughness of the fascia could not be determined under laboratory conditions. The advantage of using rabbit fascia over porcine fascia is the presence of an additional muscle (musculus panniculus carnosus) beneath the skin and adipose tissue, allowing the fascia to be removed without deterioration.

Rabbit fascia preparation: Sexually mature New Zealand white rabbits weighing at least 3 kg were used to prepare dorsal fascia samples for tribological testing. The rabbits underwent sedation with subcutaneous medetomidine (0.3 mg/kg; Domitor inj., Orion Corporation, Espoo, Finland) followed by induction of general anesthesia with intramuscular ketamine (25 mg/kg; Narkamon inj., Bioveta, Ivanovice na Hane, Czech Republic). After stunning with a captive bolt gun, the rabbits were euthanized by transecting the carotid artery

(arteria carotis communis). Following skin removal, a paravertebral incision was made to release the dorsal fascia from the spine, see Fig. 15. The fascia was then dissected bluntly from the back muscle extending up to the latissimus dorsi, tensor fasciae latae, and external oblique abdominis muscles. The collected fascia was immersed in Hanks balanced salt solution and transported to the laboratory at 4°C to maintain tissue viability. After 16 hours, the chilled fascia was removed from the transport solution and placed in a sterilized Petri dish to prevent dehydration. A section of the fascia was then spread on a glass plate and a test sample approximately 60×20 mm was cut out using dissecting scissors. This prepared sample was subsequently fixed to the tribometer for testing.

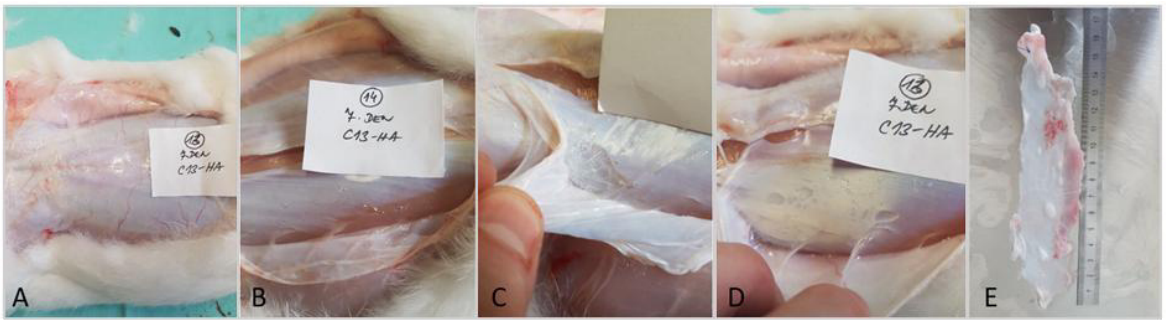

Fig. 15 Dorsal rabbit fascia preparation

Model F: An alternative two-layer model utilized commercially available synthetic fascia. This model featured a 1 mm thick replacement fascia composed of multiple layers of fibers obtained from SynDaver^{TM}, USA (Fiber Fascia, SKU: 141620), designed mainly for medical device testing and surgical training purposes. The synthetic fascia underwent pre-preparation and storage as per the manufacturer's guidelines. One drawback of this model is its relatively high cost.

5.2.2 Lubricants

Native HA with MW of 101, 316, 610 and 2000 kDa and HA derivatives (reduced HA (HA RED and lauroyl modified HA-C12)) provided by Contipro, a.s. (Dolní Dobrouč, Czech Republic) were dissolved in PBS and sterilized by filtration. Concentrations and measured viscosity of tested solutions are summarized in Tab 4. In the initial phase of the experiments, low viscosity mineral oil was used as a reference fluid having the dynamic viscosity of 0.105 Pa.s.

Tab 4 HA-based lubricants

Designation	MW (kDa)	Degree of substitution (%)	Concentration (mg/ml)	Viscosity (mPa.s, 37 °C)
-	2,000	-	10	2,348
-	610	-	20	1,191
-	316	-	20	2,02
-	101	-	20	27
-	316	-	10	59
HA-COOH5	275	18	20	122
HA-C12	318	9.1	3	37

5.3 Experimental design

5.3.1 The influence of material hardness and motion speed on fascia model friction (Study I)

As fascia is an organ that facilitates movement by its layers sliding over each other, it was necessary to investigate the effect of movement speed on friction in our model. Based on the frequency of common daily activities, which is less than 5 Hz in 90% of cases [123; 124], a test interval of 1 - 5 Hz velocity with a step of 1 Hz and an amplitude of 12 mm was determined. In addition to investigating the effect of movement velocity on fascial friction, it was necessary to investigate the effect of material stiffness. Pathological changes in the fascia cause changes in the structure, density and mechanical properties of the fascial tissue. These changes were simulated using model A - PDMS with stiffness ranging from 10 to 50 ShA, as is common in many biotribological studies dealing with compliant contacts. The pathological changes trigger the nervous system to signal the overproduction of high MW HA. Therefore, in the initial study, high viscosity HA of 2000 kDa with a concentration of 10 mg/ml was used as a lubricant. As a reference fluid, a low viscosity mineral oil (LVO) was chosen. The detailed experimental conditions, materials and lubricants used are given in Tab 5.

Contact pressure is a crucial parameter related to the material's hardness. To determine its value, we used the Finite Element Method (FEM). A non-linear analysis allowing for large deflections was conducted using Ansys Workbench. The contact type between the simulated bodies was set as frictional. A normal force of 1 N was applied to the pin,

matching the experimental conditions. The materials modelled included rubber and silicone (VMQ), with a tensile yield strength of 8.97 MPa and a density of $1.12e^{-06}$ kg/mm³. Further FEM analysis of contact pressure was not conducted due to the lack of tensile tests required for a comprehensive analysis.

5.3.2 Hyaluronic acid properties scale estimation (Study II)

In the second part of the study, the tribology tests were measured to compare friction properties of high MW (HMW) of 2,000 kDa and 10 mg/ml concentration and low MW (LMW) of 316 kDa with the same concentration, on model B, see Fig. 13. Experimental conditions could be seen in Tab 5.

Tab 5 Experimental conditions used in experiments

Study	Test time	Normal force	Frequency of the reciprocal motion	Path	Repetitions
I.	300 s	1 N	1-5 Hz	± 12 mm	3x
II.	300 s	2 N	1 Hz	± 16 mm	5x
III.	300, 3000 s	2 N	1 Hz	± 16 mm	3x, 5x
IV.	300 s	2 N	1 Hz	± 16 mm	5x

5.3.3 Tribological model development (Study III)

In the following part of the study, two phenomena were examined: the impact of the contact pair geometry and the friction within different fascia models. Detailed descriptions of the specific models are shown in Fig. 13. The experimental conditions for both phenomena under investigation are displayed in Tab 5. The selected models were designed to closely approximate real fascia-fascia contact. Initially, a top layer was added to the base material to mimic how fascia is situated in the body. In our body, muscle is followed by a fascia layer, then another fascia layer, and finally muscle or fat. Since actual fascia contact is more like a plate-on-plate configuration rather than pin-on-plate, pins with radii of 8.6 mm, 30 mm, and 50 mm were used on the most rigid model A and the most compliant model C. With these three pins, point contact R8.6 and linear contact R30 and R50, and two

models, the effect of pin geometry was studied. Additionally, the study focused on testing elastomers more compliant than PDMS, such as PU gel Phantom and PVA hydrogel, to better simulate the mechanical properties of fascia. Finally, real rabbit fascia was incorporated into the model to further enhance its realism.

As previously mentioned, fascia-fascia contact in the human body is naturally lubricated by HA. In this study, native HA as the lubricant to replicate this natural mechanism was utilized. To thoroughly investigate the effects, HA with two different MWs: 316 kDa and 610 kDa was used. For the 316 kDa HA, a concentration of 10 mg/ml was employed, while for the 610 kDa HA, a higher concentration of 20 mg/ml was used. These specific concentrations and MWs were chosen to observe how different formulations impact the frictional properties of fascia models.

5.3.4 Hyaluronic acid frictional properties (Study III and Study IV)

The previous part, which extended into the investigation of HA's frictional properties affecting fascia behavior, utilized a developed rabbit model labelled model E. In addition, to the rabbit model, this section introduces model F with synthetic fascia. Both models were also tested with four native HAs (610 kDa, 316 kDa, 101 kDa of 20 mg/ml and 316 kDa of 10 mg/ml). Furthermore, two HA derivatives from Tab 4 were included to determine if native HA can be fully replaced by a derivative while maintaining the same frictional properties, non-toxicity, and with an expected slower *in vivo* degradation. The experimental conditions remain consistent with the model development short tests, see Tab 5. To examine the stability of HA as a lubricant over an extended period, experiments were conducted for a duration of 300 and 3,000 s. Since *in vivo* degradation could not be assessed with tribological assays, this phase of the experiment was complemented by a pharmacological study with HA of 316 kDa, 10 mg/ml and HA-COOH5. Lubricants were selected based on their friction-reducing effects and frictional stability over time. To increase the clarity of the methods section, most of the chapter has been graphically represented on Fig. 16 and Fig. 17.

5.3.5 Statistical methods

Unless otherwise noted, the results were expressed as the mean of three/five measurements ± standard deviation (SD). Statistical significance was evaluated using one-way or two-way ANOVA, followed by Tukey's or Bonferroni's multiple comparisons tests, with individual variances calculated for each comparison. Statistical significance was denoted as *$P < 0.05$, **$P < 0.01$, ***$P < 0.001$, and ****$P < 0.0001$.

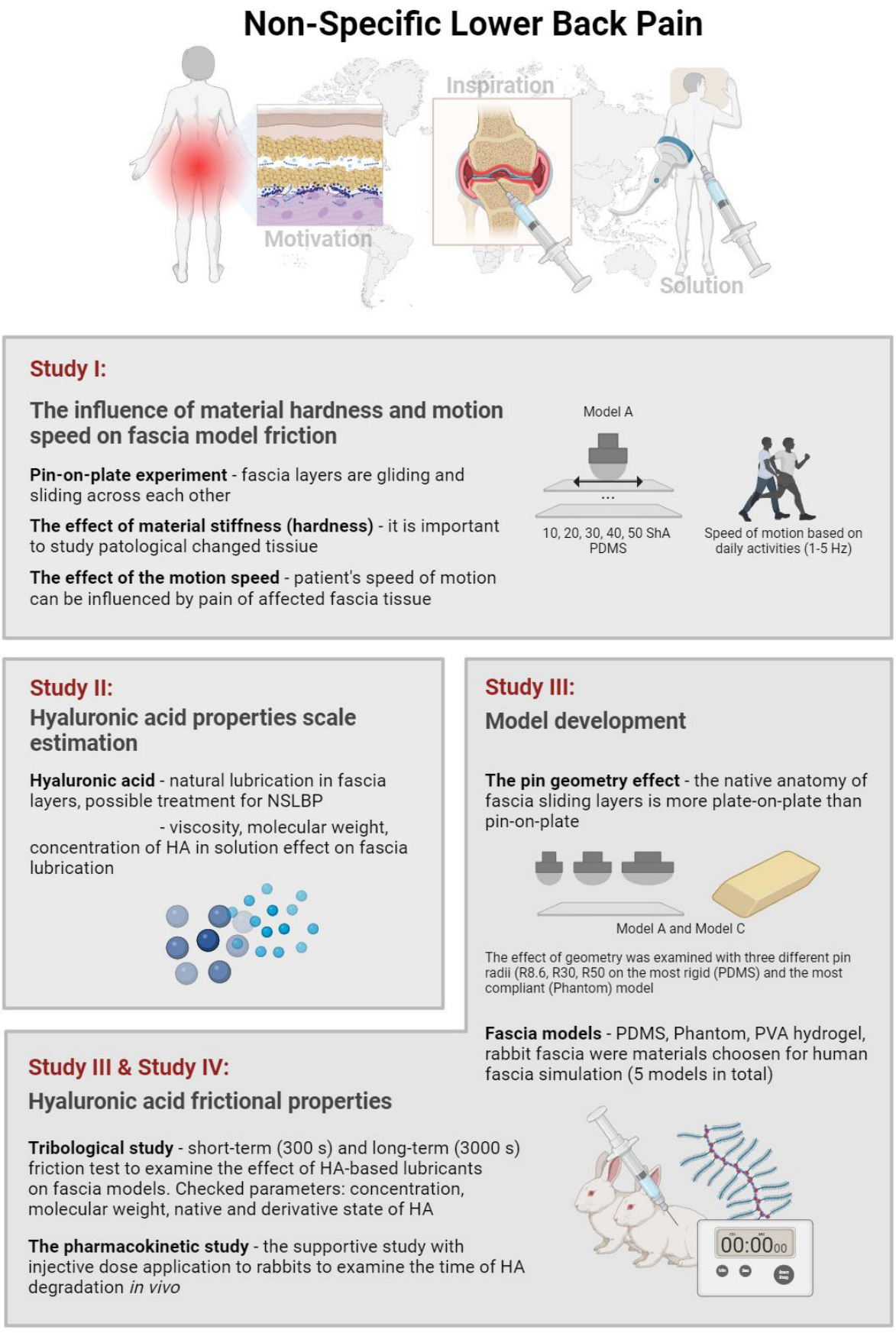

Fig. 16 Graphical illustration of issues examined in the study. Created with Biorender.com

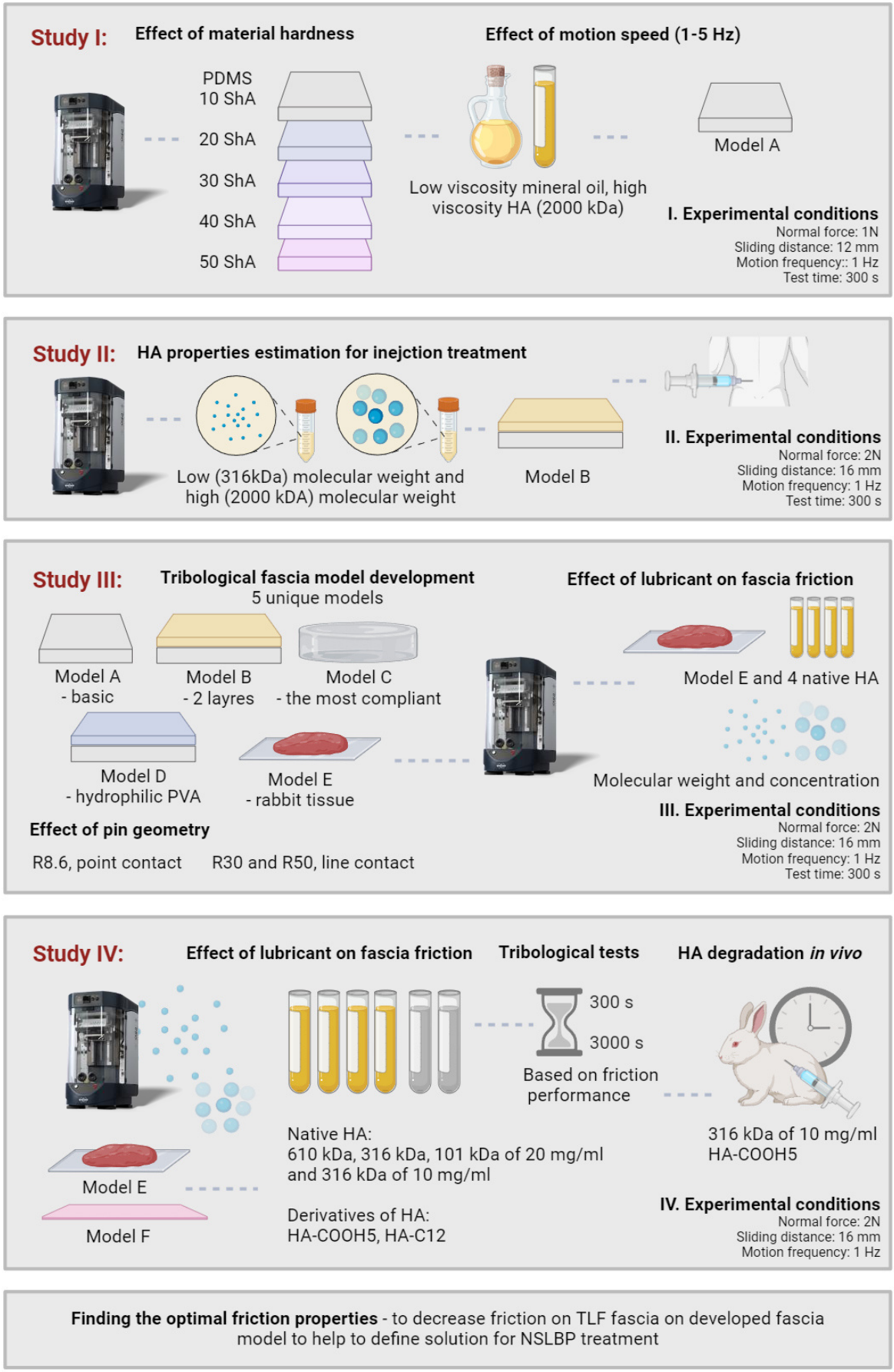

Fig. 17 Graphical illustration of methods used in different parts of the study. Created with Biorender.com

5.4 Thesis layout

First Publication [I.]: This preliminary study focuses on the behavior of compliant contacts with five levels of stiffness. It investigates the effects of changes in the speed of reciprocating linear motion on frictional responses of materials. By analysing the COF, the study examines the sensitivity of materials to these input conditions when lubricated with high and low viscosity lubricants. Thus, the first publication is important to answer the first scientific question Q1 and test the first hypothesis H1.

STREĎANSKÁ, A., D. NEČAS, M. VRBKA, I. KŘUPKA, M. HARTL, E. TOROPITSYN, J. HUSBY. Development of Tribological Model of Human Fascia: The Influence of Material Hardness and Motion Speed. *Biotribology*, Volume 30, 2022, ISSN 2352-5738.

DOI: 10.1016/j.biotri.2022.100209. [CiteScore – 3.9]

(Author's contribution 53%)

Second Publication [II.]: Developed concurrently with the third publication, this study uses one of the initial models and geometries to explore the effects of fundamental properties of two native HA-based solutions, specifically low and high MW, on friction. This multidisciplinary study provides a comprehensive view of the optimal range of MWs for HA applications. Results from friction tests, rheology, and extrusion force of HA through a needle helped in selecting property combinations for the next phase of the study published in [III.].

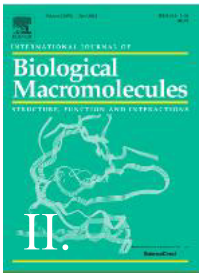

NEŠPOROVÁ, K., J. MATONOHOVÁ, J. HUSBY, E. TOROPITSYN, L. DIVOKÁ STUPECKÁ, A. HUSBY, T. SUCHÁNKOVÁ KLEPLOVÁ, A. STREĎANSKÁ, M. ŠIMEK, D. NEČAS, M. VRBKA, R. SCHLEIP, V. VELEBNÝ. Injecting hyaluronan in the thoracolumbar fascia: A model study. *International Journal of Biological Macromolecules*, Volume 253, Part 3, 2023. ISSN 0141-8130.

DOI: 10.1016/j.ijbiomac.2023.126879. [IF = 7,7]

(Author's contribution 20%)

Third Publication [III.]: This paper presents the development of more advanced models and tests mainly the hypothesis H1 from the first research question. It examines the impact of three designed geometries on the COF for materials with stiffness levels on the ShA and much more compliant Sh00 scales. The study introduces five tribological models of fascia consisting of four technical materials and one biological tissue, with varying stiffness,

roughness, and wettability. Moreover, building on the results from the second publication, this the publication examines the impact of concentration and MW of four native HA-based solutions on friction in a model with biological fascia. Thus, both the second [II.] and third [III.] publications partially address hypotheses H1, H2 from the first and second research questions.

STREĎANSKÁ, A., D. NEČAS, M. VRBKA, J. SUCHÁNEK, J. MATONOHOVÁ, E. TOROPITSYN, M. HARTL, I. KŘUPKA, K. NEŠPOROVÁ. Understanding frictional behavior in fascia tissues through tribological modeling and material substitution, Journal of the Mechanical Behavior of Biomedical Materials, Volume 155, 2024, 106566, ISSN 1751-6161.

DOI: 10.1016/j.jmbbm.2024.106566. [IF = 3,3]

(Author's contribution 47%)

Fourth Publication [IV.]: Building on the previous studies, this study uses a biological model and introduces an additional synthetic fascia model. Utilizing the same geometry and experimental conditions as in the third publication, it further investigates the second hypothesis H2 on the full substitutability of native HA with its derivative, assuming equal or better frictional properties, biocompatibility, and improved *in vivo* stability. The *in vivo* stability was examined as part of an accompanying pharmacokinetic study.

STREĎANSKÁ, A., M. ŠIMEK, J. MATONOHOVÁ, D. NEČAS, M. VRBKA, J. SUCHÁNEK, V. PAVLIŇÁKOVÁ, L. VOJTOVÁ, M. HARTL, I. KŘUPKA, K. NEŠPOROVÁ. Optimizing Hyaluronan-Based Lubricants for Treating Thoracolumbar Fascia Pathologies: Insights from Tribological and Pharmacokinetic Studies, Lubricants 2025, 13, 184.

DOI: 10.3390/lubricants13040184. [IF = 3,1]

(Author's contribution 35%)

6 RESULTS AND DISCUSSION

The following section presents a summary of the most important results. The first part is divided into four subsections according to the main research papers. The second part consists of full versions of research papers in which the results are discussed in detail.

6.1 First publication [I.]

The first research paper is a preliminary study. The experiments were conducted on a basic model, referred to as Model A, consisting of a PDMS plate and a point contact pin made from the same material. PDMS was chosen for its common use in biotribological models across various studies. The key findings of the paper are related to experimental conditions and material stiffness of PDMS on ShA scale on friction. The experiment with variable sliding velocities reveals that motion speed influences the COF in a model simulating fascial tissue interactions. Fascia's sliding potential decreases in patients with NSLBP due to adhesion. Experiments were conducted at frequencies between 1 and 5 Hz, reflecting the typical range of daily activities. Results show that both lubricants exhibit a slight increase in friction with increasing speed, likely due to the viscoelastic properties of PDMS with a hardness of 10 ShA. The COF values converge at lower speeds, indicating minimal boundary film formation due to insufficient hydrodynamic separation. These findings highlight the importance of motion speed in assessing the frictional properties of lubricated fascial tissues. Mechanical properties, particularly the stiffness of fascia, vary with pathological changes and many other factors. Increased loose connective tissue in fascia layers, described as densification (adhesion), suggests altered tissue's viscosity. The study shows no correlation between the sliding COF for HA and LVO lubricants. HA lubrication showed no significant stiffness (hardness) effect, whereas oil lubrication doubled the COF from the softest to hardest PDMS, peaking at PDMS 40 ShA. The sliding speed was set to 12 mm/s, indicating a boundary lubrication regime, confirmed for HA-lubricated samples. While PDMS roughness was consistent, LVO exhibited better lubricating properties at the lowest speed due to its low viscosity and weak boundary film formation.

6.2 Second publication [II.]

The second research paper is a multidisciplinary publication with a tribological part measured on model B. The tribological experiments, designed to mimic realistic fascia motion, were carried out a pin-on-plate configuration. This setup reflected the sliding planes of deep fascia. The study measured the COF for HMW and LMW HA solutions, both at a 10 mg/ml concentration. The results demonstrated that LMW HA had a lower COF

(around 0.031) compared to HMW HA (around 0.044), indicating better lubrication properties for fascia tissue. Unlike HMW HA, which can increase friction due to higher viscosity, LMW HA showed a positive impact on friction reduction. The reference fluid (PBS) exhibited a significantly higher COF, with stable but higher friction curves throughout the test. These findings highlight the importance of HA MW in optimizing lubrication for fascia-like tissues. Based on the findings, it is recommended to use HA-based solutions with lower MWs for further testing.

Overall, in this study, it was demonstrated for the first time that deep aponeurotic fascia can be injected with hyaluronan under ultrasound guidance. A novel combination of molecular biology techniques and an analysis of the mechanical properties of both the TLF and the HA solution established that the specific properties of HA are crucial for intrafascial application. The injection of HA into connective tissue was found to be safe, though the efficacy of this treatment for low back pain of myofascial origin remains to be tested in a clinical setting. The intrafascial injection was performed on a rabbit cadaver, which served as a suitable model for this proof-of-concept study. The characterization of the rabbit TLF composition established it as an alternative animal model for fascia research and treatment development, and for biotribological model.

6.3 Third publication [III.]

The effect of pin radius was investigated in the third study using two models: model A and model C. Each model was tested with pin radii ranging from 8.6 mm to 50 mm, while maintaining a constant applied normal load. The results revealed a significant correlation between the COF and pin radius. In model A, increasing the pin radius from 8.6 mm to 50 mm resulted in a 22% reduction in friction, though the COF remained stable between radii of 30 mm and 50 mm. In model C, a 36% reduction in friction was observed, with a more pronounced drop between radii of 30 mm and 50 mm. The friction curves in model C showed more fluctuation compared to model A. Model A displayed consistent adhesion patterns and friction curves. This model's results showed that increasing contact area reduces friction. Conversely, model C, selected for its relevance to lower back conditions, exhibited rapid changes in frictional force and asymmetrical deformation phases. This behavior reflects the viscoelastic nature of the material, which causes hysteresis and varying frictional resistance during different motion directions. The study highlights that material stiffness significantly influences friction behavior and adhesion more than contact area alone. These findings underscore the importance of considering pin shape, material properties, and normal force to accurately simulate real-life contact conditions and enhance mechanical system performance.

In the second phase of the study, Model A was re-evaluated using 316 kDa 10 mg/ml and 610 kDa, with dynamic friction assessed across different models. Model B, featuring a PU

gel layer with 75 Sh00 hardness, showed a COF decrease from 0.050 to 0.045 (316 kDa 10 mg/ml) and from 0.115 to 0.058 (610 kDa), indicating improved stability. Model C, using a PU gel with 30 Sh00 hardness, exhibited significantly higher friction for both lubricants. Model D, with PVA hydrogel for the fascia and PDMS for the muscle, had lower COF values of 0.019 (316 kDa 10 mg/ml) and 0.034 (610 kDa). Model E, incorporating rabbit fascia and PDMS, showed COF values of 0.029 (316 kDa 10 mg/ml) and 0.056 (610 kDa). Significant differences were found between Model B and Model E for 316 kDa 10 mg/ml and between Model D and Model E for 610 kDa. Friction forces were generally higher for 610 kDa, with fluctuations observed in models B, D, and E. The study aimed to develop a tribological model for fascia. Due to limited biological samples, elastomers were used as substitutes. Results showed that softer elastomers with lower elastic modulus had higher adhesion and friction. Viscous materials caused greater frictional oscillations. The friction was influenced by material stiffness, adhesion, and roughness, with a decrease in adhesive friction compared to hysteretic friction. Wettability influenced friction behavior. PDMS/PU gel and PDMS/PVA hydrogel models had friction values closest to rabbit fascia. PU gel's contact angle was similar to fascia for 610 kDa, and hydrogel matched with 316 kDa 10 mg/ml, indicating the importance of wettability. Models B and D are promising alternatives for real fascia, with PU gel better for high-viscosity lubricants and PVA hydrogel for low-viscosity ones. Model C's performance is attributed to its low rigidity and high deformation.

The third part of this study investigated the influence of MW and concentration of HA on the friction of the rabbit fascia model. The setup included a PDMS base-muscle layer with a rabbit fascia layer on top. Four HA solutions varying in MW (101 to 610 kDa) and concentrations (10 mg/ml and 20 mg/ml) were tested. The results revealed that friction values were highest (COF = 0.056) with 610 kDa at 20 mg/ml (η = 1191.47 mPa s) and lowest (COF = 0.026) with 101 kDa at the same concentration (η = 27.4923 mPa s). Additionally, HA 316 (η = 202.94 mPa s) showed a higher COF (0.040) than 316 kDa at 10 mg/ml (η = 59.72 mPa s) with a COF of 0.029. Overall, friction increased with both the MW and concentration of HA in the solution. Friction curves for 101 kDa displayed some fluctuation but remained consistent over time, while other lubricants showed a slight increase in friction over time. This study utilized a rabbit fascia model to explore the impact of HA solution properties on friction. HA is known to reduce friction in biological tissues, but its efficacy depends on its MW and concentration. In human physiology, the MW of HA varies, with higher weights typically found in synovial fluid and lower weights in rheumatoid conditions. The study found that higher viscosity HA solutions, which correspond to higher MWs and concentrations, resulted in increased friction. This is due to the densely packed polymer chains in the solution, restricting movement and increasing friction under low sliding motion and applied load. Specifically, high MW 610 kDa demonstrated higher friction compared to lower viscosity HA lubricants. These findings suggest that focusing solely on high viscosity HA solutions may not be practical for reducing friction in fascia. The primary aim was to develop a tribological model to identify ideal HA properties

for medical viscosupplements targeting low back pain, considering that HA can enhance the smooth interaction between tissue surfaces.

6.4 Fourth publication [IV.]

The beginning of fourth study investigated the effect of material preload on friction using jaw prestressing in tribological testing. Initial experiments focused on 316 kDa HA lubricant due to its medium MW and common usage. Results indicated that prestressed level had minimal impact on rabbit fascia friction. Prestressing had a more pronounced effect on synthetic fascia, with friction increasing from COF 0.0517 and 0.04931 to 0.6275 under strong prestress. Based on these findings, subsequent tribological tests were conducted on a middle-prestressed fascia. The study explored how material stretching affects fascia friction, recognizing that fascia naturally undergoes stress during muscle movement. Fascia is composed of three connective tissue sublayers with distinct densities and orientations, with collagen fibers providing resistance to tension and stretching. Rabbit fascia, structurally similar to human fascia, showed minimal friction changes under preload due to its collagen and layered structure. In contrast, synthetic fascia exhibited higher friction under heavy preload, likely due to wear and damage to its top layer, leading to increased surface roughness and hysteretic friction.

In next part of the study evaluated the effect of HA solutions with varying MW and concentrations on friction in both short-term and long-term tribological tests. The study investigated the effects of various HA solutions on friction through both short-term and long-term tribological testing. In the short-term tests lasting 300 s, HA solutions with MW of 101 kDa and 316 kDa 10 mg/ml exhibited the lowest COF for both *ex vivo* rabbit and synthetic fascia. Conversely, the 610 kDa solution displayed the highest friction, nearly doubling the COF observed with the 101 kDa and 316 kDa 10 mg/ml solutions. Notably, HA-RED showed similar efficacy to native HA in reducing friction, but its impact did not significantly differ from that of native HA of comparable MW. HA-C12, on the other hand, had the highest friction for synthetic fascia but achieved the lowest friction for rabbit fascia. In the long-term tests conducted over 3000 s, the synthetic fascia demonstrated more consistent friction behavior with fewer abrupt changes compared to other specimens. However, HA-C12 notably deteriorated the performance of synthetic fascia, indicating its unsuitability for effective tribological testing in this context. The rabbit fascia, in contrast, maintained relatively steady performance across most scenarios, though some fluctuations in friction levels were observed when using the 610 kDa HA and 316 kDa 10 mg/ml solutions. HA-RED showed potential for stability but exhibited some instability in specific cases.

The study found that higher MW and concentration of HA increased solution viscosity, which generally led to higher friction. This effect is due to the increased packing density

of polymer chains, making movement within the solution more difficult and raising friction levels. This trend was observed in the short-term tests, where higher viscosity solutions like 610 kDa HA and HA-RED exhibited higher COF. Interestingly, lower MW HA solutions (101 kDa and 316 kDa 10 mg/ml) provided lower friction, contrasting with findings in other systems like osteoarthritic joints or the eye, where higher viscosity HA often improves lubrication. The results highlight that in fascial tissues, the presence of collagen fibers allows HA to be mechanically entrapped, reducing friction and protecting against damage. This effect was less pronounced in synthetic fascia, which lacks collagen. HA-C12, despite its lower viscosity and concentration, was effective in reducing friction in rabbit fascia but showed unstable performance in synthetic fascia. This indicates that HA's interaction with collagen plays a significant role in its lubricating effectiveness.

The fourth study also involved the pharmacokinetics of HA-based intrafascial viscosupplementation, which showed that chemically modified HA-RED was eliminated within 30 days in the same manner as native HA but exhibited a longer retention time compared with native HA. Overall, the study suggests that lower MW HA solutions, particularly 316 kDa HA 10 mg/ml and HA-RED, are effective for reducing friction in fascial tissues. The findings also underscore the importance of considering MW, concentration and chemical modification to optimize HA-based lubricants for fascial viscosupplementation.

Biotribology 30 (2022) 100209

Contents lists available at ScienceDirect

Biotribology

journal homepage: www.elsevier.com/locate/biotri

Development of Tribological Model of Human Fascia: The Influence of Material Hardness and Motion Speed

Streďanská A.[a,*], D. Nečas[a], M. Vrbka[a], I. Křupka[a], M. Hartl[a], E. Toropitsyn[b], J. Husby[b]

[a] Biotribology Research Group, Faculty of Mechanical Engineering, Brno University of Technology, Technická 2896/2, 616 69 Brno, Czech Republic
[b] Contipro a.s., Dolní Dobrouč 401, 561 02 Dolní Dobrouč, Czech Republic

ARTICLE INFO

Keywords:
Soft tissues
Compliance
Friction
Hyaluronic acid

ABSTRACT

Low back pain is one of the most prevalent health disabilities worldwide. It is suggested that thoracolumbar fascia is possible causality of low back pain due to nerve innervation and pathological changes. A tribological model of fascia layers sliding across each other was developed in the present study. The influence of motion speed was investigated. The experiments were carried out in a pin-on-plate configuration using a normal load of 1 N and a range of speed from 1 to 5 Hz. Additionally, since fascia changes its structure depending on health conditions and physical activity, the influence of material hardness was studied. Therefore, different hardness of PDMS is considered to mimic different densities of the tissues. High-viscosity hyaluronic acid and low-viscosity oil were used as the lubricants. It was revealed that there is an apparent influence of lubricant viscosity with increasing material hardness. The friction increased with increasing movement speed for most of the PDMS hardness investigated. It seems the combination of high viscosity of hyaluronic acid, compliant material, and low speed can lead to low friction behaviour. Therefore, future studies will focus on finding even more compliant material for further development of the model towards mimicking the contact of human soft tissues.

1. Introduction

According to recent studies, low back pain (LBP) cases are on the rise, causing more global disability than any other condition [1]. There is emerging evidence suggesting that idiopathic LBP can be related to the thoracolumbar fascia (TLF) due to its dense sensory innervation and gliding properties [2,3]. The deep fascia is a multi-layered structure formed by two to three layers of densely packed bundles of collagen fibres shown in Fig. 1. Each layer is separated from the adjacent one by a thin layer of loose connective tissue, which is rich in hyaluronan [4]. Fibroblast-like cells, aligned on the inferior surface of fascia, called fasciacytes have been described [5]. These cells have a specialized function of hyaluronic acid (HA) synthesis and secretion.

One of the significant properties of HA is its viscoelasticity. Both the viscosity and the elasticity are not constant but vary with the rate of shear or oscillatory movement. The viscoelasticity of HA suggests that it should be an ideal biological lubricant [6]. The role of HA as the lubricant in a human body is well-known in synovial joints. Synovial fluid contains HA providing low-friction and low-wear properties to a cartilage surface [7,8]. Nowadays, HA represents a key molecule in a variety of medical, pharmaceutical, and cosmetic applications. For instance, HA is a component of eye tissue and tear fluid; hence it is the active ingredient of many eye drops [9]. It is used to treat skin irritations and support wound healing [10,11]; HA is a component of a nasal spray for chronic rhinosinusitis [12], treatment of tendon allograft [13,14] or it serves as a drug delivery system [15,16]. The physico-chemical properties of HA, such as thixotropic non-Newtonian fluid, are determined by the concentration, molecular weight, solvent ionic composition, temperature, pH, and covalent or non-covalent binding of proteins or by workload [17–21]. However, HA viscosity depends on tissue conditions where it operates as a lubricant. If the density of tissue is increased by injury or pathological changes such as densification or fibrosis [22,23], the behaviour of the whole fascia can be changed [19].

The contact of soft biological tissues, such as the fascia layers, represents a compliant contact in biotribology. The compliant materials generally reach relatively high friction coefficient values, while this phenomenon is partially related to Van der Waals forces [24,25]. Because of adhesion and large deformation between the bodies, evaluation of contact pressure and the contact area is quite a challenging issue [26,27]. Adhesion leads to larger contact areas and higher contact hardness for a given applied force relative to the Hertz model of contact mechanics.

* Corresponding author.
E-mail address: Alexandra.Stredanska@vut.cz (A. Streďanská).

https://doi.org/10.1016/j.biotri.2022.100209
Received 30 September 2021; Received in revised form 1 April 2022; Accepted 1 April 2022
Available online 4 April 2022

Hence soft contact mechanics became quite challenging in biotribology. Nevertheless, there is a large bandwidth of compliant technical models that do not involve animal testing. PDMS is one of the commonly used substitution materials of human tissues in these models. Although there are tribological models for simulating the oral cavity [28,29], artery [30], or skin [31], none, in so far as we know, have been developed for the study of fascia tribology. Therefore, this study aimed to investigate the impact of shore hardness of polydimethylsiloxane (PDMS), in terms of simulating varying hardness due to pathological changes of fascia. The PDMS was lubricated by HA, as a natural substance (endogenous) for the human fascia. The second objective of the study was to investigate how various motion speeds of a fascial layer prejudice friction between layers.

2. Materials and Methods

In this study, a commercial tribometer Bruker - UMT TriboLab was used for friction measurements. A pin-on-plate configuration was employed with a movable bottom module, where a pot was mounted. An upper module with a pin holder was stationary and was loaded against the pot with the fixed plate. The tribometer determines the coefficient of friction (COF) based on the values of the friction force F_f and the normal force F_n monitored by the sensors in time. The scheme of the experimental setup is shown in Fig. 2. For the purpose of the study, a tribological model of soft connective tissues needs to be developed.

The model should simulate the tribological contact pair of the soft tissues in the body without using biological samples. PDMS with various hardness from 10 to 50 ShA increased continuously by 10 ShA was chosen as a suitable representative. The contact pair always consisted of the pin and the plate of the same material (hardness). The plate, which was 3.5 mm thick, 70 mm long, and 35 mm wide (Fig. 2), was inserted into a stainless steel pot where lubricant can be applied to ensure fully flooded contact. The pot contains four holders with springs to avoid plate motion. The pin was formed by a PDMS sphere of radius 8.6 mm fixed in a stainless steel holder. The holder was detachably connected by a thread.

Two main issues were investigated in the study. The impact of PDMS contact pair hardness (the first case) and the impact of the frequency of linear reciprocating motion expressing the motion speed (the second case) on COF. The normal force F_n, maintained by the pin, was set to 1 N for both cases. Each step of the experiment with a 12 mm stroke was repeated three times separately on the new path and lasted 300 s. Test temperature was 25 °C. Before and after each experiment, the pot was carefully cleaned using isopropyl alcohol to avoid the influence of the measurement by the impurities from the previous test. In the first case, the bottom module moved with the frequency of 1 Hz (mean velocity 12 $mm.s^{-1}$) while material hardness varied. In the second case, the PDMS with hardness 10 ShA was chosen as the contact pair and the frequency varied. Values of the frequency were changed (1–5 Hz).

Contact pressure is the important parameter connected with the hardness of the material. The FEM method was used to determine its value. Non-linear analysis with a large deflection allowed was carried out using Ansys Workbench. The type of contact between simulated bodies was selected as frictional contact. The normal force applied to the pin was 1 N, which corresponds to the experiment. The model of the materials was Rubber, silicone (VMQ) – tensile yield strength 8.97 MPa, density $1.12e^{-06}$ $kg.mm^{-3}$.

In this study, two different lubricants were compared. Low viscosity oil (LVO), having the dynamic viscosity of 0.105 Pa.s was used as the reference. The results were then compared with those for the solution of HA. In general, HA in the body has a relatively high molecular weight (MW), therefore, HA with MW of 2000 kDa was chosen. The concentration of HA in the solution was 10 mg/ml, and PBS served as a base liquid. The viscosity was measured using a rotational viscosimeter TA Instruments Discovery HR-3 rheometer (TA Instruments, New Castle, DE, USA). Experiments were analyzed using a stainless-steel cone and plate geometry (40 mm diameter cone with a 1° cone angle). The test temperature was set to 25 °C. The experiment was repeated three times with a fresh sample of HA.

3. Results and Discussion

3.1. FEM Analysis of the Contact Area and HA Rheology

The contact area and value of the contact pressure were analyzed by FEM. The maximum value of the contact pressure was determined to be 170 kPa, and the size of the contact area was 9.95 mm^2. The respective results of normal stress and contact pressure are displayed in Fig. 3. For example, the regular contact pressure between cartilage and menisci is circa 3 MPa [32]. The average contact pressure between the Achilles tendon and the calcaneus is 160 kPa (tensile load in the tendon was 70 N) [33], and the mean pressure between the plantar fascia and the intrinsic foot muscles is 110 kPa [34].

After FEM analysis of the contact, the rheology of the model HA-based fluid was evaluated. As can be seen in Fig. 4, dynamic viscosity dramatically drops for the shear rates lower than 500 /s. Further shear

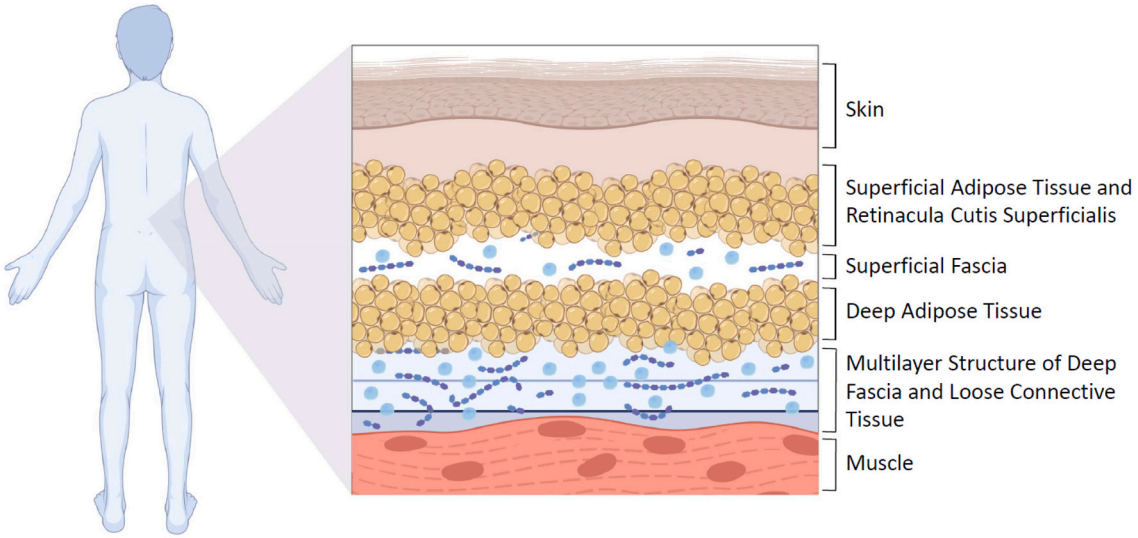

Fig. 1. Scheme of the fascia layers. Created with BioRender.com.

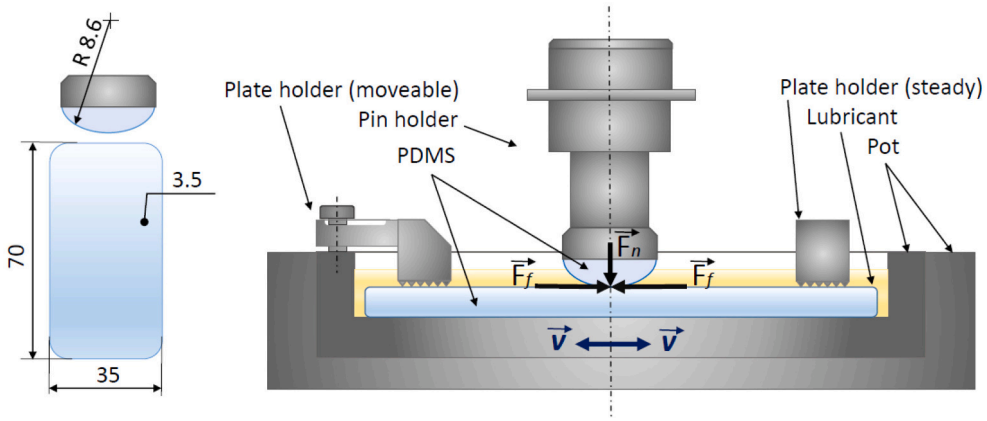

Fig. 2. Scheme of the experimental setup.

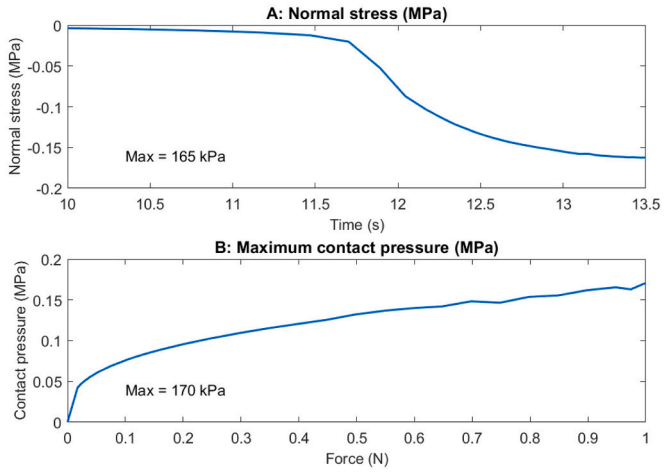

Fig. 3. A: The dependence of normal stress due to normal force on time. B: Maximum contact pressure depending on loading normal force.

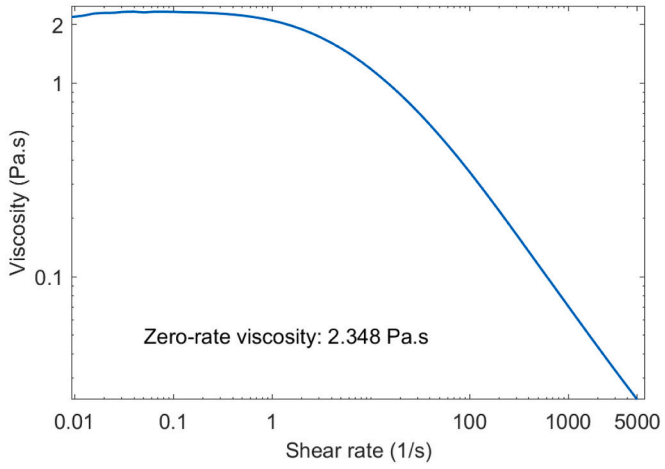

Fig. 4. The dependence of viscosity of HA 2000 kDa on shear rate.

rate increase does not lead to considerable changes in viscosity, which continuously decreases from 0.1 to 0.05 Pa.s. The curve from average values can be seen in Fig. 4. The experimental results dependent on the influence of the shear rate show that the solution of HA is the non-Newtonian and pseudoplastic fluid. These results are in agreement with a previous study about the influence of hyaluronic acid present in solution upon the rheological behaviour [35].

3.2. The Influence of Motion Speed

The pin-on-plate experiment with variable sliding velocity was carried out to determine the influence of motion speed. Fascia is a tissue composed of layers sliding across each other or against muscles [36]. However, with the increased density of fascia tissue due to the pathological state, the sliding potential of layers is reduced in patients with LBP [37]. Without pain, the representative range of kinematics of normal walk is 4–6 Hz. The spectral power analysis from walking barefoot across a force plate shows that 98% of the spectral power is under 10 Hz and above 90% under 5 Hz [38]. Plasqui et al. [39] exhibited that 99% of the acceleration performance in the walk is concentrated under 15 Hz. However, they also demonstrated that the frequency range of daily activities was between 0.3 and 3.5 Hz. Accordingly, the experiments in this chapter were carried out at the frequency from 1 to 5 Hz. Fig. 5 shows COF for both fluids tested in the range of the velocity for PDMS 10 ShA. It is known that Young's modulus of PDMS varies between around 0.57 and 3.7 MPa with a degree of cross-linking [40], McKee et al. detected that Young's modulus of muscle is approximately 7 kPa, which is two orders of magnitude lower value. Thus 10 ShA was chosen for this study. As can be seen, both lubricants showed slightly increased friction with increasing sliding speed. This phenomenon might be associated with the viscoelastic properties of PDMS. The friction that appears from the deformation of the silicone rubber alters as a function of speed due to its viscoelastic response. Moreover, in highly compliant surfaces, the contact area is determined by elastic conformity rather than plastic deformation at asperities at a lower contact load. In an account of that, the boundary lubrication regime is expected. At the lowest speed, the lubricant COF values are shifted marginally, then overlapped, showing there is a thin or even zero boundary film created. This is because the speed is insufficient to separate the surfaces hydrodynamically and there are no phospholipids which would support hydration lubrication behaviour [41]. These results are in line with previous studies [28,42,43].

3.3. The Influence of Material Hardness

Mechanical properties, especially stiffness of fascia, vary with age and gender [44], together with physical condition, hydration [45], contraction level of the muscle [46], and pathological changes [22]. Stecco et al. [36] described increased loose connective tissue in layers of fascia in ultrasound images as densification. The term suggests an alteration in the viscosity of the fascia. In addition, it is crucial to deal with the influence of material hardness since Shallamach [47] showed that the hardness of the sample considerably affects friction. Fig. 6

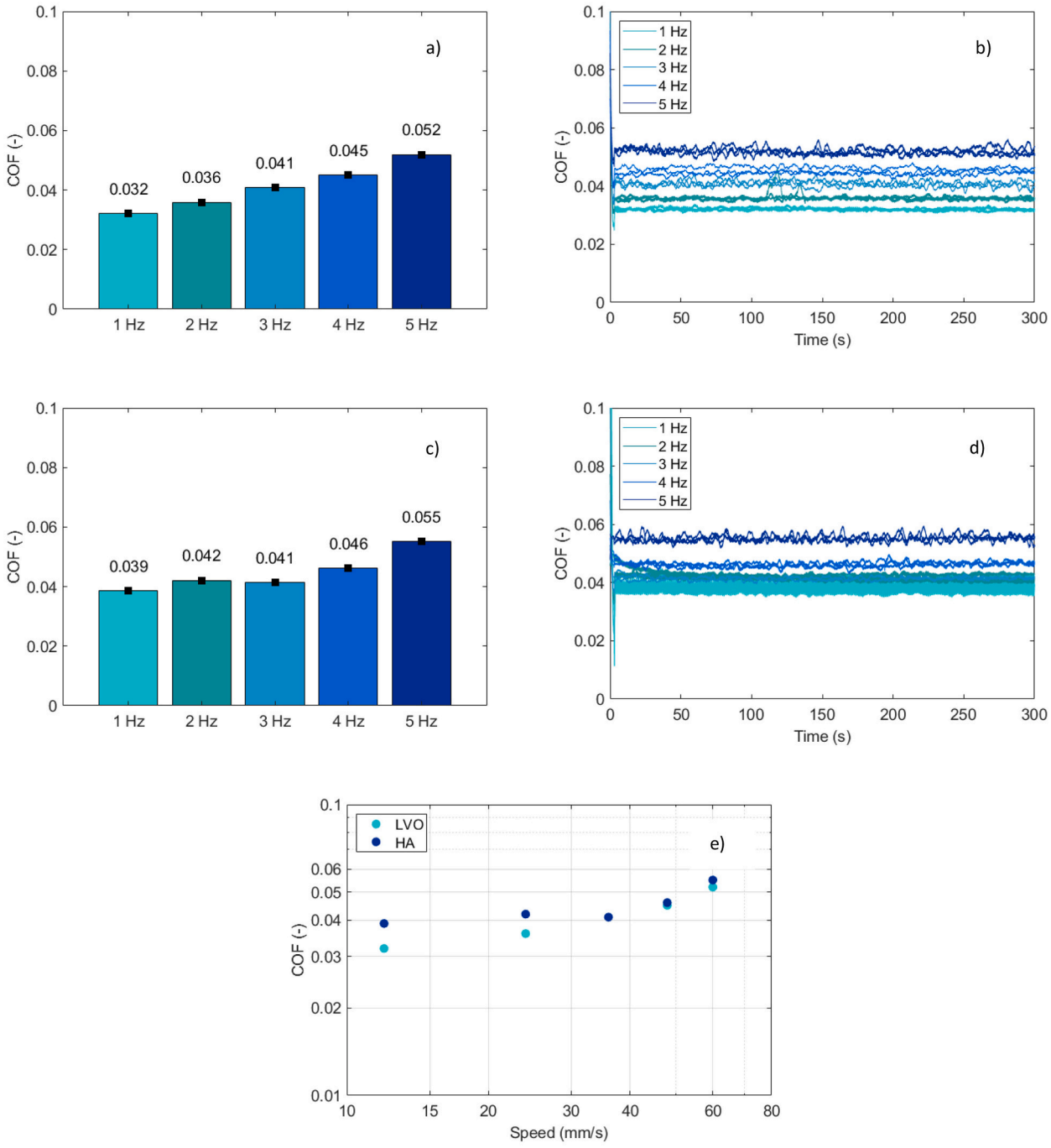

Fig. 5. Influence of the motion speed. Fig. a) and b) – LVO, the fig. c) and d) – HA 2000 kDa. Fig. a) and c) bar plots showing mean values of COF and SDD. SDD is measured between the mean value of each friction curve of the sample. Fig. b) and d), the curves showing the development of COF in time. Fig. e) In the Stribeck curve (LVO and HA).

shows sliding COF for LVO and HA. As can be seen, there is no correlation between them. While material lubricated by HA had no significant hardness effect, the hardness effect was determined when the material was lubricated by oil. The oil had doubled the value of COF from the softest to the hardest PDMS, but the maximum value reached the contact pair PDMS 40 ShA. Since the sliding speed for each test was set to 12 $mm.s^{-1}$, we expected the boundary regime to take place for all the samples. This proposes that the contact is already being self-lubricated, and lubricant is being squeezed out from the PDMS due to the pin pressure. The boundary regime was confirmed at least in samples lubricated by HA. The rubber-like PDMS is usually made by cast molding [48], independently of hardness, standards of casting as its roughness should be preserved. Thus, we can assume an analogous material roughness in all samples. However, as can be seen in Fig. 5, LVO had better lubricating properties in the boundary regime at the lowest speed. Perhaps, this can be explained by the low-viscosity behaviour of oil and better leaking to the contact forming a weak boundary film. In the study [49], it was found experimentally that the sliding friction coefficient increases with decreasing elastic modulus. However, the mentioned study investigated the contact of solid-compliant nature, while the experiments were carried out under rolling or rolling-sliding conditions. Therefore, the discrepancy between the current data and previous literature may arise from full compliance of the contact and different motion conditions.

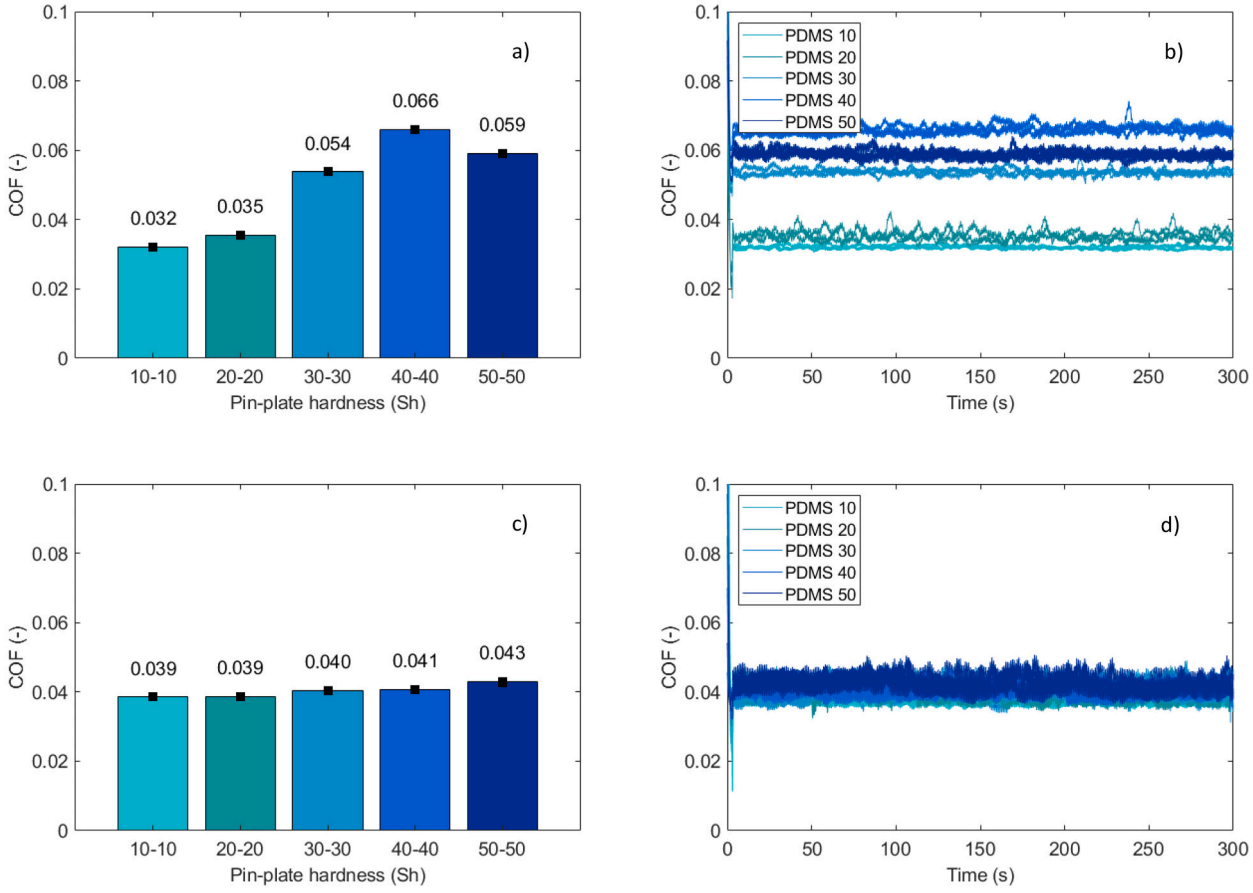

Fig. 6. Influence of the material hardness. Fig. a) and b) – LVO, the fig. c) and d) – HA 2000 kDa. Fig. a) and c) bar plots showing mean values of COF and SDD. SDD is measured between the mean value of each friction curve of the sample Fig. b) and d), the curves showing COF development in time.

The present paper provided an insight into the frictional behaviour of compliant materials, possibly mimicking human soft tissues. However, the authors admit one of the particular limitations of the study. According to studies given by Weber et al. [50] and McKee et al. [51], real biological tissues have a lower hardness than PDMS considered in multiple biotribological studies. Nevertheless, as mentioned above, PDMS is commonly used as the model material for the tribological models in many bioapplications [28–31]. Future studies should concentrate on approaching even lower contact hardness together with lower contact pressure. However, the achieved results are essential, showing some fundamentals and general trends of friction in compliant contacts.

4. Conclusion

The present study focused on the evaluation of friction coefficient in the contact of compliant PDMS samples, which might be used for mimicking the human fascia tissues contact in future research. The measurements were carried out in pin-on-plate configuration considering the reciprocating motion. The experimental investigation aimed at the effect of sample hardness, the role of lubricant, and the influence of motion speed. The main findings may be summarized in the following points:

- For high-viscosity HA there is no friction dependence on PDMS hardness.
- For LVO, there is a strong friction dependence on material hardness.
- COF increased with increasing PDMS hardness, in general.
- Both lubricants showed increased friction with increasing motion speed.

Declaration of Competing Interest

The authors declare that they have no known competing financial interests or personal relationships that could have appeared to influence the work reported in this paper.

Acknowledgments

This project (Fascia lubrication and regeneration by hyaluronan) has received funding from the Operational Programme Enterprise and Innovations for Competitiveness 2014-2020 (OPEIC) under agreement No CZ.01.1.02/0.0/0.0/19_262/0020005.

References

[1] A. Wu, L. March, X. Zheng, J. Huang, X. Wang, J. Zhao, et al., Global low back pain prevalence and years lived with disability from 1990 to 2017: estimates from the global burden of disease study 2017, Ann. Transl. Med. 8 (2020), https://doi.org/10.21037/atm.2020.02.175, 299–299.
[2] C.K. Chen, A.J. Nizar, Myofascial pain syndrome in chronic back pain patients, Korean J. Pain 24 (2011) 100–104, https://doi.org/10.3344/kjp.2011.24.2.100.
[3] J. Tesarz, U. Hoheisel, B. Wiedenhöfer, S. Mense, Sensory innervation of the thoracolumbar fascia in rats and humans, Neuroscience 194 (2011) 302–308, https://doi.org/10.1016/j.neuroscience.2011.07.066.
[4] L. Lancerotto, C. Stecco, V. MacChi, A. Porzionato, A. Stecco, R. De Caro, Layers of the abdominal wall: anatomical investigation of subcutaneous tissue and superficial fascia, Surg. Radiol. Anat. 33 (2011) 835–842, https://doi.org/10.1007/s00276-010-0772-8.
[5] C. Stecco, R. Stern, A. Porzionato, V. MacChi, S. Masiero, A. Stecco, et al., Hyaluronan within fascia in the etiology of myofascial pain, Surg. Radiol. Anat. 33 (2011) 891–896, https://doi.org/10.1007/s00276-011-0876-9.
[6] J.R.E. Fraser, T.C. Laurent, U.B.G. Laurent, Hyaluronan: its nature, distribution, functions and turnover, J. Intern. Med. 242 (1997) 27–33, https://doi.org/10.1046/j.1365-2796.1997.00170.x.

[7] T.M. Tamer, Hyaluronan and synovial joint: function, distribution and healing, Interdiscip. Toxicol. 6 (2013) 111–125, https://doi.org/10.2478/intox-2013-0019.
[8] D. Rebenda, M. Vrbka, P. Čípek, E. Toropitsyn, D. Nečas, M. Pravda, et al., On the dependence of rheology of hyaluronic acid solutions and frictional behavior of articular cartilage, Materials (Basel) 13 (2020), https://doi.org/10.3390/ma13112659.
[9] A. Fallacara, S. Vertuani, G. Panozzo, A. Pecorelli, G. Valacchi, S. Manfredini, Novel artificial tears containing cross-linked hyaluronic acid: an in vitro re-epithelialization study, Molecules 22 (2017), https://doi.org/10.3390/molecules22122104.
[10] K.L. Aya, R. Stern, Hyaluronan in wound healing: rediscovering a major player, Wound Repair Regen. 22 (2014) 579–593, https://doi.org/10.1111/wrr.12214.
[11] M.G. Neuman, L. Oruña, G. Coto, G. Lago, R. Nanau, M. Vincent, Hyaluronic acid signals for repair in ethanol-induced apoptosis in skin cells in vitro, Clin. Biochem. 43 (2010) 822–826, https://doi.org/10.1016/j.clinbiochem.2010.04.005.
[12] M. Di Cicco, G. Alicandro, L. Claut, L. Cariani, N. Luca, G. Defilippi, et al., Efficacy and tolerability of a new nasal spray formulation containing hyaluronate and tobramycin in cystic fibrosis patients with bacterial rhinosinusitis, J. Cyst. Fibros. 13 (2014) 455–460, https://doi.org/10.1016/j.jcf.2014.02.006.
[13] C. Zhao, Z. Wei, R.L. Reisdorf, A.R. Thoreson, G.D. Jay, S.L. Moran, et al., The effects of biological lubricating molecules on flexor tendon recon[1] ZHAO, Chunfeng, Zhuang WEI, Ramona L REISDORF, Andrew R THORESON, Gregory D JAY, Steven L MORAN, Kai Nan AN a Peter C AMADIO. The effects of biological lubricating molecules on flex, Plast. Reconstr. Surg. 133 (2014), https://doi.org/10.1097/PRS.0000000000000102.
[14] M.J. Forthofer, K.M. Arnold, R.L. Reisdorf, P.C. Amadio, C. Zhao, The effect of gelatin molecular weight on tendon lubrication utilizing an extrasynovialized Turkey flexor tendon model, Mil. Med. 186 (2021), https://doi.org/10.1093/milmed/usaa265 n.d.
[15] G. Huang, H. Huang, Application of hyaluronic acid as carriers in drug delivery, Drug Deliv. 25 (2018) 766–772, https://doi.org/10.1080/10717544.2018.1450910.
[16] Y.-J. Jin, T. Ubonvan, D.-D. Kim, Hyaluronic acid in drug delivery systems, J. Pharm. Investig. 40 (2010) 33–43, https://doi.org/10.4333/kps.2010.40.s.033.
[17] R. Tadmor, N. Chen, J.N. Israelachvili, Thin Film Rheology and Lubricity of Hyaluronic Acid Solutions at a Normal Physiological Concentration 61, 2002.
[18] K.G. Ganjaei, J.W. Ray, B. Waite, K.J. Burnham, The fascial system in musculoskeletal function and myofascial pain, Curr. Phys. Med. Rehabil. Reports 8 (2020) 364–372, https://doi.org/10.1007/s40141-020-00302-3.
[19] M.K. Cowman, T.A. Schmidt, P. Raghavan, A. Stecco, Viscoelastic properties of hyaluronan in physiological conditions, F1000Research 4 (2015), https://doi.org/10.12688/f1000research.6885.1.
[20] J.R.E. Fraser, T.C. Laurent, U.B.G. Laurent, The nature of hyaluronan, J. Intern. Med. 242 (1997) 27–33.
[21] M.K. Cowman, S. Matsuoka, Experimental approaches to hyaluronan structure, Carbohydr. Res. 340 (2005) 791–809, https://doi.org/10.1016/j.carres.2005.01.022.
[22] P.G. Pavan, A. Stecco, R. Stern, C. Stecco, Painful connections: densification versus fibrosis of fascia, Curr. Pain Headache Rep. 18 (2014), https://doi.org/10.1007/s11916-014-0441-4.
[23] P. Pavan, A. Stecco, R. Stern, P. Logna Prat, C. Stecco, Fibrosis and densification: Anatomical vs functional alteration of the fascia, J. Bodyw. Mov. Ther. 20 (2016) 151, https://doi.org/10.1016/j.jbmt.2015.07.029.
[24] K.L. Johnson, K. Kendall, A.D. Roberts, Surface energy and the contact of elastic solids, Proc. R Soc. Lond. A Math. Phys. Sci. 324 (1971) 301–313, https://doi.org/10.1098/rspa.1971.0141.
[25] M. Barquins, Friction and wear of rubber-like materials, Wear 160 (1993) 1–11, https://doi.org/10.1016/0043-1648(93)90400-G.
[26] B. Best, P. Meijers, A.R. Savkoor, The formation of schallamach waves, Wear 65 (1981) 385–396, https://doi.org/10.1016/0043-1648(81)90064-8.
[27] A. Schallamach, How does rubber slide? Wear 17 (1971) 301–312, https://doi.org/10.1016/0043-1648(71)90033-0.
[28] D.M. Dresselhuis, H.J. Klok, M.A.C. Stuart, R.J. De Vries, G.A. Van Aken, E.H.A. De Hoog, Tribology of o/w emulsions under mouth-like conditions: determinants of friction, Food Biophys. 2 (2007) 158–171, https://doi.org/10.1007/s11483-007-9040-9.
[29] R.S. Edmonds, T.J. Finney, M.R. Bull, A.A. Watrelot, T.L. Kuhl, Friction measurements of model saliva-wine solutions between polydimethylsiloxane surfaces, Food Hydrocoll. 113 (2021), 106522, https://doi.org/10.1016/j.foodhyd.2020.106522.
[30] S. Vad, A. Eskinazi, T. Corbett, T. McGloughlin, J.P. Vande Geest, Determination of coefficient of friction for self-expanding stent-grafts, J. Biomech. Eng. 132 (2010) 1–10, https://doi.org/10.1115/1.4002798.
[31] B.V. Farias, S.A. Khan, Probing gels and emulsions using large-amplitude oscillatory shear and frictional studies with soft substrate skin surrogates, Colloids Surf. B: Biointerfaces 201 (2021), 111595, https://doi.org/10.1016/j.colsurfb.2021.111595.
[32] T. Fukubayashi, H. Kurosawa, The contact area and pressure distribution pattern of the knee: a study of normal and osteoarthrotic knee joints, Acta Orthop. 51 (1980) 871–879, https://doi.org/10.3109/17453678008990887.
[33] T. Matsui, T. Kumai, S. Kamijo, Y. Shinohara, H. Kurokawa, A. Taniguchi, et al., Effect of ankle motion and tensile stress at the Achilles tendon on the contact pressure between the Achilles tendon and the calcaneus, J. Foot Ankle Surg. 60 (2021) 753–756, https://doi.org/10.1053/j.jfas.2021.02.008.
[34] S. Taş, A. Çetin, An investigation of the relationship between plantar pressure distribution and the morphologic and mechanic properties of the intrinsic foot muscles and plantar fascia, Gait Posture 72 (2019) 217–221, https://doi.org/10.1016/j.gaitpost.2019.06.021.
[35] A. García-Abuín, D. Gómez-Díaz, J.M. Navaza, L. Regueiro, I. Vidal-Tato, Viscosimetric behaviour of hyaluronic acid in different aqueous solutions, Carbohydr. Polym. 85 (2011) 500–505, https://doi.org/10.1016/j.carbpol.2011.02.028.
[36] J. Dommerholt, Functional atlas of the human fascial system, J. Bodyw. Mov. Ther. 19 (2015) 679–680, https://doi.org/10.1016/j.jbmt.2015.06.010.
[37] H.M. Langevin, J.R. Fox, C. Koptiuch, G.J. Badger, A.C. Greenan-Naumann, N. A. Bouffard, et al., Reduced Thoracolumbar Fascia Shear Strain in Human Chronic Low Back Pain, 2011, https://doi.org/10.1186/1471-2474-12-203.
[38] H. Jagos, J. Oberzaucher, M. Reichel, W.L. Zagler, W. Hlauschek, A multimodal approach for insole motion measurement and analysis, Procedia Eng. 2 (2010) 3103–3108, https://doi.org/10.1016/j.proeng.2010.04.118.
[39] G. Plasqui, A.G. Bonomi, K.R. Westerterp, Daily physical activity assessment with accelerometers: new insights and validation studies, Obes. Rev. 14 (2013) 451–462, https://doi.org/10.1111/obr.12021.
[40] Z. Wang, A.A. Volinsky, N.D. Gallant, Crosslinking effect on polydimethylsiloxane elastic modulus measured by custom-built compression instrument, J. Appl. Polym. Sci. 131 (2014) 1–4, https://doi.org/10.1002/app.41050.
[41] P. Hilšer, A. Suchánková, K. Mendová, K.E. Filipič, M. Daniel, M. Vrbka, A new insight into more effective viscosupplementation based on the synergy of hyaluronic acid and phospholipids for cartilage friction reduction, Biotribology 25 (2021), https://doi.org/10.1016/j.biotri.2021.100166.
[42] J.H.H. Bongaerts, K. Fourtouni, J.R. Stokes, Soft-tribology: lubrication in a compliant PDMS-PDMS contact, Tribol. Int. 40 (2007) 1531–1542, https://doi.org/10.1016/j.triboint.2007.01.007.
[43] J. de Vicente, J.R. Stokes, H.A. Spikes, Rolling and sliding friction in compliant, lubricated contact, Proc. Inst. Mech. Eng. Part J. J. Eng. Tribol. 220 (2006) 55–63, https://doi.org/10.1243/13506501JET90.
[44] M. Kirilova-Doneva, D. Pashkouleva, The effects of age and sex on the elastic mechanical properties of human abdominal fascia, Clin. Biomech. 92 (2022), 105591, https://doi.org/10.1016/j.clinbiomech.2022.105591.
[45] R. Schleip, L. Duerselen, A. Vleeming, I.L. Naylor, F. Lehmann-Horn, A. Zorn, et al., Strain hardening of fascia: static stretching of dense fibrous connective tissues can induce a temporary stiffness increase accompanied by enhanced matrix hydration, J. Bodyw. Mov. Ther. 16 (2012) 94–100, https://doi.org/10.1016/j.jbmt.2011.09.003.
[46] S. Otsuka, X. Shan, Y. Kawakami, Dependence of muscle and deep fascia stiffness on the contraction levels of the quadriceps: an in vivo supersonic shear-imaging study, J. Electromyogr. Kinesiol. 45 (2019) 33–40, https://doi.org/10.1016/j.jelekin.2019.02.003.
[47] A. Schallamach, Friction and abrasion of rubber, Wear 1 (1958) 384–417, https://doi.org/10.1016/0043-1648(58)90113-3.
[48] X. Ye, H. Liu, Y. Ding, H. Li, B. Lu, Research on the cast molding process for high quality PDMS molds, Microelectron. Eng. 86 (2009) 310–313, https://doi.org/10.1016/j.mee.2008.10.011.
[49] C. Myant, H.A. Spikes, J.R. Stokes, Influence of load and elastic properties on the rolling and sliding friction of lubricated compliant contacts, Tribol. Int. 43 (2010) 55–63, https://doi.org/10.1016/j.triboint.2009.04.034.
[50] P. Weber, C. Graf, W. Klingler, N. Weber, R. Schleip, The feasibility and impact of instrument-assisted manual therapy (IAMT) for the lower back on the structural and functional properties of the lumbar area in female soccer players: a randomised, placebo-controlled pilot study design, Pilot Feasibility Stud. 6 (2020) 1–10, https://doi.org/10.1186/s40814-020-00592-3.
[51] C.T. McKee, J.A. Last, P. Russell, C.J. Murphy, Indentation versus tensile measurements of young's modulus for soft biological tissues, Tissue Eng. Part B Rev. 17 (2011) 155–164, https://doi.org/10.1089/ten.teb.2010.0520.

International Journal of Biological Macromolecules 253 (2023) 126879

Contents lists available at ScienceDirect

International Journal of Biological Macromolecules

journal homepage: www.elsevier.com/locate/ijbiomac

Injecting hyaluronan in the thoracolumbar fascia: A model study

Kristina Nešporová [a,*], Jana Matonohová [a], Jarmila Husby [a], Evgeniy Toropitsyn [a], Lenka Divoká Stupecká [a], Aaron Husby [a], Tereza Suchánková Kleplová [b], Alexandra Streďanská [c], Matěj Šimek [a], David Nečas [c], Martin Vrbka [c], Robert Schleip [d,e], Vladimír Velebný [a]

[a] Contipro a.s., Dolní Dobrouč 401, 561 02 Dolní Dobrouč, Czech Republic
[b] Department of Dentistry, Charles University, Faculty of Medicine in Hradec Kralove and University Hospital Hradec Kralove, 500 05 Hradec Kralové, Czech Republic
[c] Biotribology Research Group, Faculty of Mechanical Engineering, Brno University of Technology, 616 69 Brno, Czech Republic
[d] DIPLOMA Hochschule, 37242 Bad Sooden-Allendorf, Germany
[e] Conservative and Rehabilitative Orthopedics, Department of Sport and Health Sciences, Technical University of Munich, 80333 Munich, Germany

ARTICLE INFO

Keywords:
Hyaluronan
Thoracolumbar fascia
Intrafascial injection

ABSTRACT

Hyaluronan (HA) has been recently identified as a key component of the densification of thoracolumbar fascia (TLF), a potential contributor to non-specific lower back pain (LBP) currently treated with manual therapy and systemic or local delivery of anti-inflammatory drugs. The aim of this study was to establish a novel animal model suitable for studying ultrasound-guided intrafascial injection prepared from HA with low and high Mw. Effects of these preparations on the profibrotic switch and mechanical properties of TLF were measured by qPCR and rheology, respectively, while their lubricating properties were evaluated by tribology. Rabbit proved to be a suitable model of TLF physiology due to its manageable size enabling both TLF extraction and in situ intrafascial injection. Surprisingly, the tribology showed that low Mw HA was a better lubricant than the high Mw HA. It was also better suited for intrafascial injection due to its lower injection force and ability to freely spread between TLF layers. No profibrotic effects of either HA preparation in the TLF were observed. The intrafascial application of HA with lower MW into the TLF appears to be a promising way how to increase the gliding of the fascial layers and target the myofascial LBP.

1. Introduction

Lower back pain (LBP) is one of the common health problems that up to 80 % of adults experience at some point in their life and is the most frequent cause of disability worldwide [1]. Densification and changes in HA content of deep thoracolumbar fascia (TLF) are considered one of the causes of LBP [2–4]. The fascia is a ubiquitous network surrounding all organs, muscles, and nerves consisting of cellular components and extracellular matrix. Its unique layered structure and hyaluronan (HA)-rich ECM enable gliding and thus proper mechanical force transfer.

Similarly to the ubiquitous presence of fascia in our body, HA is prevalent in most tissues. It is an anionic, non-sulphated linear polysaccharide with the structure of simple design (disaccharide sequences of D-glucuronic acid and *N*-acetyl-D-glucosamine), but with multifaceted functions and biological effects. In case of the TLF, HA is a major component of loose connective tissue separating the layers of dense collagen-rich tissue of deep fascia [5]. In normal functioning fascia, HA provides the hydration and lubrication, but acute injury and/or chronic inflammation can cause changes in HA rheological and lubrication properties leading to fascia densification, stiffness, and pain [6]. These pathological changes have been recently connected to the over-production of HA with lower molecular weight. On the other hand, HA is successfully used as a lubricant in different indications including arthritis [7] and plantar fasciitis [8] thanks to its high biocompatibility, safety, and total biodegradability.

The development of fascia-targeted therapy can be problematic due to the limited knowledge about this ubiquitous structure but also the lack of proven animal models. In this work, we have established a new animal model for the study of the TLF. Using this model and several in vitro tribological and rheological methods, the HA with the highest potential to beneficially affect the gliding of fascia has been selected and its safety was tested ex vivo. Also, the intrafascial application under ultrasound (US) guidance has been evaluated in this animal model hinting at its possibility in human patients.

* Corresponding author.
E-mail address: kristina.nesporova@contipro.com (K. Nešporová).

https://doi.org/10.1016/j.ijbiomac.2023.126879
Received 9 February 2023; Received in revised form 30 August 2023; Accepted 10 September 2023
Available online 12 September 2023

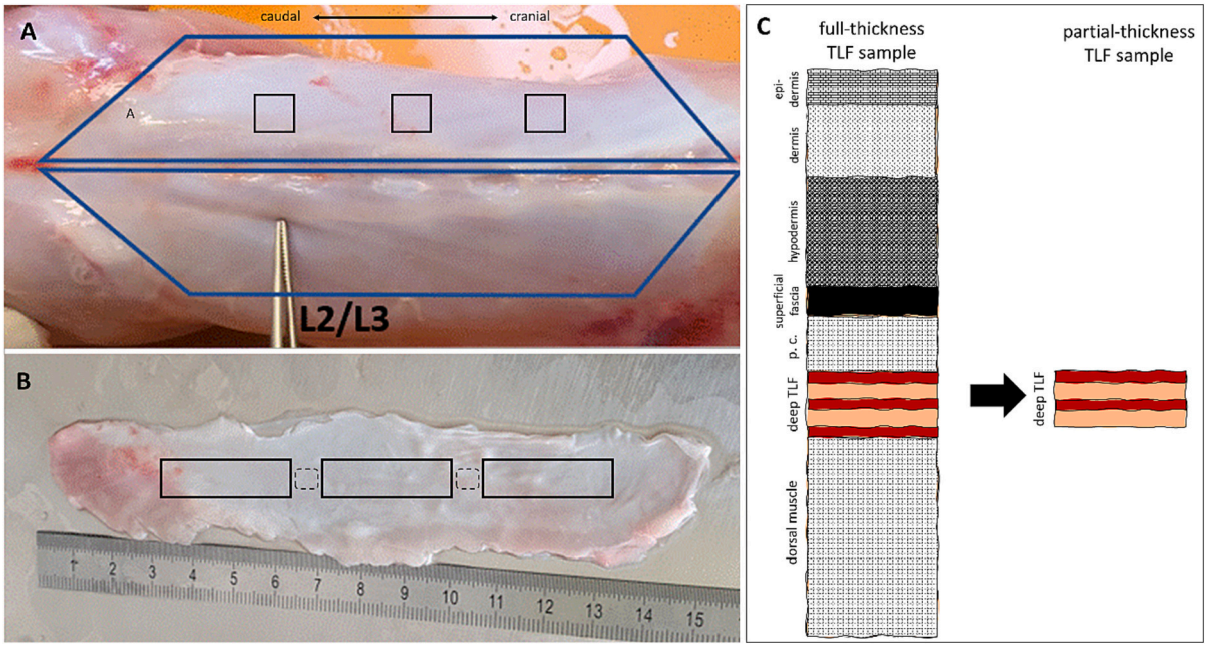

Fig. 1. Rabbit TLF sampling strategy. (A) Anatomic localization of TLF in the skinned rabbit dorsal area with the depiction of sampling location for full-thickness TLF samples for histology and HA quantification by LC-MS/MS. (B) Partial-thickness TLF excised from the rabbit back with the depiction of sampling location for partial-thickness TLF samples for gene expression analysis (smaller squares) and mechanical properties measurement (larger rectangles). (C) Schematic depiction of TLF complexity in full-thickness and partial thickness samples. p.c.; panniculus carnosus.

2. Materials and methods

2.1. Source of fascia tissue samples

For this study, healthy sexually mature (3–4 months old) male New Zealand white rabbits (2.7–3.5 kg) were purchased from a certified laboratory animal breeder and supplier VELAZ (VELAZ, Ltd., Czech Republic). The rabbits were housed in clean cages under standardized environmental conditions (12-hour light/dark cycle, temperature 17–21 °C, air humidity 30–70 %). The animals had access ad libitum to the standard diet for rabbits (VELAZ Ltd., Czech Republic) and drinking water.

Fascia tissue was studied in situ or collected for further evaluation solely from rabbit cadavers. It is important to note that, at the time of conducting the experiment in 2020, obtaining ethical committee approval for this type of experiment was not required under the Czech law, Act No. 246/1992 Sb.

2.2. Fascie tissue harvesting

The rabbits were euthanised by intracardial application of pentobarbital in combined premedication by ketamin and meloxicam. The TLF tissue samples (app. 15 × 3 cm) were obtained from rabbit cadavers in the region defined by the Th10 - L6 vertebrae and the attachment sites of the tensor fasciae latae, external oblique abdominis, and latissimus dorsi muscles (area used for sampling and harvested sample of TLF are visualised in Fig. 1A, B).

The TLF tissue samples were harvested either as partial-thickness deep fascia samples (without the epimysial layer) or as full-thickness tissue samples including the skin and muscle above and underneath, respectively (Fig. 1C). Tissue samples were collected from both the left and right sides of the spine as separated samples. For all type of experiments at least three samples of TLF from three different animals have been used (if not specified otherwise).

2.3. Histology

Rabbit full-thickness samples of deep TLF (app. 1 × 1 cm) from lumbar area including the muscular and cutaneous tissue below and above deep TLF, respectively, were fixed in 4 % paraformaldehyde followed by a standard procedure of dehydration, formation of paraffin blocks (TP1020 processor and EG1150H paraffin embedding station; Leica), slicing 5 μm histological sections (RM 2250 rotary microtome; Leica), deparaffinization, rehydration, and Masson's trichrome (MT) staining. For HA staining the samples were processed by the method by Šínová [9]. The detailed method for MT and HA staining and microscopic analysis is included in the Supplementary material. Histological examination was performed on 3 different samples of deep TLF from different rabbits.

2.4. HA quantification in rabbit myofascial tissue by liquid chromatography with mass spectrometric detection (LC-MS/MS)

Rabbit full-thickness samples of deep TLF (app. 1 × 1 cm) from lumbar area including the muscular and cutaneous tissue below and above deep TLF, respectively, were used for HA quantification. Harvested samples from cadavers were stored at 4 °C for max 2 h. Before enzymatic digestion the tissue was separated into 3 distinct samples, muscle (with the epimysium removed), TLF (which included epimysium) and skin (including the subcutaneous tissue with superficial fascia and panniculus carnosus). The HA amount was measured as described by Šimek [10]. Briefly, 100 μl of tissue homogenate was digested with actinase E and with HA lyase yielding unsaturated HA disaccharides. The chromatography separation was carried out with a Phenomenex Jupiter Proteo 4 μm 90 Å column (250 × 4.6 mm) column using Acquity UPLC I-class chromatographic system (Waters, UK). The separation was carried out at RT by gradient elution with 0.1 % formic acid in water and methanol. The flow rate was set at 0.5 ml/min, and the following gradient of methanol was applied: 0–15 % in 3–15 min, 15–80 % in 15–16 min. MS was performed using a triple quadrupole mass spectrometer equipped with an electrospray ion source (Xevo TQ-XS, Waters, UK) operating in the negative ionization mode. For both compounds,

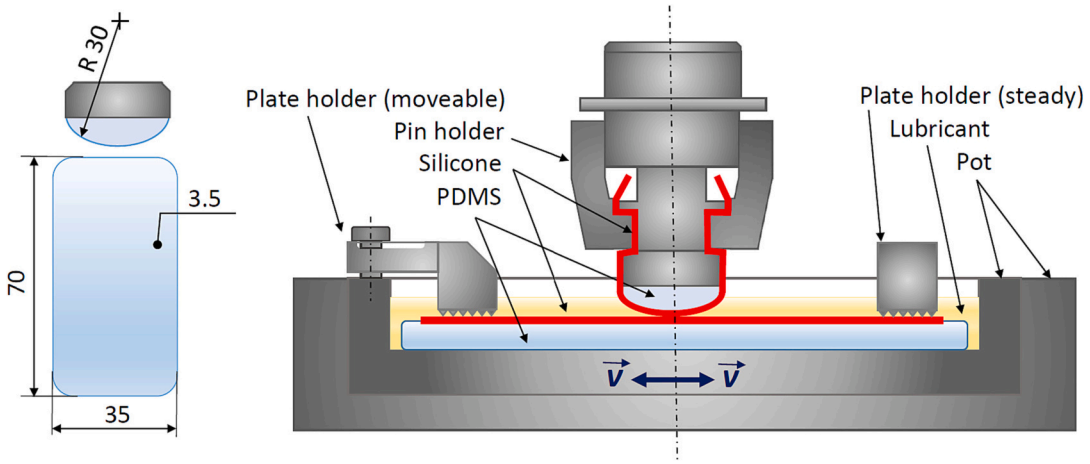

Fig. 2. Detail of the contact samples (left); scheme of the experimental configuration (right).

two characteristic product ions were monitored.

2.5. Preparation of HA solutions

High molecular weight HA (HMW HA, Mw = 1444.7 ± 13.0 kDa, Mn/Mw = 1.639 ± 0.031) and low molecular weight HA (LMW HA, Mw = 312.4 ± 6.2 kDa, Mn/Mw = 1.711 ± 0.038) were provided by Contipro a.s. (Czech Republic). Mw and polydispersity (Mn/Mw) were measured by SEC-MALS (miniDAWN TREOS, Wyatt). HA solutions were prepared in normal saline (0.9 % NaCl) or phosphate-buffered saline (PBS) at a concentration of 10 and 20 mg/ml, sterilized by filtration and for the biological test, the endotoxin levels were measured by Endosafe NexGen-PTS, and only apyrogenic samples (endotoxin levels <0.1 IU/ml) were used for testing.

2.6. Evaluation of rabbit thoracolumbar fascia mechanical and viscoelastic properties

The mechanical and viscoelastic properties of partial-thickness samples of rabbit deep TLF were determined using a Discovery Hybrid Rheometer - 3 equipped with a dynamic mechanical accessory with a humidity chamber (TA Instruments). Freshly dissected TLF was transported at 2–8 °C placed between two PBS-soaked medical grade towels and further processed within 2 h. Tissue was cut into rectangular pieces with dimensions 3 × 1 cm (max. 3 samples were prepared from one TLF). Individual samples of the tissue were placed between two solid rectangular fixtures and the initial gap was set to 1 cm.

The stress-strain curves of the tissue samples were measured in the humidity chamber at a temperature of 37 °C and relative humidity of 95 %. All samples were conditioned for at least 5 min to reach the equilibrium state before the tensile test was set to begin. After sample conditioning, stress emerged due to humidity and temperature changes, and was offset to zero. Tensile measurements were carried out uniaxially at a constant linear rate of 250 μm/s. The results were calculated as average values and the standard deviations were counted. The relation between stress and strain was evaluated, including the calculation of ultimate tensile strength (UTS), force, and ultimate deformation.

Oscillation frequency tests were performed to determine the viscoelastic properties of fascia samples incubated for 18 h in PBS (negative control) and 1 % LMW HA. Facia samples incubated for 18 h without any tested solution (at 95 % humidity) were used as the nonincubated control to evaluate the effect of tissue swelling on its viscoelastic properties. All samples were conditioned for at least 5 min at a temperature of 37 °C and relative humidity of 95 %. Subsequently, the initial deformation force (stress) was set to 0.5 N and 5.0 N to describe the properties of the fascia at different stress levels. Measurements were performed at a constant axial displacement of 25 μm (strain 0.25 %) over a frequency range of 1–10 Hz. The results were calculated as average values and the standard deviations were counted. A minimum of 6 fascia samples from 3 different animals were used in measurements.

2.7. Evaluation of rheological properties of HA solutions

The rheological properties of HA solutions were determined using a Discovery Hybrid Rheometer - 3. The viscosity of samples was measured using a stainless-steel cone geometry (60 mm diameter cone with a 1° cone angle) at a temperature of 25 °C. Experiments were performed under steady shear conditions and the viscosity was evaluated as a function of the shear rate applied to the tasted samples over the range of 0.01 to 3000 s^{-1}. All samples of HA solutions were equilibrated for 2 min before each measurement. After equilibration, the dependency of viscosity on shear rate was laid down and resulting viscosity flow curves were plotted on a logarithmic scale. All performed measurements were repeated at least three times with new samples. Zero shear rate viscosity of HA solutions was calculated by using the Careau-Yasuda model via TRIOS software. The results were calculated as average values (+/- the standard deviations).

2.8. Injection force measurements

Injection force and pressure were measured using a universal test machine (Single Column Materials Testing System Instron 3342) in compression mode. The HA solutions were transferred into 3 ml syringes with an inner diameter of 8.9 mm (Mediware servoprax GmbH). A needle of 25 G × 40 mm (Neopoint servoprax GmbH) was attached to the syringe for the measurements. The testing speed was set to 10 $mm{\cdot}min^{-1}$. The Instron device with a compression plate measured the injection force subjected to the plunger with a maximum load capacity of 500 N. The plunger displacement and the injection force were recorded by the software Bluehill. Maximum and average values of the injection force and pressure were evaluated. All performed measurements were repeated at least three times. The results were calculated as average values (+/- the standard deviations).

2.9. Tribological measurements of HA solutions

The friction experiments were carried out using the commercial tribometer Bruker UMT TriboLab and the experimental configuration consisted of the pin and the plate. The pin was fixed in a top mount holder, which is stationary. It has a convex surface shape, being 30 mm wide and having a radius of curvature of 30 mm. The plate is flat, 3.5 mm thick, 35 mm wide, and 70 mm long. It is mounted in a bottom

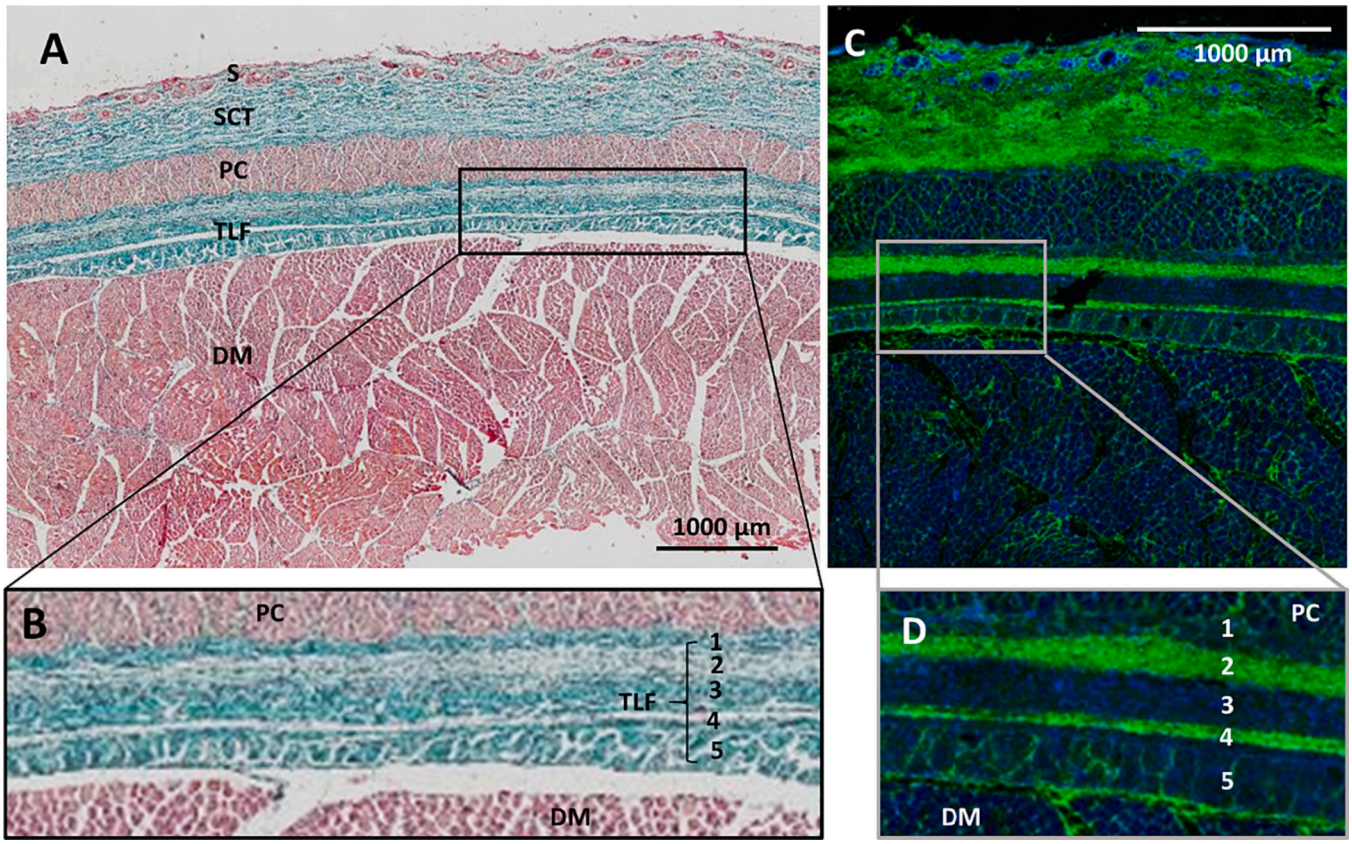

Fig. 3. Histology of rabbit deep TLF. (A, B) Masson's trichrome staining of full-thickness samples from rabbit back. S, skin; SCT, subcutaneous tissue; PC, panniculus carnosus; TLF, deep thoracolumbar fascia; DM, dorsal muscle. (C, D) HA detection by fluorescent HABP. Green, HA; blue, nuclei. (B, D) details of TLF, with five distinct layers. Layer 5 is consistent with the epimysium, layers 1 and 3 are another two dense collagen-rich layers while layers 2 and 4 represent HA-rich loose connective tissue layers of TLF.

holder, which undergoes a reciprocating motion. The contact of two soft fascia tissues connected to the muscles beneath was substituted by the contact of polydimethylsiloxane (PDMS) with thin silicone layers attached to the bottom of the pin and the same materials representing the plate itself. The scheme of the experiment is shown in Fig. 2.

The effect of HMW HA and LMW HA on resulting friction within the contact was tested at room temperature. PBS was used as a reference fluid. The applied vertical (normal) load maintained by the pin was set to 2 N, which results in the contact pressure of 95 kPa, which was revealed thanks to finite element method analysis. Each experiment lasted 300 s, while the stroke length was set to 16 mm. The experiments were carried out at a frequency of 1 Hz (sliding speed of 16 mm/s). Each experiment was repeated five times, enabling a basic statistical evaluation.

2.10. Gene expression in ex vivo fascia

Freshly dissected partial-thickness samples of deep TLF was transported at 2–8 °C placed between two PBS-soaked medical grade towels and further processed within 2 h. TLF tissue was placed on a sterile Petri dish with PBS and cut into pieces (5 mm × 5 mm). Those were placed in the 24well culture plate (1 fascia sample per well) and were submerged in the cultivation media (0.9 ml). In selected wells, 0.1 ml of HA solutions (1 % in physiological saline) was added. Fascia samples were cultivated at 37 °C, 5 % CO2, and 95 % humidity for 24 h. The 20 ng/ml TGFβ1 was used as a positive control of the profibrotic switch in fascia tissue. 0.1 ml of saline was used as a negative control.

After 24 h incubation, the samples were washed in sterile PBS and then homogenized (TissueLyser II, Qiagen). Total RNA was isolated using the RNeasy isolation kit (Qiagen). The RNA concentration and quality were assessed spectrophotometrically (NanoDrop One, ThermoFisher Scientific). cDNA synthesis was carried out using SuperScript III First Strand Synthesis System (Thermo Fisher Scientific). Primers for qPCR were synthesized by Generi Biotech (Czech Republic) and their sequences are in Table S1. The Power SYBR Green PCR Master Mix (Thermo Fisher Scientific) was used in qPCR reactions performed in QuantStudio Real-Time PCR (Applied Biosystems). Data were normalized to ACTB mRNA levels, and gene expression fold change was calculated using the $2^{-\Delta\Delta CT}$ method. The statistical significance of the differences between the treated and negative control samples (each $n = 3$) was compared using Student's *t*-test (Excel, Microsoft Office).

2.11. Injecting TLF of rabbit cadavers with hyaluronan

To prove the possibility to apply the HMW HA or LMW HA in the proper layer of the TLF, the rabbit cadavers (see Chapter 2.1) with intact fascia were divided into two groups. The applied solutions were dyed blue utilizing Toluidine blue stain, for better visualization. Before injection, beginning the L2-3 intervertebral space was manually identified by counting the vertebral spinous processes starting from the sacrum.

The rabbits in the first group were skinned, and after exposing the TLF the space between the superficial and deep layers of deep TLF was injected with 1 ml of 2 % HMW HA or 1 % LMW HA via a needle of 25G in diameter under the direct eye view. The application sites were then manually massaged to evaluate the ability of HA to spread between fascial layers.

In the second group, the rabbits were shaved on their backs and using the 25G needle under the US guidance were intrafascially injected with 1 ml of HMW HA or LMW HA. App-based ultrasound device Philips Lumify ultrasound system with linear array transducer Philips Lumify

Table 1
The amount of endogenous HA in rabbit TLF.

Tissue	HA content (μg HA/g of tissue)
TLF	411.9 ± 72.8
muscle (without epimysium)	12.8 ± 1.9
skin (including subcutaneous tissue)	561.6 ± 83.7

The uncertainty of HA concentration comes from method validation [10].

L12–4 Android (Philips Ultrasound, Inc., USA) connected to tablet has been used. The US probe was operated in a sagittal plane and glided laterally left approximately one centimeter, maintaining the top of the image in a cephalad position.

3. Results and discussion

3.1. Rabbit as a model of TLF physiology

TLF's role in proper posture and movement is critical and its pathological changes, e.g. densification, are connected to various pathologies including the LBP. The study of TLF is due to its anatomically complex but also structurally thin and planar nature rather difficult. Nowadays, the most common animal models to study TLF in vivo are mice [11], rats [12], and pigs [13]. Small animals allow studying various pharmacological interventions (topical and systemic) due to their relatively low cost and ease of manipulation. Pigs are on the other hand better suited to act as a close anatomical models of human TLF due to their size, e.g. TLF injury was modeled and examined via US in pigs [13], but are hard to handle and costly. In this work, we have for the first time used a rabbit as a broadly available animal model (due to relatively small size, ease of handling and low cost) and described the morphological structure of rabbit TLF. Of course, the main limitation of any animal model, including the rabbit, is their different anatomic structure compared to the human connected to the unique human posture and bipedalism [14].

3.1.1. Histological evaluation of rabbit TLF

Rabbit TLF is a multilayered wide sheet of tough, white fascia covering the thoracolumbar region (Fig. 1A). The TLF is divided by the spine into the left and right portions, and the spine and TLF are firmly connected. Ventrali the TLF is connected with the external and internal oblique muscles, musculus latissimus dorsi, and inferior trapezius. While there is currently no detailed analysis of rabbit fascial anatomy published, it is reasonable to assume that it may share a similar basic arrangement in the thoracolumbar region, as has been extensively described for humans, horses, and dogs. In a study by Ahmed et al. [15], where the thoracolumbar fascia in horses and dogs exhibit a comparable three-layered orientation, with the two more superficial layers attaching to the spinous processes and the deepest layer attaching to the transverse processes. Further research is needed to determine whether the fascial anatomy of the lumbar region in rabbits differs significantly or not compared to other mammals.

Histology of a full-thickness sample of rabbit low back revealed that deep TLF from lumbar region is present between erector spinae and subcutaneous musculus panniculus (Fig. 3A). Deep TLF itself consists of three layers of dense connective tissue with high collagen content (based on MT staining). The deepest layer is consistent with the description and function of epimysium as it is connected to the dorsal muscle underneath. This layer is segmented and interwoven with HA (Fig. 3C, D). Between dense layers, two HA-rich layers are present. Except for epimysium, TLF's dense layers are mobile and are gliding on each other.

Overall, the macroscopic and microscopic structure of rabbit TLF is very close to the structure of the human TLF [16].

3.1.2. HA content in rabbit TLF

The high HA content in rabbit TLF was confirmed by LC-MS analysis. The full-thickness sample of shaved rabbit back was divided into three separate samples: deep TLF (including the epimysium), the underlying back muscle (without epimysium), and the skin and subcutaneous tissue (including superficial fascia and panniculus carnosus). Table 1 shows that HA content in deep TLF was very similar to the HA content in skin and surrounding tissues, while the dorsal muscle itself contains only a small amount of HA. Values for skin and muscle are consistent with previously reported HA concentration in rabbit skin (500 μg/g of tissue) and muscle (27 μg/g) by Armstrong and Bell [17] and Laurent and Tengblad [18], respectively. The rabbit TLF is very rich in HA, at least in comparison to the analysis of human fascia by Fede et al. [5]. Differences between rabbit and human TLF can be caused by the different needs for load-bearing in rabbits and humans and by the differences in fascia sampling and analytical techniques.

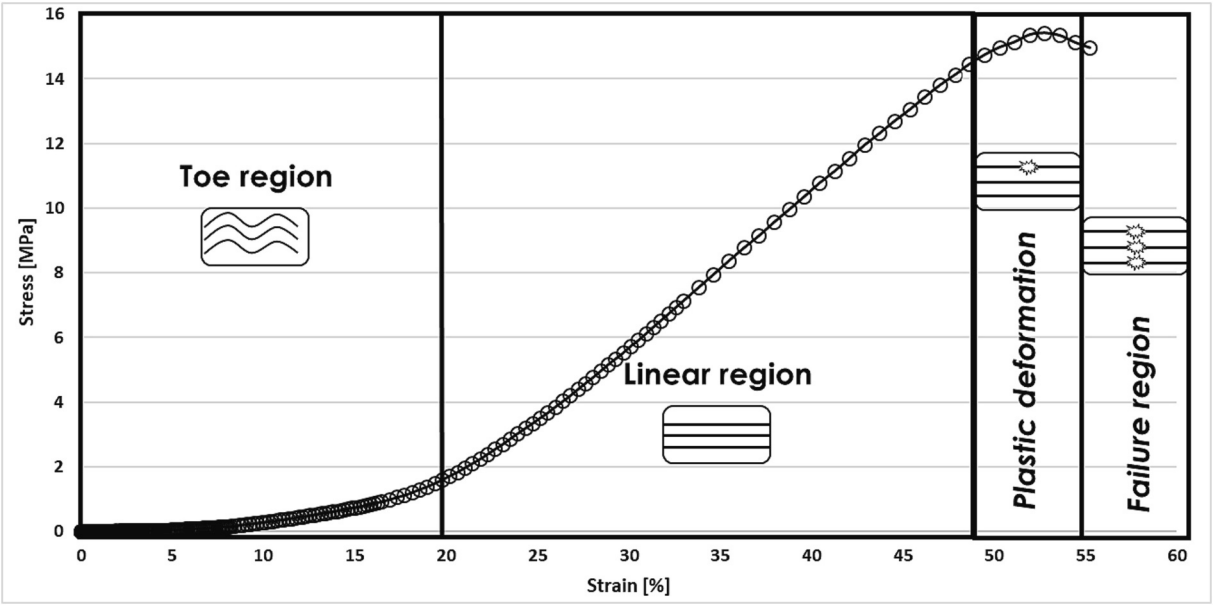

Fig. 4. Stress-strain curve of a representative sample of the rabbit TLF.

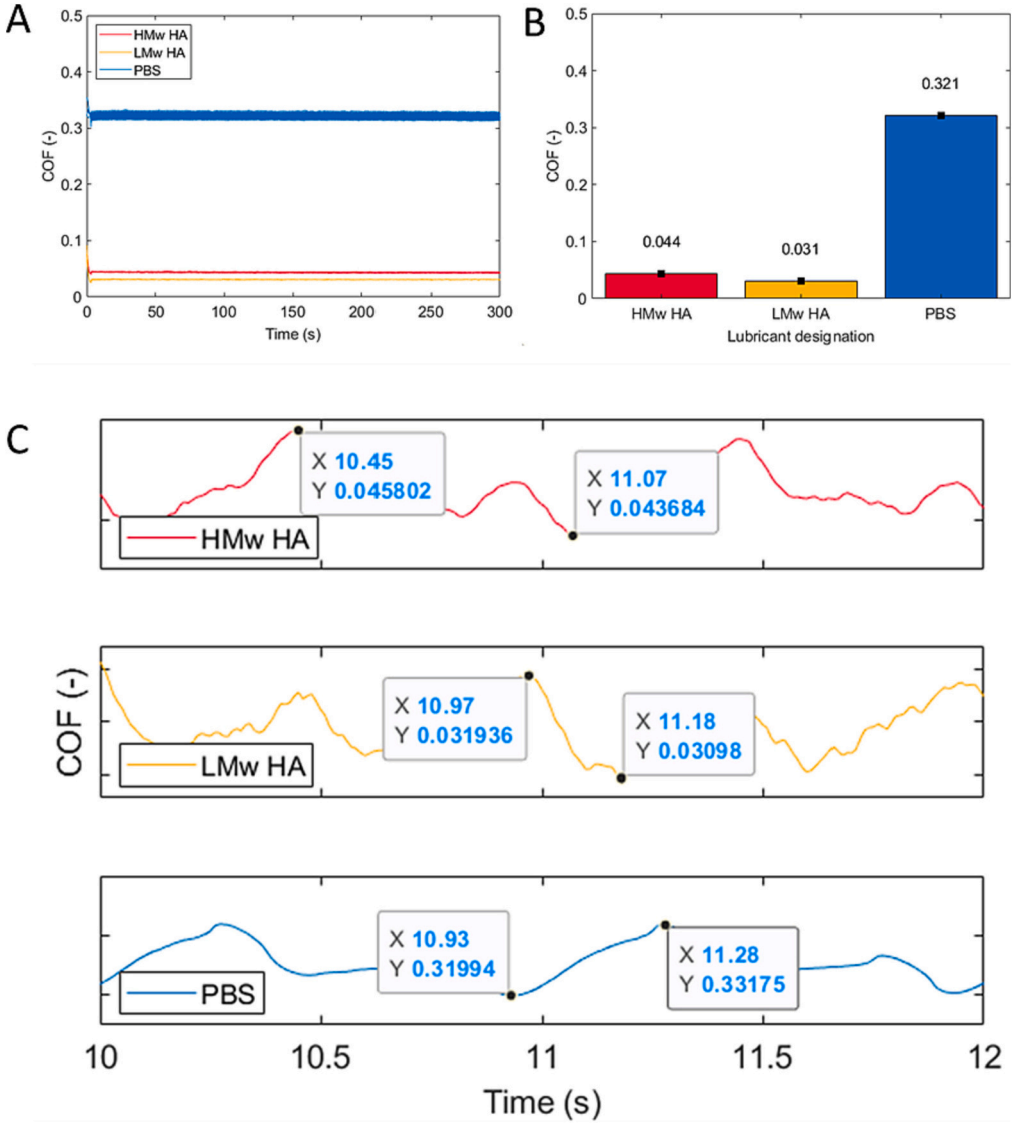

Fig. 5. Friction curves. (A) Development of COF - friction curves. (B) Barplots of average values of COF. (C) Details of amplitudes of each friction curve with peak data points for HMW HA, LMW HA, and PBS.

3.1.3. *Mechanical properties of rabbit fascia*

First, the tensile tests were conducted to evaluate the basic properties of tissue. The typical stress-strain curve of rabbit fascia is illustrated in Fig. 4. It is worth noting that mechanical analysis was performed only with the partial-thickness TLF which is missing the lowest epimysial layer tightly connected to the muscle underneath. This method was chosen since the process of muscle tissue removal from TLF caused major damage to the TLF and increased the variability of measurement significantly.

The obtained stress-strain curve is typical for soft tissues, such as tendons and fascia [19–21]. The toe region is a non-linear part of the curve which is characterized by the stretching of fascia collagen fibers. In the linear region, the collagen fibers orient themselves in the direction of the mechanical tensile load and begin to stretch. The deformation is elastic (reversible) and fascia samples return to their initial length when unloaded. Plastic deformation describes the level of strain when the load exceeds the physiological limit of fascia and inter- and intramolecular bonds between the structure molecules fail, which leads to irreversible deformation. Obtained results are very similar to the mechanical properties of human crural fascia described by Stecco et al. [22] including the overall behavior of the material and the yield point, however, the linear region of rabbit TLF was longer. In comparison with human lumbodorsal fascia properties [23], rabbit TLF was significantly less stiff, which might be due to the nature of the sample origin (old human cadavers vs young rabbits). Average ultimate tensile strength (21.4 ± 4.3 MPa), ultimate tensile force (32.1 ± 6.5 N), and ultimate deformation (58.2 ± 15.5 %) of rabbit TLF were determined. As only the partial-thickness TLF samples were used for the tensile measurement, we have chosen the uniaxial mode of measurement based on the orientation of the fiber present in the samples. Main source of variability in the tensile measurement was exact localization of sample which probably corresponds with the TLF layer thickness changes along the studied area.

3.2. *Intrafascial application of LMW HA*

HA is used intraarticularly in orthopedics to alleviate joint pains in osteoarthritis patients. Viscosupplementations are usually based on HMW HA or crosslinked chemically modified HA to ensure the highest level of high viscosity, cushioning, and lubrication [24]. Off-label use of HA viscosupplementation has been also reported in plantar fascitis [8,25,26]. On the other hand, the densification of TLF has been connected to the changes in HA content and MW. The viscous HMW HA can

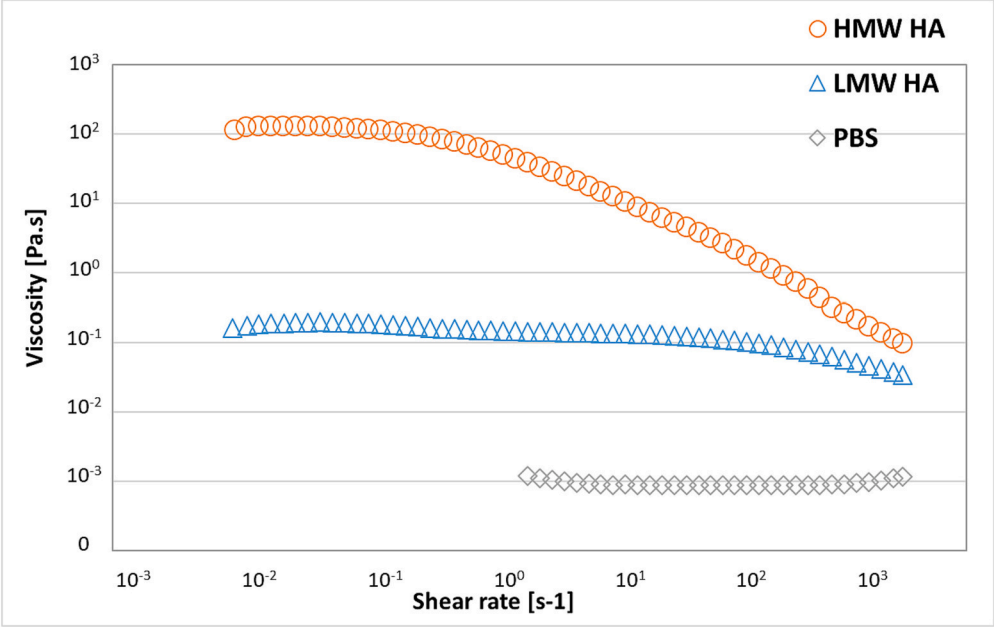

Fig. 6. Viscosity curves of HMW HA, LMW HA, and PBS (control).

be also difficult to apply between the fascial layers. For this reason, we have utilized the solutions of 1 % LMW HA and tested its tribological, rheological, and safety profiles.

3.2.1. *Tribological evaluation of HA solutions*

The tribological experiments were carried out considering the linear reciprocating motion to mimic the realistic fascia motion. From the geometrical point of view, the deep fascia represents a couple of planes sliding against each other. Hence, the experimental configuration consists of the pin and the plate, representing an established biotribological approach described by Streďanská et al. [27]. Considering the contact mechanics, it is evident that fascia is a very soft material. It is challenging to investigate natural biological soft tissues since these are usually non-uniform in terms of structure, thickness, and material properties.

First, the coefficient of friction (COF) of the HMW and LMW HA solutions was measured to evaluate the hypothesis that the LMW solution would be a superior lubricant [28]. While commercially available HMW HA preparations are often more concentrated, the concentration of both HA solutions was fixed at 1 %, as the concentration of HA is a crucial parameter affecting its frictional behavior. The results of COF depending on MW together with the friction of referential PBS are shown in Fig. 5, which illustrates that lowering the MW has a positive impact on friction. It is just opposite to friction tests of the cartilage-cartilage interface, where HMW HA is more effective with the formation of a viscous layer to reduce static friction [29]. However, in compliant contact, while HMW causes high viscosity of the lubricant, friction potentially grows [30,31].

The LMW HA and HMW HA solutions exhibited COF values around 0.031 and 0.044, respectively (Fig. 5B). In both HA solutions, there is a slight drop to lower values in the beginning, while an intact lubricating film covers the silicone surface. After the decline, the COF increased and started to oscillate around its average value in the long-term range. The friction coefficient for the reference fluid is considerably higher compared to HA solutions, as there are no molecules of HA, while similar behavior was observed by Yakubov et al. [32]. Furthermore, in PBS, a substantial drop at the beginning of the test was not observed. Instead, the friction curves remained constant and stable, showing a larger repeated deviation (Fig. 5C).

Table 2
Maximum pressure and force, average pressure, and dynamic glide force (DGF) determined during extrusion of HMW HA, LMW HA, and PBS.

Sample	Maximum pressure [kPa]	Average pressure [kPa]	Maximum force [N]	Dynamic glide force (DGF) [N]
PBS	40.95 ± 4.96	26.06 ± 1.92	2.55 ± 0.31	1.62 ± 0.12
LMW HA	189.69 ± 2.11*	188.31 ± 2.05*	11.80 ± 0.13*	11.71 ± 0.13*
HMW HA	361.33 ± 1.66*#	359.88 ± 1.78*#	22.48 ± 0.10*#	22.39 ± 0.11*#

n = 3, * $p < 0.001$ comparing the LMW and HMW solutions to the PBS, # $p < 0.001$ comparing the LMW and HMW solutions (Student's *t*-test).

3.2.2. *Viscosity and injection force of HA solutions*

Injectability and viscosity are two of the most important physicochemical parameters of parenteral dosage forms. The viscosity of LMW HA solution (10 mg/ml) which was considered a suitable solution for intrafascial injection, was compared with HMW HA solution (20 mg/ml) representing commercially available preparations used in treating plantar fasciitis [25,26], and PBS. The viscosity curves of HMW HA, LMW HA, and PBS are shown in Fig. 6. Samples of HMW HA and LMW HA exhibit non-Newtonian shear-thinning behavior and PBS behaves like a Newtonian fluid.

Using the Careau-Yasuda model, HMW HA has been shown to have the highest viscosity with a zero-rate viscosity value of 136.52 ± 2.23 Pa·s, which is 10^3-fold higher than the viscosity of LMW HA solution (0.197 ± 0.050 Pa·s), and 10^5-fold higher than PBS (0.001 ± 0.00001 Pa·s).

The observed difference in viscosity among the samples is due to the fact that high MW and concentration of HA contribute to intermolecular entanglement formation.

The injection force of the samples was determined by using one of the most common needle sizes (25G) for subcutaneous dosing [33]. The results of the injection force measurements are illustrated in Fig. S1. 2 % HMW HA solution required the highest force to extrude by a 3 ml syringe with a 25G needle. The force needed to extrude the 1 % LMW HA solution was two-fold lower and the PBS solution without HA required a ten-fold lower extrusion force compared to the HMW HA.

Maximum pressure and force, average pressure, and dynamic glide

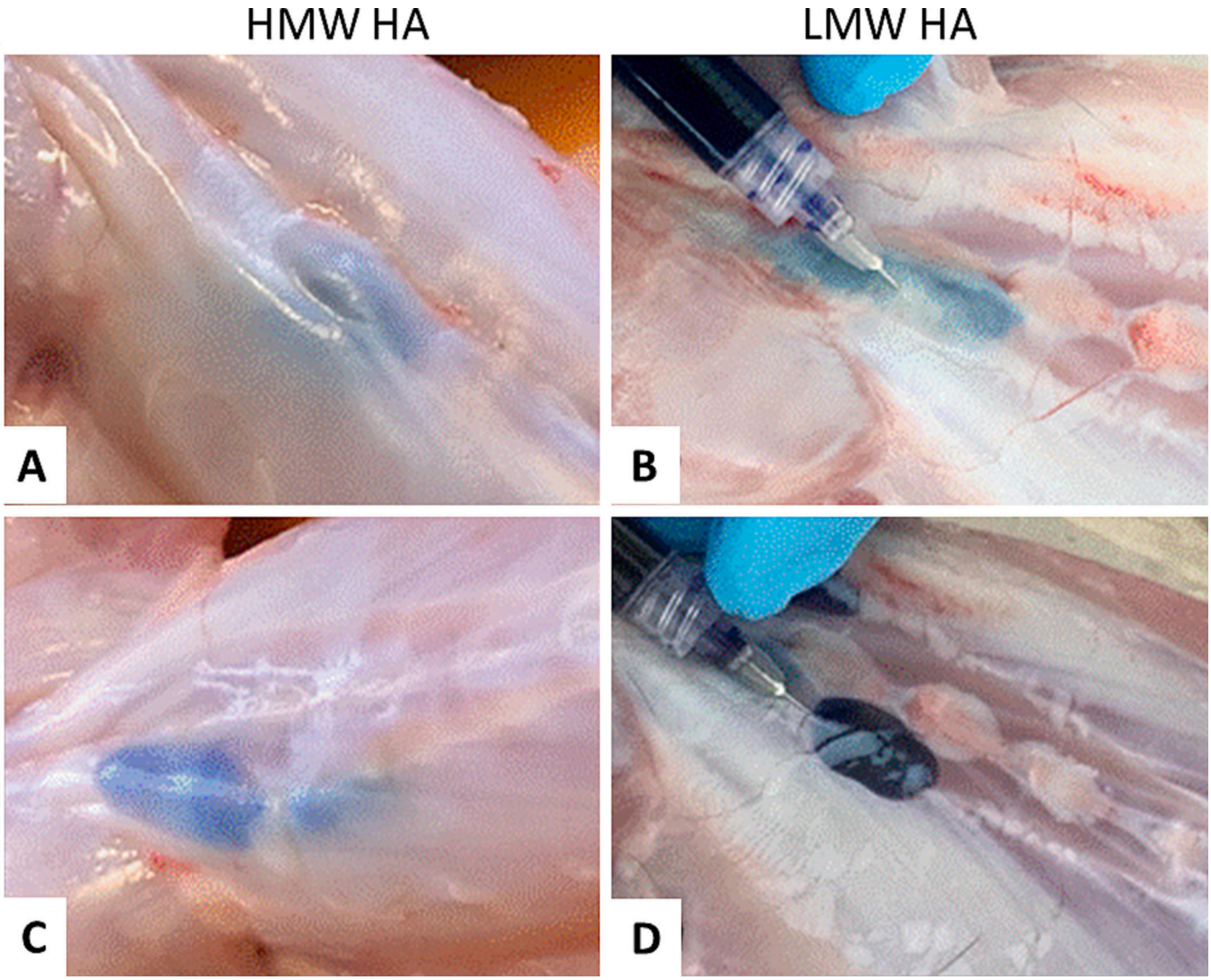

Fig. 7. Application of HA solutions (stained with toluidine blue) into deep TLF of rabbit cadaver. (A, C) HMW HA and (B, D) LMW HA were injected between (A, B) deep and middle dense layers of TLF or between (C, D) middle and superficial dense layers of TLF.

force (DGF) determined during the extrusion of HMW HA, LMW HA, and PBS are summarized in Table 2. All measurements were performed in triplicate and results were evaluated as average values. The average maximum force that can be performed with the thumb pushing on the plunger is 79.8 N [34], but clinically relevant injection forces are typically <20 N, while the maximum acceptable injection force is 40 N [35]. In the case of intrafascial injections which should be performed under ultrasound guidance, the injection force of ~20 N can be problematic.

Table 3
G′ of rabbit TLF.

Sample	Initial deformation force 0.5 N		Initial deformation force 5 N	
	G′ (2.5 Hz) [MPa]	tan δ (2.5 Hz)	G′ (2.5 Hz) [MPa]	tan δ (2.5 Hz)
Non-incubated fascia samples	58.8 ± 16.6	0.075 ± 0.021	259.5 ± 19.4	0.060 ± 0.005
Fascia samples incubated in PBS	40.7 ± 11.6	0.073 ± 0.024	252.5 ± 23.1	0.055 ± 0.10
Fascia samples incubated in HA	40.4 ± 5.6	0.116 ± 0.050	303.5 ± 33.6*	0.067 ± 0.014

$n = 6$. * $p < 0.05$ the fascia samples incubated in PBS compared to the non-incubated samples at the initial deformation force of 5 N (Student's *t*-test).

DGF of PBS solution which does not contain any dissolved polymer is low, and for a 3 ml syringe, it is 1.62 ± 0.12 N. In the case of LMW HA solution DGF for a 3 ml syringe is much higher than for PBS, 11.71 ± 0.13 N, but comfortably under the limit of 20 N. HMW HA solution has the highest DGF of 22.39 ± 0.11 N, which exceeds the limit and therefore is not suitable for intrafascial injection.

The effect of HMW HA's high viscosity is also prominent in injectability experiments. Both LMW and HMW HA solutions have been successfully injected intrafascially in both loose connective tissue compartments of TLF (Fig. 7). When applying the HMW HA we noticed that the applied solution formed a bolus (Fig. 7A, C), and even using the manual massage we did not reach a homogeneous spreading of the HMW HA in between the TLF layers. In contrast, the LMW HA spread in between the layers spontaneously during application (Fig. 7B, D) and manual massage spread LMW HA and covered the whole area of the TLF layer (Video S1). HMW HA solution is not suitable for intrafascial injection because it tends to form a mass that distributes very slowly in between the layers.

3.2.3. Ex vivo evaluation of the effect of LMW HA on the fascia characteristics

Viscoelastic properties of rabbit partial-thickness deep TLF and the effect of LMW HA on them were measured by DMA. The initial

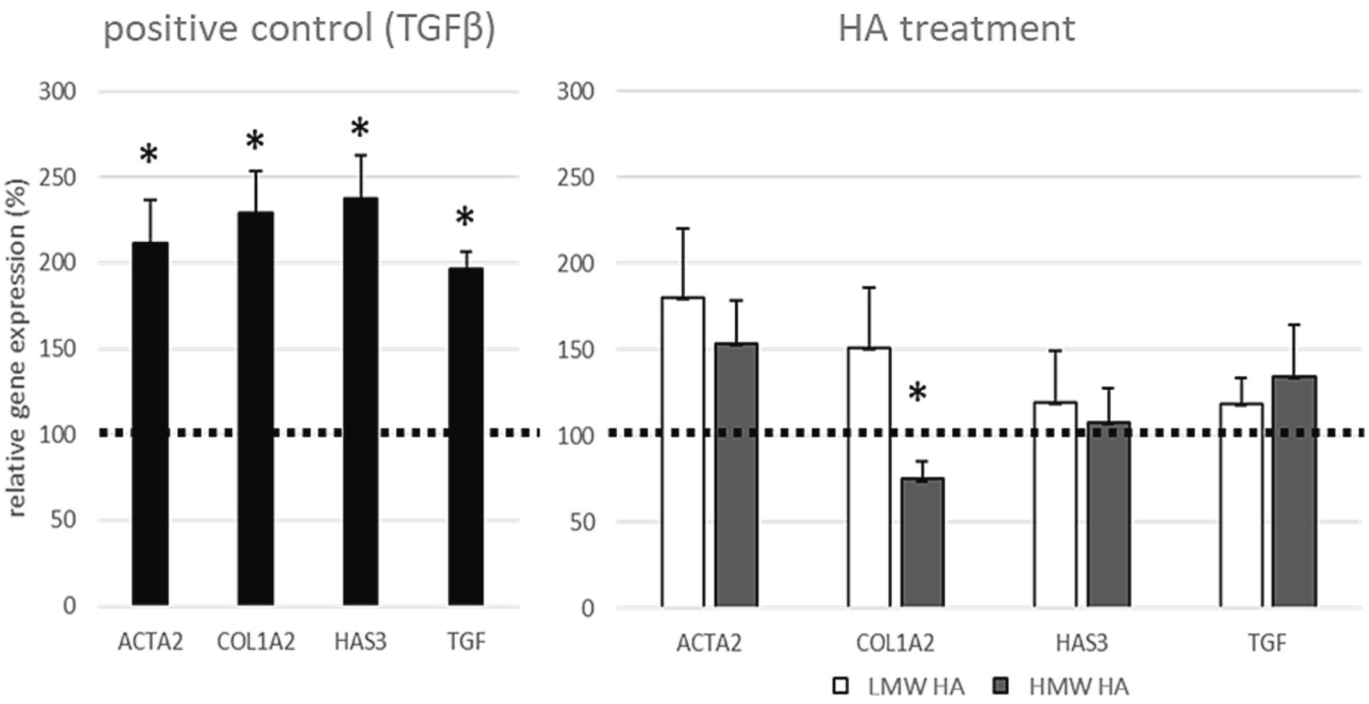

Fig. 8. Changes in gene expression after cultivation TLF with HA solutions. TGFβ was used as a positive control and a statistically significant increase was detected in all analyzed genes (ACTA2, COL1A2, HAS3, and TGF). HA solution of neither Mw (LMW and HMW HA) did not cause similar changes in fascial fibrosis-related gene expressions. $N = 3$, error bars represent S.E.M. * $p < 0.05$.

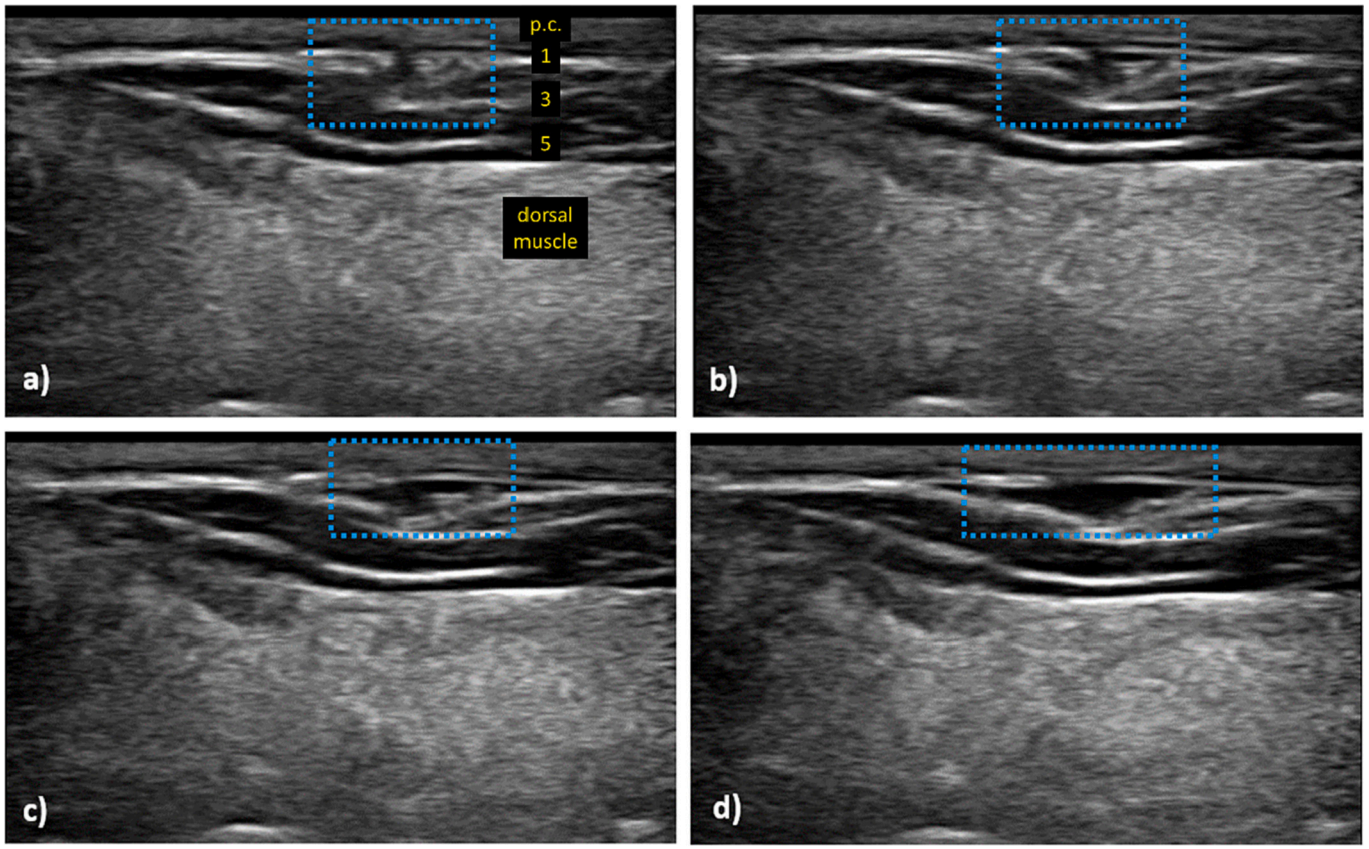

Fig. 9. Application of HA guided via US visualization, during which time it can be observed the superficial and deep fascial layers being separated by the formation of an anechoic pocket created by HA (blue rectangle). a) The individual TLF layer is labelled same as in the histological evaluation (Fig. 3).

deformation force for DMA analysis was set to 0.5 N and 5.0 N, which correspond to the toe region at almost zero load and the elastic region at physiologically acceptable load, respectively. The goal was to determine the viscoelastic properties of rabbit fascia under conditions close to physiological. For these purposes, frequency sweep experiments were carried out. Elastic (G′) and viscous (G″) moduli of fascia samples were studied by oscillatory test at a constant axial amplitude of 25 μm over a frequency range of 1–10 Hz (Fig. S2), the physiological frequency range of the knee joint during movement [36]. The frequency range for TLF during movement is not known, but it can be assumed that as a part of the body's load-sharing systems the frequency during movement should be similar in TLF. G′ and tan δ at a frequency of 2.5 Hz (the knee joint movement during running [36] and initial load 0.5 N and 5 N) were determined (Table 3). The observed results showed that G′ determined at initial load 5 N is 5 times higher than G′ determined at initial load 0.5 N for all samples, suggesting that rabbit fascia samples exhibit more elastic behavior at higher frequencies. These results showed that fresh rabbit fascia samples incubated in PBS and LMW HA solution exhibit similar viscoelastic properties at an initial load of 0.5 N. Whereas non incubated samples have slightly higher G′. When the load was increased to 5 N no difference can be seen between non-incubated samples and samples incubated in PBS, but G′ of samples incubated in LMW HA solution had significantly higher G′. Based on this it can be assumed that HA can increase the elasticity of fascia tissue. The HA (probably in its HMW form, Mw >1000 kDa) is a normal and abundant component of animal and human fascia. Its increased production has been implicated in fascia densification and fibrosis [6]. On the other hand, the exogenously added purified HA can also act as a lubricant enabling the sliding and normal function of fascial layers. The treatment of partial-thickness deep TLF by exogenously added LMW HA or HMW HA didn't cause any significant changes in the expression of genes connected to the pro-fibrotic signalling. In Fig. 8, the gene expression of α-smooth muscle actin (ACTA2) [37], type 1 collagen (COL1A2) [38], hyaluronan synthases 3 (HAS3) [39] and endogenous TGFβ [11] in ex vivo fascia treated with human TGFβ was significantly increased. Type 3 collagen was also assessed but its expression hasn't been detected in any fascia sample (data not shown). These effects haven't been observed after ex vivo TLF incubation with HA (either LMW or HMW). The presence of HA itself does not induce a profibrotic process in the fascia. The HA accumulation in fascia pathologies is probably the result of pro-inflammatory and pro-fibrotic activities of different bioactive molecules and exogenous HA should be safe in fascia treatment.

3.3. Proof-of-concept of the US-guided intrafascial injection of LMW HA

Based on the above-described data we have prepared the model medical device based on the 1 % LMW HA in the 3 ml syringe equipped with the 25G needle. Approximately 1 ml of this preparation was then injected intrafascially in the rabbit deep TLF at the level of L2-3 under the US visualization to the virtual space between the first and second dense layers of the deep TLF (Fig. 9). A discrete anechoic space could be observed developing during the application of the HA between the superficial and deep layers of the L2-3 TLF. Even in much finer fascial tissue in rabbits, it was possible to achieve the intrafascial application of 1 % LMW HA. US-guided intrafascial injection has been already used in the treatment of LBP and other myofascial pain in patients. 5–10 ml of physiological saline has been applied by the 25G needle under US guidance [40] as was a 15 ml solution of levobupivacaine and triamcinolone [41]. This type of intervention is often used to administer a bolus which should decrease the myofascial pain, in our case we hypothesized that the application of a highly lubricating natural component of loose connective tissue between dense fascial layers can lead to a better gliding fascial layer onto each other and relief from the myofascial pain without necessary creation of bolus which can further damage the fine mesh of loose connective tissue of TLF. By using the natural and relatively low concentrated preparation of HA we can also avoid the risk of chemically induced fascial LBP [42]. This assumption must be confirmed on a larger number of animals and the influence of HA concentration and Mw should be tested in preclinical tests.

There are several limitations of presented study, which should be addressed in following research. No comprehensive fascial anatomy of rabbits has been published up to date which complicates the extrapolation of presented data to the other animals and/or humans. Also, only fresh fascia from cadavers was measured and no pathology was induced in rabbit which limits the efficacy evaluation of the proposed intervention.

4. Conclusion

In this study we have for the first time shown that the deep aponeurotic fascia is injectable with hyaluronan under US guidance. Utilizing a novel combination of molecular biology and analysis of mechanical properties of both the TLF and HA solution we have established that specific properties of HA do matter for the intrafascial application. HA injected into connective tissue is safe, the efficacy of this treatment approach to low back pain of myofascial origin will yet need to be tested in a clinical setup. This intrafascial injection was performed on the rabbit cadaver which was used as a suitable model for a proof-of-the-concept study of TLF intervention and thanks to our description of rabbit TLF composition, it has been established as an alternative animal model in fascia research and treatment development.

Supplementary data to this article can be found online at https://doi.org/10.1016/j.ijbiomac.2023.126879.

CRediT authorship contribution statement

Kristina Nešporová: Methodology, Investigation, Formal analysis, Writing – original draft, Visualization, Writing – review & editing. **Jana Matonohová:** Methodology, Investigation, Formal analysis, Writing – review & editing. **Jarmila Husby:** Conceptualization, Methodology, Investigation. **Evgeniy Toropitsyn:** Methodology, Investigation, Formal analysis, Writing – original draft. **Lenka Divoká Stupecká:** Methodology, Investigation. **Aaron Husby:** Investigation. **Tereza Suchánková Kleplová:** Methodology, Investigation. **Alexandra Streďanská:** Methodology, Investigation, Formal analysis. **Matěj Šimek:** Investigation, Formal analysis. **David Nečas:** Investigation. **Martin Vrbka:** Supervision. **Robert Schleip:** Conceptualization, Writing – review & editing. **Vladimír Velebný:** Supervision.

Declaration of competing interest

The authors declare the following financial interests/personal relationships which may be considered as potential competing interests: Robert Schleip reports a relationship with Contipro a.s. that includes: consulting or advisory and paid expert testimony. Vladimir Velebny reports a relationship with Contipro a.s. that includes: board membership and equity or stocks.

Data availability

No data was used for the research described in the article.

Acknowledgement

This project (Fascia lubrication and regeneration by hyaluronan) has received funding from the Operational Programme Enterprise and Innovations for Competitiveness 2014–2020 (OPEIC) under agreement No CZ.01.1.02/0.0/0.0/19_262/0020005.

References

[1] F. Fatoye, T. Gebrye, I. Odeyemi, Real-world incidence and prevalence of low back pain using routinely collected data, Rheumatol. Int. 39 (4) (2019) 619–626.
[2] J. Wilke, et al., The lumbodorsal fascia as a potential source of low back pain: a narrative review, Biomed. Res. Int. 2017 (2017), p. 5349620.
[3] C. Stecco, et al., Hyaluronan within fascia in the etiology of myofascial pain, Surg. Radiol. Anat. 33 (10) (2011) 891–896.
[4] P.G. Pavan, et al., Painful connections: densification versus fibrosis of fascia, Curr. Pain Headache Rep. 18 (8) (2014) 441.
[5] C. Fede, et al., Quantification of hyaluronan in human fasciae: variations with function and anatomical site, J. Anat. 233 (4) (2018) 552–556.
[6] E.J. Hughes, K. McDermott, M.F. Funk, Evaluation of hyaluronan content in areas of densification compared to adjacent areas of fascia, J. Bodyw. Mov. Ther. 23 (2) (2019) 324–328.
[7] J. Hermans, et al., The effectiveness of high molecular weight hyaluronic acid for knee osteoarthritis in patients in the working age: a randomised controlled trial, BMC Musculoskelet. Disord. 20 (1) (2019) 196.
[8] T. Kumai, et al., Short-term efficacy and safety of hyaluronic acid injection for plantar fasciopathy, Knee Surg. Sports Traumatol. Arthrosc. 26 (3) (2018) 903–911.
[9] R. Sinova, et al., Anti-HA antibody does not detect hyaluronan, Glycobiology 31 (5) (2021) 520–523.
[10] M. Simek, et al., LC-MS/MS study of in vivo fate of hyaluronan polymeric micelles carrying doxorubicin, Carbohydr. Polym. 209 (2019) 181–189.
[11] M.E.D. Franca, et al., Manipulation of the fascial system applied during acute inflammation of the connective tissue of the thoracolumbar region affects transforming growth factor-beta1 and Interleukin-4 levels: experimental study in mice, Front. Physiol. 11 (2020) 587373.
[12] S.M. Corey, et al., Sensory innervation of the nonspecialized connective tissues in the low back of the rat, Cells Tissues Organs 194 (6) (2011) 521–530.
[13] J.H. Bishop, et al., Ultrasound evaluation of the combined effects of thoracolumbar fascia injury and movement restriction in a porcine model, PloS One 11 (1) (2016), e0147393.
[14] L. Vieira, Phylogenetics of the fascial system, Cureus. 12 (10) (2020), e10787.
[15] W. Ahmed, et al., A comparative multi-site and whole-body assessment of fascia in the horse and dog: a detailed histological investigation, J. Anat. 235 (6) (2019) 1065–1077.
[16] L. Benetazzo, et al., 3D reconstruction of the crural and thoracolumbar fasciae, Surg. Radiol. Anat. 33 (10) (2011) 855–862.
[17] S.E. Armstrong, D.R. Bell, Measurement of high-molecular-weight hyaluronan in solid tissue using agarose gel electrophoresis, Anal. Biochem. 308 (2) (2002) 255–264.
[18] U.B.G. Laurent, A. Tengblad, Determination of hyaluronate in biological samples by a specific radioassay technique, Anal. Biochem. 109 (2) (1980) 386–394.
[19] R. Kelc, et al., The physiology of sports injuries and repair processes, in: H. Michael, D. Nick, K. Yaso (Eds.), Current Issues in Sports and Exercise Medicine, IntechOpen, Rijeka, 2013 p. Ch. 2.
[20] K.K. Rami, S. Simo, Biomechanics and modeling of skeletal soft tissues, in: K. Vaclav (Ed.), Theoretical Biomechanics, IntechOpen, Rijeka, 2011 p. Ch. 6.
[21] M. Puksec, et al., Biomechanical comparison of the temporalis muscle fascia, the fascia lata, and the dura mater, J Neurol Surg B Skull Base 80 (1) (2019) 23–30.
[22] C. Stecco, et al., Investigation of the mechanical properties of the human crural fascia and their possible clinical implications, Surg. Radiol. Anat. 36 (1) (2014) 25–32.
[23] L.H. Yahia, P. Pigeon, E.A. DesRosiers, Viscoelastic properties of the human lumbodorsal fascia, J. Biomed. Eng. 15 (5) (1993) 425–429.
[24] J. Park, et al., Viscosupplementation in the therapy for osteoarthritic knee, Appl. Sci. 11 (24) (2021) 11621.
[25] G.F. Ferreira, et al., Comparison of the effect of hyaluronic acid injection versus extracorporeal shockwave therapy on chronic plantar fasciitis: protocol for a randomized controlled trial, PloS One 16 (6) (2021), e0250768.
[26] S.A. Raeissadat, et al., Ultrasound-guided injection of high molecular weight hyaluronic acid versus corticosteroid in management of plantar fasciitis: a 24-week randomized clinical trial, J. Pain Res. 13 (2020) 109–121.
[27] A. Streďanská, et al., Development of Tribological model of human fascia: the influence of material hardness and motion speed, Biotribology 30 (2022) 100209.
[28] M.K. Cowman, et al., Viscoelastic Properties of Hyaluronan in Physiological Conditions **4**, F1000Res, 2015, p. 622.
[29] D. Rebenda, et al., Rheological and frictional analysis of viscosupplements towards improved lubrication of human joints, Tribology International 160 (2021) 107030.
[30] C. Myant, H.A. Spikes, J.R. Stokes, Influence of load and elastic properties on the rolling and sliding friction of lubricated compliant contacts, Tribol. Int. 43 (1) (2010) 55–63.
[31] S.J. Falcone, D.M. Palmeri, R.A. Berg, Rheological and cohesive properties of hyaluronic acid, J. Biomed. Mater. Res. A 76 (4) (2006) 721–728.
[32] G.E. Yakubov, et al., Viscous boundary lubrication of hydrophobic surfaces by mucin, Langmuir 25 (4) (2009) 2313–2321.
[33] F. Cilurzo, et al., Injectability evaluation: an open issue, AAPS PharmSciTech 12 (2) (2011) 604–609.
[34] A. Vo, M. Doumit, G. Rockwell, The biomechanics and optimization of the needle-syringe system for injecting triamcinolone acetonide into keloids, J Med Eng 2016 (2016) 5162394.
[35] R.P. Watt, H. Khatri, A.R.G. Dibble, Injectability as a function of viscosity and dosing materials for subcutaneous administration, Int. J. Pharm. 554 (2019) 376–386.
[36] E. Balazs, Viscoelastic Properties of Hyaluronan and Its Therapeutic Use. (2004) 415–455.
[37] D.C. Rockey, N. Weymouth, Z. Shi, Smooth muscle alpha actin (Acta2) and myofibroblast function during hepatic wound healing, PloS One 8 (10) (2013), e77166.
[38] M. Fragiadaki, et al., Interstitial fibrosis is associated with increased COL1A2 transcription in AA-injured renal tubular epithelial cells in vivo, Matrix Biol. 30 (7–8) (2011) 396–403.
[39] S.D. Collum, et al., Inhibition of hyaluronan synthesis attenuates pulmonary hypertension associated with lung fibrosis, Br. J. Pharmacol. 174 (19) (2017) 3284–3301.
[40] S. Kongsagul, et al., Ultrasound-guided physiological saline injection for patients with myofascial pain, J Med Ultrasound 28 (2) (2020) 99–103.
[41] E. Piraccini, R.M. Corso, S. Maitan, Ultrasound guided erector spinae plane block for myofascial pain syndrome, J. Clin. Anesth. 57 (2019) 121.
[42] A. Schilder, et al., Sensory findings after stimulation of the thoracolumbar fascia with hypertonic saline suggest its contribution to low back pain, Pain 155 (2) (2014) 222–231.

journal of the mechanical behavior of biomedical materials 155 (2024) 106566

Contents lists available at ScienceDirect

Journal of the Mechanical Behavior of Biomedical Materials

journal homepage: www.elsevier.com/locate/jmbbm

Understanding frictional behavior in fascia tissues through tribological modeling and material substitution

A. Streďanská [a,*], D. Nečas [a], M. Vrbka [a], J. Suchánek [b], J. Matonohová [c], E. Toropitsyn [c], M. Hartl [a], I. Křupka [a], K. Nešporová [c]

[a] Biotribology Research Group, Faculty of Mechanical Engineering, Brno University of Technology, Technická 2896/2, 616 69, Brno, Czech Republic
[b] Faculty of Medicine in Hradec Králové, Charles University, Šimkova 870, 500 03, Hradec Králové, Czech Republic
[c] Contipro a.s., Dolní Dobrouč 401, 561 02, Dolní Dobrouč, Czech Republic

ARTICLE INFO

Keywords:
Fascia
Tribological model
Soft material
Hyaluronic acid
Friction test

ABSTRACT

The objective of this study is to develop a reliable tribological model to enable a more thorough investigation of the frictional behavior of fascia tissues connected to non-specific lower back pain. Several models were designed and evaluated based on their coefficient of friction, using a low-frequency, low-load reciprocating motion. The study found that two technical elastomers, layered on PDMS to simulate the fascia and underlying muscle, are suitable substitutes for biological tissue in the model. The influence of tribopair geometry was also examined, and the results showed that greater conformity of contact leads to a lower COF, regardless of the material combination used. Finally, the friction properties of HA of various molecular weights and concentrations were tested.

1. Introduction

Lower back pain (LBP) is a common health condition that affects almost everyone at some point in their lives, often leading to job incapacity and high treatment costs, which can result in severe socio-economic issues (Chen et al., 2022; Balagué et al., 2012). Unfortunately, the cause of LBP is often unidentified or misdiagnosed, leading to a prolonged treatment process. However, recent research suggests that the thoracolumbar fascia (TLF) may be a potential cause of non-specific LBP due to its rich innervation and function within the vertebrate body (Chen and Nizar, 2011; Tesarz et al., 2011; Langevin et al., 2011).

The TLF is a type of connective tissue composed of layers of pearly-white fibrous sheets. Its purpose is to provide a broad attachment area for muscles, and isolate underlying muscles from surrounding muscles or adipose tissue. Spanning the length of the back, the TLF consists of two or three layers of collagen fibers separated by loose connective tissues (Stecco et al., 2011a; Blasi et al., 2015). These tissues contain fasciacytes, specialized cells responsible for producing hyaluronic acid (HA), which lubricates the fascia (Stecco et al., 2011b). This lubrication is crucial as it enables the different layers of the TLF to glide over each other smoothly, facilitating free movement. The pathological changes of the fascial tissue, such as fibrosis and densification, can lead to increased friction between the layers, which may be a factor in the development of LBP (Pavan et al., 2014, 2016). Therefore, injecting a viscosupplement therapy into the fascia layers (as shown in Fig. 1) could potentially provide relief for LBP. To precisely define the friction-reducing properties of viscosupplements, it is necessary to investigate the effects of HA as a native lubricant on fascial friction.

While there are numerous biotribological models available to study friction in the eye (Černohlávek et al., 2021), skin (Dąbrowska et al., 2017; Derler et al., 2007), or mouth (Dresselhuis et al., 2008; Edmonds et al., 2021; Watrelot et al., 2019), there is currently no model of fascia layers to study different conditions that influence friction in such an important organ that may be causing pain. As a result, this paper aims to develop a fascia model that can simulate real fascia and study friction in both healthy and afflicted tissue. By creating such a model, we hope to gain a better understanding of the role of the fascia in LBP and potentially improve treatment options for this common and debilitating condition. In a previous study (Streďanská et al., 2022), a preliminary model of fascia was created using polydimethylsiloxane (PDMS) as an elastomer with low elastic moduli. However, this model was found to be unsuitable for mimicking fascia because of high stiffness of material pair and non-realistic point contact. Consequently, efforts are currently focused on the search for a more authentic elastomer to develop a

* Corresponding author.
E-mail address: Alexandra.Stredanska@vut.cz (A. Streďanská).

https://doi.org/10.1016/j.jmbbm.2024.106566
Received 11 March 2024; Received in revised form 12 April 2024; Accepted 3 May 2024
Available online 5 May 2024

tribological fascia model. The development of artificial models based on technical materials is usually based on friction comparisons. Of course, friction is affected by the model configuration and conditions, so it is a good idea to base the model on the standard conditions (configurations) used for the application - i.e. two muscles divided by fascia layers. To achieve this objective, more compliant technical materials are being utilized, and a comparison is being made between their coefficient of friction (COF) and that of real fascia. Initially, rabbit TLF was considered as the most authentic model; nevertheless, employing biological tissue like rabbit fascia can be inconvenient due to the necessity for dissection, transportation, and time-sensitive testing to prevent tissue decay. Moreover, the mechanical properties of fascia undergo changes when frozen, which adds to the difficulties involved in working with it. For more reason, see the Limitations. Therefore, the search is ongoing for a technical material that can function as a dependable fascia tribological model.

Previous studies by Bongaerts et al. (Bongaerts et al., 2007) found that an increase in material roughness led to a decrease in COF in the boundary lubrication regime, and the viscosity of the Newtonian lubricant decreased friction in rougher contacts. Additionally, the contact angle of the plate-lubricant interaction was found to be related to friction, with a lower contact angle leading to a lower COF. Sadowski et al. (Sadowski and Stupkiewicz, 2019) investigated the influence of substrate configuration and viscoelasticity on friction using a PDMS-PDMS configuration and found that hysteresis losses contributed significantly to friction. Selway et al. (Selway et al., 2017) studied the effects of fluid viscosity and wetting on viscoelastic lubrication and found that rough contacts produced higher viscoelastic hysteresis, increasing friction. The wettability of elastomers was also studied by Schneemilch et al. (Schneemilch and Quirke, 2007) and Hillborg et al. (Hillborg et al., 2001) before and after surface oxidization. Tribological studies on compliant planes with solid pins have been conducted by several other researchers. Schallamach (Schallamach, 1971) discovered instability waves in sliding compliant contacts, leading to fatigue fractures and wear, with the frequency and number of waves dependent on the elastic modulus of the elastomer. De Vicente et al. (de Vicente et al., 2006) studied rolling and sliding friction in compliant tribopairs and found that sliding friction was strongly dependent on the SRR in the EHL regime, but had no effect in the boundary and mixed regimes, while rolling friction was independent of SRR. Myant et al. (Myant et al., 2010) found that reducing elastic moduli leads to a drop in friction, and Xu et al. (Xu et al., 2021) investigated the interfacial deformation of compliant contacts under the influence of traction and normal force through numerical simulation, finding that the material deformed unsymmetrically, and the cavity served as a lubricant reservoir.

The findings of these studies are important in the development of a tribological fascia model that accurately represents compliant contacts involving biological samples. Understanding the effects of material roughness, viscosity, wetting, and elastic moduli on friction can aid in finding the technical material that mimics fascia more authentically. The tribology of compliant contacts is well-researched and relevant to our study on the friction of fascia. The aim of this study is to develop a tribological model of fascia through tribological modeling and material substitution and study friction in these models. Thus, the model could be used to investigate viscosupplement treatment, which aims to reduce pain by decreasing friction in the fascia through the use of HA solution in the later stage of our investigation. This paper builds on a previous study with a basic PDMS model (Streďanská et al., 2022) and presents an advanced tribological fascia model with sheets to better mimic the real contact between layers of tissue.

2. Materials and methods

2.1. Experimental apparatus and setup

Determination of the frictional properties of the model and HA lubricants was performed on the tribometer Bruker UMT TriboLab (Bruker, Billerica, MA, USA). Sliding tests were conducted in pin-on-plate configuration. The pin was stationary, holding the normal force of 2 N. Unfortunately, no biomechanical study examined forces between fascia and muscle or fascia layers. Nevertheless, the planned viscosupplement is meant to be utilized in conjunction with manual therapy. According to a study by Albert et al. (Albert et al., 2006) mean hand force measured for different massage techniques was 8.1 ± 2.7 N. The human hand presents a larger contact surface during massage, and also, some of the load will be lost in the skin and fat, and the actual load on the fascia may therefore be less. Plasqui et al. (Plasqui et al., 2013) demonstrated that the frequency range of motion of daily activities was between 0.3 and 3.5 Hz. Therefore, the plate performed a linear reciprocal movement with a frequency of 1 Hz (avg. velocity 24 mm s^{-1} as can be seen in Fig. 2. The influence of motion speed was examined in our previous study (Streďanská et al., 2022). Each step of the experiment with a 12 mm stroke was repeated 3 times separately on the new path and lasted 300 s. The length of the path of 12 mm was determined by the study (Langevin et al., 2011). The range of fascia movement in this study was in men/women without pain 16.90 ± 1.89/16.89 ± 1.55 mm, with pain 9.74 ± 0.86/16.28 ± 1.92 mm. The scheme of the experimental setup is shown in Fig. 2.

For the model development and experiments, a holder and a pin were designed. The pot consisted of internal and external parts, where one is inserted into the other. The internal pot is used to insert a plate representing a muscle. The maximum possible size of the plate is 70 × 30 mm. The external pot was used to mount the tribometer platform and, at the same time, to heat the entire jig assembly. Heating is ensured by heating cartridges which maintain a temperature of 37 °C. There are studs on the external pot, on which holders for the models or real fasciae are inserted.

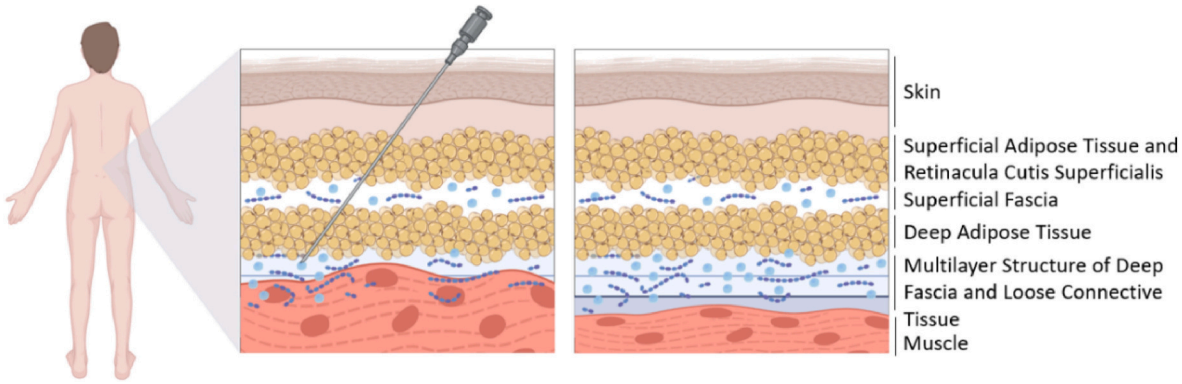

Fig. 1. Left side – Injection treatment of fascia by HA-based viscosupplement between to layers of patological deep fascia. Right side – Situation between layers of deep fascia after viscosupplemetation theraphy. Created by Biorender.com.

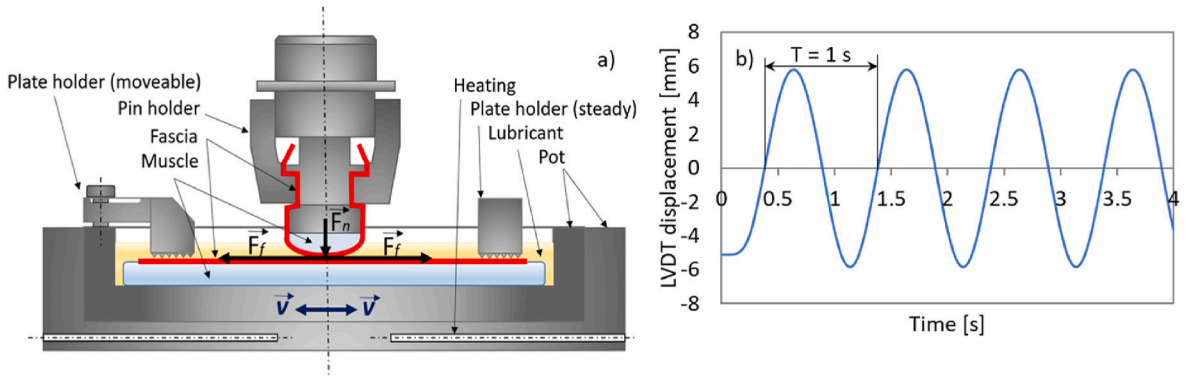

Fig. 2. a) scheme of experimental apparatus, b) velocity profile of bottom module for 1 Hz frequency and 12 mm path shown by the position of the LVDT sensor over time.

One holder is static and the other is movable. Both holders are tightened with wing nuts. In the case of a movable holder, its position is also secured by double-head screws. First, the fascia is held in place by a static holder, then it is pre-tensioned with a movable holder, which is then secured. This design allows for easy replacement of fascia or tested lubricants.

The real fascia contact approaches the plate-on-plate configuration as friction arises between the tissue layers. Although plate-on-plate configuration was omitted for undesirable edge effects. To approach this situation and to study the influence of tribopair geometry, the original pin of 8.6 mm radius was supplemented by two sizes of cylindrical surface radii – 30 mm (R30) and 50 mm (R50), which allows for the use of base material thicknesses of 3.5 mm. The construction of the pin consisted of the pin itself and two holders. The pin is formed by a cylindrical tip that is in contact with the bath during the experiments. The muscle model is glued to the cylindrical contact surface. The fascia is fastened in one holder and then manually prestressed over the cylindrical surface and fastened with the other holder. The pin prepared in this way is inserted and secured in the upper part of the tribometer.

2.2. Materials

Models representing muscles and fascia are made up of PDMS, PU Gels, PVA hydrogel, and referent rabbit fascia; see Fig. 3, where the individual material pairs are listed. The basic PDMS-PDMS model described in (Streďanská et al., 2022) was used as the first model A. The second model B is composed of PDMS-PDMS 10 ShA (acetoxy-PDMS, Elastosil® E43 Transparent, Wacker Chemie AG), Ra = 1.08 μm and

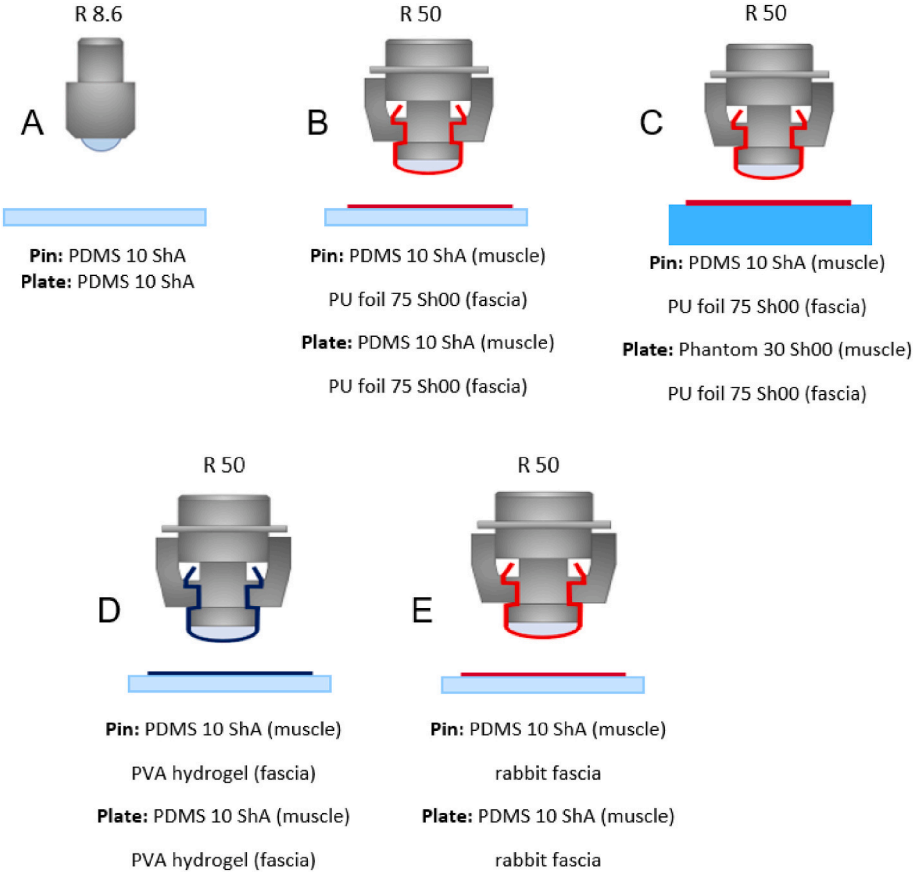

Fig. 3. Investigated tribological models of fascia.

3000 kPa tensile strength, with interlayers of PU gel 75 Sh00 Phantom (BTG Standard 75, Technogel®, Germany GmbH), Ra = 211.2 nm and >800 kPa tensile strength mimicking the fascia layers on the muscle. Since the fascia tissue is a membrane on the muscle or adipose tissue, this model approached the situation of the human body. Model B used a pin with a linear contact with a 50 mm radius. The third model C consists of the PDMS 10 ShA pin and the PU gel plate labeling Phantom (BTG S 130 AX, Technogel®, Germany GmbH) with 30 Sh00 stiffness, Ra = 1.1 μm and 60–70 kPa tensile strength, which is much more compliant than PDMS, so mimicking the muscle more faithfully. For this purpose, even the pin was upgraded to a larger radius of 50 mm, preserving the linear contact. Model D returned to PDMS-PDMS with interlayers, this time made up of hydrogel. The PVA hydrogel (Ra = 793. 42 nm) was chosen based on its hydrophilic surface properties. Model E was a reference model and the most real one from PDMS-PDMS and interlayers of rabbit fascia with 21 ± 4 MPa tensile strength. Mechanical properties were measured as part of our other study (Nešporová et al., 2023). The surface roughness of the fascia could not be determined under our laboratory conditions. Compared to porcine, the rabbit has one big advantage because there is an extra muscle (musculus panniculus carnosus) under the layer of skin and adipose tissue. Thanks to this muscle, the fascia is not embedded in fat, as it is in humans and pigs, and can be removed without deterioration. PDMS plates for the pin and also for the plate were 3.5 mm thick, while Phantom was 8 mm thick. Interlayer materials were 0.75–1 mm thick.

2.3. Lubricants

The solutions of HA were used as lubricants as it is in a real fascia. It is a non-Newtonian lubricant where the degree of polymerization results in differences in viscosity. This depends on chemical properties such as molecular weight and concentration of the solution. In general, increased molecular weight and concentration lead to increased lubricant viscosity. Four different combinations were chosen to lubricate fascia, as shown in Table 1. A commercial rheometer Discovery HR 30 (New Castle, DE, USA) was used in a cone-plate configuration at 37 °C for viscosity measurements. The experiments were carried out using a stainless-steel cone and plate geometry (40 mm diameter with a 1° cone angle). The results are shown in Table 1 and the rheological curves can be seen in Appendix A.

The wettability of the materials has also been measured to check whether the surfaces are hydrophobic or hydrophilic concerning the lubricants HA610a, HA316b and deionized water as a reference. A small amount of lubricant (6 μl) was applied to the material surface, and the contact angle was measured in 2D using a microscope (Fig. 4). Individual contact angles are shown in Table 2.

2.4. Statistical methods

The findings were shown as the average of 3 measurements along with their standard deviation (SD). The statistical analysis involved two-way ANOVA, followed by either Tukey's comparison tests. For each comparison, individual variances were calculated. In all cases, significance was determined as *P < 0.05, **P < 0.01, ***P < 0.001, and ****P < 0.0001.

Table 1
List of lubricants used in the experimental study.

Designation	Molecular weight	Concentration	Viscosity (37 °C)
HA610a	610 kDa	20 mg/ml	1191.47 mPa s
HA316a	316 kDa	20 mg/ml	202.94 mPa s
HA101a	101 kDa	20 mg/ml	27.49 mPa s
HA316b	316 kDa	10 mg/ml	59.72 mPa s

3. Results

3.1. Effect of tribopair geometry

The effect of three different radii was investigated on two models: a model A (a commonly used model in biotribology to simulate compliant contacts) and a PDMS-Phantom model (model C, the least stiff material of those used in this study). Each test condition was assessed by focusing on dynamic friction. This involved selecting a subset of the stroke within a region where the friction remains relatively stable, devoid of maximum peaks – where the static friction occurred. More information can be found at Appendix A. Fig. 5(d–i) illustrates an example of a set of strokes in both directions. The strokes within each curve were averaged to represent friction curves shown in Fig. 5(b–c) and singular friction data points in the figure presented in Fig. 5(a). The COF was compared for each measurement where the pin radius increased from 8.6 mm through 30–50 mm (Fig. 5(a–c)). Expanding the contact area through an increase in pin radius, while maintaining the same applied normal load, results in a reduction of contact pressure. In this particular phase of the experiment, both models were lubricated with HA101a. The results revealed a significant correlation between COF and pin radius. In the model A, increasing the contact area led to an overall friction reduction of 22% from R8.6 to R50. However, COF between R30 and R50 remained unchanged. The friction curves remained consistent throughout the duration of the test and showed the same shape and progression. Similarly, in the model C, increasing the contact area led to an overall 36% reduction in friction, but the drop between R30 and R50 was more evident. In this case, the friction curves fluctuated compared to those observed in the model A. The fluctuation of the curves is closely related to the friction force, shown in Fig. 5(d–i), and will be discussed in more detail in the discussion.

3.2. Testing of friction in fascia models

The second step of the study involved the simultaneous development of the models alongside the first step. In this phase, model A from the preliminary study was also subjected to testing using HA316b and HA610a. Each test condition was evaluated with a focus on dynamic friction as in the test before - examples are shown in Fig. 6(b–k). The strokes within each curve were averaged to represent singular friction data points in Fig. 6(a). The sliding friction coefficient was then compared between the developed versions, as illustrated in Fig. 6(a). Firstly, model B with pin R50 and with an additional upper layer of PU gel with a hardness of 75 Sh00 was introduced to simulate the fascia layer. Comparing it to the preliminary model A reported COF values of 0.050; SD = 0.005588 for HA316b and 0.115; SD = 0.005236 for HA610a, the COF decreased for both HA316b to 0.045; SD = 0.002489 and HA610a to 0.058; SD = 0.004945. The friction curves exhibited more consistent progress over the testing time and became more stable. Secondly, model C utilized PU gel with a hardness of 30 Sh00 (Phantom) instead of PDMS as the muscle, along with the R50 pin. Notably, the application of Phantom resulted in a significantly higher level of friction testing for both lubricants, exceeding the others by an order of magnitude. Next, model D reverted to PDMS as the muscle while retaining the R50 pin. The fascia was represented by the use of PVA hydrogel. Model D reported COF values of 0.019; SD = 0.000102 for HA316b and 0.034; SD = 0.001976 for HA610a, indicating a decrease in friction compared to model B. Finally, the model E with rabbit fascia was developed, with the base muscle layers composed of PDMS. The model utilized the largest designed contact area of the tribopair using the R50 pin. Model E reported COF values of 0.029; SD = 0.000814 for HA316b and 0.056; SD = 0.001553 for HA610a. As can be seen in Table 3 in comparison to rabbit fascia model, models B and D exhibited the most similar friction properties for both lubricants. The comparison between Model B and Model E showed a statistically significant difference for HA316b (**; P = 0.0029), while for HA610a, the comparison did not exhibit statistical

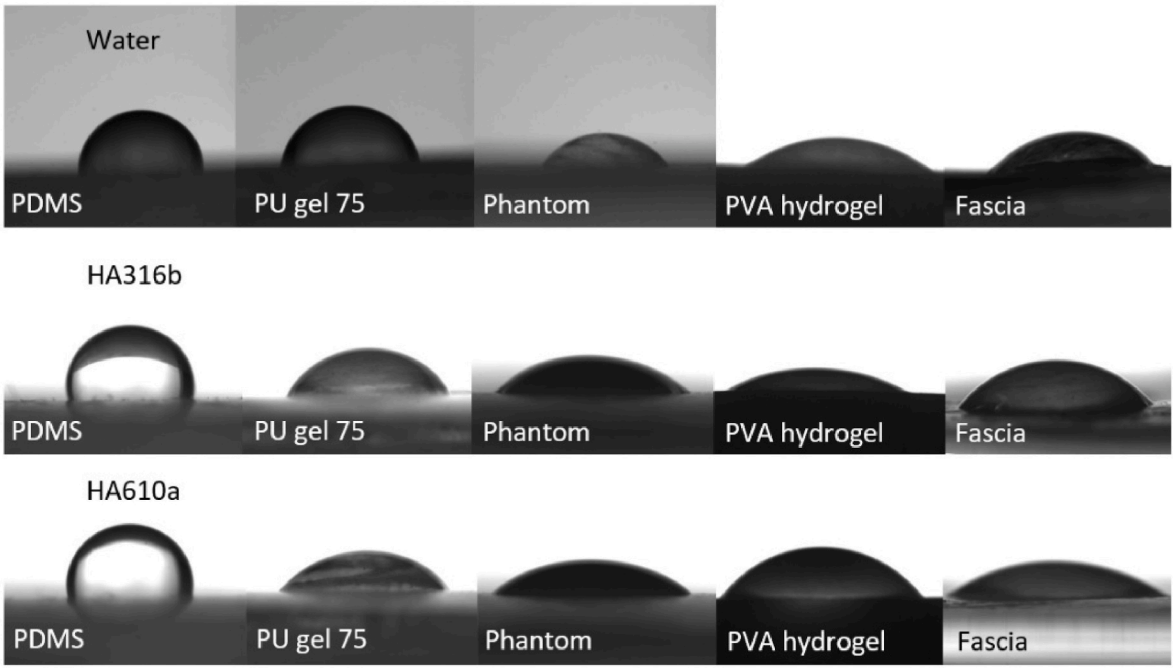

Fig. 4. Wettability of rubbing surfaces.

Table 2
Contact angles between fluids and materials.

Lubricant	PDMS	PU gel 75	Phantom	PVA hydrogel	Fascia
HA610a	100.09°	52.03°	41.27°	45.31°	50.09°
HA316b	107.65°	63.05°	45.00°	31.02°	28.33°
Water - reference	82.63°	78.95°	41.20°	25.33°	39.28°

significance (ns; P = 0.9823). When comparing Model D and Model E, the analysis revealed that there was no statistically significant difference for HA316b (ns; P = 0.1168). However, for HA610a, the comparison demonstrated a highly significant difference (****; P < 0.0001). The other models show a high level of significance for both lubricants compared to model E.

As shown in Fig. 6(b–k), even models B, D, and E exhibited the fluctuations. The friction forces for HA610a were generally higher than those for HA316b, and the shape of the friction force curves was quite similar across the models for both lubricants. However, the friction force curves differed between the models themselves.

3.3. Friction tests of rabbit fascia – model E

The third part of this study focused on investigating the influence of molecular weight and concentration of HA on the friction of the rabbit fascia model E. The pin and plate consisted of a PDMS base-muscle layer with a rabbit fascia layer on top. Four solutions (listed in Table 1) of HA were utilized, varying in molecular weight from 101 to 610 kDa and concentrations of 10 mg/ml and 20 mg/ml. The results indicated that the friction values were highest (0.056; SD = 0.001552) when using HA610a with a concentration of 20 mg/ml (η = 1191.47 mPa s), while the lowest friction values (0.026; SD = 0.0008719) were observed with HA101a at the same concentration (η = 27.4923 mPa s). Furthermore, HA316a at a concentration of 20 mg/ml (η = 202.94 mPa s) exhibited a higher COF (0.040; SD = 0.001574) compared to HA316b at 10 mg/ml (η = 59.72 mPa s), which resulted in a COF of 0.029; SD = 0.0008141. Therefore, as depicted in Fig. 7, friction increased with both increasing molecular weight and concentration of HA in the solution. The progression of friction over time is also illustrated in Fig. 7(b). Friction curves for HA101 showed some fluctuation but otherwise consistent behavior over time. In contrast, for the other lubricants, the friction curves exhibited a slight increase over time.

4. Discussion

4.1. Effect of tribopair geometry

In this section of the experiment, two models were employed: model A and model C. Model A was selected due to its widespread use in biotribological studies, specifically in areas like the eye-eyelid (Černohlávek et al., 2021) or mouth (Vinke et al., 2018; Vlădescu et al., 2023). Model C was chosen based on input from physiotherapists and their sensory experiences during manual therapy of the lower back. The redesign of the pin's shape and dimensions aimed to make it more closely resemble real fascia contact. The study's findings suggest that friction levels decrease as the contact area increase in both model A and model C contacts. These results align with previous studies (Mahdi et al., 2015; Rand and Crosby, 2009; Rennie et al., 2005) that established a correlation between the increased COF and increased normal load respectively contact pressure in compliant contact. The data in (Mahdi et al., 2015) indicates that, for both cylindrical and spherical probes, the friction due to deformation rises as the normal load and sliding speed increase. Moreover, this study indicates that in a lubricated condition, an increase in both speed and normal load leads to a tendency for the balance between adhesion and deformation to approach a 50/50 ratio. The split between the adhesive and deformation components is investigated by two terms friction model (Adams et al., 2007; Van Kuilenburg et al., 2015). The first component - adhesive - relies on the mechanism the energy that's lost when small connections break between two surfaces sliding against each other. These connections happen because of short-range attractions between molecules, like the ones in van der Waals interactions (Adams et al., 2007).

The role of adhesion in contributing significantly to the total friction of compliant contacts is widely known (Schallamach, 1958). Hence, it is valuable to examine not only the COF curves but also the frictional force curves themselves. These curves are notably influenced by the variable geometry of the contact area, clearly showcasing the presence of

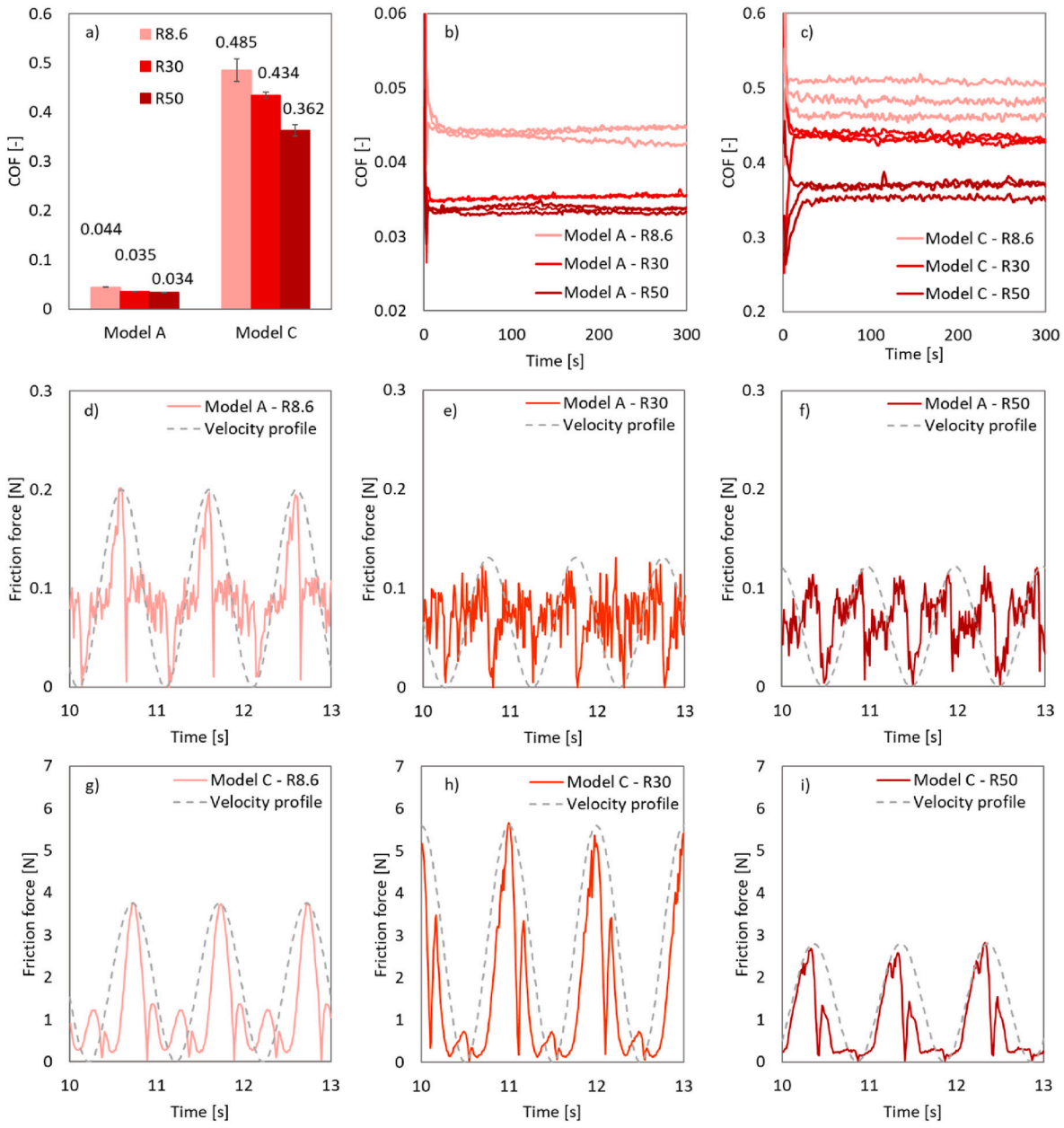

Fig. 5. Influence of tribopair geometry on friction lubricated by HA101a. a) summary bar plot of COF, b) and c) development of friction in time, d) -i) individual friction force curves with velocity profile (Stredˈanská et al., 2022).

adhesive behavior rather than pure sliding indicating boundary lubrication regime. The tangential movements on the elastomer surface which can be seen in Fig. 5, suggest that friction arises from the interplay between adhesive dragging and an ongoing relaxation process at the microscale level. In model A, the frictional force increased during the forward motion, with multiple small adhesion cycles until peak occurred. An explanation is offered by Barquins (Barquins, 1992), who describes that elastomer molecules undergo thermal agitation at the interface, with their jump directions being random in the absence of external stress. The application of a frictional force guides these jumps to alleviate stress. During sliding, molecular bonds consistently detach from and reattach to the slider, causing small jumps in the elastomer chain ends. The transitions from peak to valley happened almost instantly, as a result of a change of direction into a movement of the opposite sense. At this point, the pin velocity is zero, so the COF value corresponds to the static friction value.

On the other hand, model C exhibited a rapid increase to the peak and a similarly quick decrease during the sinusoidal cycle. Interestingly, while the adhesion pattern and shape were relatively consistent in model A for both motion direction, except for an increase in the peak value not used to calculate the COF, model C displayed unsymmetrical deformation phase at all holder sizes. In positive stage of motion there is a steep increase of tangential force almost without adhesion jumps. The dissipation of frictional force not only mirrors the strength of interfacial bonds but also signifies the viscoelastic loss characteristics of the elastomer. In the other words, the elastomer friction mechanism is a viscoelastic process (Barquins, 1992; Schallamach, 1971). Nevertheless, the shift towards the negative direction doesn't occur abruptly but rather follows an exponential pattern. This suggests that the extensive deformation and accumulation of material in front of the pin are substantial enough for the elastomer deformation to entirely take precedence. This dominance arises from the material's high ductility and slow relaxation resulting in high resistance to movement. Consequently, during the pin's movement in the opposite direction, we observe the

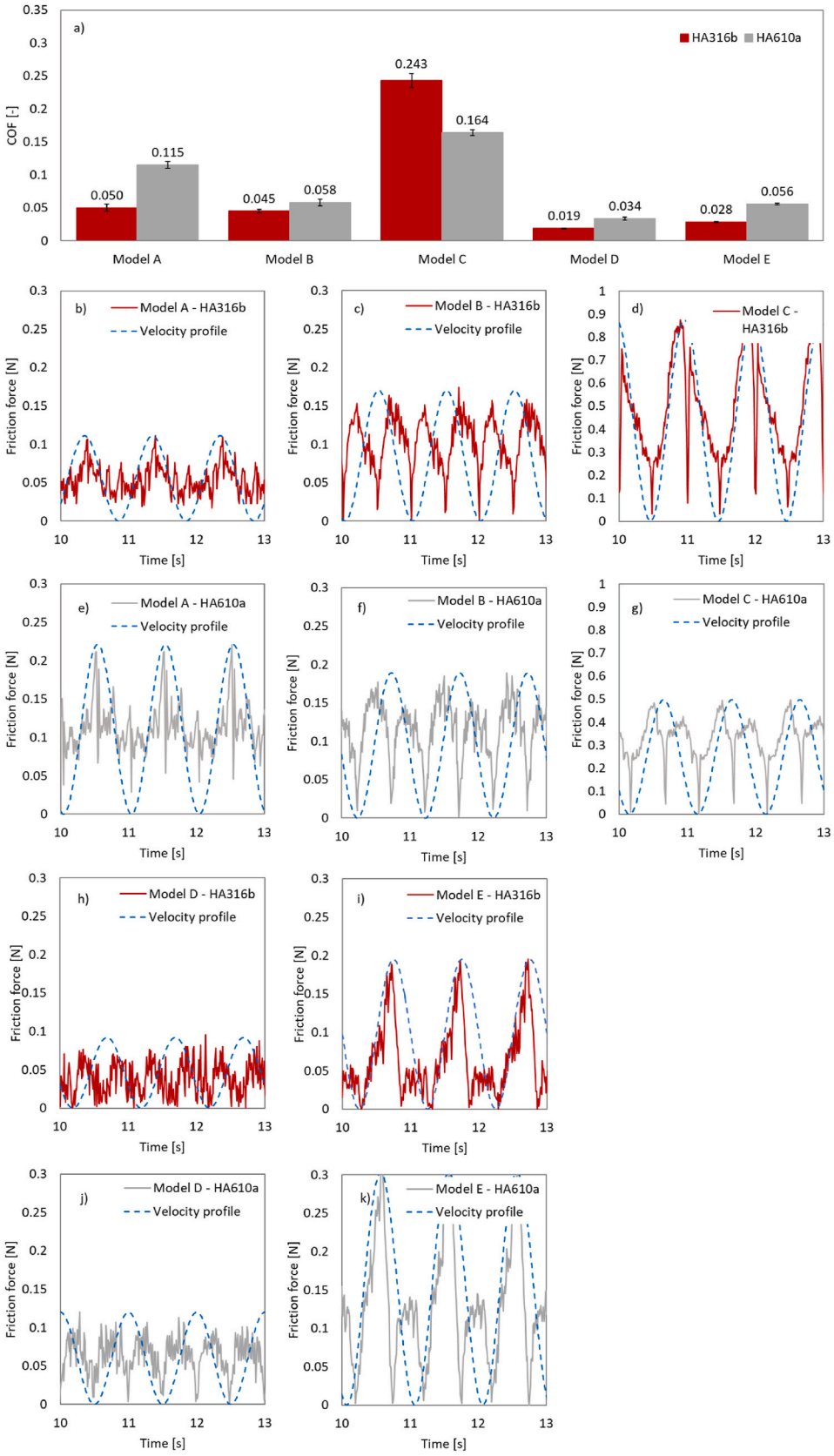

Fig. 6. Friction of tribological fascia models. a) summary bar plot, b)-k) individual friction force curves with velocity profile (Streďanská et al., 2022).

Table 3
Statistical analysis of tribological fascia models comaprison.

Designation	HA316b		HA610a	
	Significance	Adjusted P value	Significance	Adjusted P value
"Model A vs. Model B"	ns	0.7082	****	<0.0001
"Model A vs. Model C"	****	<0.0001	****	<0.0001
"Model A vs. Model D"	****	<0.0001	****	<0.0001
"Model A vs. Model E"	***	0.0002	****	<0.0001
"Model B vs. Model C"	****	<0.0001	****	<0.0001
"Model B vs. Model D"	****	<0.0001	****	<0.0001
"Model B vs. Model E″	**	**0.0029**	**ns**	**0.9823**
"Model C vs. Model D"	****	<0.0001	****	<0.0001
"Model C vs. Model E"	****	<0.0001	****	<0.0001
"Model D vs. Model E″	**ns**	**0.1168**	****	**<0.0001**

material attempting to relax, facilitated by the moving pin. As a result, the deformation in the negative direction is considerably smaller, leading to an asymmetry in the frictional force between both movement directions. So, this is a nice demonstration of the hysteresis of the material (Popov, 2010). As the contact changed to R30 and R50, the adhesion became evident. Moreover, as the contact area increased, the peak value of the maximum friction force decreased. This indicates that material stiffness plays a more significant role in influencing the occurrence, origin and characterisation of adhesion and deformation in both model A and C, rather than the contact area. This observation is supported by other relevant studies (Berdichevsky et al., 2004; Xue et al., 2016).

In summary, these experiments highlighted the importance of pin shape, material properties, and normal force in determining friction behavior in compliant contacts. The findings emphasized the need for careful consideration of these factors to accurately simulate real *in-vivo* contact conditions and optimize performance in mechanical systems.

4.2. Testing of friction in fascia models

The primary objective of this study was to develop a tribological model for fascia. While the most sophisticated model would involve rabbit fascia, the scarcity and limited availability of biological samples prompted the search for a suitable technical equivalent within elastomers. In this regard, it is well-known that the sliding friction coefficient increases as the elastic modulus of elastomers decreases (Myant et al., 2010). This aligns with the understanding that a less stiff material has the capacity to produce a greater resistive force when subjected to shearing – therefore the friction force increases (Adam et al., 2019; Voll and Popov, 2014). Put simply, softer compounds exhibited higher adhesion at the same velocities due to time-dependent viscoelasticity. Additionally, employing a more viscous material in the tribopair resulted in more pronounced oscillations in the friction force (Kim et al., 2020), as we can observe in Fig. 5(d–i) and Fig. 6(b–k). The observed increase in friction can be attributed to the contribution of friction caused by adhesion and hysteresis losses occurring in compliant contact (Mahdi et al., 2015; Sadowski and Stupkiewicz, 2019; Schallamach, 1971). This results in a significant difference in friction magnitude between PDMS- and Phantom-based models, as elaborated earlier in the discussion. The control of the adhesion primarily lies with the stiffness, as previously observed (Adam et al., 2019; Tiwari et al., 2017). Furthermore, what's particularly intriguing is that the adhesion remains unaffected by the type or viscosity of the lubricant used; rather, it is predominantly influenced by the materials in the tribopair (Kim et al., 2020). However, in the boundary and mixed lubrication regimes, friction is significantly influenced by material roughness, as asperities serve as lubricant reservoirs within the contact (Selway et al., 2017). It's worth noting that silicone-like elastomers, including those utilized in this study, generally exhibit relatively high roughness due to the manufacturing process (Ye et al., 2009). Specific roughness values are given in Materials and methods. However, in study by Tiwari et al. (Tiwari et al., 2017) the impact of raised roughness varied based on the stiffness of the elastomer compound. This distinct behavior can be clarified by considering the extra elastic energy accumulated when stiffer elastomer makes contact with a rough surface and the supplementary contact area observed in the case of more compliant, softer elastomer. Which, in the case of a compliant elastomers, indicates the contribution of hysteresis friction. Due to hysteresis friction being attributed to internal energy dissipation related to elastomer deformation, the friction force rises with the increasing deformation of elastomer asperities. Consequently, the hysteresis friction is likely to increase with a higher Ra of the elastomer, resulting in an elevated friction coefficient (Ido et al., 2019). However, considering the generally low friction in all models except for model C, it can be inferred that the adhesive component of friction decreases in the representation of the hysteretic component.

The hydrophilicity and hydrophobicity of the interface between the

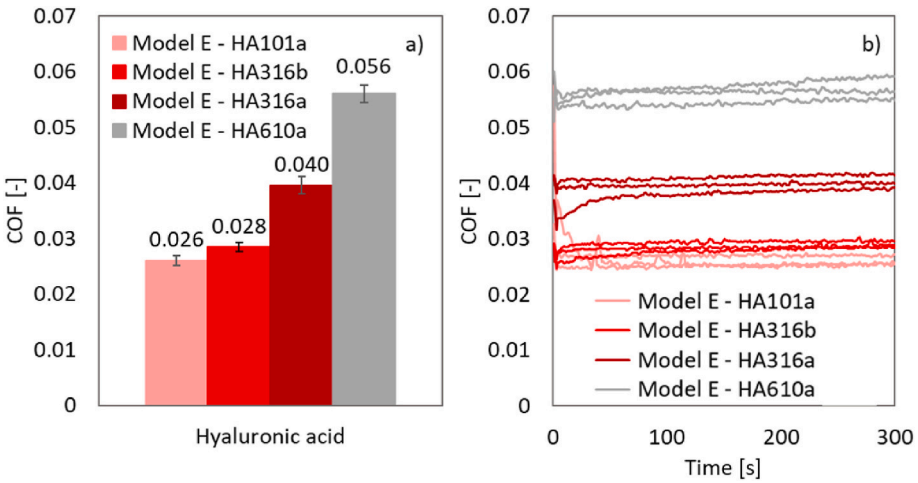

Fig. 7. Influence of concentration and molecular weight on the friction of rabbit fascia (Stredˈanská et al., 2022).

material and the lubricant represent additional material properties that influence contact behavior (Bongaerts et al., 2007). All the materials used to create the fascial model were measured with the two lubricants employed in the tribological testing of the developed models. The data presented in Table 2 provide information on these properties. Based on the data analysis, it is evident that the PDMS/PU gel and PDMS/PVA hydrogel models exhibited friction values closest to the rabbit fascia model for both lubricants. In terms of wettability, the PU gel exhibited a comparable contact angle to the fascia for HA610a, indicating a similar COF. The same situation is repeated for hydrogel, rabbit fascia and HA316b lubricant. Therefore, it can be assumed that this parameter influences the friction results. A previous study (Zhao et al., 2018) investigating the wettability of pure hydrogel reported strong hydrophilicity when in contact with water, which may explain the similar COF measured for the low viscous HA316b (the viscosity data can be seen in Table 1). Consequently, both models (B and D) show promise as replacements for real fascia, with the PU gel being more suitable for high viscous lubricants and the PVA hydrogel for low viscous lubricants. The opposing trend of lubrication observed in the C model is likely attributed to the combination of low rigid material, hydrophobicity, and substantial deformations. The effects of the lubricants used will be discussed more in the next part of the discussion.

In conclusion, this study addressed the development of a tribological model for fascia by considering alternative materials due to the limited availability of biological samples. The results indicate that the choice of material properties, such as elastic modulus, roughness, and wettability affects the friction behavior in compliant contact. The PDMS/PU gel (model B) and PDMS/PVA hydrogel (model D) exhibited friction values closest to the rabbit fascia model (model E) for the lubricants tested. These findings provide valuable insights for the selection of suitable technical equivalents for fascia in future tribological studies.

4.3. Friction tests of rabbit fascia

The rabbit fascia model was utilized in this study to explore the impact of HA solution properties on friction using a biological tissue. It is worth mentioning that HA is known for its effect to reduce friction, for example between the eye and the eyelid or in the natural and artificial joints (Černohlávek et al., 2021; Nečas et al., 2019, 2023; Rebenda et al., 2021). Together with other substances such as phospholipids or proteins, HA can lubricate brilliantly even in boundary regime. However, friction-reducing properties of HA are strongly depended on its properties such as molecular weight and concentration. In general, molecular weight in the body varies. For example, in human physiological synovial fluid, it typically ranges from 6000 to 7000 kDa but, in rheumatoid fluid, the molecular weight is comparatively lower, falling within the range of 3000–5000 kDa (Fraser et al., 1997; Laurent et al., 1996). In addition, the estimated thickness of the HA fluid layer within the fascia is on the order of tens of microns (Fede et al., 2018), which is significant compared to the size of the molecules and even the roughness of the fascia (Choi et al., 2011). Consequently, in cases where the concentration or molecular weight of HA is high, the increased viscosity resulting from the resistance to flow can impact lubrication (Cowman et al., 2015; Falcone et al., 2006). Indicating that full-film lubrication likely prevails within the closed fascial system, it is quite sensible to explore how the specific properties of individual solutions influence friction in the fascia.

The findings in the study indicated that an increase in the viscosity of HA in the solution corresponded to an increase in the COF. The viscosity of an ideal polymer solution is proportional to the fraction of the solution volume occupied by polymer chains. This occupied volume fraction can also be expressed in terms of the mass concentration of the polymer multiplied by the polymer specific volume (Cowman et al., 2015). In other words, viscosity is influenced by the length and number of polymer chains in the solution, as well as the size of the molecules. As the molecular weight and concentration increase, the presence of densely packed polymer chains restricts the ability of the polymer to find space for movement within the solution. Consequently, under conditions of low sliding motion and applied load, friction between the molecules has the potential to increase. This is finally confirmed by the results of the experiment carried out.

In our investigation of the developed fascial model, high molecular weight HA610a was utilized. This lubricant exhibits a relatively high viscosity. As depicted in the results presented in Fig. 7, it demonstrates increased friction when paired with the fascia compared to the lower viscosity lubricants employed. It's important to remember that the primary objective of this study was to create a tribological model for fascia, driven by the potential application of identifying ideal HA properties for a medical viscosupplement designed to address low back pain. Elevated HA production represents the body's initial response to enhance the smooth interaction between two surfaces, similar to the mechanism observed in a synovial joint (Pavan et al., 2014). When HA is present within thin connective tissue layers, the HA chains can intertwine, thereby contributing to the hydrodynamic properties of the solution (Matteini et al., 2009). Consequently, based on the initial results, it appears impractical to exclusively concentrate on high viscosity, and therefore high molecular weight, and/or highly concentrated HA solutions in future research.

4.4. Limitations

The authors acknowledge several potential limitations in the current study. The initial section of the publication concentrates on assessing the impact of pin geometry using materials of varying rigidity. This aspect of the experiment has been carried out using a single lubricant, specifically designated as HA101a. The decision to utilize only one lubricant was influenced by literature, such as Kim et al. (Kim et al., 2020), which suggests that the primary factor influencing outcomes should be the material in the tribopair rather than the lubricant. Consequently, there is a strong basis to presume that the friction trends observed for the specified material models and pin geometry will persist when employing any other lubricant.

Further, in examining the five developed models, the choice of employing HA316b and HA610a lubricants is justified as follows. HA610a was selected due to its high viscosity, being the most viscous lubricant available for the study. The authors note in the current discussion that in lubricated parts of the human body, such as joints, HA tends to have a higher molecular weight. On the other hand, HA316b is among the less viscous lubricants used in the study, containing half the concentration of HA compared to HA101a. This led to concerns about the lower stability of the solution as a fascia lubricant, though this concern was ultimately not substantiated. However, testing all five models with all four lubricants would have been excessively time-consuming, prompting the authors to opt for the more streamlined approach of using the two specified lubricants.

Other possible limitation of this study is that rabbit fascia was used as a representative tissue for human fascia. Typically, porcine and bovine specimens are more frequently employed as human models. However, in these animals, it remains unclear how to separate deep fascia from fat without causing damage. This aspect suggests a major challenge for future research using biological samples to investigate friction and lubrication of fascia.

5. Conclusions

The aim of this study was to develop a tribological model of the fascia through tribological modelling and material substitution and to study the friction in these models. Four tribological models of fascia were constructed from technical elastomers and one from rabbit fascia. This paper was built upon the preliminary study (Streďanská et al., 2022) and presents the following findings:

- increased contact area resulting in improved pressure distribution and decreased friction for both the basic and the most compliant model. With the more compliant model, the change in geometry had a significantly more positive effect,
- PVA hydrogel and PU gel (stiffness of 75 Sh00) tribopair was identified as potential replacements for real biological samples based on comparing four different tribological models,
- concerning high-viscosity HA lubricant, PU gel is more suitable replacement of fascia, while PVA is recommended when focusing on low-viscosity lubricants,
- a strong correlation between friction and HA solution's molecular weight and concentration was found based on investigating rabbit fascia model.

The findings and models from the study will be further used for a follow-up study to define the properties leading to low friction in the fascia and will serve as a basis for the development of a viscosupplement for the treatment of lower back pain.

Ethical approval

Ethical review and approval were waived for this study due to the sole use of animal cadavers for tissue harvesting. The use of tissue from animal cadavers was in accordance with relevant guidelines and regulations in Czech Republic. The procedure for obtaining the thoracolumbar fascia was approved by the Ethics Committee of the MINISTRY OF EDUCATION, YOUTH AND PHYSICAL EDUCATION ID: MSMT- 2036/2022-3. Human Ethics and Consent to Participate declarations: not applicable.

CRediT authorship contribution statement

A. Stredˈanská: Writing – original draft, Investigation, Data curation. **D. Nečas:** Writing – review & editing, Supervision, Data curation, Conceptualization. **M. Vrbka:** Supervision, Project administration, Methodology. **J. Suchánek:** Methodology, Conceptualization. **J. Matonohová:** Project administration, Investigation, Formal analysis. **E. Toropitsyn:** Methodology, Investigation. **M. Hartl:** Funding acquisition. **I. Křupka:** Project administration, Resources. **K. Nešporová:** Project administration, Methodology, Funding acquisition, Conceptualization.

Declaration of competing interest

The authors declare that they have no known competing financial interests or personal relationships that could have appeared to influence the work reported in this paper.

Data availability

The research data is published on the ZENODO with the source in the article.

Acknowledgment

This publication was supported by the project "Mechanical Engineering of Biological and Bio-inspired Systems", funded as project No. CZ.02.01.01/00/22_008/0004634 by Programme Johannes Amos Comenius, call Excellent Research.

This project (Fascia lubrication and regeneration by hyaluronan) has received funding from the Operational Programme Enterprise and Innovations for Competitiveness 2014–2020 (OPEIC) under agreement No CZ.01.1.02/0.0/0.0/19_262/0020005.

Appendix A

The rheological properties of HA solutions

Due to the non-Newtonian behavior of HA solutions, we not only provide the viscosity value at zero shear rate but also publish viscosity curves within the shear gradient range of 1–1000 1/s. The zero-shear rate viscosity of HA solutions was determined using the Careau-Yasuda model through TRIOS software.

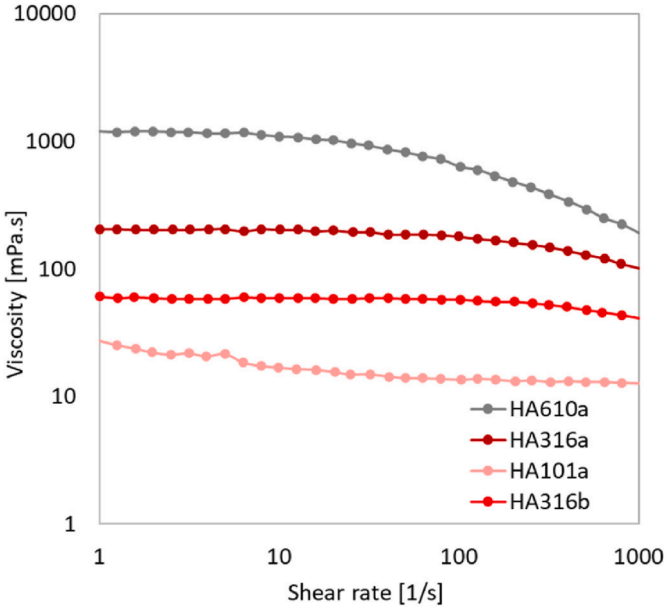

Fig. 8. The rheological curves - HA solutions.

Data analysis

In order to separate dynamic friction from static friction, a post-process analysis using Matlab software is performed after the data has been measured.

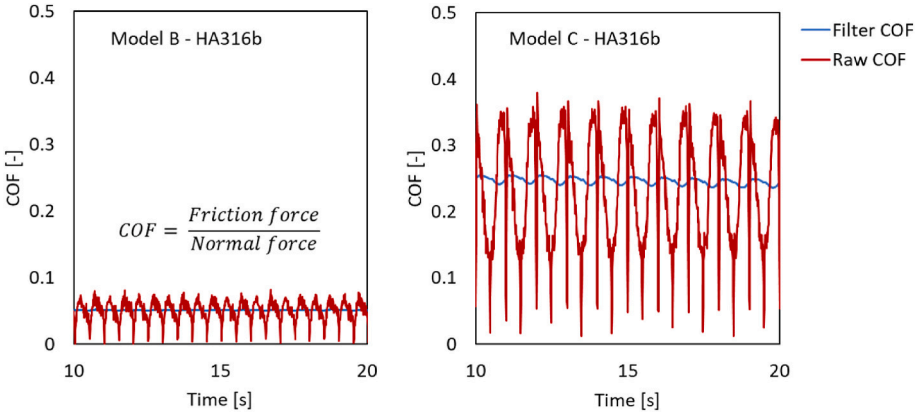

Fig. 9. Post-process data analysis example on Model B and C lubricated by HA316b.

Matlab function – *sgolayfilt*: translates the raw COF curve by a third-degree polynomial and thus filters out static friction. The result is a blue filter COF curve.

Tab. 4
The comparison of raw and filtered mean COF values.

	Model B	Model C
Raw mean COF (−)	0.045758863	0.233958
Filtered mean COF (−)	0.045739873	0.243161

References

Adam, A., Paulkowski, D., Mayer, B., 2019. Friction and deformation behavior of elastomers. Mater. Sci. Appl. 10, 527–542. https://doi.org/10.4236/msa.2019.108038.

Adams, M., Briscoe, B., Johnson, S., 2007. Friction and lubrication of human skin. Tribol. Lett. 26, 239–253. https://doi.org/10.1007/s11249-007-9206-0.

Albert, W., Duncan, C., Currie-Jackson, N., Gaudet, V., Callaghan, J., 2006. Biomechanical Assessment of Massage Therapists, Occupational Ergonomics, vol. 6, pp. 1–11. https://doi.org/10.3233/OER-2006-6101.

Balagué, F., Mannion, A., Pellisé, F., Cedraschi, C., 2012. Non-specific low back pain. Lancet 379, 482–491. https://doi.org/10.1016/S0140-6736(11)60610-7.

Barquins, M., 1992. Adherence, friction and wear of rubber-like materials. Wear 158, 87–117. https://doi.org/10.1016/0043-1648(92)90033-5.

Berdichevsky, Y., Khandurina, J., Guttman, A., Lo, Y., 2004. UV/ozone modification of poly(dimethylsiloxane) microfluidic channels. Sensor. Actuator. B Chem. 97, 402–408. https://doi.org/10.1016/j.snb.2003.09.022.

Blasi, M., Blasi, J., Domingo, T., Pérez-Bellmunt, A., Miguel-Pérez, M., 2015. Anatomical and histological study of human deep fasciae development. Surg. Radiol. Anat. 37, 571–578. https://doi.org/10.1007/s00276-014-1396-1.

Bongaerts, J., Fourtouni, K., Stokes, J., 2007. Soft-tribology: lubrication in a compliant PDMS–PDMS contact. Tribol. Int. 40, 1531–1542. https://doi.org/10.1016/j.triboint.2007.01.007.

Černohlávek, M., Brandejsová, M., Štěpán, P., Vagnerová, H., Hermannová, M., Kopecká, K., Kulhánek, J., Nečas, D., Vrbka, M., Velebný, V., Huerta-Angeles, G., 2021. Insight into the lubrication and adhesion properties of hyaluronan for ocular drug delivery. Biomolecules 11. https://doi.org/10.3390/biom11101431.

Chen, C., Nizar, A., 2011. Myofascial pain syndrome in chronic back pain patients. Korean J. Pain 24, 100–104. https://doi.org/10.3344/kjp.2011.24.2.100.

Chen, S., Chen, M., Wu, X., Lin, S., Tao, C., Cao, H., Shao, Z., Xiao, G., 2022. Global, regional and national burden of low back pain 1990–2019: a systematic analysis of the Global Burden of Disease study 2019. J. Orthopaedic Transl. 32, 49–58. https://doi.org/10.1016/j.jot.2021.07.005.

Choi, S., Shin, J., Cheong, Y., Lee, H., Jin, K., Park, H., 2011. Nanostructural investigation of frontalis sling biomaterial surfaces. Scanning 33, 419–425. https://doi.org/10.1002/sca.20233.

Cowman, M., Schmidt, T., Raghavan, P., Stecco, A., 2015. Viscoelastic properties of hyaluronan in physiological conditions. F1000Research 4, 6–22. https://doi.org/10.12688/f1000research.6885.1.

Dąbrowska, A., Rotaru, G., Spano, F., Affolter, C., Fortunato, G., Lehmann, S., Derler, S., Spencer, N., Rossi, R., 2017. A water-responsive, gelatine-based human skin model. Tribol. Int. 113, 316–322. https://doi.org/10.1016/j.triboint.2017.01.027.

de Vicente, J., Stokes, J., Spikes, H., 2006. Rolling and sliding friction in compliant, lubricated contact. Proc. IME J. J. Eng. Tribol. 220, 55–63. https://doi.org/10.1243/13506501JET90.

Derler, S., Schrade, U., Gerhardt, L., 2007. Tribology of human skin and mechanical skin equivalents in contact with textiles. Wear 263, 1112–1116. https://doi.org/10.1016/j.wear.2006.11.031.

Dresselhuis, D., Dehoog, E., Cohenstuart, M., Vanaken, G., 2008. Application of oral tissue in tribological measurements in an emulsion perception context. Food Hydrocolloids 22, 323–335. https://doi.org/10.1016/j.foodhyd.2006.12.008.

Edmonds, R., Finney, T., Bull, M., Watrelot, A., Kuhl, T., 2021. Friction measurements of model saliva-wine solutions between polydimethylsiloxane surfaces. Food Hydrocolloids 113. https://doi.org/10.1016/j.foodhyd.2020.106522.

Falcone, S., Palmeri, D., Berg, R., 2006. Rheological and cohesive properties of hyaluronic acid. J. Biomed. Mater. Res. 76A, 721–728. https://doi.org/10.1002/jbm.a.30623.

Fede, C., Angelini, A., Stern, R., Macchi, V., Porzionato, A., Ruggieri, P., De Caro, R., Stecco, C., 2018. Quantification of hyaluronan in human fasciae: variations with function and anatomical site. J. Anat. 233, 552–556. https://doi.org/10.1111/joa.12866.

Fraser, J., Laurent, T., Laurent, U., 1997. Hyaluronan: its nature, distribution, functions and turnover. J. Intern. Med. 242, 27–33. https://doi.org/10.1046/j.1365-2796.1997.00170.x.

Hillborg, H., Sandelin, M., Gedde, U., 2001. Hydrophobic recovery of polydimethylsiloxane after exposure to partial discharges as a function of crosslink density. Polymer 42, 7349–7362. https://doi.org/10.1016/S0032-3861(01)00202-6.

Ido, T., Yamaguchi, T., Shibata, K., Matsuki, K., Yumii, K., Hokkirigawa, K., 2019. Sliding friction characteristics of styrene butadiene rubbers with varied surface roughness under water lubrication. Tribol. Int. 133, 230–235. https://doi.org/10.1016/j.triboint.2019.01.015.

Kim, A., Cholewinski, A., Mitra, S., Zhao, B., 2020. Viscoelastic tribopairs in dry and lubricated sliding friction. Soft Matter 16, 7447–7457. https://doi.org/10.1039/D0SM00516A.

Langevin, H., Fox, J., Koptiuch, C., Badger, G., Greenan- Naumann, A., Bouffard, N., Konofagou, E., Lee, W., Triano, J., Henry, S., 2011. Reduced thoracolumbar fascia shear strain in human chronic low back pain. BMC Muscoskel. Disord. 12 https://doi.org/10.1186/1471-2474-12-203.

Laurent, T., Laurent, U., Fraser, J., 1996. The structure and function of hyaluronan: an overview. Immunol. Cell Biol. 74, a1–a7. https://doi.org/10.1038/icb.1996.32.

Mahdi, D., Riches, A., Gester, M., Yeomans, J., Smith, P., 2015. Rolling and sliding: separation of adhesion and deformation friction and their relative contribution to total friction. Tribol. Int. 89, 128–134. https://doi.org/10.1016/j.triboint.2014.12.021.

Matteini, P., Dei, L., Carretti, E., Volpi, N., Goti, A., Pini, R., 2009. Structural behavior of highly concentrated hyaluronan. Biomacromolecules 10, 1516–1522. https://doi.org/10.1021/bm900108z.

Myant, C., Spikes, H., Stokes, J., 2010. Influence of load and elastic properties on the rolling and sliding friction of lubricated compliant contacts. Tribol. Int. 43, 55–63. https://doi.org/10.1016/j.triboint.2009.04.034.

Nečas, D., Sadecká, K., Vrbka, M., Gallo, J., Galandáková, A., Křupka, I., Hartl, M., 2019. Observation of lubrication mechanisms in knee replacement: a pilot study. Biotribology 17, 1–7. https://doi.org/10.1016/j.biotri.2019.02.001.

Nečas, D., Kulíšek, V., Štěpán, P., Ondreáš, F., Čípek, P., Huerta-Angeles, G., Vrbka, M., 2023. Friction and lubrication of eye/lens/lid interface: the effect of lubricant and contact lens material. Tribol. Lett. 71 https://doi.org/10.1007/s11249-023-01787-4.

Nešporová, K., Matonohová, J., Husby, J., Toropitsyn, E., Stupecká, L., Husby, A., Suchánková Kleplová, T., Streďanská, A., Šimek, M., Nečas, D., Vrbka, M., Schleip, R., Velebný, V., 2023. Injecting hyaluronan in the thoracolumbar fascia: a model study. Int. J. Biol. Macromol. 253 https://doi.org/10.1016/j.ijbiomac.2023.126879.

Pavan, P., Stecco, A., Stern, R., Stecco, C., 2014. Painful connections: densification versus fibrosis of fascia. Curr. Pain Headache Rep. 18 https://doi.org/10.1007/s11916-014-0441-4.

Pavan, P., Stecco, A., Stern, R., logna Prat, P., Stecco, C., 2016. Fibrosis and densification: anatomical vs functional alteration of the fascia. J. Bodyw. Mov. Ther. 20 https://doi.org/10.1016/j.jbmt.2015.07.029.

Plasqui, G., Bonomi, A., Westerterp, K., 2013. Daily physical activity assessment with accelerometers: new insights and validation studies. Obes. Rev. 14, 451–462. https://doi.org/10.1111/obr.12021.

Popov, V., 2010. Contact mechanics and friction, 362. https://doi.org/10.1007/978-3-642-10803-7.

Rand, C., Crosby, A., 2009. Friction of soft elastomeric wrinkled surfaces. J. Appl. Phys. 106 https://doi.org/10.1063/1.3226074.

Rebenda, D., Vrbka, M., Nečas, D., Toropitsyn, E., Yarimitsu, S., Čípek, P., Pravda, M., Hartl, M., 2021. Rheological and frictional analysis of viscosupplements towards improved lubrication of human joints. Tribol. Int. 160 https://doi.org/10.1016/j.triboint.2021.107030.

Rennie, A., Dickrell, P., Sawyer, W., 2005. Friction coefficient of soft contact lenses: measurements and modeling. Tribol. Lett. 18, 499–504. https://doi.org/10.1007/s11249-005-3610-0.

Sadowski, P., Stupkiewicz, S., 2019. Friction in lubricated soft-on-hard, hard-on-soft and soft-on-soft sliding contacts. Tribol. Int. 129, 246–256. https://doi.org/10.1016/j.triboint.2018.08.025.

Schallamach, A., 1958. Friction and abrasion of rubber. Wear 1, 384–417. https://doi.org/10.1016/0043-1648(58)90113-3.

Schallamach, A., 1971. How does rubber slide? Wear 17, 301–312. https://doi.org/10.1016/0043-1648(71)90033-0.

Schneemilch, M., Quirke, N., 2007. Effect of oxidation on the wettability of poly (dimethylsiloxane) surfaces. J. Chem. Phys. 127 https://doi.org/10.1063/1.2770723.

Selway, N., Chan, V., Stokes, J., 2017. Influence of fluid viscosity and wetting on multiscale viscoelastic lubrication in soft tribological contacts. Soft Matter 13, 1702–1715. https://doi.org/10.1039/C6SM02417C.

Stecco, C., Macchi, V., Porzionato, A., Duparc, F., De Caro, R., 2011a. The fascia: the forgotten structure. J. Anat. Embryol. 116 (3), 127–138. https://doi.org/10.13128/IJAE-10683.

Stecco, C., Stern, R., Porzionato, A., Macchi, V., Masiero, S., Stecco, A., De Caro, R., 2011b. Hyaluronan within fascia in the etiology of myofascial pain. Surg. Radiol. Anat. 33, 891–896. https://doi.org/10.1007/s00276-011-0876-9.

Streďanská, A., Nečas, D., Vrbka, M., Křupka, I., Hartl, M., Toropitsyn, E., Husby, J., 2022. Development of tribological model of human fascia: the influence of material hardness and motion speed. Biotribology 30. https://doi.org/10.1016/j.biotri.2022.100209.

Streďanská, A., Nečas, D., Vrbka, M., Suchánek, J., Matonohová, J., Toropitsyn, E., Hartl, M., Křupka, I., Nešporová, K.. Understanding frictional behavior in fascia tissues through tribological modeling and material substitution. Zenodo. https://doi.org/10.5281/zenodo.11108538.

Tesarz, J., Hoheisel, U., Wiedenhöfer, B., Mense, S., 2011. Sensory innervation of the thoracolumbar fascia in rats and humans. Neuroscience 194, 302–308. https://doi.org/10.1016/j.neuroscience.2011.07.066.

Tiwari, A., Dorogin, L., Bennett, A., Schulze, K., Sawyer, W., Tahir, M., Heinrich, G., Persson, B., 2017. The effect of surface roughness and viscoelasticity on rubber adhesion. Soft Matter 13, 3602–3621. https://doi.org/10.1039/C7SM00177K.

Van Kuilenburg, J., Masen, M., van der Heide, E., 2015. A review of fingerpad contact mechanics and friction and how this affects tactile perception. Proc. IME J. J. Eng. Tribol. 229, 243–258. https://doi.org/10.1177/1350650113504908.

Vinke, J., Kaper, H., Vissink, A., Sharma, P., 2018. An ex vivo salivary lubrication system to mimic xerostomic conditions and to predict the lubricating properties of xerostomia relieving agents. Sci. Rep. 8 https://doi.org/10.1038/s41598-018-27380-7.

Vlădescu, S., Agurto, M., Myant, C., Boehm, M., Baier, S., Yakubov, G., Carpenter, G., Reddyhoff, T., 2023. Protein-induced delubrication: how plant-based and dairy proteins affect mouthfeel. Food Hydrocolloids 134. https://doi.org/10.1016/j.foodhyd.2022.107975.

Voll, L., Popov, V., 2014. Experimental investigation of the adhesive contact of an elastomer. Phys. Mesomech. 17, 232–235. https://doi.org/10.1134/S1029959914030096.

Watrelot, A., Kuhl, T., Waterhouse, A., 2019. Friction forces of saliva and red wine on hydrophobic and hydrophilic surfaces. Food Res. Int. 116, 1041–1046. https://doi.org/10.1016/j.foodres.2018.09.043.

Xu, Y., Cartwright, B., Advincula, L., Myant, C., Stokes, J., 2021. Generalised scaling law for soft contact tribology: influence of load and asymmetric surface deformation. Tribol. Int. 163 https://doi.org/10.1016/j.triboint.2021.107192.

Xue, L., Pham, J., Iturri, J., del Campo, A., 2016. Stick–slip friction of PDMS surfaces for bioinspired adhesives. Langmuir 32, 2428–2435. https://doi.org/10.1021/acs.langmuir.6b00513.

Ye, X., Liu, H., Ding, Y., Li, H., Lu, B., 2009. Research on the cast molding process for high quality PDMS molds. Microelectron. Eng. 86, 310–313. https://doi.org/10.1016/j.mee.2008.10.011.

Zhao, T., Wang, G., Hao, D., Chen, L., Liu, K., Liu, M., 2018. Macroscopic layered organogel-hydrogel hybrids with controllable wetting and swelling performance. Adv. Funct. Mater. 28 https://doi.org/10.1002/adfm.201800793.

lubricants

MDPI

Article

Optimizing Hyaluronan-Based Lubricants for Treating Thoracolumbar Fascia Pathologies: Insights from Tribological and Pharmacokinetic Studies

Alexandra Streďanská [1], Matěj Šimek [2], Jana Matonohová [2], David Nečas [1], Martin Vrbka [1,*], Jakub Suchánek [3], Veronika Pavliňáková [4], Lucy Vojtová [4], Martin Hartl [1], Ivan Křupka [1] and Kristina Nešporová [2]

[1] Biotribology Research Group, Faculty of Mechanical Engineering, Brno University of Technology, Technická 2896/2, 616 69 Brno, Czech Republic; alexandra.stredanska@vut.cz (A.S.); david.necas@vut.cz (D.N.); martin.hartl@vut.cz (M.H.); ivan.krupka@vut.cz (I.K.)
[2] Contipro a.s., Dolní Dobrouč 401, 561 02 Dolní Dobrouč, Czech Republic; matej.simek@contipro.com (M.Š.); jana.matonohova@contipro.com (J.M.); kristina.nesporova@contipro.com (K.N.)
[3] Faculty of Medicine in Hradec Králové, Charles University, Šimkova 870, 500 03 Hradec Králové, Czech Republic; suchanekj@lfhk.cuni.cz
[4] CEITEC—Central European Institute of Technology, Brno University of Technology, Purkyňova 656/123, 612 00 Brno, Czech Republic; veronika.pavlinakova@ceitec.vutbr.cz (V.P.); lucy.vojtova@ceitec.vutbr.cz (L.V.)
* Correspondence: martin.vrbka@vut.cz

Abstract: In a world where the incidence of non-specific lower back pain (LBP) is steadily increasing, researchers are still searching for effective solutions for patients. Hyaluronic acid (HA) viscosupplementation is commonly used to restore lubrication in osteoarthritis (OA) and other medical applications, but its rapid metabolism limits efficacy. This study evaluates whether an HA derivative can replace native HA for the treatment of non-specific LBP while maintaining or enhancing its frictional properties and improving in vivo stability. Six HA-based lubricants, both native and derivatized, were tested in a tribological rabbit fascia model and a new synthetic model. Reduced HA derivative showed better tribological properties and longer in vivo residence time compared to native HA, as demonstrated in pharmacokinetic studies in rabbits. The 316 kDa HA and reduced HA exhibited the most stable tribological properties, which were influenced by their molecular weight and concentration. These findings suggest that both native and reduced HA are promising viscosupplements for intrafascial injection in the treatment of LBP, with reduced HA potentially enhancing effectiveness through a prolonged effect.

Keywords: lower back pain; hyaluronic acid; fascia; friction; viscosupplementation

Received: 6 March 2025
Revised: 14 April 2025
Accepted: 15 April 2025
Published: 16 April 2025

Citation: Streďanská, A.; Šimek, M.; Matonohová, J.; Nečas, D.; Vrbka, M.; Suchánek, J.; Pavliňáková, V.; Vojtová, L.; Hartl, M.; Křupka, I.; et al. Optimizing Hyaluronan-Based Lubricants for Treating Thoracolumbar Fascia Pathologies: Insights from Tribological and Pharmacokinetic Studies. *Lubricants* **2025**, *13*, 184. https://doi.org/10.3390/lubricants13040184

1. Introduction

In recent years, there has been a significant increase in cases of lower back pain (LBP) among individuals [1,2]. The treatment for LBP can be financially burdensome and prolonged, often without accurately diagnosing the underlying cause. As a result, many individuals may experience work incapacity [1]. Research suggests that one possible cause of LBP could be the thoracolumbar fascia (TLF), which undergoes pathological changes [3–5]. Healthy fascia typically consists of two or three layers of connective tissue that glide smoothly and are lubricated by hyaluronic acid (HA) [6]. However, an unhealthy lifestyle and overuse syndromes can lead to structural changes in the fascia.

Such changes in the fascia can include densification and fibrosis, which are distinct pathological alterations. The two alterations often occur simultaneously. Fibrosis refers to a

pathological change in the fibrous component of the fascia, characterized by the random accumulation of collagen fibers. This type of change is challenging to modify manually during rehabilitation. On the other hand, densification is a change in the viscosity of the loose connective tissue within the fascia, resulting from the more viscous HA [7–9]. This causes patients with chronic LBP to exhibit reduced gliding of the TLF [5]. Furthermore, it has been proposed that heightened muscle exertion elevates the molecular weight (MW) of HA, consequently increasing its viscosity [10,11], while the increase in viscosity of HA is also associated with immobilization [12]. This elevation in viscosity may impede normal muscle movement within loose connective tissue. Analogous to its function in joint and synovial fluid, heightened HA production represents an initial effort by the fascia to enhance its mobility. At elevated concentrations, HA behaves similarly to a non-Newtonian fluid, exhibiting increased viscosity as the HA chains entangle, thereby contributing to the solution's hydrodynamic characteristics [6]. The heightened viscosity of HA, coupled with the sparsity of connective tissue due to pathological alterations within and upon the fascia, reduces the sliding between the collagen fiber layers of the deep fascia, consequently resulting, again, in a sensation of stiffness in the patient's back.

Viscosupplementation with HA is widely used to restore lubrication and improve the gliding of connective tissues in osteoarthritis (OA), as well as to reduce friction and enhance comfort between contact lenses and the eye [13]. Intrafascial injections of HA, a promising therapeutic approach recently introduced by our group, could similarly restore the reduced gliding ability of the fascia by reducing friction between its layers [14]. However, a key limitation of using HA in medicine is its relatively rapid degradation in the human body, which restricts its duration of action. To extend its residence time at the application site, HA can be chemically modified [15] while preserving its essential mucoadhesiveness and biocompatibility [16]. For example, a form of HA with partially reduced carboxyl groups offers increased thermal stability and enzymatic resistance [16]. While reduced HA has not yet been studied for LBP treatment, it has been widely researched for restoring joint lubrication in OA [17]. The amphiphilic form of HA is known for its resistance to enzymatic degradation and its ability to interact through both ionic and hydrophobic interactions [18]. Compared to native HA, this derivative exhibits significantly enhanced shear-thinning behavior [19]. It has been previously studied for use in eye drops to treat dry eyes [20], where this form demonstrated extremely low friction and effectively prevented surface eye cells from drying out, outperforming regular HA.

Therefore, this study aims to determine if native HA used in viscosupplementation for treating non-specific LBP can be effectively replaced with a derivative that maintains or even enhances its frictional properties while offering improved in vivo stability. We rigorously tested six HA-based lubricants, in both native and derivatized forms, on a tribological model of rabbit fascia introduced in [21]. Simultaneously, a new synthetic model was introduced to verify the lubricants' influence on fascia friction. The most promising derivative based on tribological testing, reduced HA [22], exhibits nontoxic properties and biodegradability comparable to native HA, as demonstrated in a pharmacokinetic study involving rabbits.

2. Materials and Methods

2.1. Lubricants

Native HA (101, 316 and 610 kDa) and HA derivatives (reduced HA (HA RED and lauroyl-modified HA (HA-C12)), provided and biotechnologically manufactured by Contipro a.s. (Dolní Dobrouč, Czech Republic), were dissolved in PBS and sterilized by filtration. Concentrations and viscosity of tested solutions are summarized in Table 1. Structures of HA derivatives are displayed in Figure S1.

Table 1. Lubricants used for tribological tests.

Designation	Molecular Weight (kDa)	Degree of Substitution	Concentration (mg/mL)	Viscosity (mPa·s, 37 °C)
610 kDa HA	610	-	20	1191
316 kDa HA	316	-	20	202
101 kDa HA	101	-	20	27
316 kDa HA (lower conc.)	316	-	10	59
HA-RED	275	18%	20	122
HA-C12	318	9.1%	3	37

For the pharmacokinetics study, a solution of ^{13}C-labelled 316 kDa HA and a solution of HA-RED were prepared in normal saline (0.9% NaCl) at a concentration of 10 mg/mL. Labelling of HA with the nonradioactive isotope ^{13}C was used to distinguish the administered HA from endogenous HA [23]. After sterilization by filtration, they were additionally autoclaved. Apyrogenicity of the solutions was then verified using a portable endotoxin testing system (Endosafe® nexgenPTS™ testing system, Charles River Laboratories, Wilmington, MA, USA) and only apyrogenic samples (endotoxin levels < 0.1 IU/mL) were used for study.

2.2. Tribological Setup

Bruker UMT TriboLab (Bruker, Billerica, MA, USA) was used to measure friction and lubrication properties of test samples in a pin-on-plate configuration. The tribometer sensor recorded the normal and friction force, from which the value of the friction coefficient was calculated as a function of time. The static pin was loaded with 2 N normal force. The plate moved with a 1 Hz frequency of reciprocal linear motion and 12 mm track length. The same amount of lubricant and test temperature were kept for each test (2 mL of lubricant, 37 °C). Two types of experiments were conducted based on changes in the test time. The short-term 300 s tests and the preload effect tests were repeated five times. The long-term 3000 s tests were tested three times. Experimental conditions were chosen based on physiological conditions, therapy, and the limitations of the test facility. For more information, refer to the Materials and Methods Section in the previous publication [21].

The experimental apparatus, in pin-on-plate configuration, consisted of a pot and pin part. The pin has a convex surface with a 50 mm radius on which the polydimethylsiloxane (PDMS) with a 1 mm thickness is embedded. The fascia is stretched over the surface of the pin and PDMS, which is attached with jaws screwed into the pin. The pot is divided into two main parts. The lower part provides attachment to the tribometer, heating cartridges, and an assembly of jaws to hold the sample. In the bottom part, PDMS is inserted and, over it, fascia is prestressed by the jaws. This study examines the effect of different levels of prestressing when the fascia is stretched to three degrees: strong, medium, and weak. These levels are defined by the width of the fascia when stretched at the center and edges of the specimen. The lubricants examined in this study were laid on elastomer PDMS of 10 ShA stiffness simulating underlying muscle. Sliding friction tests were carried out for prepared thoracolumbar rabbit fascia and SynDaver™ (Tampa, FL, USA) synthetic fibrous fascia tissue.

2.3. Preparation of Samples of Rabbit TLF

Sexually mature New Zealand white rabbits, with body weights of at least 3 kg, were used for preparation of TLF for tribological testing. The rabbits were first sedated by subcutaneous administration of medetomidine (0.3 mg/kg; Domitor inj., Orion Corporation, Espoo, Finland) and then induced into general anesthesia by intramuscular administration

of ketamine (25 mg/kg; Narkamon inj., Bioveta, Ivanovice na Hane, Czech Republic). Subsequently, the animals were stunned with a captive bolt gun and then exsanguinated by transecting the carotid artery (arteria carotis communis). After removing the skin from the cadaver, a paravertebral incision was made, thereby releasing the TLF from the spine. Then, the fascia was released by blunt dissection from the back muscle up to the latissimus dorsi muscle, tensor fascia late muscle and external oblique abdominis muscle. The collected TLF was immersed in a transport solution (Hanks balanced salt solution) and transported to the laboratory at 4 °C. The chilled fascia was removed from the test tube after 16 h at 4 °C and moved, along with the transport solution, to a sterilized Petri dish to prevent the tissue from drying out. Subsequently, the right or left part of the fascia was taken out and spread on a glass plate, see Figure 1. After measuring, a sample of approximately 60 × 20 mm of the test sample was cut out with dissecting scissors. The prepared sample was attached to the tribometer.

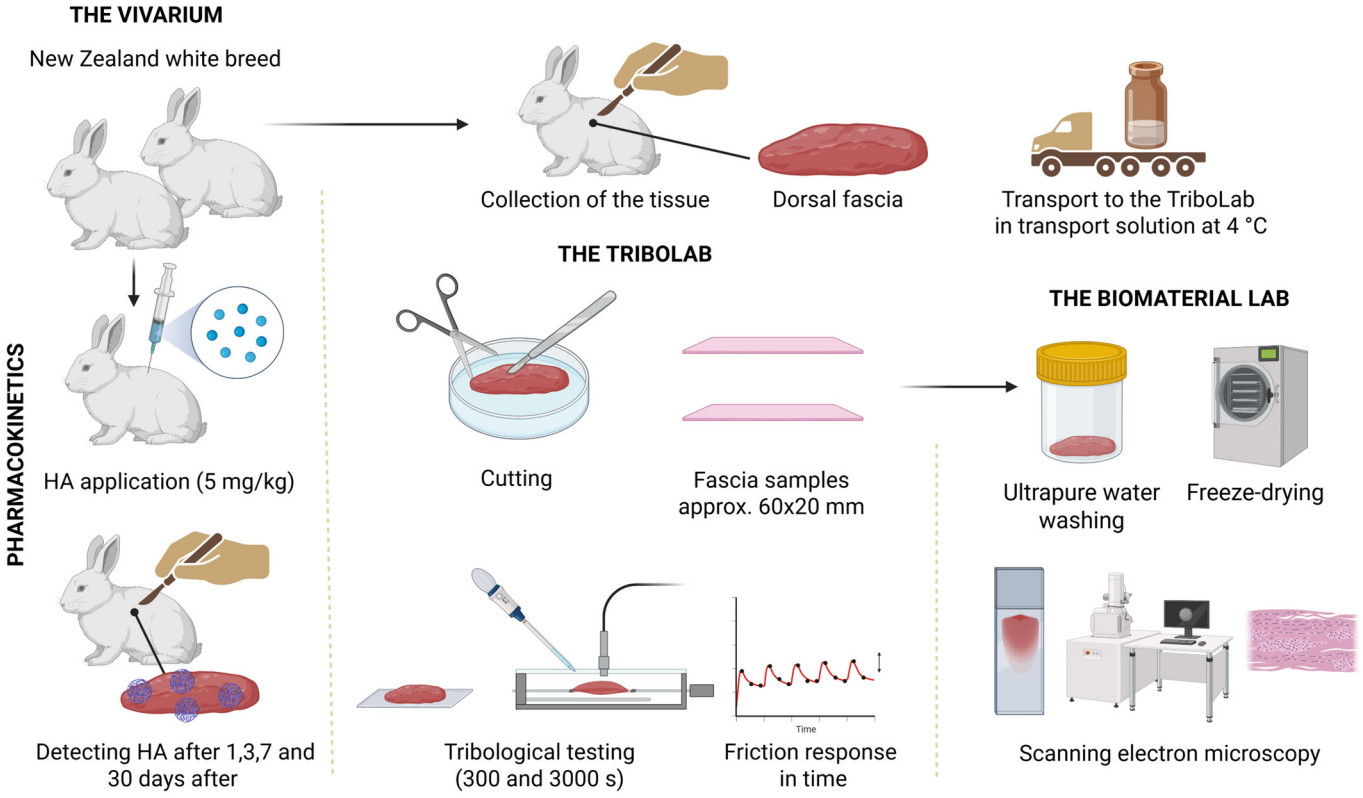

Figure 1. A summary diagram of the methods used for rabbit fascia in the present study. Created with www.Biorender.com (accessed on 21 May 2024).

Fascia for electron microscopy scanning was washed with ultrapure water (Type II according to ISO 3696 [24], prepared on an Elix 5 UV Water Purification System (Merck, Darmstadt, Germany)). Then, the specimen was freeze-dried on an Epsilon 2-10D machine (Martin Christ, Osterode am Hartz, Germany). A scanning electron microscope, MIRA3 (TESCAN, Brno, Czech Republic), was used to study the morphology of the dried fascia sample. Images were taken in secondary electron emission mode; the scan mode was DEPTH, the beam density was 10, and the high voltage was 10 kV. The working distance was set to 15 mm. The surface of the sample was coated with a 15 nm thin layer of Au using an EM ACE 600 (Leica Microsystems, Wetzlar, Germany).

2.4. Pharmacokinetic Study

This study was approved by the Ethics Committee of the Ministry of Education, Youth and Sports (approval No. MSMT-2036/2022-3). For this study, 48 healthy, sexually mature

New Zealand white male rabbits (weighing 2.7–3.5 kg) obtained from a certified laboratory animal breeder and supplier, VELAZ, Ltd. (Prague, Czech Republic), were used. The rabbits were acclimated for a period of two weeks before the experiment began. The animals were housed individually in clean stainless-steel cages under standardized environmental conditions (12-h light/dark cycle, temperature 17–21 °C, air humidity 30–70%). The rabbits had access ad libitum to the standard diet for rabbits (VELAZ Ltd., Prague, Czech Republic) and drinking water. The rabbits were randomly allocated into eight groups, with six rabbits per group. The groups differed in the amount of intrafascial injected solution (HA-RED/^{13}C-labelled 316 kDa HA) and in the euthanasia time after the solution administration (1/3/7/30 days). The rabbits were first sedated by subcutaneous administration of medetomidine (0.3 mg/kg; Domitor inj., Orion Corporation, Espoo, Finland) and then induced into general anesthesia by intramuscular administration of ketamine (25 mg/kg; Narkamon inj., Bioveta, Ivanovice na Hane, Czech Republic). Subsequently, the rabbits were shaved on their backs (approximately 4 × 4 cm in the application sites of the thoracolumbar spine area), and, using a 25G needle under ultrasound guidance (Lumify, Philips, Amsterdam, The Netherlands), they were injected with a 1% solution of ^{13}C-labelled 316 kDa HA or a 1% solution of HA-RED (according to their experimental group) in the amount of 0.7 mL on each side between the superficial and deep layers of the thoracolumbar fascia at the level of the L2–L3 intervertebral junction, 50 mm lateral to the spine (left and right). The application sites were then gently massaged manually to evenly spread the injected solution between the fascial layers throughout the entire extent of the fascia. At 1, 3, 7, or 30 days after the intrafascial administration of HA-RED or ^{13}C-labelled 316 kDa HA solution, depending on the experimental group, the animals were sedated by subcutaneous administration of medetomidine (0.3 mg/kg; Domitor inj., Orion Corporation, Espoo, Finland) and then induced into general anesthesia by intramuscular administration of ketamine (25 mg/kg; Narkamon inj., Bioveta, Ivanovice na Hane, Czech Republic). A non-coagulated blood sample (1 mL) was then collected from the central ear artery (arteria auricularis centralis), centrifuged, and the plasma was separated. Subsequently, the animals were stunned with a captive bolt gun and then exsanguinated by transecting the carotid artery (arteria carotis communis). Then, after removing the skin from the rabbit cadavers, the TLF tissue samples were obtained as two separate samples: a partial-thickness fascia (without the epimysial layer) by separation from the spine through a paravertebral incision and releasing by blunt dissection from the back muscles, and the corresponding epimysial layer with muscle tissue underneath. Both types of samples were weighed separately, frozen individually at −20 °C, and transported to the laboratory for quantification of administered ^{13}C-labelled 316 kDa HA and HA-RED in the fascia and muscle by LC-MS.

2.5. Determination of Isotopically Labelled HA and HA-RED in Rabbit Fascia and Muscle

For the quantification of HA derivatives, a modified LC-MS method based on quantification of HA disaccharides after enzymatic hydrolysis was employed [25] (Figure S2). Briefly, weighted samples of fascia and muscle were diluted with buffer (100 mM PBS with 10 mM EDTA, pH 7.4) and homogenized with Precellys Evolution homogenizer (Bertin Technologies, France). To 100 µL aliquot, internal standard of fully isotopically labelled 8×^{13}C-HA (lower conc.) was added, and samples were incubated for 3 h at 45 °C with 40 µL of 1% Actinase E solution (Merck, Germany) in HEPES buffer (pH 8). Afterwards, 1 µL of solution of hyaluronan lyase from Streptococcus pneumoniae (Contipro a.s., Czech Republic) was added and samples were incubated for 30 min at 37 °C. Finally, 400 µL of acetonitrile (LC-MS grade, VWR, Radnor, PA, USA) was added, the samples were centrifuged (30 s, 10,000 rpm) and supernatants were analyzed by LC-MS. A Vanquish Horizon chromatography system and a TQS Altis plus triple quadrupole mass spectrometer (both

Thermo Fisher Scientific, Waltham, MA, USA) were used for analysis. A total of 2 µL of sample were injected onto an Acquity BEH HILIC Amide (2.1 × 100 mm) analytical column (Waters, Wilmslow, UK) tempered at 60 °C. The mobile phases consisted of 0.1% formic acid (*v*/*v*) (LC-MS grade, Merck, Germany) and acetonitrile (LC-MS grade, VWR, USA). The gradient of acetonitrile was as follows: 0–0.5 min 90%, 0.5–5 min 90–74%, 5–7 min 74–40%, 7–7.5 min 40–90%, 7.5–9 min 90%. The electrospray settings for the analysis were as follows: capillary voltage −4000 V, Sheath gas 50, Aux gas 10, Sweep gas 0.5, ion transfer tube temp. 275 °C, vaporizer temp. 350 °C. MRM transitions of unsaturated disaccharides for $1\times^{13}$C-316 kDa HA (lower conc.) and fully labelled HA together with unsaturated tetrasaccharide of HA-RED were detected during the analysis.

2.6. Preparation of Tribological Samples from Synthetic Fascia

The 1 mm synthetic substitute fascia, consisting of multiple fiber planes, was purchased from SynDaver^{TM} (*Fibrous fascia*, SKU: 141620), and is designed primarily for medical device design testing and for medical professionals to practice surgery. Pre-preparation and storage of synthetic fascia were performed according to manufacturer's instructions. The procedure for cutting, sizing, and mounting the specimens further coincides with the preparation of tribological samples from rabbit fascia.

2.7. Statistical Methods

Results were presented as a mean from three measurements ± SD (standard deviation) unless otherwise stated. Statistical criteria were verified by one-way or two-way ANOVA followed by Tukey's or Bonferroni's multiple comparisons tests, with individual variances computed for each comparison. The Tukey test was applied for short-term friction tests involving multiple group comparisons to detect significant differences while controlling the overall error rate, while the Bonferroni correction was used for long-term tests with a limited number of planned comparisons to minimize the risk of false positives. For all tests, * $p < 0.05$, ** $p < 0.01$, *** $p < 0.001$, and **** $p < 0.0001$ were considered to be significant.

3. Results

3.1. Testing of Preload Effect of Fascia on Friction

In tribological testing, the material in the experimental setup is preloaded to simulate the conditions experienced during muscle movement. Since stress levels can significantly impact friction results, this study begins by parametrically analyzing the effect of material preload on friction, utilizing jaw prestressing. Subsequent friction experiments were conducted five times using the 316 kDa HA lubricant, chosen due to its medium MW and widespread use among the lubricants in this study. Figure 2 illustrates that the bias level's effect on friction had almost no effect on rabbit fascia when the fascia is prestressed. Statistical analysis revealed the following significance levels: $p = 0.0427$ for the difference between weak and middle bias levels, $p = 0.0542$ for the difference between weak and strong, and $p = 0.9752$ for the difference between middle and strong for synthetic fascia. However, the influence of fascia prestressing emerges as a slightly more significant factor in synthetic fascia. In instances where the fascia is moderately or not prestressed, friction levels are lower compared to instances where the fascia is strongly prestressed. The coefficient of friction (COF) increased from 0.0517 (SD = 0.0076) or 0.04931 (SD = 0.0016) to 0.6275 (SD = 0.0023). Importantly, the bias level ceases to affect friction in cases of strong prestress levels. For rabbit fascia, the significance levels were $p = 0.8523$ between weak and middle, $p = 0.2301$ between weak and strong, and $p = 0.0002$ between middle and strong bias levels. Considering the results from the parametric study, the tribological tests in the following parts of the study were performed on a middle-prestressed fascia.

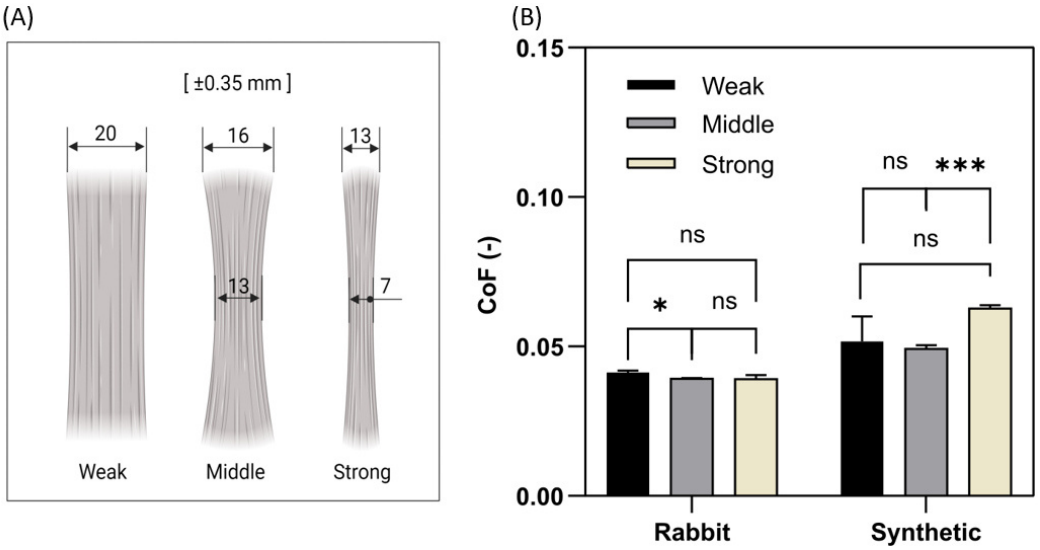

Figure 2. Level and friction influence of material prestressing of rabbit and synthetic fascia in experimental apparatus. (**A**) Illustration of specimen stretching and the locations of verifying specimen width measurements to categorize them as weak, medium, and strong. (**B**) Friction results of tribological testing. One-way ANOVA was used for statistical analysis.

3.2. Short-Term and Long-Term Testing of Fascia Friction

The friction experiments were conducted in two distinct stages. Initially, short-term tribological tests were conducted for 300 s. The results in Figure 3 were analyzed to determine which lubricant most effectively reduces the friction of the fascia and its layers. This information is valuable in identifying suitable properties for Visco supplements for treating non-specific LBP. Statistical performance between the different lubricants is listed in Table S1. 101 kDa HA and 316 kDa HA (lower conc.) exhibited the lowest COF for both materials. However, 316 kDa HA and HA-RED also demonstrated low friction with no significant difference observed for both ex vivo rabbit and synthetic fascia. Conversely, HA-C12 displayed the highest friction and standard deviation (SD) for synthetic fascia but the lowest for rabbit fascia. Lastly, 610 kDa HA exhibited the highest friction, nearly double that of 101 kDa HA and 316 kDa HA (lower conc.), for both materials. The results of the short-term tests indicate that HA-RED has the same efficacy on fascia friction as native HA with the same concentration and molecular weight. However, the interchangeability of HA-C12 with native HA remains debatable. Among the native HAs, 101 kDa HA and 316 kDa HA (lower conc.) are the most effective candidates for successfully reducing friction in fascia and its layers.

The second phase aimed to confirm the suitability of the lubricant for fascia lubrication based on long-term effects. Long-term tribological tests were conducted for 3000 s with other experimental conditions maintained. The results were presented for each material in Figure 4, illustrating the evolution of friction over time for rabbit fascia and synthetic fascia, respectively. These graphs are depicted as curves because the behavior of the lubricant in contact over time is deemed more important than the final or average friction value. An overview of the graph indicates that synthetic fascia exhibited more consistent behavior throughout the long-term test compared to other specimens, with fewer abrupt transitions and instabilities in the friction curves. However, HA-C12 lubrication notably deteriorated the performance of synthetic fascia, rendering it unsuitable for effective tribological testing with this lubricant. Conversely, the performance of rabbit fascia remained relatively steady across most scenarios, showing no significant deterioration in either case. Nonetheless, when paired with 610 kDa HA lubricant, slight fluctuations in performance were observed, with friction levels gradually increasing over time. A similar but more nuanced trend was

observed with 316 kDa HA (lower conc.) lubrication of rabbit fascia. Regarding HA-RED lubrication, one friction curve of rabbit fascia exhibited instability and a slight upward trend over time. The results of the long-term assays are consistent with the results of the short-term assays, confirming that HA-RED can replace native HA with the same properties if it demonstrates longer stability in vivo. While HA-C12 exhibits low friction on biological fascia, its performance on synthetic fascia raises questions about its long-term lubricating effects. Therefore, the benefits of HA-C12 compared with HA-RED need to be carefully evaluated. Native HAs generally demonstrated good stability over time. However, lower MW is associated with greater temporal stability, and lower concentrations result in reduced friction. Therefore, the best native candidate for reducing friction in the fascia and its layers is 316 kDa HA (lower conc.).

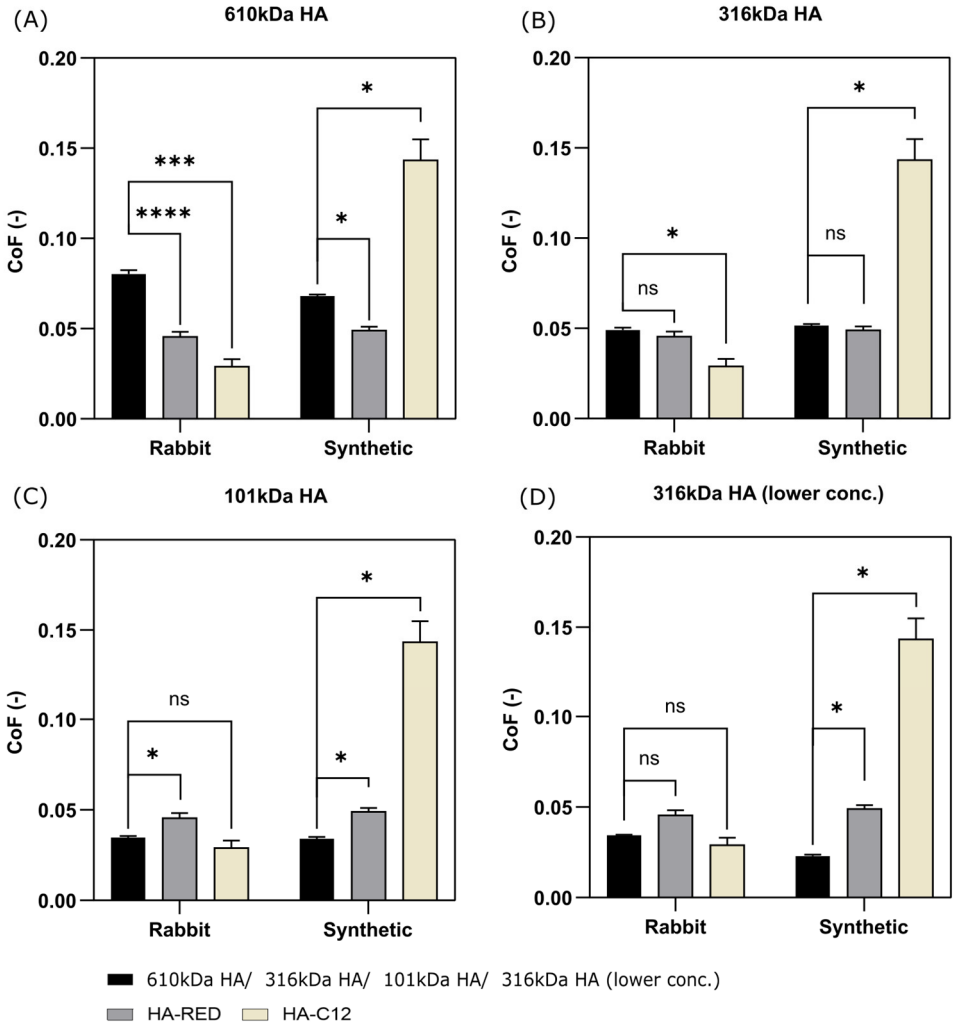

Figure 3. COF comparison of HA-based lubricants on rabbit and synthetic models. Two-way ANOVA was used for statistical analysis. Differences between native HA lubricants and derivatives tested on synthetic fascia were * $p < 0.05$, shown in Table S1. The graph presents a comparison of native HA forms against derivatives, therefore the results for HA-RED and HA-C12 are the same for parts (**A**–**D**). Black bar is labelled in terms of the plot name.

3.3. Pharmacokinetics of 316 kDa HA (Lower Conc.) and HA-RED After Application to the Fascia

Based on the tribological results, 316 kDa HA (lower conc.) and HA-RED were singled out as the candidates for the development of viscosupplementation for the treatment of non-specific LBP. To determine the pharmacokinetics of both materials and biodegradability of HA-RED, ^{13}C-labelled HA and HA-RED were administered to live rabbits via intrafascial

injection and the number of administered materials were quantified in fascia and muscle by LC-MS.

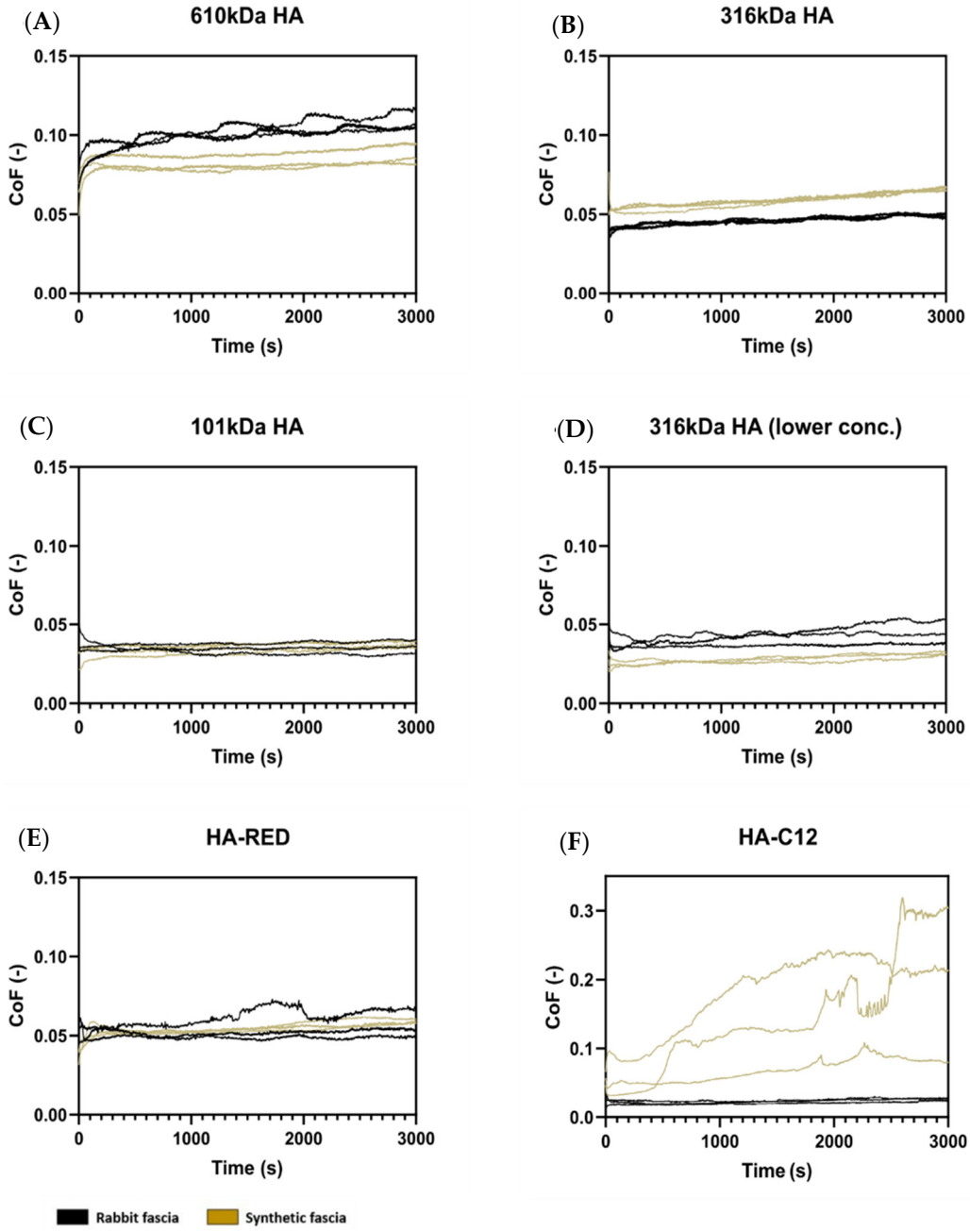

Figure 4. Development of friction in time of 3000 (s) for rabbit and synthetic fascia. One-way ANOVA was used for statistical analysis.

Although a relatively large amount of 316 kDa HA (lower conc.) is injected into the fascia (14 mg corresponds to a dose of 5 mg/kg), after 3 days the amount of exogenous HA present in the fascia is very small (<2%) relative to the amount of endogenous HA in the tissue (see Figure 5). The amount of endogenous HA in fascia was determined to be 412 ± 73 µg/g and in muscle 12.8 ± 1.9 µg/g. Thus, the ratio of the concentration of ^{13}C-HA in the fascia to that of endogenous HA decreased during 1, 3, 7 and 30 days as follows: 25.3%, 1.7%, 0.1%, 0.0%, respectively. In muscle, the ratio is then 14.4%, 0.3%, and 0.1% at 3 days, 7 days, and 30 days, respectively. The rate of elimination of applied ^{13}C-HA from the fascia is thus relatively rapid. The elimination half-life in fascia and muscle was

determined to be 20.1 h and 15.7 h, respectively. The concentration of ^{13}C-HA was also determined in plasma and was determined to be below the detection limit of <100 ng/mL.

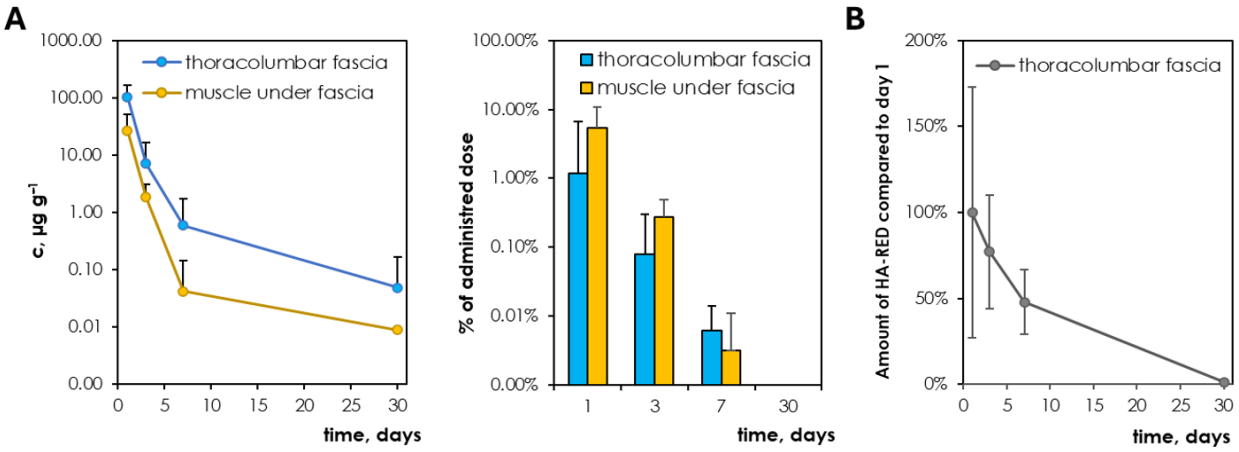

Figure 5. Pharmacokinetics of 13C-316 kDa HA (lower conc.) after injection into the fascia expressed as (**A**) the concentration of 13C-316 kDa HA (lower conc.) per 1 g of tissue and (**B**) the amount of 13C-316 kDa HA (lower conc.) in the tissue expressed as a proportion of the total amount injected. One-way ANOVA was used for statistical analysis.

Quantification of HA-RED in fascial and muscle tissue by LC-MS was problematic since the main unique product of enzymatic degradation, unsaturated disaccharide of HA-RED, lacks an ionizable carboxyl group and was undetectable by LC-MS (Figure S2). Therefore, unsaturated tetrasaccharide, the site product of enzymatic depolymerization, was used for detection. However, the low abundance of tetrasaccharide and interferents present in the fascia and muscle specimens prevented accurate quantification of HA-RED, and, thus, its abundance in fascia and muscle was evaluated at least semiquantitatively. The HA-RED signal was detected at 1, 3 and 7 days after administration. As in the case of ^{13}C-HA, only trace amounts were present in the samples 30 days after administration. The elimination half-life in fascia was around 108 h. The rate of elimination could not be accurately evaluated, but the signal at 7 days was still significant, and the elimination half-life in fascia was around 108 h, suggesting that the HA-RED is a biodegradable material with a slightly slower elimination rate than native HA.

4. Discussion

In this study, we examined six HA-based lubricants using ex vivo and synthetic fascia to identify optimal HA properties that minimize friction within the fascia and its layers. HA plays a crucial role in facilitating smooth movement within the fascia. Pathological conditions cause HA to thicken, leading to tissue adhesion. In a previous study [14], we proposed a promising treatment involving native HA intrafascial injections to reduce tissue friction and alleviate pain. Effective agents must possess specific properties for optimal functionality. Therefore, our experiments focused on understanding how the MW, chemical modification and concentration of HA influence friction in fascia and its layers. The most promising HA derivative from tribological experiments, HA-RED, was also tested for biodegradability using rabbits to ensure its safety use for intrafascial injections.

4.1. Influence of Preload of Fascia on Friction

This study begins by examining how stretching materials affect fascia friction. This investigation is motivated by several factors. Firstly, during testing, the material is held in place and slightly prestressed to mimic the natural tension fascia experiences. Fascia, which separates muscles or fat, naturally undergoes stress with every movement due to

muscle contractions or external forces [26]. Structurally, fascia consists of three sublayers of connective tissue with different densities and orientations [27,28]. Studies have shown that within each sublayer collagen fibers run parallel, but the fibers in adjacent layers are oriented at angles of about 70–80 degrees to each other [27]. Research on rabbit dorsal fascia demonstrated a similar structure to human TLF, with collagen fibers and loose connective tissue [14]. Notably, only the superficial sublayer is richly innervated and contains few elastic fibers [28]. Collagen fibers, visible in the study's images (see Figure 6), provide resistance to tension and stretching, common in various fascial tissues like ligaments, tendons, sheaths, muscular fascia, and deeper fascial sublayers [29]. The collagen and three-layer structure of the fascia, designed to allow fiber sliding within each layer [30,31], likely explains why preloading did not affect the friction of HA within the rabbit fascia. In contrast, synthetic fascia showed higher friction under heavier preload. The synthetic material, consisting of three sublayers with hydrophilic polymer on the top and bottom and fibers in the middle, might have experienced top-layer wear under increased stress.

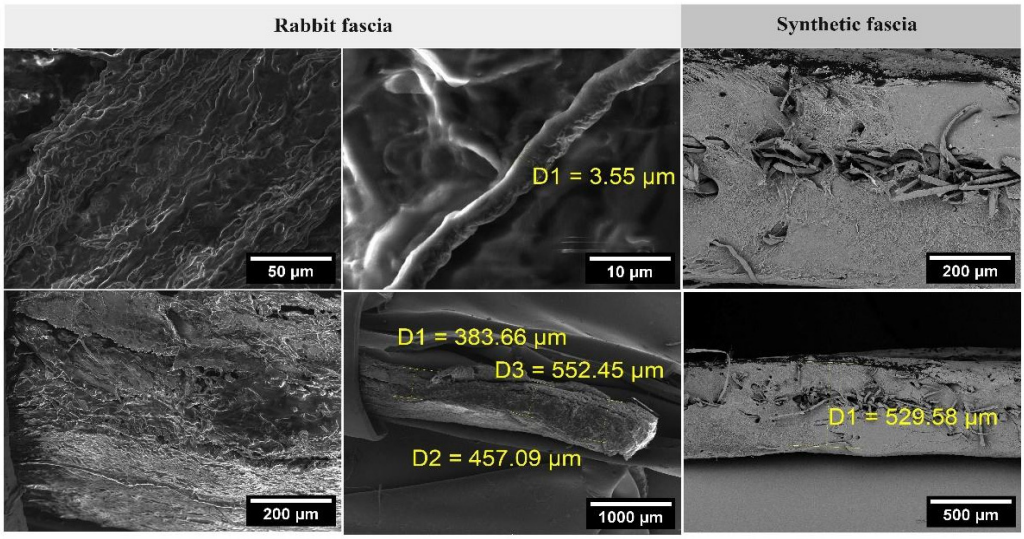

Figure 6. Close-ups of the fascia specimens used, captured using the SEM method.

These thinner layers are more prone to damage from stretching and tangential forces during friction tests, leading to rougher fiber surfaces (Figure 7). When the top fiber surface contacts the material, additional contact area is observed with more compliant elastomers, indicating hysteretic friction [32]. Hysteretic friction likely increases with higher surface roughness, leading to a higher COF [33]. However, this hypothesis requires further analysis. Future viscosupplements should maintain low friction levels without being compromised by stress and wear in pathological conditions. Additionally, future experiments should note that there is no significant difference in friction between lightly and moderately prestressed material, so materials will not be overstressed in further tests.

4.2. Selection of Appropriate Properties of HA-Based Solution as a Viscosupplement of TLF Fascia Based on Friction Results

As mentioned in the Introduction, one of the main limitations of HA in medical applications is its quick degradation in the human body, which reduces its effectiveness over time. To extend its presence at the application site, HA can undergo chemical modifications. In this study, both native HA (610 kDa, 316 kDa and 101 kDa HA) and two HA derivatives (HA-RED and HA-C12, see Figure S1) were tested. HA-RED is HA with carboxyl groups partly reduced to primary alcohols [22]. Comparing the results of native HA and HA-RED with similar MW (316 vs. 275 kDa), we observe that the reduction of carboxyl groups

had no significant impact on fascia friction. Despite a minor decrease in viscosity, the influential factors remained MW and concentration parameters. HA-C12 is an amphiphilic form of HA [18]. In studies [19,20], HA-C12 showed extremely low friction and effectively prevented surface eye cells from drying out, surpassing the effectiveness of regular HA. However, the effect of HA-C12 derivation on fascia friction alone cannot be assessed as the lubricant has a different concentration than the others used.

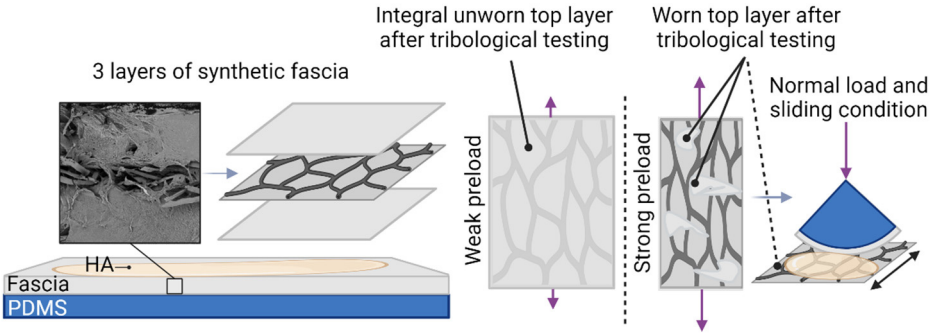

Figure 7. Synthetic fascia layers' behavior under the preloading, normal load and sliding conditions. The direction of the purple arrows shows the direction of stress on the material.

In this study, the viscosity of HA solutions increased with increasing MW and concentration, as shown in Table 1. The reason for this increase is straightforward: the viscosity of a polymer solution depends on the proportion of the solution's volume taken up by the polymer chains. This proportion can be described by the concentration of the polymer multiplied by its specific volume [6]. In simpler terms, viscosity is influenced by the length and number of polymer chains in the solution, as well as the size of the molecules themselves. As MW and concentration rise, the polymer chains become more tightly packed, making it harder for them to move freely within the solution. Consequently, when minimal sliding and pressure are applied, friction between the molecules increases. This conclusion is supported by the findings of the short-term friction experiments, as seen in Figure 3.

The tribological experiments also supported the statement that a high-viscosity solution may not be ideal for promoting fascial glide [10–12]. These solutions (610 kDa HA, 316 kDa HA, and HA-RED) exhibited higher friction coefficients. In contrast, Figure 3 shows a noticeable decrease in friction of native HA (101 kDa HA and 316 kDa HA (lower conc.)) with decreasing MW and concentration for both fascial models. Surprisingly, this is the opposite of what happens in an osteoarthritic joint [34,35] or the eye and eyelid [13]. The most interesting comparison is with HA-C12, which may explain how HA behaves toward fascia. For rabbit fascia, a solution with a concentration of 3 mg/mL and a low MW of 318 kDa achieved super-low friction. However, the friction of the synthetic fascia was almost five times higher. This demonstrates that HA has limited capacity to adhere to both hydrophilic and hydrophobic artificial surfaces [36]. In contrast, for tissue, collagen fibers on cartilage deform under boundary lubrication [37], reducing gaps laterally while maintaining size normally. This deformation allows collagen fibers to mechanically entrap HA molecules. While the forces binding the molecules to the fibers are not strong enough to create a complete lubricating layer [38], unlike phospholipids and HA [39–41], the HA trapped in this manner can still serve as a boundary layer, preventing cartilage damage. HA-C12 has a low concentration and viscosity, forming a weaker lubricating film (Table 1). Therefore, the synergy between collagen fibers and HA helps protect fascia against wear and damage. Synthetic fascia, lacking collagen, does not form this layer, leading to rapid wear. Even a concentration as small as 3 mg/mL is a suitable option for viscosupplementation of fascia.

The HA-collagen synergy is likely manifested in other cases as well. For 610 kDa HA, the longitudinal test curves for synthetic fascia show a smooth progression throughout the experiment, as seen in Figure 4. The *MW* and concentration of 610 kDa HA and the likely low roughness of the synthetic fascia contributed to forming a minimally weak lubricating film, protecting the fascia from damage. For rabbit fascia, regular waves can be seen in the progress. This may be explained by the viscoelastic properties of HA at higher MWs, as shown by [42], combined with how collagen entraps HA between its fibers [37]. The friction gradually increases until it reaches its peak and then decreases gradually. This suggests that 610 kDa HA, due to its large macromolecular clusters [6], does not reach deep between the collagen fibers but attaches mechanically to their surface, causing an increase in friction. Due to the viscoelastic properties of HA and the shear frictional bias, the chains tear into smaller ones, as described in [6,43,44], again protecting the fascia from damage. The interaction between lubricin and HA also plays a crucial role in the lubrication of connective tissues, reducing friction and preventing tissue adhesion [45]. Lubricin penetrates chemically bound HA, forming a viscoelastic gel that lowers the COF and enhances surface resistance to wear. Increasing lubricin concentration further improves lubrication by elevating the threshold load before wear occurs and reducing friction between HA-coated surfaces. Additionally, the HA-lubricin gel forms a stable lubricating film, maintaining its thickness under load [46]. Its shear viscosity increases significantly under confinement, and lubricin's interaction with HA prevents further adsorption onto negatively charged surfaces, potentially minimizing tissue adhesion.

4.3. HA Degradation in Living Organisms and Viscosupplement Confrontation

The suitability of native versus reduced HA for treating non-specific LBP was further assessed through pharmacokinetics (Figure 5). The viscosupplement is designed to dilute endogenous HA, which becomes highly viscous due to pathological changes in fascial tissue [10,11]. Based on friction results, 316 kDa HA (lower conc.) and HA-RED (275 kDa) were selected for comparison. However, previous research has shown that HA solutions degrade more slowly in vivo with higher MW compared to lower MW [23]. Consequently, 101 kDa HA, despite having the same COF but a lower MW, was not chosen for in vivo experiments. The turnover rate of endogenous HA in the body is relatively rapid, with a half-life of 2–5 min in the bloodstream [47] and a few days in tissues [48]. If low doses of exogenous HA are used (~μg kg^{-1}), its elimination is fast and similar to elimination of endogenous HA; however, if HA is dosed at relatively high doses in the range of mg kg^{-1} HA elimination follows saturable kinetics, where the elimination half-life can reach several hours for HA. HA is eliminated from the body through local cleavage reactions and systemic elimination via the liver, lymphatics, and kidneys. At the cellular level, HA undergoes non-specific degradation by free radicals or specific depolymerization by various enzymes [23].

HA administered via intrafascial injection at a dose of 5 mg/kg exhibited an elimination half-life which is expected for this MW [23]. It is appealing to use HA with higher MW to prolong its stay in fascia and enhance the effectiveness of the viscosupplement. However, formulations with excessively high MW have been reported to cause local harm [49] and its application is problematic due to the high viscosity of solutions of high-MW HA [14]. The chemical derivatization of HA seems a more promising approach to prolong the stay of viscosupplementation at application sites, as the viscosity is unaltered and resistance to enzymatic degradation is enhanced [50]. The pharmacokinetics of HA-RED showed excellent biocompatibility and biodegradability, since after 30 days all HA-RED was eliminated similarly to native HA of similar *MW*. HA-RED exhibited a longer elimination half-life (108 h) than native HA (20.1 h), as seen in Figure 5. Although chemical modification of HA

ensures higher in vivo stability, the elimination of viscosupplementation remains relatively fast. Despite this, viscosupplementation based on HA can be effective, as evidenced in the case of viscosupplementation for OA. Although the on-site quantification of HA-RED was challenging and only allowed for semi-quantitative determination, the prolonged retention of HA-RED was inferred from its elimination kinetics, where the limitations of semi-quantitative analysis do not affect the validity of the conclusion.

Viscosupplementation with HA is a well-established treatment for OA of the joints, where the administered HA is absorbed within days [51]. However, the clinical efficacy of intra-articular HA injections for managing knee OA pain reaches its maximum around 6–8 weeks after administration, with uncertain benefits at 6 months [52]. This extended relief may be attributed to HA's ability to initiate secondary processes despite its rapid degradation. HA can reduce nerve impulses and sensitivity linked to OA pain [53]. In experimental OA models, HA has shown protective effects on cartilage, likely mediated by its molecular and cellular interactions observed in vitro. Exogenous HA stimulates HA and proteoglycan synthesis in chondrocytes, reduces the production and activity of proinflammatory mediators and matrix metalloproteinases, and modulates immune cell behavior. Furthermore, dermal HA fillers are known to enhance fibroblast production and alleviate inflammatory skin conditions [54]. Fasciacytes [55], which produce HA in the fascia, are fibroblast-like cells contributing to these effects. HA has documented wound-healing properties [56] and it is crucial in regulating cell behavior and promoting cell proliferation within an HA-rich extracellular matrix [57]. These physiological effects collectively contribute to the mechanisms through which HA exerts its clinical benefits in the viscosupplement treatment, even for fascia tissue and non-specific LBP.

5. Conclusions

In this study, HA-based lubricants were tribologically tested to optimize the solution's properties, leading to low friction of fascia tissue. The aim of this study was to assess whether the HA derivative could substitute the native HA form, preserving its superior frictional properties with an assumed slower degradation in vivo. Tribological tests were supplemented by pharmacokinetics of the two most promising lubricants using a living rabbit model, contributing to the development of advanced therapeutic solutions. To summarize the main conclusions and contributions of the study:

- Tribological model—Optimization of fascia prestressing: The medium rabbit and synthetic fascia prestress ensures that the final friction results will be influenced by the effect of the lubricant without being affected by the degree of fascia tension;
- Lubricants: 316 kDa HA and HA-RED were identified as having the best and most stable tribological properties for fascia lubricants, driven by their MW and concentration;
- Pharmacokinetics of intrafascial HA-based viscosupplementation: Chemically modified HA (HA-RED) is eliminated within 30 days as well as native HA; however, it exhibits a longer residence time compared to native HA.

Supplementary Materials: The following supporting information can be downloaded at: https://www.mdpi.com/article/10.3390/lubricants13040184/s1, Figure S1: Structures of native HA and its derivatives: reduced HA (HA-RED) and lauroyl-modified HA (HA-C12). Figure S2: Enzymatic depolymerization of fully labelled native HA (14×^{13}C-HA), reduced-HA (HA) and 2×^{13}C-labelled native HA (2×^{13}C-HA) into unsaturated oligosaccharides. Figure S3: COF comparison of HA-based lubricants on rabbit and synthetic models. Table S1: Significance of friction results between individual lubricants.

Author Contributions: A.S.—investigation, conceptualization, writing—original draft preparation, data curation, methodology; M.Š.—visualization, investigation, writing—original draft preparation,

data curation, methodology; J.M.—writing-original draft preparation, formal analysis; D.N.—writing-review and editing, supervision; M.V.—visualization, supervision, project administration; J.S.—resources, methodology; V.P.—methodology, writing—review and editing; L.V.—resources, funding acquisition; M.H.—supervision; I.K.—funding acquisition; K.N.—supervision, resources, project administration. All authors have read and agreed to the published version of the manuscript.

Funding: This publication was supported by the project "Mechanical Engineering of Biological and Bio-inspired Systems", funded as project No. CZ.02.01.01/00/22_008/0004634 by Programme Johannes Amos Comenius, call Excellent Research. This work was partly supported by the Ministry of Health of the Czech Republic under project No. NU22-08–00454. CzechNanoLab project LM2023051 funded by MEYS CR is gratefully acknowledged for the financial support of the measurements/sample fabrication at CEITEC Nano Research Infrastructure.

Institutional Review Board Statement: The study was approved by the Ethics Committee of the Ministry of Education, Youth and Sports (approval No. MSMT-2036/2022-3).

Data Availability Statement: Experimental data for *Hyaluronic Acid-Based Lubricants Tribology for Alleviating Non-Specific Lower Back Pain* available at resource https://doi.org/10.5281/zenodo.11239441 (accessed on 22 February 2024).

Conflicts of Interest: Authors Matěj Šimek, Jana Matonohová, Kristina Nešporová were employed by Contipro a.s. The remaining authors declare that the research was conducted in the absence of any commercial or financial relationships that could be construed as a potential conflict of interest.

Abbreviations

The following abbreviations are used in this manuscript:

LBP	lower back pain
HA	hyaluronic acid
OA	osteoarthritis
SD	standard deviation
COF	coefficient of friction
PDMS	polydimethylsiloxane

References

1. Wu, A.; March, L.; Zheng, X.; Huang, J.; Wang, X.; Zhao, J.; Blyth, F.M.; Smith, E.; Buchbinder, R.; Hoy, D. Global low back pain prevalence and years lived with disability from 1990 to 2017: Estimates from the Global Burden of Disease Study 2017. *Ann. Transl. Med.* **2020**, *8*, 299. [CrossRef] [PubMed]
2. Hoy, D.; Bain, C.; Williams, G.; March, L.; Brooks, P.; Blyth, F.; Woolf, T.V.; Buchbinder, R. A systematic review of the global prevalence of low back pain. *Arthritis Rheumatol.* **2012**, *64*, 2028–2037. [CrossRef] [PubMed]
3. Casato, G.; Stecco, C.; Busin, R. Role of fasciae in nonspecific low back pain. *Eur. J. Transl. Myol.* **2019**, *29*, 8330. [CrossRef] [PubMed]
4. Wilke, J.; Schleip, R.; Klingler, W.; Stecco, C. The Lumbodorsal Fascia as a Potential Source of Low Back Pain: A Narrative Review. *Biomed Res. Int.* **2017**, *2017*, 5349620. [CrossRef]
5. Langevin, H.M.; Fox, J.R.; Koptiuch, C.; Badger, G.J.; Greenan-Naumann, A.C.; Bouffard, N.A.; Konofagou, E.A.; Lee, W.-N.; Triano, J.J.; Henry, S.M. Reduced thoracolumbar fascia shear strain in human chronic low back pain. *BMC Musculoskelet. Disord.* **2011**, *12*, 203. [CrossRef]
6. Cowman, M.K.; Schmidt, T.A.; Raghavan, P.; Stecco, A. Viscoelastic Properties of Hyaluronan in Physiological Conditions. *F1000Research* **2015**, *4*, 622. [CrossRef]
7. Matteini, P.; Dei, L.; Carretti, E.; Volpi, N.; Goti, A.; Pini, R. Structural Behavior of Highly Concentrated Hyaluronan. *Biomacromolecules* **2009**, *10*, 1516–1522. [CrossRef]
8. Fede, C.; Angelini, A.; Stern, R.; Macchi, V.; Porzionato, A.; Ruggieri, P.; De Caro, R.; Stecco, C. Quantification of hyaluronan in human fasciae: Variations with function and anatomical site. *J. Anat.* **2018**, *233*, 552–556. [CrossRef]
9. Stecco, A.; Meneghini, A.; Stern, R.; Stecco, C.; Imamura, M. Ultrasonography in myofascial neck pain: Randomized clinical trial for diagnosis and follow-up. *Surg. Radiol. Anat.* **2014**, *36*, 243–253. [CrossRef]

10. Stecco, A.; Gesi, M.; Stecco, C.; Stern, R. Fascial Components of the Myofascial Pain Syndrome. *Curr. Pain Headache Rep.* **2013**, *17*, 352. [CrossRef]
11. Stecco, A.; Stern, R.; Fantoni, I.; De Caro, R.; Stecco, C. Fascial Disorders: Implications for Treatment. *Phys. Med. Rehabil.* **2016**, *8*, 161–168. [CrossRef] [PubMed]
12. Wilke, J.; Schleip, R.; Yucesoy, C.A.; Banzer, W. Not merely a protective packing organ? A review of fascia and its force transmission capacity. *J. Appl. Physiol.* **2018**, *124*, 234–244. [CrossRef] [PubMed]
13. Iwashita, H.; Mabuchi, K.; Itokawa, T.; Okajima, Y.; Suzuki, T.; Hori, Y. Evaluation of the Lubricating Effect of Hyaluronic Acid on Contact Lenses Using a Pendulum-Type Friction Tester Under Mimicking Physiological Conditions. *Eye Contact Lens* **2022**, *48*, 83–87. [CrossRef] [PubMed]
14. Nešporová, K.; Matonohová, J.; Husby, J.; Toropitsyn, E.; Stupecká, L.D.; Husby, A.; Kleplová, T.S.; Stred'anská, A.; Šimek, M.; Nečas, D.; et al. Injecting hyaluronan in the thoracolumbar fascia: A model study. *Int. J. Biol. Macromol.* **2023**, *253*, 126879. [CrossRef]
15. Hintze, V.; Schnabelrauch, M.; Rother, S. Chemical Modification of Hyaluronan and Their Biomedical Applications. *Front. Chem.* **2022**, *10*, 830671. [CrossRef]
16. Griesser, J.; Hetényi, G.; Bernkop-Schnürch, A. Thiolated Hyaluronic Acid as Versatile Mucoadhesive Polymer: From the Chemistry Behind to Product Developments—What Are the Capabilities? *Polymers* **2018**, *10*, 243. [CrossRef]
17. Ikeda, J.; Zhao, C.; Sun, Y.-L.; An, K.-N.; Amadio, P.C. Carbodiimide-Derivatized Hyaluronic Acid Surface Modification of Lyophilized Flexor Tendon: A biomechanical study in a canine in vitro model. *JBJS* **2010**, *92*, 388–395. [CrossRef]
18. Huerta-Ángeles, G.; Brandejsová, M.; Kopecká, K.; Ondreáš, F.; Medek, T.; Židek, O.; Kulhánek, J.; Vagnerová, H.; Velebný, V. Synthesis and Physicochemical Characterization of Undecylenic Acid Grafted to Hyaluronan for Encapsulation of Antioxidants and Chemical Crosslinking. *Polymers* **2020**, *12*, 35. [CrossRef]
19. Huin-Amargier, C.; Marchal, P.; Payan, E.; Netter, P.; Dellacherie, E. New physically and chemically crosslinked hyaluronate (HA)-based hydrogels for cartilage repair. *J. Biomed. Mater. Res. Part A* **2006**, *76A*, 416–424. [CrossRef]
20. Černohlávek, M.; Brandejsová, M.; Štěpán, P.; Vagnerová, H.; Hermannová, M.; Kopecká, K.; Kulhánek, J.; Nečas, D.; Vrbka, M.; Velebný, V.; et al. Insight into the Lubrication and Adhesion Properties of Hyaluronan for Ocular Drug Delivery. *Biomolecules* **2021**, *11*, 1431. [CrossRef]
21. Stred'anská, A.; Nečas, D.; Vrbka, M.; Suchánek, J.; Matonohová, J.; Toropitsyn, E.; Hartl, M.; Křupka, I.; Nešporová, K. Understanding frictional behavior in fascia tissues through tribological modeling and material substitution. *J. Mech. Behav. Biomed. Mater.* **2024**, *155*, 106566. [CrossRef] [PubMed]
22. Buffa, R.; Klejch, T.; Hermannová, M.; Hejlová, L.; Svozil, V.; Vágnerová, H.; Škubalová, H.; Nešporová, K.; Velebný, V. Modified hyaluronic acid with enhanced resistance to degradation. *Carbohydr. Polym.* **2023**, *320*, 121241. [CrossRef] [PubMed]
23. Šimek, M.; Nešporová, K.; Kocurková, A.; Foglová, T.; Ambrožová, G.; Velebný, V.; Kubala, L.; Hermannová, M. How the molecular weight affects the in vivo fate of exogenous hyaluronan delivered intravenously: A stable-isotope labelling strategy. *Carbohydr. Polym.* **2021**, *263*, 117927. [CrossRef] [PubMed]
24. *ISO 3696:1987*; Water for Analytical Laboratory Use—Specification and Test Methods. International Organization for Standardization: Geneva, Switzerland, 1987.
25. Šimek, M.; Turková, K.; Schwarzer, M.; Nešporová, K.; Kubala, L.; Hermannová, M.; Foglová, T.; Šafránková, B.; Šindelář, M.; Šrůtková, D.; et al. Molecular weight and gut microbiota determine the bioavailability of orally administered hyaluronic acid. *Carbohydr. Polym.* **2023**, *313*, 120880. [CrossRef]
26. Schleip, R.; Klingler, W.; Lehmann-Horn, F. Active fascial contractility: Fascia may be able to contract in a smooth muscle-like manner and thereby influence musculoskeletal dynamics. *Med. Hypotheses* **2005**, *65*, 273–277. [CrossRef]
27. Stecco, C.; Pavan, P.G.; Porzionato, A.; Macchi, V.; Lancerotto, L.; Carniel, E.L.; Natail, A.N.; De Caro, R. Mechanics of crural fascia: From anatomy to constitutive modelling. *Surg. Radiol. Anat.* **2009**, *31*, 523–529. [CrossRef]
28. Benetazzo, L.; Bizzego, A.; De Caro, R.; Frigo, G.; Guidolin, D.; Stecco, C. 3D reconstruction of the crural and thoracolumbar fasciae. *Surg. Radiol. Anat.* **2011**, *33*, 855–862. [CrossRef]
29. Kumka, M.; Bonar, J. Fascia: A morphological description and classification system based on a literature review. *J. Can. Chiropr. Assoc.* **2012**, *56*, 179–191.
30. Yahia, L.H.; Rhalmi, S.; Newman, N.; Isler, M. Sensory innervation of human thoracolumbar fascia. *Acta Orthop. Scand.* **2009**, *63*, 195–197. [CrossRef]
31. Stecco, C.; Porzionato, A.; Lancerotto, L.; Stecco, A.; Macchi, V.; Ann Day, J.; De Caro, R. Histological study of the deep fasciae of the limbs. *J. Bodyw. Mov. Ther.* **2008**, *12*, 225–230. [CrossRef]
32. Tiwari, A.; Dorogin, L.; Bennett, A.I.; Schulze, K.D.; Sawyer, W.G.; Tahir, M.; Heinrich, G.; Persson, B.N.J. The effect of surface roughness and viscoelasticity on rubber adhesion. *Soft Matter* **2017**, *13*, 3602–3621. [CrossRef] [PubMed]
33. Ido, T.; Yamaguchi, T.; Shibata, K.; Matsuki, K.; Yumii, K.; Hokkirigawa, K. Sliding friction characteristics of styrene butadiene rubbers with varied surface roughness under water lubrication. *Tribol. Int.* **2019**, *133*, 230–235. [CrossRef]

34. Anadere, I.; Chmiel, H.; Laschner, W. Viscoelasticity of "normal" and pathological synovial fluid. *Biorheology* **1979**, *16*, 179–184. [PubMed]
35. Balazs, E.A. Viscosupplementation for treatment of osteoarthritis: From initial discovery to current status and results. *Surg. Technol.* **2004**, *12*, 278–289.
36. Chang, D.P.; Abu-Lail, N.I.; Coles, J.M.; Guilak, F.; Jay, G.D.; Zauscher, S. Friction force microscopy of lubricin and hyaluronic acid between hydrophobic and hydrophilic surfaces. *Soft Matter* **2009**, *5*, 3438–3445. [CrossRef]
37. Greene, G.W.; Zappone, B.; Banquy, X.; Lee, D.W.; Söderman, O.; Topgaard, D.; Israelachvili, J.N. Hyaluronic acid–collagen network interactions during the dynamic compression and recovery of cartilage. *Soft Matter* **2012**, *8*, 9906–9914. [CrossRef]
38. Jay, G.D.; Torres, J.R.; Warman, M.L.; Laderer, M.C.; Breuer, K.S. The role of lubricin in the mechanical behavior of synovial fluid. *Proc. Natl. Acad. Sci. USA* **2007**, *104*, 6194–6199. [CrossRef]
39. Hilšer, P.; Suchánková, A.; Mendová, K.; Filipič, K.E.; Daniel, M.; Vrbka, M. A new insight into more effective viscosupplementation based on the synergy of hyaluronic acid and phospholipids for cartilage friction reduction. *Biotribology* **2021**, *25*, 100166. [CrossRef]
40. Herzog, M.; Li, L.; Galla, H.-J.; Winter, R. Effect of hyaluronic acid on phospholipid model membranes. *Colloids Surf. B Biointerfaces* **2019**, *173*, 327–334. [CrossRef]
41. Dėdinaitė, A.; Wieland, D.C.F.; Bełdowski, P.; Claesson, P.M. Biolubrication synergy: Hyaluronan—Phospholipid interactions at interfaces. *Adv. Colloid Interface Sci.* **2019**, *274*, 102050. [CrossRef]
42. Rebenda, D.; Vrbka, M.; Čípek, P.; Toropitsyn, E.; Nečas, D.; Pravda, M.; Hartl, M. On the Dependence of Rheology of Hyaluronic Acid Solutions and Frictional Behavior of Articular Cartilage. *Materials* **2020**, *13*, 2659. [CrossRef] [PubMed]
43. Balazs, E.A. Viscoelastic properties of hyaluronic acid and biological lubrication. *Univ. Mich. Med. Cent. J.* **1968**, 255–259.
44. Tamer, T.M. Hyaluronan and synovial joint: Function, distribution and healing. *Interdiscip. Toxicol.* **2013**, *6*, 111–125. [CrossRef]
45. Han, M.; Russo, M.J.; Desroches, P.E.; Silva, S.M.; Quigley, A.F.; Kapsa, R.M.; Moulton, S.E.; Greene, G.W. Calcium ions have a detrimental impact on the boundary lubrication property of hyaluronic acid and lubricin (PRG-4) both alone and in combination. *Colloids Surf. B Biointerfaces* **2024**, *234*, 113741. [CrossRef]
46. Das, S.; Banquy, X.; Zappone, B.; Greene, G.W.; Jay, G.D.; Israelachvili, J.N. Synergistic Interactions between Grafted Hyaluronic Acid and Lubricin Provide Enhanced Wear Protection and Lubrication. *Biomacromolecules* **2013**, *14*, 1669–1677. [CrossRef]
47. Fraser, J.R.F.; Laurent, T.C.; Pertoft, H.; Baxter, E. Plasma clearance, tissue distribution and metabolism of hyaluronic acid injected intravenously in the rabbit. *Biochem. J.* **1981**, *200*, 415–424. [CrossRef]
48. Kogan, G.; Šoltés, L.; Stern, R.; Schiller, J.; Mendichi, R. Hyaluronic Acid: Its Function and Degradation in in vivo Systems. *Bioact. Nat. Prod. (Part N)* **2008**, *34*, 789–882. [CrossRef]
49. Reichenbach, S.; Blank, S.; Rutjes, A.W.; Shang, A.; King, E.A.; Dieppe, P.A.; Jüni, P.; Trelle, S. Hylan versus hyaluronic acid for osteoarthritis of the knee: A systematic review and meta-analysis. *Arthritis Care Res.* **2007**, *57*, 1410–1418. [CrossRef]
50. Klejch, T.; Buffa, R.; Šimek, M.; Nešporová, K.; Exnerová, A.; Bednařík, J.; Brandejsová, M.; Vágnerová, H.; Fiala, F.; Velebný, V. Enzymatically stable unsaturated hyaluronan-derived oligosaccharides with selective cytostatic properties. *Carbohydr. Polym.* **2024**, *336*, 122129. [CrossRef]
51. Larsen, N.E.; Dursema, H.D.; Pollak, C.T.; Skrabut, E.M. Clearance kinetics of a hylan-based viscosupplement after intra-articular and intravenous administration in animal models. *J. Biomed. Mater. Res. Part B Appl. Biomater.* **2012**, *100B*, 457–462. [CrossRef]
52. Trigkilidas, D.; Anand, A. The effectiveness of hyaluronic acid intra-articular injections in managing osteoarthritic knee pain. *Ann. R. Coll. Surg. Engl.* **2013**, *95*, 545–551. [CrossRef] [PubMed]
53. Moreland, L.W. Intra-articular hyaluronan (hyaluronic acid) and hylans for the treatment of osteoarthritis: Mechanisms of action. *Arthritis Res. Ther.* **2003**, *5*, 54–67. [CrossRef] [PubMed]
54. Walker, K.; Basehore, B.M.; Goyal, A.; Zito, P.M. Hyaluronic Acid. Statpearls [Internet]. Available online: https://www.ncbi.nlm.nih.gov/books/NBK482440/ (accessed on 19 June 2024).
55. Stecco, C.; Fede, C.; Macchi, V.; Porzionato, A.; Petrelli, L.; Biz, C.; Stern, R.; De Caro, R. The fasciacytes: A new cell devoted to fascial gliding regulation. *Clin. Anat.* **2018**, *31*, 667–676. [CrossRef] [PubMed]
56. Fallacara, A.; Vertuani, S.; Panozzo, G.; Pecorelli, A.; Valacchi, G.; Manfredini, S. Novel Artificial Tears Containing Cross-Linked Hyaluronic Acid: An In Vitro Re-Epithelialization Study. *Molecules* **2017**, *22*, 2104. [CrossRef]
57. Owen, S.C.; Kuo, J.-W.; Prestwich, G.D. 2.14 Hyaluronic Acid. *Compr. Biomater. II* **2017**, *2*, 306–331. [CrossRef]

Supplementary Materials:

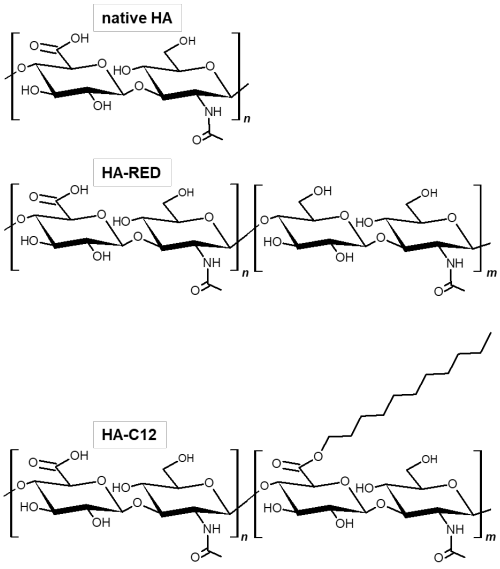

Figure S1 Structures of native HA and its derivatives: reduced HA (HA-RED) and lauroyl-modified HA (HA-C12)

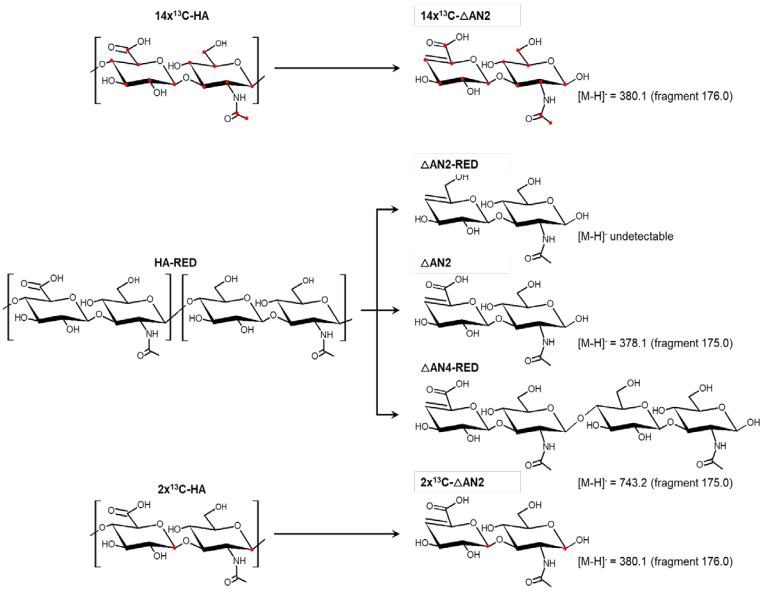

Figure S2 Enzymatic depolymerization of fully labelled native HA (14x^{13}C-HA), reduced-HA (HA) and 2x^{13}C-labelled native HA (2x^{13}C-HA) into unsaturated oligosaccharides. Fragmentations of deprotonated unsaturated oligosacharides were measured in negative ion mode. Unsaturated disacchide of HA-RED lacks of ionizable carboxyl group and was undetecable in LC-MS, therefore unsaturated tetrasaccharide, the site product of enzymatic degradation was used for quantification.

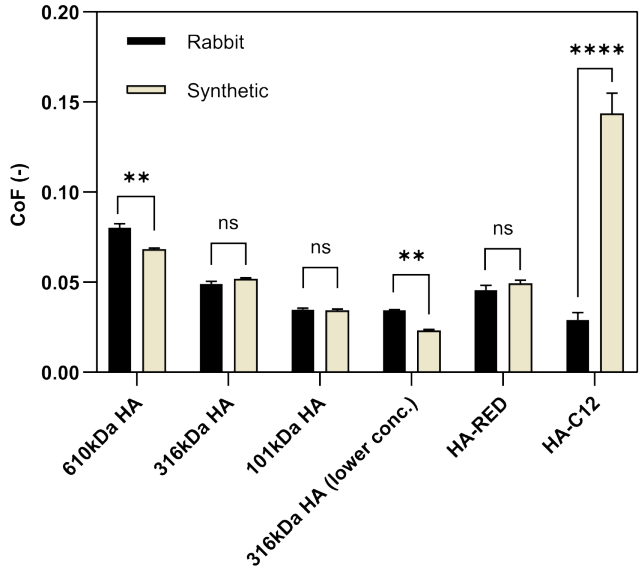

Figure S3 COF comparison of HA-based lubricants on rabbit and synthetic models.

To demonstrate how the synthetic fascia compares to real rabbit tissue in friction and lubrication studies. Six HA-based lubricants with different formulations were used, and the friction results, along with further statistical significance of the different models shown in **Figure S3,** illustrate how each material performed with each lubricant. For 316kDa HA, 101kDa HA, and HA-RED, the friction results indicated complete interchangeability and no significant difference in COF (ns; $P > 0.9999$). A slight difference was observed for 610kDa HA (**; $P = 0.0037$) and 316kDa HA (lower conc.) (**; $P = 0.0064$), while HA-C12 (****; $P < 0.0001$) showed the most significant differences. As can be seen, synthetic fascia has become an interchangeable model of rabbit fascia.

Table S1 Significance of friction results between individual lubricants.

Designation	*Ex vivo* rabbit fascia		Synthetic fascia	
	Significance	Adjusted P value	Significance	Adjusted P value
610kDa HA vs. 316kDa HA	***	0.0009	**	0.0013
610kDa HA vs. 101kDa HA	***	0.0002	****	<0.0001
610kDa HA vs. 316kDa HA (lower conc.)	***	0.0007	****	<0.0001
610kDa HA vs. HA-RED	****	<0.0001	*	0.0164
610kDa HA vs. HA-C12	***	0.0003	*	0.0273
316kDa HA vs. 101kDa HA	****	<0.0001	****	<0.0001

316kDa HA vs. 316kDa HA (lower conc.)	*	0.0117	***	0.0007
316kDa HA vs. HA-RED	ns	0.2122	ns	0.3113
316kDa HA vs. HA-C12	*	0.0239	*	0.0168
101kDa HA vs. 316kDa HA (lower conc.)	ns	0.9949	*	0.0172
101kDa HA vs. HA-RED	*	0.0422	*	0.0116
101kDa HA vs. HA-C12	ns	0.3129	*	0.0121
316kDa HA (lower conc.) vs. HA-RED	ns	0.0674	*	0.0134
316kDa HA (lower conc.) vs. HA-C12	ns	0.4369	*	0.0125
HA-RED vs. HA-C12	**	0.0080	*	0.0125

7 LIMITATIONS

Despite the successful development of a tribological model to simulate fascial tissues and the comprehensive evaluation of HA-based solutions for friction reduction, several limitations must be acknowledged.

First, while the selected technical materials provided a practical approximation of biological fascial tissue, they cannot fully replicate the complex, hierarchical structure, biochemical composition, and dynamic remodelling capacity of native fascia. Thus, certain microstructural and time-dependent behaviors observed *in vivo* may not have been completely captured.

Second, although various sliding velocities, preloads, and contact geometries were incorporated into the experimental design to simulate physiological conditions, these parameters still represent a simplification compared to the full range of mechanical forces and multi-axial movements occurring within the human body.

Third, the experimental environment was controlled and static in terms of temperature and humidity, whereas *in vivo* conditions involve fluctuations in hydration, biochemical milieu, and mechanical loading over time, all of which can affect tissue lubrication and adhesion mechanisms.

Fourth, the study focused primarily on healthy fascial tissue properties and modelled pathological adhesion conditions through technical means. However, pathological fascia (e.g., fibrotic, inflamed) might display additional changes, such as altered collagen cross-linking or proteoglycan composition, which were not fully simulated in the present work.

Fifth, although extensive statistical analysis was conducted to validate findings, the sample size for certain biological experiments was limited due to the availability of biological tissue, which may have influenced the robustness of some comparisons.

8 CONCLUSIONS

The motivation behind this work was to develop, in cooperation with Contipro, a.s., a HA-based viscosupplement that would be injected into the TLF layers, where it would reduce the impact of adhesion of fascial tissues inflamed by pathological changes. Whereby this phenomenon is associated with NSLBP, a health problem affecting the entire world across generations. The incidence of NSLBP is increasing and is expected to continue to increase, leading to significant socioeconomic consequences, including loss of employment and reduced participation in social activities. Effective solutions are therefore urgently needed. Current treatment options have proved inadequate, with patients often expressing dissatisfaction with the results.

For the research, it was essential to investigate the frictional properties of HA-based solutions on fascial tissue under conditions that closely mimic the physiological environment. However, a review of the existing literature showed that no tribological model has been specifically developed for this purpose. Therefore, a primary aim of this work was to develop a tribological model of TLF that accurately simulates *in vivo* conditions, which facilitated targeted investigations for the benefit of patients. Through a series of experimental setups and biological simulations, the aim of this research was to identify the critical factors influencing HA lubrication and to develop an appropriate TLF model. Subsequently, as a second aim, the factors influencing the lubrication mechanisms of fascial tissue were investigated and a definitive recommendation of HA-based solution composition in the development of a viscosupplement for the treatment of NSLBP was made. The major outcomes may be summarized as follows:

1. Impact of sliding velocity: In models simulating fascial tissue interactions, sliding velocity (ranging from 1 to 5 Hz) affected the COF. This indicates that motion speed plays a crucial role in the frictional behavior of fascia, particularly in conditions like NSLBP where fascial adhesion might be a factor.
2. Material stiffness and friction in PDMS models: The frictional properties of PDMS models, used to simulate fascial tissue, are influenced by material stiffness (measured on the ShA scale). The COF doubled when moving from softer to harder PDMS, with the highest COF observed at 40 ShA. This highlights the importance of material selection in biotribological modeling.
3. Effect of pin radius on friction: In experiments with elastomer models, increasing pin radius led to reduced friction. Specifically, harder PDMS, friction decreased by 22% when the pin radius increased from 8.6 mm to 50 mm, and similar trends were observed in much softer elastomer Phantom, with a notable reduction in friction between 30 mm and 50 mm radii.
4. Material preload and friction: The effect of material preload on friction differed between rabbit and synthetic fascia. For rabbit fascia, preload had minimal impact

due to its collagen structure, while synthetic fascia experienced significant friction increases under heavy preload. This suggests that the structural properties of fascia influence how preload affects frictional behavior.

5. Influence of HA MW, concentration and derivation: High viscous HA solutions (610 kDa, 20 mg/ml) resulted in increased friction due to the dense packing of polymer chains which restricted movement. Conversely, lower viscous HA solutions (101 kDa, 20 mg/ml; 316 kDa, 10 mg/ml) were associated with lower COF, indicating that HA MW and concentration are critical in optimizing lubrication. The type of derivation had no effect on fascia lubrication showing the MW and concentration remains dominant factors. However, the derivative of HA has the advantage of slower degradation in a living organism as pharmacokinetics study showed.

Regarding the tested hypotheses, the obtained results are summarized in the following remarks:

Q1: What material parameters are crucial in developing a tribological model to accurately simulate fascial tissues and reliably identify the adhesive mechanisms in pathological conditions?

To develop a tribological model that accurately simulates fascial tissues and identifies adhesive mechanisms in pathological conditions, several material parameters must be carefully considered. Material stiffness has a significant impact on friction; lower stiffness is generally associated with higher friction coefficients. The viscoelastic properties of the materials are equally crucial, as they influence frictional behavior through their effect on movement within the lubricant layer. For example, lower MW HA solutions were observed to reduce friction more effectively compared to higher MW solutions, which increased friction due to their higher viscosity. Surface roughness and wettability also contribute to frictional behavior, with increased roughness and variations in contact angles influencing friction values. Furthermore, preload and contact area are critical parameters; variations in pin radius and applied preload were shown to significantly affect friction in experimental tests. Dynamic conditions, such as sliding velocity, must also be incorporated to accurately replicate the frictional response under different movement scenarios. The results obtained were subjected to statistical analysis, and significant differences were identified, thereby confirming the trends observed in material behavior and frictional response. **Based on these statistically validated results, the first hypothesis was confirmed within the scope of the proposed thesis.**

Q2: What is the mechanism of friction reduction of HA lubricated adhesive fascial tissue induced by various solution compositions?

The mechanism of friction reduction in HA-lubricated adhesive fascial tissue is influenced by several factors related to the composition of the HA solutions. Lower MW HA solutions demonstrate better lubrication properties compared to higher MW solutions. This effect is attributed to the lower viscosity of lower MW HA solutions, which facilitates smoother movement between tissue surfaces and minimizes the resistance associated with more viscous fluids. Consequently, they reduce friction more effectively. Additionally, the concentration of HA solutions plays a significant role in friction reduction; lower concentrations generally result in improved lubrication due to reduced viscosity, whereas higher concentrations tend to increase viscosity and, consequently, friction. The presence of collagen fibers in fascial tissues further affects this mechanism. HA interacts with these fibers, enhancing lubrication by reducing direct surface-to-surface contact and limiting excessive adhesion, thereby contributing to a lower friction coefficient and protecting the tissue from damage under pathological conditions. In summary, the friction reduction mechanism is primarily governed by the MW and concentration of the HA solution, as well as its interaction with collagen fibers in the fascial tissue. The type of HA derivative does not influence fascial friction but provides the advantage of slower degradation *in vivo* compared to the native solution. The experimental findings were statistically analyzed, and significant differences in frictional behavior were confirmed across various HA compositions. **Based on these statistically validated results, the second hypothesis was confirmed within the scope of the proposed thesis.**

Fig. 18 Fascigel - HA-based viscosupplement for NSLBP

At the conclusion of this thesis, the key findings and outcomes of the research are presented. Through the development of models, extensive testing, and analysis, clear recommendations were established for creating a viscosupplement for the treatment of NSLBP. The resulting product, named *Fascigel,* see Fig. 18, was successfully developed and has passed all required tests, including clinical trials on patients. *Fascigel* is now on a promising trajectory toward regulatory approval, with the potential to alleviate pain and improve the quality of life for those affected by NSLBP.

9 LIST OF PUBLICATIONS

STREĎANSKÁ, A., D. NEČAS, M. VRBKA, I. KŘUPKA, M. HARTL, E. TOROPITSYN, J. HUSBY. Development of Tribological Model of Human Fascia: The Influence of Material Hardness and Motion Speed. Biotribology, 2022, vol. 30. ISSN 2352-5738. Doi: 10.1016/j.biotri.2022.100209

NEŠPOROVÁ, K., J. MATONOHOVÁ, J. HUSBY, E. TOROPITSYN, L. DIVOKÁ STUPECKÁ, A. HUSBY, T. SUCHÁNKOVÁ KLEPLOVÁ, A. STREĎANSKÁ, M. ŠIMEK, D. NEČAS, M. VRBKA, R. SCHLEIP, V. VELEBNÝ. Injecting hyaluronan in the thoracolumbar fascia: A model study. International Journal of Biological Macromolecules, Vol. 253, Part 3, 2023. ISSN 0141-8130. Doi: 10.1016/j.ijbiomac.2023.126879.

STREĎANSKÁ, A., D. NEČAS, M. VRBKA, J. SUCHÁNEK, J. MATONOHOVÁ, E. TOROPITSYN, M. HARTL, I. KŘUPKA, K. NEŠPOROVÁ. Understanding frictional behavior in fascia tissues through tribological modeling and material substitution, Journal of the Mechanical Behavior of Biomedical Materials, Volume 155, 2024, 106566, ISSN 1751-6161. Doi: 10.1016/j.jmbbm.2024.106566.

STREĎANSKÁ, A., M. ŠIMEK, J. MATONOHOVÁ, D. NEČAS, M. VRBKA, J. SUCHÁNEK, V. PAVLIŇÁKOVÁ, L. VOJTOVÁ, M. HARTL, I. KŘUPKA, K. NEŠPOROVÁ. Optimizing Hyaluronan-Based Lubricants for Treating Thoracolumbar Fascia Pathologies: Insights from Tribological and Pharmacokinetic Studies, Lubricants 2025, 13, 184. Doi: 10.3390/lubricants13040184.

10 LITERATURE

[1] F.Balagué, A.Mannion, F.Pellisé, C.Cedraschi, Non-specific low back pain, The Lancet. vol. 379 (2012) 482-491. https://doi.org/10.1016/S0140-6736(11)60610-7.

[2] Chronic Back Pain, (2003). https://hpi.georgetown.edu/backpain/ (accessed 2024-08-20).

[3] M.Ferreira, K.de Luca, L.Haile, J.Steinmetz, G.Culbreth, M.Cross, J.Kopec, P.Ferreira, F.Blyth, R.Buchbinder, J.Hartvigsen, A.Wu, S.Safiri, A.Woolf, G.Collins, K.Ong, S.Vollset, A.Smith, J.Cruz, K.Fukutaki, S.Abate, M.Abbasifard, M.Abbasi-Kangevari, Z.Abbasi-Kangevari, A.Abdelalim, A.Abedi, H.Abidi, Q.Adnani, A.Ahmadi, R.Akinyemi, A.Alamer, A.Alem, Y.Alimohamadi, M.Alshehri, M.Alshehri, H.Alzahrani, S.Amini, S.Amiri, H.Amu, C.Andrei, T.Andrei, B.Antony, J.Arabloo, J.Arulappan, A.Arumugam, T.Ashraf, S.Athari, N.Awoke, S.Azadnajafabad, T.Bärnighausen, L.Barrero, A.Barrow, A.Barzegar, L.Bearne, I.Bensenor, A.Berhie, B.Bhandari, V.Bhojaraja, A.Bijani, B.Bodicha, S.Bolla, J.Brazo-Sayavera, A.Briggs, Global, regional, and national burden of low back pain, 1990–2020, its attributable risk factors, and projections to 2050: a systematic analysis of the Global Burden of Disease Study 2021, The Lancet Rheumatology. vol. 5 (2023). https://doi.org/10.1016/S2665-9913(23)00098-X.

[4] J.Hartvigsen, M.Hancock, A.Kongsted, Q.Louw, M.Ferreira, S.Genevay, D.Hoy, J.Karppinen, G.Pransky, J.Sieper, R.Smeets, M.Underwood, R.Buchbinder, J.Hartvigsen, D.Cherkin, N.Foster, C.Maher, M.Underwood, M.van Tulder, J.Anema, R.Chou, S.Cohen, L.Menezes Costa, P.Croft, M.Ferreira, P.Ferreira, J.Fritz, S.Genevay, D.Gross, M.Hancock, What low back pain is and why we need to pay attention, The Lancet. vol. 391 (2018) 2356-2367. https://doi.org/10.1016/S0140-6736(18)30480-X.

[5] D.Hoy, C.Bain, G.Williams, L.March, P.Brooks, F.Blyth, A.Woolf, T.Vos, R.Buchbinder, A systematic review of the global prevalence of low back pain, Arthritis & Rheumatology. vol. 64 (2012) 2028-2037. https://doi.org/https://pubmed.ncbi.nlm.nih.gov/22231424/.

[6] M.Ferreira, G.Machado, J.Latimer, C.Maher, P.Ferreira, R.Smeets, Factors defining care-seeking in low back pain – A meta-analysis of population based surveys, European Journal of Pain. vol. 14 (2010). https://doi.org/10.1016/j.ejpain.2009.11.005.

[7] J.St. Sauver, D.Warner, B.Yawn, D.Jacobson, M.McGree, J.Pankratz, L.Melton, V.Roger, J.Ebbert, W.Rocca, Why Patients Visit Their Doctors: Assessing the Most Prevalent Conditions in a Defined American Population, Mayo Clinic Proceedings. vol. 88 (2013) 56-67. https://doi.org/10.1016/j.mayocp.2012.08.020.

[8] R.Deyo, J.Weinstein, Low Back Pain, New England Journal of Medicine. vol. 344 (2001) 363-370. https://doi.org/10.1056/NEJM200102013440508.

[9] P.Pavan, A.Stecco, R.Stern, C.Stecco, Painful Connections: Densification Versus Fibrosis of Fascia, Current Pain and Headache Reports. vol. 18 (2014). https://doi.org/10.1007/s11916-014-0441-4.

[10] J.Wilke, R.Schleip, C.Yucesoy, W.Banzer, Not merely a protective packing organ? A review of fascia and its force transmission capacity, Journal of Applied Physiology. vol. 124 (2018) 234-244. https://doi.org/10.1152/japplphysiol.00565.2017.

[11] H.Langevin, J.Fox, C.Koptiuch, G.Badger, A.Greenan- Naumann, N.Bouffard, E.Konofagou, W.Lee, J.Triano, S.Henry, Reduced thoracolumbar fascia shear strain in human chronic low back pain, BMC Musculoskeletal Disorders. vol. 12 (2011). https://doi.org/10.1186/1471-2474-12-203.

[12] P.Pavan, A.Stecco, R.Stern, P.logna Prat, C.Stecco, Fibrosis and densification: Anatomical vs functional alteration of the fascia, Journal of Bodywork and Movement Therapies. vol. 20 (2016). https://doi.org/10.1016/j.jbmt.2015.07.029.

[13] C.Stecco, R.Schleip, A fascia and the fascial system, Journal of Bodywork and Movement Therapies. vol. 20 (2016) 139-140. https://doi.org/10.1016/j.jbmt.2015.11.012.

[14] C.Stecco, R.Stern, A.Porzionato, V.Macchi, S.Masiero, A.Stecco, R.De Caro, Hyaluronan within fascia in the etiology of myofascial pain, Surgical and Radiologic Anatomy. vol. 33 (2011) 891-896. https://doi.org/10.1007/s00276-011-0876-9.

[15] J.Wilke, R.Schleip, W.Klingler, C.Stecco, The Lumbodorsal Fascia as a Potential Source of Low Back Pain: A Narrative Review, BioMed Research International. vol. 2017 (2017) 1-6. https://doi.org/10.1155/2017/5349620.

[16] G.Casato, C.Stecco, R.Busin, Role of fasciae in nonspecific low back pain, European Journal of Translational Myology. vol. 29 (2019) 159-163. https://doi.org/10.4081/ejtm.2019.8330.

[17] F.Willard, A.Vleeming, M.Schuenke, L.Danneels, R.Schleip, The thoracolumbar fascia: anatomy, function and clinical considerations, Journal of Anatomy. vol. 221 (2012) 507-536. https://doi.org/10.1111/j.1469-7580.2012.01511.x.

[18] R.Drake, W.Vogl, A.Mitchell, Gray's basic anatomy, Elsevier - Churchill Livingstone, Philadelphia, 2012.

[19] J.Macintosh, N.Bogduk, S.Gracovetsky, The biomechanics of the thoracolumbar fascia, Clinical Biomechanics. vol. 2 (1987) 78-83. https://doi.org/10.1016/0268-0033(87)90132-X.

[20] H.Lee, J.Petrofsky, N.Daher, L.Berk, M.Laymon, I.Khowailed, Anterior cruciate ligament elasticity and force for flexion during the menstrual cycle, Medical Science Monitor. vol. 19 (2013) 1080-1088. https://doi.org/10.12659/MSM.889393.

[21] E.Eiling, A.Bryant, W.Petersen, A.Murphy, E.Hohmann, Effects of menstrual-cycle hormone fluctuations on musculotendinous stiffness and knee joint laxity, Knee Surgery, Sports Traumatology, Arthroscopy. vol. 15 (2007) 126-132. https://doi.org/10.1007/s00167-006-0143-5.

[22] A.Duffin, A.Lam, R.Kidd, A.Chan, K.Donaghue, Ultrasonography of plantar soft tissues thickness in young people with diabetes, Diabetic Medicine. vol. 19 (2002) 1009-1013. https://doi.org/10.1046/j.1464-5491.2002.00850.x.

[23] V.Trindade, P.Martins, S.Santos, M.Parente, R.Natal Jorge, A.Santos, L.Santos, J.Fernandes, Experimental study of the influence of senescence in the biomechanical properties of the temporal tendon and deep temporal fascia based on uniaxial tension tests, Journal of Biomechanics. vol. 45 (2012) 199-201. https://doi.org/10.1016/j.jbiomech.2011.09.018.

[24] D.Wojtysiak, Effect of Age on Structural Properties of Intramuscular Connective Tissue, Muscle Fibre, Collagen Content and Meat Tenderness in Pig longissimus lumborum muscle, Folia Biologica. vol. 61 (2013) 221-226. https://doi.org/10.3409/fb61_3-4.221.

[25] O.Trabold, S.Wagner, C.Wicke, H.Scheuenstuhl, M.Hussain, N.Rosen, A.Seremetiev, H.Becker, T.Hunt, Lactate and oxygen constitute a fundamental regulatory mechanism in wound healing, Wound Repair and Regeneration. vol. 11 (2003) 504-509. https://doi.org/10.1046/j.1524-475X.2003.11621.x.

[26] J.Bishop, J.Fox, R.Maple, C.Loretan, G.Badger, S.Henry, M.Vizzard, H.Langevin, D.Miao, Ultrasound Evaluation of the Combined Effects of Thoracolumbar Fascia Injury and Movement Restriction in a Porcine Model, PLOS ONE. vol. 11 (2016). https://doi.org/10.1371/journal.pone.0147393.

[27] I.Gatej, M.Popa, M.Rinaudo, Role of the pH on Hyaluronan Behavior in Aqueous Solution, Biomacromolecules. vol. 6 (2005) 61-67. https://doi.org/10.1021/bm040050m.

[28] L.Yahia, S.Rhalmi, N.Newman, M.Isler, Sensory innervation of human thoracolumbar fascia, Acta Orthopaedica Scandinavica. vol. 63 (2009) 195-197. https://doi.org/10.3109/17453679209154822.

[29] J.Tesarz, U.Hoheisel, B.Wiedenhöfer, S.Mense, Sensory innervation of the thoracolumbar fascia in rats and humans, Neuroscience. vol. 194 (2011) 302-308. https://doi.org/10.1016/j.neuroscience.2011.07.066.

[30] Low back pain, in: World Health Organization, 2023. https://www.who.int/news-room/fact-sheets/detail/low-back-pain (accessed 2024-06-05).

[31] D.Cunha e Silva, J.Dourado, M.Dias, W.Menezes, F.Jesus-Moraleida, A.Nunes, LOW BACK PAIN TREATMENT STRATEGIES IN PRIMARY CARE AND USER SATISFACTION: CROSS-SECTIONAL STUDY OF USER PERSPECTIVES, Brazilian Journal of Physical Therapy. vol. 28 (2024). https://doi.org/10.1016/j.bjpt.2024.100701.

[32] I.Bernstein, Q.Malik, S.Carville, S.Ward, Low back pain and sciatica: summary of NICE guidance, BMJ. (n.d.). https://doi.org/10.1136/bmj.i6748.

[33] M.Almeida, B.Saragiotto, B.Richards, C.Maher, Primary care management of non-specific low back pain: key messages from recent clinical guidelines, Medical Journal of Australia. vol. 208 (2018) 272-275. https://doi.org/10.5694/mja17.01152.

[34] W.IJzelenberg, T.Oosterhuis, J.Hayden, B.Koes, M.van Tulder, S.Rubinstein, A.de Zoete, Exercise therapy for treatment of acute non-specific low back pain: a Cochrane systematic review and meta-

analysis of randomised controlled trials, Archives of Physical Medicine and Rehabilitation. (2024). https://doi.org/10.1016/j.apmr.2024.02.732.

[35] B.Ercole, S.Antonio, D.Julie Ann, C.Stecco, How much time is required to modify a fascial fibrosis?, Journal of Bodywork and Movement Therapies. vol. 14 (2010) 318-325. https://doi.org/10.1016/j.jbmt.2010.04.006.

[36] K.Arumugam, K.Harikesavan, Effectiveness of fascial manipulation on pain and disability in musculoskeletal conditions. A systematic review, Journal of Bodywork and Movement Therapies. vol. 25 (2021) 230-239. https://doi.org/10.1016/j.jbmt.2020.11.005.

[37] Y.Isaji, D.Sasaki, Y.Kon, Y.Kurasawa, T.Kitagawa, Fascial manipulation for musculoskeletal disorders: A scoping review, Journal of Bodywork and Movement Therapies. vol. 40 (2024) 23-29. https://doi.org/10.1016/j.jbmt.2024.04.006.

[38] T.Wiewelhove, A.Döweling, C.Schneider, L.Hottenrott, T.Meyer, M.Kellmann, M.Pfeiffer, A.Ferrauti, A Meta-Analysis of the Effects of Foam Rolling on Performance and Recovery, Frontiers in Physiology. vol. 10 (2019). https://doi.org/10.3389/fphys.2019.00376.

[39] R.Grieve, F.Goodwin, M.Alfaki, A.Bourton, C.Jeffries, H.Scott, The immediate effect of bilateral self myofascial release on the plantar surface of the feet on hamstring and lumbar spine flexibility: A pilot randomised controlled trial, Journal of Bodywork and Movement Therapies. vol. 19 (2015) 544-552. https://doi.org/10.1016/j.jbmt.2014.12.004.

[40] X.Mao, H.He, J.Ding, Efficacy of Laser Acupuncture for Treatment of Chronic Low Back Pain: A Systematic Review and Meta-Analysis, Pain Management Nursing. (2024). https://doi.org/10.1016/j.pmn.2024.05.001.

[41] E.Balazs, Chemistry and Molecular Biology of the Intercellular Matrix, 3 ed., Academic Press, 1970.

[42] E.Balazs, T.Laurent, R.Jeanloz, Nomenclature of hyaluronic acid, Biochemical Journal. vol. 235 (1986) 903-903. https://doi.org/10.1042/bj2350903.

[43] J.Scott, Secondary Structures in Hyaluronan Solutions: Chemical and Biological Implications, Ciba Foundation Symposium 143 - The Biology of Hyaluronan. (2007) 6-20. https://doi.org/10.1002/9780470513774.ch2.

[44] E.Balazs, Viscoelastic properties of hyaluronic acid and biological lubrication, University of Michigan Medical Center Journal. (1968) 255-259.

[45] T.LAURENT, U.LAURENT, J.FRASER, The structure and function of hyaluronan: An overview, Immunology and Cell Biology. vol. 74 (1996) a1-a7. https://doi.org/10.1038/icb.1996.32.

[46] D.Amiel, K.Ishizue, E.Billings, M.Wiig, J.Berg, W.Akeson, R.Gelberman, Hyaluronan in flexor tendon repair, The Journal of Hand Surgery. vol. 14 (1989) 837-843. https://doi.org/10.1016/S0363-5023(89)80085-1.

[47] L.Hagberg, B.Gerdin, Sodium hyaluronate as an adjunct in adhesion prevention after flexor tendon surgery in rabbits, The Journal of Hand Surgery. vol. 17 (1992) 935-941. https://doi.org/10.1016/0363-5023(92)90474-4.

[48] J.Burns, K.Skinner, J.Colt, A.Sheidlin, R.Bronson, Y.Yaacobi, E.Goldberg, Prevention of Tissue Injury and Postsurgical Adhesions by Precoating Tissues with Hyaluronic Acid Solutions, Journal of Surgical Research. vol. 59 (1995) 644-652. https://doi.org/10.1006/jsre.1995.1218.

[49] W.CHEN, G.ABATANGELO, Functions of hyaluronan in wound repair, Wound Repair and Regeneration. vol. 7 (1999) 79-89. https://doi.org/10.1046/j.1524-475X.1999.00079.x.

[50] D.Johns, K.Rodgers, W.Donahue, T.Kiorpes, G.diZerega, Reduction of adhesion formation by postoperative administration of ionically cross-linked hyaluronic acid, Fertility and Sterility. vol. 68 (1997) 37-42. https://doi.org/10.1016/S0015-0282(97)81472-0.

[51] S.Na, S.Oh, K.Song, J.Lee, Hyaluronic acid/mildly crosslinked alginate hydrogel as an injectable tissue adhesion barrier, Journal of Materials Science: Materials in Medicine. vol. 23 (2012) 2303-2313. https://doi.org/10.1007/s10856-012-4689-0.

[52] Y.Yeo, C.Highley, E.Bellas, T.Ito, R.Marini, R.Langer, D.Kohane, In situ cross-linkable hyaluronic acid hydrogels prevent post-operative abdominal adhesions in a rabbit model, Biomaterials. vol. 27 (2006) 4698-4705. https://doi.org/10.1016/j.biomaterials.2006.04.043.

[53] L.Li, N.Wang, X.Jin, R.Deng, S.Nie, L.Sun, Q.Wu, Y.Wei, C.Gong, Biodegradable and injectable in situ cross-linking chitosan-hyaluronic acid based hydrogels for postoperative adhesion prevention, Biomaterials. vol. 35 (2014) 3903-3917. https://doi.org/10.1016/j.biomaterials.2014.01.050.

[54] K.Röck, K.Fischer, J.Fischer, Hyaluronan Used for Intradermal Injections Is Incorporated into the Pericellular Matrix and Promotes Proliferation in Human Skin Fibroblasts in vitro, Dermatology. vol. 221 (2010) 219-228. https://doi.org/10.1159/000318905.

[55] M.Asparuhova, D.Kiryak, M.Eliezer, D.Mihov, A.Sculean, Activity of two hyaluronan preparations on primary human oral fibroblasts, Journal of Periodontal Research. vol. 54 (2019) 33-45. https://doi.org/10.1111/jre.12602.

[56] S.Meran, D.Thomas, P.Stephens, S.Enoch, J.Martin, R.Steadman, A.Phillips, Hyaluronan Facilitates Transforming Growth Factor-β1-mediated Fibroblast Proliferation, Journal of Biological Chemistry. vol. 283 (2008) 6530-6545. https://doi.org/10.1074/jbc.M704819200.

[57] S.Shepard, H.Becker, J.Hartmann, Using Hyaluronic Acid to Create a Fetal-like Environment in vitro, Annals of Plastic Surgery. vol. 36 (1996) 65-69. https://doi.org/10.1097/00000637-199601000-00013.

[58] M.David-Raoudi, F.Tranchepain, B.Deschrevel, J.Vincent, P.Bogdanowicz, K.Boumediene, J.Pujol, Differential effects of hyaluronan and its fragments on fibroblasts: Relation to wound healing, Wound Repair and Regeneration. vol. 16 (2008) 274-287. https://doi.org/10.1111/j.1524-475X.2007.00342.x.

[59] D.Andreutti, A.Geinoz, G.Gabbiani, Effect of hyaluronic acid on migration, proliferation and alpha-smooth muscle actin expression by cultured rat and human fibroblasts, J Submicrosc Cytol Pathol. 31 (1999) 173-7.

[60] M.Yagi, N.Sato, Y.Mitsui, M.Gotoh, T.Hamada, K.Nagata, Hyaluronan Modulates Proliferation and Migration of Rabbit Fibroblasts Derived From Flexor Tendon Epitenon and Endotenon, The Journal of Hand Surgery. vol. 35 (2010) 791-796. https://doi.org/10.1016/j.jhsa.2010.02.010.

[61] M.Chen, L.Li, Z.Wang, P.Li, F.Feng, X.Zheng, High molecular weight hyaluronic acid regulates P. gingivalis–induced inflammation and migration in human gingival fibroblasts via MAPK and NF-κB signaling pathway, Archives of *Oral Biology*. vol. 98 (**2019**) 75-80. https://doi.org/10.1016/j.archoralbio.2018.10.027.

[62] M.Šimek, K.Nešporová, A.Kocurková, T.Foglová, G.Ambrožová, V.Velebný, L.Kubala, M.Hermannová, How the molecular weight affects the in vivo fate of exogenous hyaluronan delivered intravenously: A stable-isotope labelling strategy, Carbohydrate Polymers. vol. 263 (2021). https://doi.org/10.1016/j.carbpol.2021.117927.

[63] J.Fraser, T.Laurent, H.Pertoft, E.Baxter, Plasma clearance, tissue distribution and metabolism of hyaluronic acid injected intravenously in the rabbit, Biochemical Journal. vol. 200 (1981) 415-424. https://doi.org/10.1042/bj2000415.

[64] G.Kogan, L.Šoltés, R.Stern, J.Schiller, R.Mendichi, Hyaluronic Acid: Its Function and Degradation in in vivo Systems, Bioactive Natural Products (Part N). (2008) 789-882. https://doi.org/10.1016/S1572-5995(08)80035-X.

[65] J.Necas, L.Bartosikova, P.Brauner, J.Kolar, Hyaluronic acid (hyaluronan): a review, Veterinární medicína. vol. 53 (2008) 397-411. https://doi.org/10.17221/1930-VETMED.

[66] Y.Liu, X.Shu, G.Prestwich, Reduced postoperative intra-abdominal adhesions using Carbylan-SX, a semisynthetic glycosaminoglycan hydrogel, Fertility and Sterility. vol. 87 (2007) 940-948. https://doi.org/10.*1016*/j.fertnstert.2006.07**.**1532.

[67] Y.Yeo, E.Bellas, C.Highley, R.Langer, D.Kohane, Peritoneal adhesion prevention with an in situ cross-linkable hyaluronan gel containing tissue-type plasminogen activator in a rabbit repeated-injury model, Biomaterials. vol. 28 (2007) 3704-3713. https://doi.org/10.1016/j.biomaterials.2007.04.033.

[68] P.De Laco, M.Stefanetti, D.Pressato, S.Piana, M.Donà, A.Pavesio, A novel hyaluronan-based gel in laparoscopic adhesion prevention: preclinical evaluation in an animal model, Fertility and Sterility. vol. 69 (1998) 318-23. https://doi.org/10.1016/s0015-0282(98)00496-8.

[69] R.Leach, J.Burns, E.Dawe, M.SmithBarbour, M.Diamond, Reduction of Postsurgical Adhesion Formation in the Rabbit Uterine Horn Model with Use of Hyaluronate/ Carboxymethylcellulose Gel, Fertility and Sterility. vol. 69 (1998) 415-418. https://doi.org/10.1016/S0015-0282(97)00573-6.

[70] C.Kong, Y.In, H.Cho, K.Suhl, The effects of applying adhesion prevention gel on the range of motion and pain after TKA, The Knee. vol. 18 (2011) 104-107. https://doi.org/10.1016/j.knee.2009.12.007.

[71] R.Buffa, T.Klejch, M.Hermannová, L.Hejlová, V.Svozil, H.Vágnerová, H.Škubalová, K.Nešporová, V.Velebný, Modified hyaluronic acid with enhanced resistance to degradation, Carbohydrate Polymers. vol. 320 (2023). https://doi.org/10.1016/j.carbpol.2023.121241.

[72] N.Berriaud, M.Milas, M.Rinaudo, Rheological study on mixtures of different molecular weight hyaluronates, International Journal of Biological Macromolecules. vol. 16 (1994) 137-142. https://doi.org/10.1016/0141-8130(94)90040-X.

[73] S.Falcone, D.Palmeri, R.Berg, Rheological and cohesive properties of hyaluronic acid, Journal of Biomedical Materials Research Part A. 76A (2006) 721-728. https://doi.org/10.1002/jbm.a.30623.

[74] A.Dodero, R.Williams, S.Gagliardi, S.Vicini, M.Alloisio, M.Castellano, A micro-rheological and rheological study of biopolymers solutions: Hyaluronic acid, Carbohydrate Polymers. vol. 203 (2019) 349-355. https://doi.org/10.1016/j.carbpol.2018.09.072.

[75] D.Rebenda, M.Vrbka, P.Čípek, E.Toropitsyn, D.Nečas, M.Pravda, M.Hartl, On the Dependence of Rheology of Hyaluronic Acid Solutions and Frictional Behavior of Articular Cartilage, Materials. vol. 13 (2020). https://doi.org/10.3390/ma13112659.

[76] B.Forthofer, M.Arnold, B.Reisdorf, M.Amadio, M.Zhao, The Effect of Gelatin Molecular Weight on Tendon Lubrication Utilizing an Extrasynovialized Turkey Flexor Tendon Model, Military Medicine. vol. 186 (2021) 729-736. https://doi.org/10.1093/milmed/usaa265.

[77] J.Ikeda, C.Zhao, Y.Sun, K.An, P.Amadio, Carbodiimide-Derivatized Hyaluronic Acid Surface Modification of Lyophilized Flexor Tendon, vol. 92 (2010) 388-395. https://doi.org/10.2106/JBJS.H.01641.

[78] P.Raghavan, Y.Lu, M.Mirchandani, A.Stecco, Human Recombinant Hyaluronidase Injections For Upper Limb Muscle Stiffness in Individuals With Cerebral Injury: A Case Series, EBioMedicine. vol. 9 (2016) 306-313. https://doi.org/10.1016/j.ebiom.2016.05.014.

[79] T.Pereira, P.Jüni, P.Saadat, D.Xing, L.Yao, P.Bobos, A.Agarwal, C.Hincapié, B.da Costa, Viscosupplementation for knee osteoarthritis: systematic review and meta-analysis, BMJ. (n.d.) /bmj/378/bmj-2022-069722.atom. https://doi.org/10.1136/bmj-2022-069722.

[80] J.Peck, A.Slovek, P.Miro, N.Vij, B.Traube, C.Lee, A.Berger, H.Kassem, A.Kaye, W.Sherman, A.Abd-Elsayed, A Comprehensive Review of Viscosupplementation in Osteoarthritis of the Knee, Orthopedic Reviews. vol. 13 (2021). https://doi.org/10.52965/001c.25549.

[81] G.Greene, B.Zappone, X.Banquy, D.Lee, O.Söderman, D.Topgaard, J.Israelachvili, Hyaluronic acid–collagen network interactions during the dynamic compression and recovery of cartilage, Soft Matter. vol. 8 (2012). https://doi.org/10.1039/c2sm26330k.

[82] Z.Zhou, Z.Jin, Biotribology: Recent progresses and future perspectives, Biosurface and Biotribology. vol. 1 (2015) 3-24. https://doi.org/10.1016/j.bsbt.2015.03.001.

[83] W.Lin, R.Mashiah, J.Seror, A.Kadar, O.Dolkart, T.Pritsch, R.Goldberg, J.Klein, Lipid-hyaluronan synergy strongly reduces intrasynovial tissue boundary friction, Acta Biomaterialia. vol. 83 (2019) 314-321. https://doi.org/10.1016/j.actbio.2018.11.015.

[84] B.Moor, L.Nagy, J.Snedeker, A.Schweizer, Friction between finger flexor tendons and the pulley system in the crimp grip position, Clinical Biomechanics. vol. 24 (2009) 20-25. https://doi.org/10.1016/j.clinbiomech.2008.10.002.

[85] J.Prinz, R.de Wijk, L.Huntjens, Load dependency of the coefficient of friction of oral mucosa, Food Hydrocolloids. vol. 21 (2007) 402-408. https://doi.org/10.1016/j.foodhyd.2006.05.005.

[86] J.de Vicente, J.Stokes, H.Spikes, Soft lubrication of model hydrocolloids, Food Hydrocolloids. vol. 20 (2006) 483-491. https://doi.org/10.1016/j.foodhyd.2005.04.005.

[87] D.DRESSELHUIS, E.DEHOOG, M.COHENSTUART, G.VANAKEN, Application of oral tissue in tribological measurements in an emulsion perception context, Food Hydrocolloids. vol. 22 (2008) 323-335. https://doi.org/10.1016/j.foodhyd.2006.12.008.

[88] T.Rovers, G.Sala, E.Van der Linden, M.Meinders, Potential of Microbubbles as Fat Replacer: Effect on Rheological, Tribological and Sensorial Properties of Model Food Systems, Journal of Texture Studies. vol. 47 (2016) 220-230. https://doi.org/10.1111/jtxs.12175.

[89] K.Liu, M.Stieger, E.van der Linden, F.van de Velde, Fat droplet characteristics affect rheological, tribological and sensory properties of food gels, Food Hydrocolloids. vol. 44 (2015) 244-259. https://doi.org/10.1016/j.foodhyd.2014.09.034.

[90] A.Krzeminski, K.Prell, M.Busch-Stockfisch, J.Weiss, J.Hinrichs, Whey protein–pectin complexes as new texturising elements in fat-reduced yoghurt systems, International Dairy Journal. vol. 36 (2014) 118-127. https://doi.org/10.1016/j.idairyj.2014.01.018.

[91] A.Sonne, M.Busch-Stockfisch, J.Weiss, J.Hinrichs, Improved mapping of in-mouth creaminess of semi-solid dairy products by combining rheology, particle size, and tribology data, LWT - Food Science and Technology. vol. 59 (2014) 342-347. https://doi.org/10.1016/j.lwt.2014.05.047.

[92] T.Wilson, R.Aeschlimann, S.Tosatti, Y.Toubouti, J.Kakkassery, K.Osborn Lorenz, Coefficient of Friction of Human Corneal Tissue, Cornea. vol. 34 (2015) 1179-1185. https://doi.org/10.1097/ICO.0000000000000524.

[93] O.Sterner, C.Karageorgaki, M.Zürcher, S.Zürcher, C.Scales, Z.Fadli, N.Spencer, S.Tosatti, Reducing Friction in the Eye: A Comparative Study of Lubrication by Surface-Anchored Synthetic and Natural Ocular Mucin Analogues, vol. 9 (2017) 20150-20160. https://doi.org/10.1021/acsami.6b16425.

[94] M.Černohlávek, M.Brandejsová, P.Štěpán, H.Vagnerová, M.Hermannová, K.Kopecká, J.Kulhánek, D.Nečas, M.Vrbka, V.Velebný, G.Huerta-Angeles, Insight into the Lubrication and Adhesion Properties of Hyaluronan for Ocular Drug Delivery, Biomolecules. vol. 11 (2021). https://doi.org/10.3390/biom11101431.

[95] D.Nečas, V.Kulíšek, P.Štěpán, F.Ondreáš, P.Čípek, G.Huerta-Angeles, M.Vrbka, Friction and Lubrication of Eye/Lens/Lid Interface: The Effect of Lubricant and Contact Lens Material, Tribology Letters. vol. 71 (2023). https://doi.org/10.1007/s11249-023-01787-4.

[96] D.Flom, A.Bueche, Theory of Rolling Friction for Spheres, Journal of Applied Physics. vol. 30 (1959) 1725-1730. https://doi.org/10.1063/1.1735043.

[97] K.Ludema, D.Tabor, The friction and visco-elastic properties of polymeric solids, Wear. vol. 9 (1966) 329-348. https://doi.org/10.1016/0043-1648(66)90018-4.

[98] K.Grosch, The relation between the friction and visco-elastic properties of rubber, Proceedings of the Royal Society of London. Series A. Mathematical and Physical Sciences. vol. 274 (1963) 21-39. https://doi.org/10.1098/rspa.1963.0112.

[99] Y.Xu, B.Cartwright, L.Advincula, C.Myant, J.Stokes, Generalised scaling law for soft contact tribology: Influence of load and asymmetric surface deformation, Tribology International. vol. 163 (2021). https://doi.org/10.1016/j.triboint.2021.107192.

[100] C.Quinn, D.Nečas, P.Šperka, M.Marian, M.Vrbka, I.Křupka, M.Hartl, Experimental investigation of friction in compliant contact: The effect of configuration, viscoelasticity and operating conditions, Tribology International. vol. 165 (2022). https://doi.org/10.1016/j.triboint.2021.107340.

[101] P.Sadowski, S.Stupkiewicz, Friction in lubricated soft-on-hard, hard-on-soft and soft-on-soft sliding contacts, Tribology International. vol. 129 (2019) 246-256. https://doi.org/10.1016/j.triboint.2018.08.025.

[102] J.de Vicente, J.Stokes, H.Spikes, Rolling and sliding friction in compliant, lubricated contact, Proceedings of the Institution of Mechanical Engineers, Part J: Journal of Engineering Tribology. vol. 220 (2006) 55-63. https://doi.org/10.1243/13506501JET90.

[103] D.Mahdi, A.Riches, M.Gester, J.Yeomans, P.Smith, Rolling and sliding: Separation of adhesion and deformation friction and their relative contribution to total friction, Tribology International. vol. 89 (2015) 128-134. https://doi.org/10.1016/j.triboint.2014.12.021.

[104] N.Selway, V.Chan, J.Stokes, Influence of fluid viscosity and wetting on multiscale viscoelastic lubrication in soft tribological contacts, Soft Matter. vol. 13 (2017) 1702-1715. https://doi.org/10.1039/C6SM02417C.

[105] M.Scaraggi, B.Persson, Theory of viscoelastic lubrication, Tribology International. vol. 72 (2014) 118-130. https://doi.org/10.1016/j.triboint.2013.12.011.

[106] A.Adam, D.Paulkowski, B.Mayer, Friction and Deformation Behavior of Elastomers, Materials Sciences and Applications. vol. 10 (2019) 527-542. https://doi.org/10.4236/msa.2019.108038.

[107] C.Myant, H.Spikes, J.Stokes, Influence of load and elastic properties on the rolling and sliding friction of lubricated compliant contacts, Tribology International. vol. 43 (2010) 55-63. https://doi.org/10.1016/j.triboint.2009.04.034.

[108] A.Kim, A.Cholewinski, S.Mitra, B.Zhao, Viscoelastic tribopairs in dry and lubricated sliding friction, Soft Matter. vol. 16 (2020) 7447-7457. https://doi.org/10.1039/D0SM00516A.

[109] A.Tiwari, L.Dorogin, A.Bennett, K.Schulze, W.Sawyer, M.Tahir, G.Heinrich, B.Persson, The effect of surface roughness and viscoelasticity on rubber adhesion, Soft Matter. vol. 13 (2017) 3602-3621. https://doi.org/10.1039/C7SM00177K.

[110] J.Bongaerts, K.Fourtouni, J.Stokes, Soft-tribology: Lubrication in a compliant PDMS–PDMS contact, Tribology International. vol. 40 (2007) 1531-1542. https://doi.org/10.1016/j.triboint.2007.01.007.

[111] A.Pitenis, J.Urueña, K.Schulze, R.Nixon, A.Dunn, B.Krick, W.Sawyer, T.Angelini, Polymer fluctuation lubrication in hydrogel gemini interfaces, Soft Matter. vol. 10 (2014) 8955-8962. https://doi.org/10.1039/C4SM01728E.

[112] A.Elsharkawy, Visco-elastohydrodynamic lubrication of line contacts, Wear. vol. 199 (1996) 45-53. https://doi.org/10.1016/0043-1648(96)07212-2.

[113] C.Hooke, P.Huang, Elastohydrodynamic lubrication of soft viscoelastic materials in line contact, Proceedings of the Institution of Mechanical Engineers, Part J: Journal of Engineering Tribology. vol. 211 (1997) 185-194. https://doi.org/10.1243/1350650971542417.

[114] A.Pandey, S.Karpitschka, C.Venner, J.Snoeijer, Lubrication of soft viscoelastic solids, Journal of Fluid Mechanics. vol. 799 (2016) 433-447. https://doi.org/10.1017/jfm.2016.375.

[115] C.Putignano, D.Dini, Soft Matter Lubrication: Does Solid Viscoelasticity Matter?, vol. 9 (2017) 42287-42295. https://doi.org/10.1021/acsami.7b09381.

[116] C.Putignano, Soft lubrication: A generalized numerical methodology, Journal of the Mechanics and Physics of Solids. vol. 134 (2020). https://doi.org/10.1016/j.jmps.2019.103748.

[117] C.Putignano, A.Campanale, Squeeze lubrication between soft solids: A numerical study, Tribology International. vol. 176 (2022). https://doi.org/10.1016/j.triboint.2022.107824.

[118] Y.Zhao, H.Liu, G.Morales-Espejel, C.Venner, Effects of solid viscoelasticity on elastohydrodynamic lubrication of point contacts, Tribology International. vol. 171 (2022). https://doi.org/10.1016/j.triboint.2022.107562.

[119] T.He, Q.Wang, X.Zhang, Y.Liu, Z.Li, H.Kim, S.Pack, Visco-elastohydrodynamic lubrication of layered materials with imperfect layer-substrate interfaces, International Journal of Mechanical Sciences. vol. 189 (2021). https://doi.org/10.1016/j.ijmecsci.2020.105993.

[120] M.Roman, H.Chaudhry, B.Bukiet, A.Stecco, T.Findley, Mathematical Analysis of the Flow of Hyaluronic Acid Around Fascia During Manual Therapy Motions, Journal of Osteopathic Medicine. vol. 113 (2013) 600-610. https://doi.org/10.7556/jaoa.2013.021.

[121] H.Chaudhry, B.Bukiet, M.Roman, A.Stecco, T.Findley, Squeeze film lubrication for non-Newtonian fluids with application to manual medicine, Biorheology. vol. 50 (2013) 191-202. https://doi.org/10.3233/BIR-130631.

[122] K.Nešporová, J.Matonohová, J.Husby, E.Toropitsyn, L.Stupecká, A.Husby, T.Suchánková Kleplová, A.Streďanská, M.Šimek, D.Nečas, M.Vrbka, R.Schleip, V.Velebný, Injecting hyaluronan in the thoracolumbar fascia: A model study, International Journal of Biological Macromolecules. vol. 253 (2023). https://doi.org/10.1016/j.ijbiomac.2023.126879.

[123] G.Plasqui, A.Bonomi, K.Westerterp, Daily physical activity assessment with accelerometers: new insights and validation studies, Obesity Reviews. vol. 14 (2013) 451-462. https://doi.org/10.1111/obr.12021.

[124] H.Jagos, J.Oberzaucher, M.Reichel, W.Zagler, W.Hlauschek, A multimodal approach for insole motion measurement and analysis, Procedia Engineering. vol. 2 (2010) 3103-3108. https://doi.org/10.1016/j.proeng.2010.04.118.

LIST OF FIGURES

Fig. 1 How back pain affects feelings. Graphs are taken and adapted from [2] 8

Fig. 2 How back pain affects work and social life. Graphs are taken and adapted from [2] 9

Fig. 3 NSLBP caused by TLF and placement of TLF under the skin. Created by Biorender.com 11

Fig. 4 Zero-rate viscosity of HA as the function of concentration. Adapted from [73] 15

Fig. 5 The dependence of dynamic moduli (G' and G" in Pa) of HA and hylan (HA-based gel) preparation on frequency. The concentration is 10 mg/ml. MW is MW [44] 16

Fig. 6 Viscosity as a function of shear rate for HA solutions with different MWs; (b) Elastic (G′) and viscous (G″) moduli as a function of frequency for HA solutions with different MW [75] 17

Fig. 7 A multi-scale viscoelastic conceptual model has been proposed to elucidate the effects of lubricant viscosity and static wetting on the tribological characteristics of both smooth and rough contacts. Adapted from [104]. 22

Fig. 8 Real contact area (%) dependence of growing nominal surface pressure of elastomers [106] 23

Fig. 9 Plot of the friction coefficient against the preload at each sliding velocity of dry, glycerol and water friction [108] 24

Fig. 10 Stribeck curves for a hydrophobic–hydrophobic tribopair (disk roughness = 382 nm) [110] 25

Fig. 11 The friction coefficient of PTFE ball tribological contact with (A) a smooth and (B) a rough PDMS disc [104] 26

Fig. 12 Developed fascia holder for tribological testing and promo picture of UMT Tribolab from Bruker.com 33

Fig. 13 Models configuration presentation 35

Fig. 14 Redesigned pin from point contact to linear contact with R30 and R50. Fascia is prestressed over the glued PDMS and hold with two rough holders avoiding slipping on the sides 36

Fig. 15 Dorsal rabbit fascia preparation 38

Fig. 16 Graphical illustration of issues examined in the study. Created with Biorender.com 42

Fig. 17 Graphical illustration of methods used in different parts of the study. Created with Biorender.com 43

Fig. 18 Fascigel - HA-based viscosupplement for NSLBP 103

LIST OF TABLES

Tab 1 Concentration and turnover of HA in different tissues. Adapted and modified from [65] 14

Tab 2 Body parts models in the biotribological studies. Poly(dimethylsiloxane) mentioned as PDMS 19

Tab 3 HA advantages in medical usage [44-61] 29

Tab 4 HA-based lubricants 39

Tab 5 Experimental conditions used in experiments 40

LIST OF ABBREVIATIONS AND SYMBOLS

η	Viscosity	**mg**	Miligram
η_{SP}	Specific viscosity	**ml**	Mililiter
%	Percentage by weight	**mm**	Milimeter
[η]	Intrisic viscosity	**mN**	Milinewton
°	Degree	**MPa**	Megapascals
°C	Degree of Celsius	**MTM**	Mini Traction Machine
µg	Microgram	**MW**	Molecular weight
µm	Micrometer	**N**	Newton
c	Concentration	**NaCL**	Sodium chloride
COF	Coefficient of friction	**NBR**	Nitrile butadiene rubber
Da	Daltons	**NIPAM**	N-Isopropylacrylamide
DMA	Dynamic mechanical analysis	**nm**	Nanometer
EHL	Elastohydrodynamic lubrication	**NSLBP**	Non-specific lower back pain
EPDM	Ethylene-propylene diene monomer	**OA**	Osteoarthritis
FEM	Finite Element Method	**Pa**	Pascal
FM	Fascial manipulation	**PBS**	Phosphate-buffered saline
g	Gram	**PDMS**	Poly(dimethylsiloxane)
G''	Dynamic viscous modulus	**PTFE**	Polytetrafluorethylen
G'	Dynamic elastic modulus	**PU**	Polyurethan
GECO	Epichlorohydrin−ethylene oxide−allyl glycidyl ether	**PVA**	Polyvinyl alcohol
HA	Hyaluronic acid	**Ra**	Roughness
HMW	High molecular weight	**rpm**	Rotates per minute
HNBR	Hydrogenated nitrile butadiene rubber	**s**	Second
Hz	Hertz	**SEM**	Scanning electron microscope

kDa	Kilodalton	**Sh00**	Shore 00 Hardness
kg	Kilogram	**ShA**	Shore A Hardness
kPa	Kilopascal	**$t_{1/2}$**	Half-life
LBP	Lower back pain	**TGF-β3**	Transforming growth factor beta-3
LMW	Low molecular weight	**TLF**	Thoracolumbar fascia
LVO	Low viscosity oil	**wt%**	Percentage by weight